January 2018

Investigation Of The In Vivo Activity Of Ribosome-Targeting Peptides And Aminoglycosides In Escherichia Coli

Nisansala Sarangi Thilakarathne Muthunayake
Wayne State University, es5848@wayne.edu

INVESTIGATION OF THE *IN VIVO* ACTIVITY OF RIBOSOME-TARGETING PEPTIDES AND AMINOGLYCOSIDES IN *ESCHERICHIA COLI*

by

NISANSALA SARANGI THILAKARATHNE MUTHUNAYAKE

DISSERTATION

Submitted to the Graduate School

of Wayne State University,

Detroit, Michigan

in partial fulfillment of the requirements

for the degree of

DOCTOR OF PHILOSOPHY

2018

MAJOR: CHEMISTRY (Biochemistry)

Approved by:

_____

Advisor Date

_____

_____

_____

DEDICATION

This thesis work is dedicated to my parents Swarnalatha Wijayalath, Thilakarathne Muthunayake and my aunt Kamala Wijayalath and to my loving husband Nadeesha Prabath Wimalaweera.

Thank you very much for your everlasting love, support, blessings and understanding.

ACKNOWLEDGMENTS

First and foremost, I would like to express my deep and sincere gratitude to my advisor Dr. Christine Chow for her wonderful guidance, generous support, and understanding. I am grateful for the wonderful opportunities she gave me to improve my skill set as a scientist. Especially, I would like to thank her for letting me to work as the graduate research assistant for the Broadening Experience in Scientific Training (BEST) program for two years, which was an unique experience I had as a doctoral student and provided further benefits for my future. I really appreciate her personal qualities such as being an efficient worker, having exceptional writing skills and possessing great critical thinking. I learnt a lot from her. Her excellent mentorship and motivation have continuously inspired me and led me to this finish line. I wish to extend my gratitude to the dissertation committee members, Dr. Ashok Bhagwat, Dr. Sarah Trimpin, and Dr. Athar Ansari for their time and critical comments on my dissertation work. Also I would like to thank my main collaborators, Dr. Philip Cunningham, Dr. Wesley Colangelo, Dr. Ellen Inutan for providing such a wonderful collaborative environment, within which I was able to pursue my research goals. I also want to thank Professor Michael O' Connor from the University of Missouri-Kansas city for providing bacterial strains for our research.

I want to convey my deepest gratitude to Dr. Ambika Mathur, Dean of the Graduate School of Wayne State University for giving me the great opportunity to work as the Graduate research Assistant for the NIH-BEST program. Dean Mathur always tried to convince me my potential beyond biochemical research. She encouraged me to attend conferences representing the WSU-BEST program and gave me an opportunity to become a co-author of several manuscripts providing me with the experience necessary for a career outside of graduate school. I would like to thank her for showing me the great potential women have in science. Many

thanks to all the Chow group, past and present members, for being great co-workers, friends, and supporters. Specially, I would like to thank Dr. Gayani Dedduwamudalige for training me in the lab, when I first started. It was a great pleasure to work with Supuni Thalalla Gamage, Prabuddha Madubashitha, Bett Kimutai, Evan Jones, Rabiul Islam and Alan Mlotkowski. I particularly grateful to Supuni for wonderful discussions and feedback on my work and being a great collaborator, a friend and a sister. I would also like to thank the previous students from Chow lab, Dr. Hyosuk Seo, Dr. Danielle Dremann, Dr. Xun Bao, Dr. Jung Jiang, Dr. Yogo Sakakibara, Dr. Moninderpal Kaur and Daya Nidhi Kharel for being great labmates. Many thanks go to all of the undergraduate students who worked with me for last six years. These people include Laura Hajjar, Susan White, Marwa Abdel-Maguid, Amer Abu-kuwaik, Alexandra Cvetkovska, Sherrell Haney and Mackenzie Olbrys. Also I would like to thank the Ahn group members for their friendship and helpful discussions.

I also want to thank the great team I had in the graduate school. Many thanks go to Dr. Heidi Kenaga, Mary Wood, Michael Khol, Mustafa Ziyad, Dr. Annmarie Cano, and Dr. Andrew Feig for being great team workers. I would like to thank the all graduate school staff for creating a friendly and positive environment. I wish to express my gratitude to the Wayne State University and especially the Department of Chemistry, for giving me this wonderful opportunity to carry out my graduate studies. It is with great pleasure that I am remembering my undergraduate institution, the University of Kelaniya in Sri Lanka for giving me all the basic knowledge and experience, which undoubtedly helped me in my graduate studies. I also want to convey my gratitude to Kotelawla Defence University, especially to Major General Milinda Peiris, for providing me an unique opportunity to explore myself as a chemistry lecturer. I also want to convey my heartfelt gratitude to Maliyadeva Girls College, Kurunegala, Sri Lanka where

I learnt my first science lessons that inspired me to become a scientist. I would like to thank all my teachers who paved the path to earn this PhD. I also want to thank all my friends for being there for me and my husband. I am privileged to live within a large Sri Lankan community here at Wayne State, which is a rare occasion for a person who stays away from the home country.

Finally, I would like to thank my loving parents, Swarnalatha Wijayalath and Thilakarathne Muthunayake and my ever loving aunt Kamala Wijayalath for raising me to the level that I am today. They always appreciate my accomplishments more than I do and taught me to behave with great patience and humanity in front of the challenges. Specially, my mother's and aunt's effort towards my education was enormous and their courage was outstanding. Without them I wouldn't be here today. I also want to thank my ever loving sister Pathumvila Chathurangi and my brother and Nuwan Deshitha for their endless love, friendship and motivation. Thank you for giving me a wonderful childhood with lot of good memories and adventures which I always remember happily. I want to convey my sincere gratitude to my loving parent-in-laws Ananda and Tulin Wimalaweera and sister and brother-in-laws Geevani and Ruwan Wimalaweera for their love, support, motivation and understanding.

I am truly and deeply grateful to my ever loving husband, Nadeesha Prabath Wimalaweera, for his true love, moral support, and encouragement given to me and for staying at my side during the past seven years. He is my constant source of inspiration for self-improvement and ambition. Without his support, positive advice about life, silent patience and sacrifices, this Ph.D. would never have been possible. Finally I would like to thank my beautiful daughter Yenuli Vivanya Wimalaweera for her innocent smile and bunch of love that always make my life beautiful and complete.

TABLE OF CONTENTS

LIST OF TABLES

LIST OF FIGURES

LIST OF ABBREVIATIONS

2-DOS	2-deoxy streptamine
AMP	antimicrobial peptides
DMS	dimethyl sulfate
EF	elongation factor
GFP	green fluorescent protein
h44	helix 44
H69	helix 69
H92	helix 92
IF	initiation factor
MALDI MS	matrix assisted laser desorption ionization mass spectroscopy
MIC	minimum inhibitory concentration
mRNA	messenger RNA
PCR	polymerse chain reaction
PrAMP	Proline-rich antimicrobial peptides
PTC	peptidyl transferase center
RF	release factor
RRF	ribosome recycling factor
rRNA	ribosomal RNA
SPPS	solid phase peptide synthesis
TEV	tobacco etch virus
tRNA	transfer RNA
Ψ	pseudouridine

CHAPTER 1 INTRODUCTION

1.1 Introduction to the ribosome

According to the central dogma of molecular biology, the genetic information stored in DNA molecules is first transcribed into messenger RNA (mRNA) molecules and then translated into proteins.[1] The ribosome, which is a ribonucleoprotein complex, plays a significant role in the translation process in all living organisms.[2] The bacterial ribosome was first described as a small particulate component by a cell biologist, George Palade, in 1955.[3] The term "ribosome" was proposed by scientist Richard B. Roberts at the end of the 1960s.[4] In 1974, the Nobel Prize in physiology was shared by Palade and two other scientists, Albert Claude and Christian de Duve, for their work focusing on the discovery of the ribosome.[5] Although it was known that the ribosomes consist of ribonucleic acids (RNA) as well as proteins and they were capable of synthesizing proteins, the main challenge was to determine the exact mechanistic steps of translation.

In 1967, Carl Woese, Francis Crick, and Leslie Orgel were the first to suggest that RNA could act as a catalyst, based on their determination of complex RNA secondary structures.[6] In the early 1980s, Thomas Cech and Sidney Altman independently demonstrated the catalytic properties of RNA.[7,8] In 1989, they won the Nobel Prize in Chemistry for their discovery.[7,8] The breakthroughs in RNA catalysis helped advance ribosomal RNA-focused research as well.[9-12] By this time, it was clear that the ribosome, composed of RNA and protein, was capable of performing protein translation with the RNA component acting as the catalyzing force for function.[9,10] In 2009, Venkatraman Ramakrishnan, Thomas A. Steiz, and Ada E. Yonath won the Nobel Prize for their invaluable contributions to determining the structure and function of the ribosome.[13-15] With these exciting discoveries and a greater appreciation from the scientific community, the ribosome research field has been growing fast with still much to be learned

about this fascinating organelle. A detailed view of the structure, dynamics, and function of the bacterial ribosome will be discussed next.

1.2 Components that form the bacterial and eukaryotic ribosome

The ribosome is composed of two major subunits, referred to as large and small, which are characterized by the sedimentation rate known as the Svedberg unit (S).[16] One Svedberg (S) is equal to 10^{-13} s. The bacterial ribosome is about 25 nm in diameter with a molecular mass of 2.4×10^{6} Da and a sedimentation coefficient of 70S.[17,18] As shown in **Figure 1.1**, the 70S bacterial ribosome contains a large subunit known as 50S and a small subunit known as 30S. Association of the 50S and 30S subunits leads to the complete 70S ribosome.

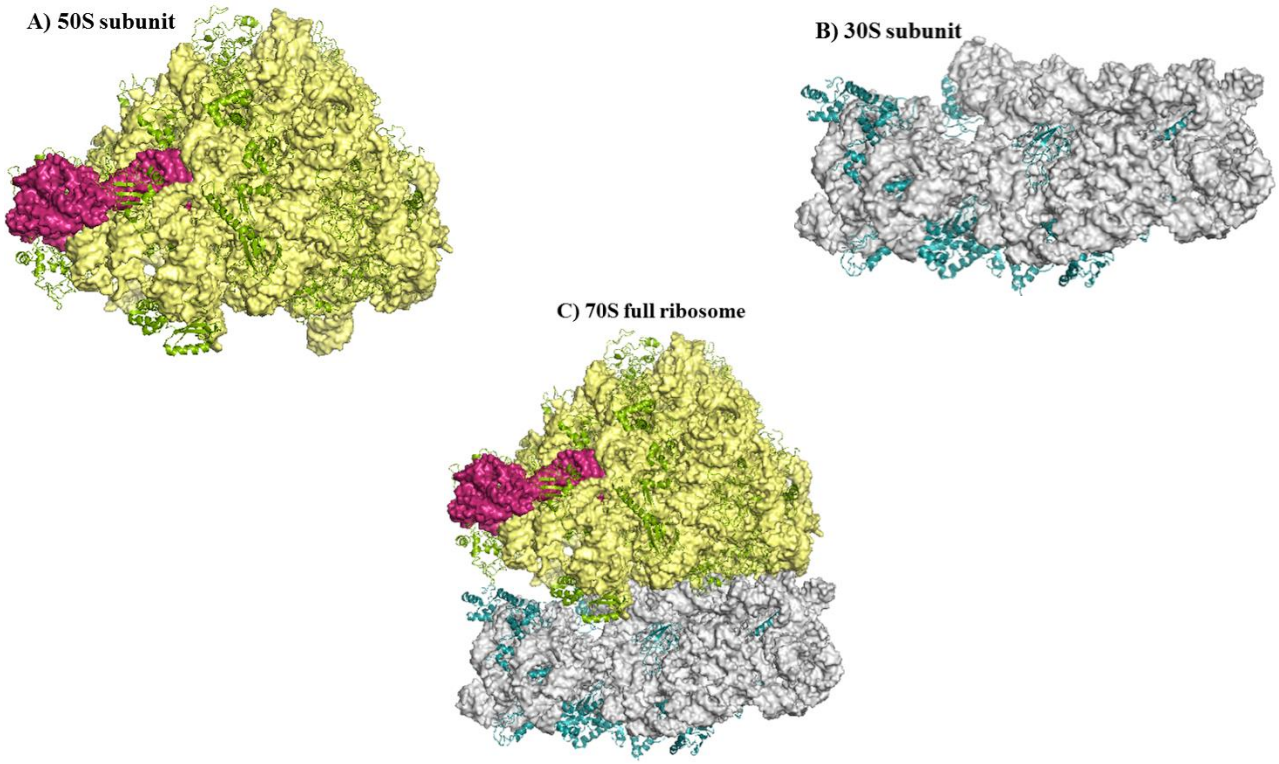

Figure 1.1 *E. coli* bacterial ribosome. (A) The large 50S subunit[19] is composed of 23S rRNA in yellow, 5S rRNA in pink, and 34 rproteins in green. (B) The small 30S subunit is composed of 16S rRNA in grey and 21 rproteins in cyan. (C) Association of the large and small subunits forms the complete 70S ribosome (PDB ID: 2AW4).

The eukaryotic ribosome is larger than the bacterial ribosome with 60S and 40S subunits that together form the 80S ribosome.[20] The ribosome is a ribonucleoprotein complex. Each subunit of the ribosome can be further broken down into individual components, ribosomal RNA (rRNA) and ribosomal proteins (rproteins). In bacterial ribosomes, the 50S subunit comprises 5S rRNA, which contains 120 nucleotides, and 23S rRNA, which contains 2904 nucleotides.[18] The 50S contains 34 rproteins. The 30S subunit comprises 16S rRNA, which contains 1542 nucleotides and 21 rproteins.[19] The eukaryotic ribosome is about 25 nm in diameter with a molecular mass of 4.2×10^6 Da.[21] The 60S subunit comprises 28S rRNA containing 4718 nucleotides, 5.8S rRNA with 160 nucleotides, and 5S rRNA with 120 nucleotides. The 60S contains 49 rproteins. The small subunit 40S contains 18S rRNA with 1874 nucleotides and 33 rproteins.[20] Although the bacterial and eukaryotic ribosomes differ in overall size, they have many highly conserved regions that are essential for the ribosomal functions.[22] Since this thesis work mainly focuses on the bacterial ribosome, all figures and explanations will be in reference to the *E. coli* system.

1.3 Function and significance of the bacterial ribosome

In the late 1950s, Francis Crick proposed the central dogma of molecular biology.[1] As illustrated in **Figure 1.2**, the flow of genetic information is from "DNA to RNA to protein". During the first step, DNA produces complementary DNA through a process called replication.[1] Following replication, the genetic information in DNA is transcribed into a messenger RNA (mRNA) molecule. Finally, the genetic information encoded by the mRNA is translated into a polypeptide chain. The ribosome is the machinery responsible for protein synthesis.[9,10] In the translation process, the ribosome can be considered as the working station, with mRNA as the template and tRNA carrying the building blocks required for the synthesis.[9,10]

The ribosome translation process involves four important steps: mRNA decoding, peptidyl transfer, translocation, and termination. Each ribosomal subunit plays an important and distinct role in the process. The major function of the large ribosomal subunit is to catalyze peptide-bond formation between the amino acid on the aminoacyl transfer RNA (aa-tRNA) in the aminoacyl site (A site) and the nascent polypeptide chain on the peptidyl site (P site), whereas the main function of the small subunit is mRNA decoding in which the sequence is "read" by the machinery.[9,10] In the following section, these steps of bacterial protein translation will be discussed in more detail.

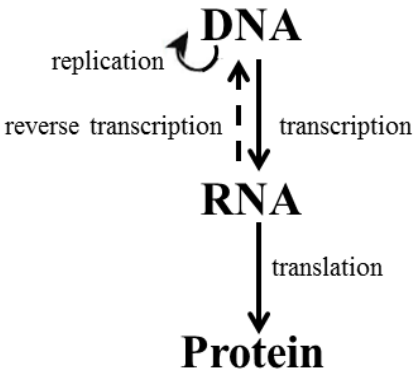

Figure 1.2 The central dogma of molecular biology. This chart shows the flow of genetic information from DNA to proteins. The genetic information in DNA is first transcribed into RNA and then translated into proteins. DNA can undergo replication to produce more DNA, and RNA can undergo reverse transcription to make DNA.

1.3.1 Translation initiation

As shown in **Figure 1.3**, translation initiation begins when the 30S subunit encounters a single-stranded mRNA transcript. The initiator fMet-tRNA$_f^{Met}$ is positioned over the start codon of mRNA in the P site. Correct placement of the start codon on the ribosome is accomplished by base pairing between the Shine-Dalgarno sequence upstream of the start codon and the anti-Shine-Dalgarno sequence at the 3' end of the 16S rRNA.[23,24]

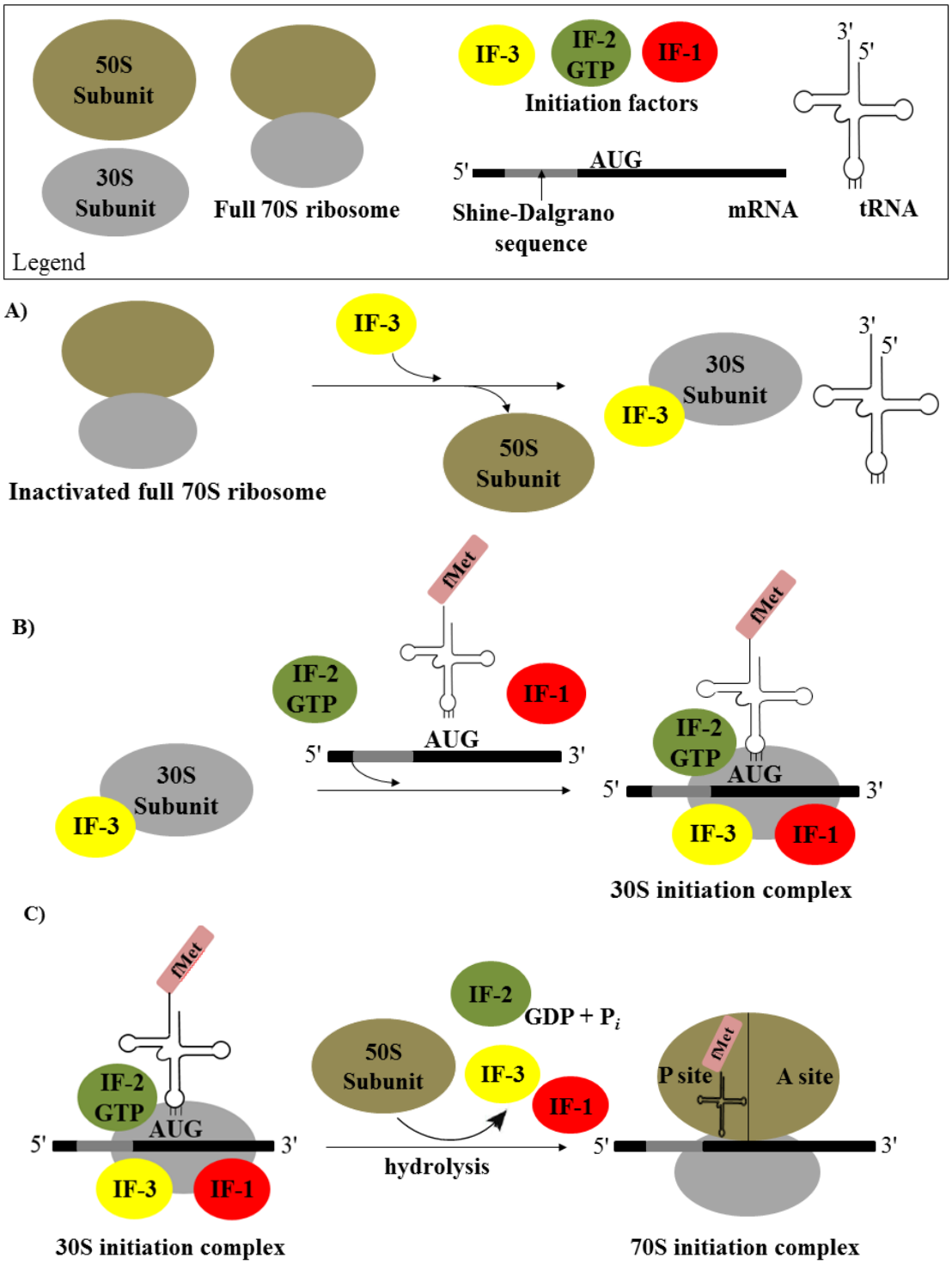

Figure 1.3 Translation initiation of the bacterial ribosome. A) An inactivated 70S ribosome is approached by IF-3, which promotes subunit dissociation. IF-3 remains bound to the 30S subunit. B) The mRNA with the start codon AUG and Shine-Dalgarno sequence upstream of the start codon is recruited to the 30S subunit along with IF-1 and IF-2-GTP-fMet-tRNA$_f^{Met}$ complex. This combination forms the 30S initiation complex. C) IF-1 and IF-3 are released, allowing for subunit association, and hydrolysis of GTP releases IF-2. The 70S initiation complex is formed, allowing for elongation to begin.

The initiation step is facilitated by additional proteins called initiation factors. The first step in initiation is recycling of the 30S subunit, which dissociates from the 50S in the previous translation cycle (described more in **Section 1.3.3**). Initiator factor 3 (IF-3) binding releases the mRNA and deacylated tRNA on 30S remaining from the previous translation cycle.[24] The 30S-IF-3 complex binds to mRNA, initiator factor 1 (IF-1), initiator factor 2 (IF-2), and initiator tRNA (fMet-$tRNA_f^{Met}$) to form the 30S initiation complex. Initiation factor 2 (IF-2) promotes binding of the 50S subunit to form the 70S initiation complex accompanied by IF-3 release. After GTP hydrolysis of IF-2, fMet-$tRNA_f^{Met}$ moves to the peptidyl transferase center (PTC) and the ribosome is ready for the elongation phase. [25-27]

1.3.2 Translation elongation

The intact ribosome has three compartments as follows. The A site binds incoming aminoacyl-tRNAs (aa-tRNAs). The P site binds tRNAs carrying the growing polypeptide chain. The E site is important for dissociation of the tRNAs so that they can be recharged with amino acids. The initiator tRNA, fMet-$tRNA_f^{Met}$, binds directly to the P site. This creates an initiation complex with a free A site ready to accept the aa-tRNA corresponding to the next codon after the AUG start codon.[25,27] The second stage of protein translation is known as elongation. In the elongation cycle, the polypeptide chain is extended in the N to the C terminus direction by sequential addition of amino acids. As shown in **Figure 1.4**, the elongation cycle is composed of three main steps: decoding, transpeptidation, and translocation. The elongation process is facilitated by two proteins called elongation factors. Elongation factor Tu (EF-Tu) delivers the aa-tRNA to the ribosomal A site, and elongation factor G (EF-G) catalyzes translocation of the tRNA and mRNA with respect to the ribosome.[18] The aa-tRNA is delivered as a ternary complex with EF-Tu and GTP.

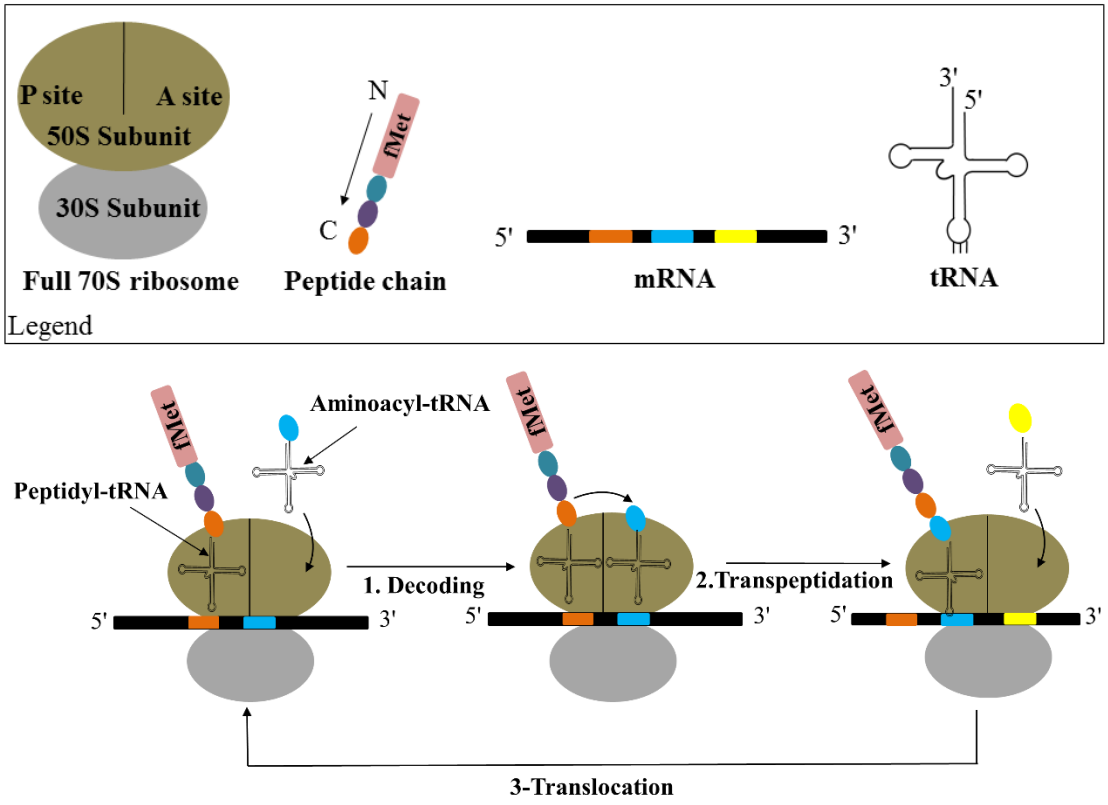

Figure 1.4 Translation elongation of the bacterial ribosome. Elongation is broken down into three steps: decoding, transpeptidation, and translocation. These steps work in a cyclic fashion in conjunction with the three elongation factors (EF-Tu, EF-Ts, and Ef-G; not pictured) until the polypeptide sequence is complete.

The initial binding of the aa-tRNA ternary complex to the ribosome involves Watson-Crick base pairing between the mRNA codon and aa-tRNA anticodon. The mRNA and cognate aa-tRNA interaction induces a conformational change of the universally conserved residues A1493, A1492, and G530 in the 16S rRNA in order to stabilize the codon-anticodon interaction. The complete accommodation of tRNA in the A site requires GTP hydrolysis on EF-Tu.[28,29] This process takes place at the GTPase center on the 50S subunit.[30] After transmitting information regarding the correct codon-anticodon interaction, GTP hydrolysis leads to dissociation of EF-Tu from the ribosome. The tRNA aminoacyl end orients towards the PTC, which is located entirely on the 50S subunit.[31] The next step of elongation is transpeptidation, in which peptide-bond

formation occurs. In the peptidyl-transferase reaction, the α-amino group of the aa-tRNA in the A site attacks the carbonyl carbon of the ester linkage of the peptidyl tRNA in the P site.[32-34] As a result of the peptide bond formation, the nascent polypeptide chain on the P-site tRNA is transferred to the A-site tRNA. After peptidyl transfer, the P site contains deacylated tRNA and the A site contains peptidyl-tRNA. In order to empty the A site for the next incoming aa-tRNA ternary complex, the P-site tRNA and A-site peptidyl tRNA have to move to the E site and P site, respectively. This process is known as translocation, which is facilitated by EF-G.[35] During each translocation step, tRNAs shift from the P to E site and A to P site. During this process, the ribosome undergoes a ratchet-like intersubunit rotation, in which the 30S subunit rotates counter-clockwise with respect to the 50S subunit.[35-38]

During translocation, tRNAs go from classical A/A and P/P configurations to A/P and P/E hybrid configurations. The E site traps the hybrid P/E tRNA efficiently and facilitates the translocation.[39] GTP hydrolysis occurs on EF-G, which triggers back-ratcheting of the 30S subunit into the unrotated ribosome conformation.[39,40] Upon complete back-ratcheting of the 30S subunit, the entire ribosome moves by three nucleotides (one codon) on the mRNA. The ribosome is now translocated to the next codon on the mRNA and ready for the next incoming aa-tRNA into the open A site.

1.3.3 Translation termination

The final step of protein translation is termination. The addition of amino acids to the polypeptide chain continues until a stop codon reaches the A site. When the ribosome encounters a stop-codon sequence —UAA UAG, or UGA— on the mRNA, termination occurs. Stop codons are recognized by a protein called release factor (RF) instead of a tRNA. RF-1 decodes UAA and UAG stop codons whereas RF-2 decodes UAA and UGA stop codons (**Figure 1.5**). RF-3 forms

a complex with GTP, then binds to the ribosome and induces hydrolysis of the nascent polypeptide chain from the P-site tRNA. The cleaved polypeptide chain then exits the ribosome through the exit tunnel.[41,42] Ribosome recycling factor (RRF) can then bind to the A site in conjunction with EF-G/GTP complex.[43] The hydrolysis of EF-G allows RRF to be translocated to the P site, in a similar fashion described in the elongation step, which shifts the remaining tRNAs out and into the E site. This process ultimately releases the RRF and hydrolyzed EF-G/GTP complex with mRNA, leaving behind an inactive 70S ribosome.

1.4 Ribosomal RNA structure and modifications

Ribosomal RNA has a primary functional role in all stages of protein synthesis. The discovery of the catalytic activity of RNA provided support for rRNA as the basic functional element of the ribosome. Previous studies in which ribosomal proteins were removed from ribosomes followed by activity assays indicated catalytic activity of the rRNA.[44,45] Determination of the secondary structures of the 5S, 16S, and 23S rRNAs expanded their possible functional roles.[22,46,47] Most importantly, solving the crystal structures of ribosomes vastly increased our understanding of the protein synthesis machinery and verified the role of rRNA as the catalytic domain for translation.[14,48]

Ribosomal RNA is post-transcriptionally modified in several sites by a variety of ribosome-related enzymes. The sites and the number of rRNA modifications vary across phylogeny.[19,49,50] The *E. coli* ribosome contains a total of 36 of modifications, 11 in 16S rRNA and 25 in 23S rRNA.[22] The list of all nucleotide modifications present in *E. coli* 16S rRNA and responsible enzymes are shown in **Table 1.1**. The same information for 23S rRNA is given in **Table 1.2**. There are three main types of nucleotide modification in rRNA: 1) isomerization of

uridine to pseudouridine (Ψ); 2) methylation of 2' hydroxyls (Nm); and 3) alterations to bases, most of which undergo methylation at different positions (mN).[49,51]

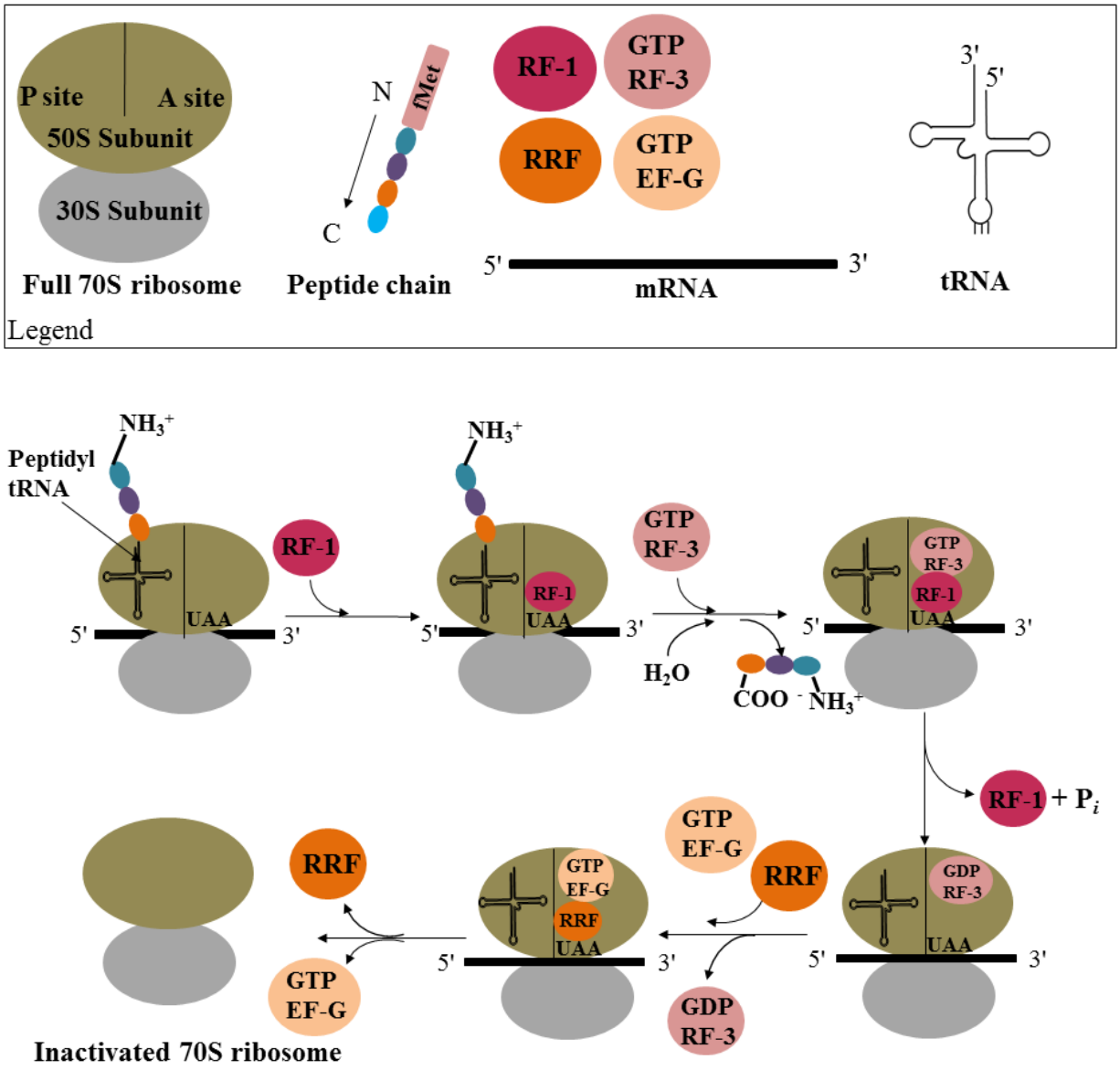

Figure 1.5 Translation termination of the bacterial ribosome. Release factor one (RF-1) or release factor two (RF-2) recognize the stop codon (*e.g.*, UAA). This stimulates the recruitment of RF-3 bound to GTP, which, upon hydrolysis, recruits EF-G bound to GTP and the ribosome recycling factor (RRF) upon its release. Upon a second hydrolysis of the GTP bound to EF-G, the mRNA, remaining tRNA, and termination factors are released, leaving an inactivated 70S ribosome.

According to the secondary structural maps (**Figures 1.6 & 1.7**) and high-resolution x-ray crystal structures of the ribosome, modified nucleotides are highly localized in the most functionally important regions of the ribosome.[19,50] In particular, regions such as the A site, PTC, polypeptide exit channel, and intersubunit bridge region are highly modified. Their occurrence in functionally important regions of the ribosome suggests possible roles of modified nucleotides in protein translation.[19,50]

Table 1.1 Nucleotide modifications in *E. coli* 16S rRNA

Modification	Position	Enzyme	Enzyme class	References
m^2G	966	RsmD	MT	52-55
m^7G	527	RsmG	MT	56-58
m^2G	1207	RsmC	MT	53,54,59,60
m^2G	1516	RsmJ	MT	53, 61,62
m^5C	967	RsmB	MT	63-65
m^5C	1407	RsmF	MT	66,67
m^4Cm	1402	RsmH	MT	66-73
$m^2{}_6A$	1518	RsmA	MT	39
$m^2{}_6A$	1519	RsmA	MT	74-76
m^3U	1498	RsmE	MT	74,75
Ψ	516	RsmA	PS	76-78

MT: methyltransferase; PS: pseudouridine synthase

The importance of post-transcriptional modification for protein synthesis was first revealed by carrying out *in vitro* protein translation with *E. coli* ribosomes reconstituted with unmodified 16S and 23S rRNA.[79] In these experiments, the greater ability of fully modified ribosomes to carryout protein synthesis compared with unmodified ribosome was revealed.

Therefore, it is suggested that rRNA modifications play an important role in structure and function of the ribosome.

Table 1.2 Nucleotide modifications in *E. coli* 23S rRNA

Base	Modification	Position	Enzyme	Enzyme Class	References
G	m^1G	745	RlmA(l)	MT	80-82
G	m^2G	1835	RlmG	MT	53,83
G	m^7G	2069	RlmKL	MT	83-87
G	Gm	2251	Mrm1	MT	87
C	m^5C	1968	Rlml	MT	88-90
C	Cm	2498	RlmM	MT	67,91
C	s^2C	2501	-	-	51
A	m^6A	1618	RlmF	MT	92
A	m^6A	2030	RlmJ	MT	93-99
A	m^2A	2503	Cfr	MT	93-99
U	Ψ	746	RluA	PS	76,100-104
U	m^5U	747	RlmCD	MT	105,106
U	Ψ	955	RluC	PS	106,107
U	Ψ	1911	RluD	PS	108
U	Ψ	1915	RluD	PS	109-113
U	$m^3Ψ$	1915	RluH	PS	88,109-114
U	Ψ	1917	RluD	PS	108,115-117
U	m^5U	1939	RlmD	MT	111,118-121
U	D	2446	-	MT	-
U	Ψ	2457	RluE	PS	122
U	Ψ	2504	RluC	PS	106-108
U	Um	2552	RlmE	MT	123-126
U	Ψ	2580	RluC	PS	127
U	Ψ	2604	RluB	PS	121,128-130
U	Ψ	2605	RluF	PS	121,131

MT: methyl transferase; PS: pseudouridine synthase

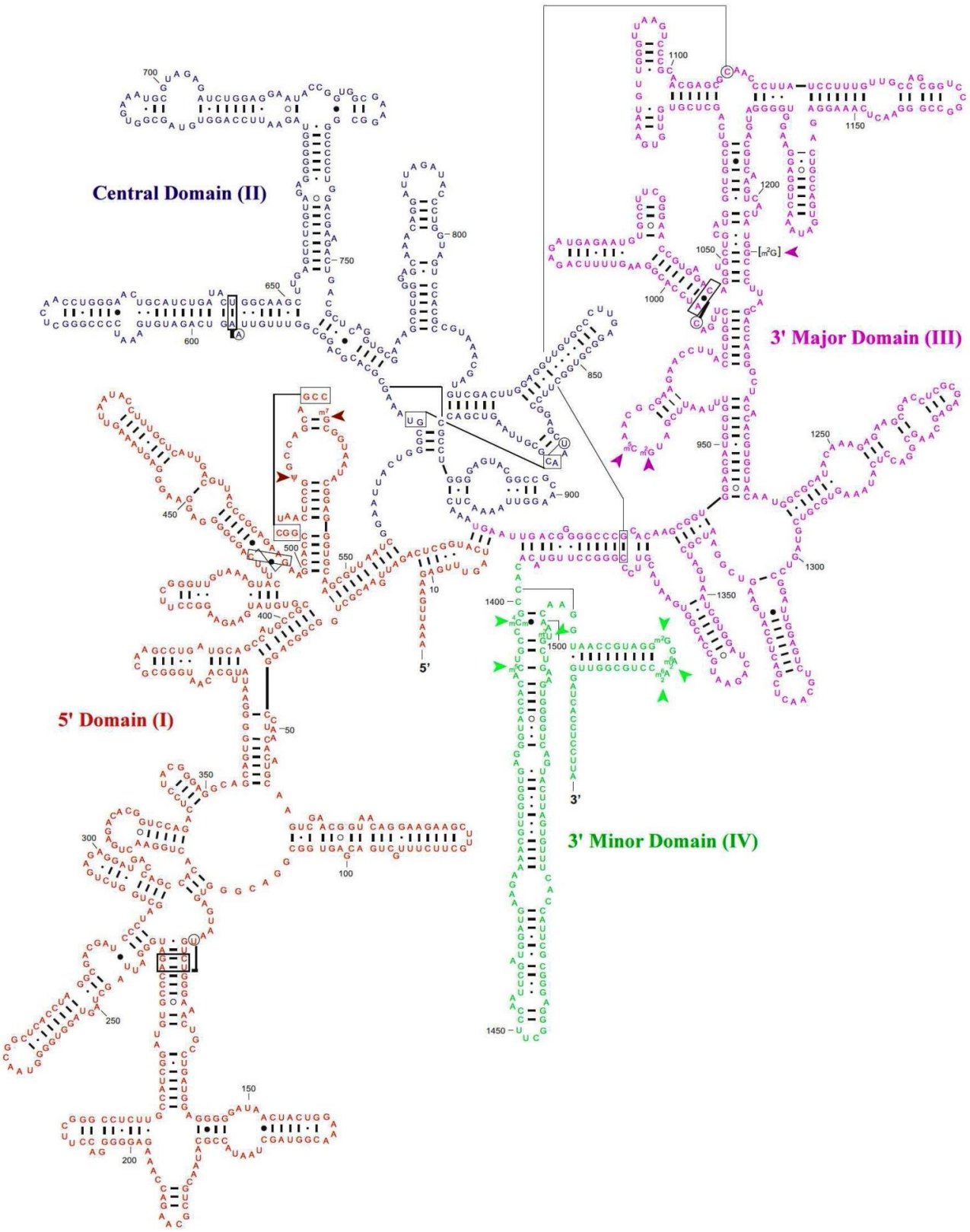

Figure 1.6 Secondary structure of *E. coli* 16S rRNA. [14] Modified RNA nucleotides are labeled with arrows.

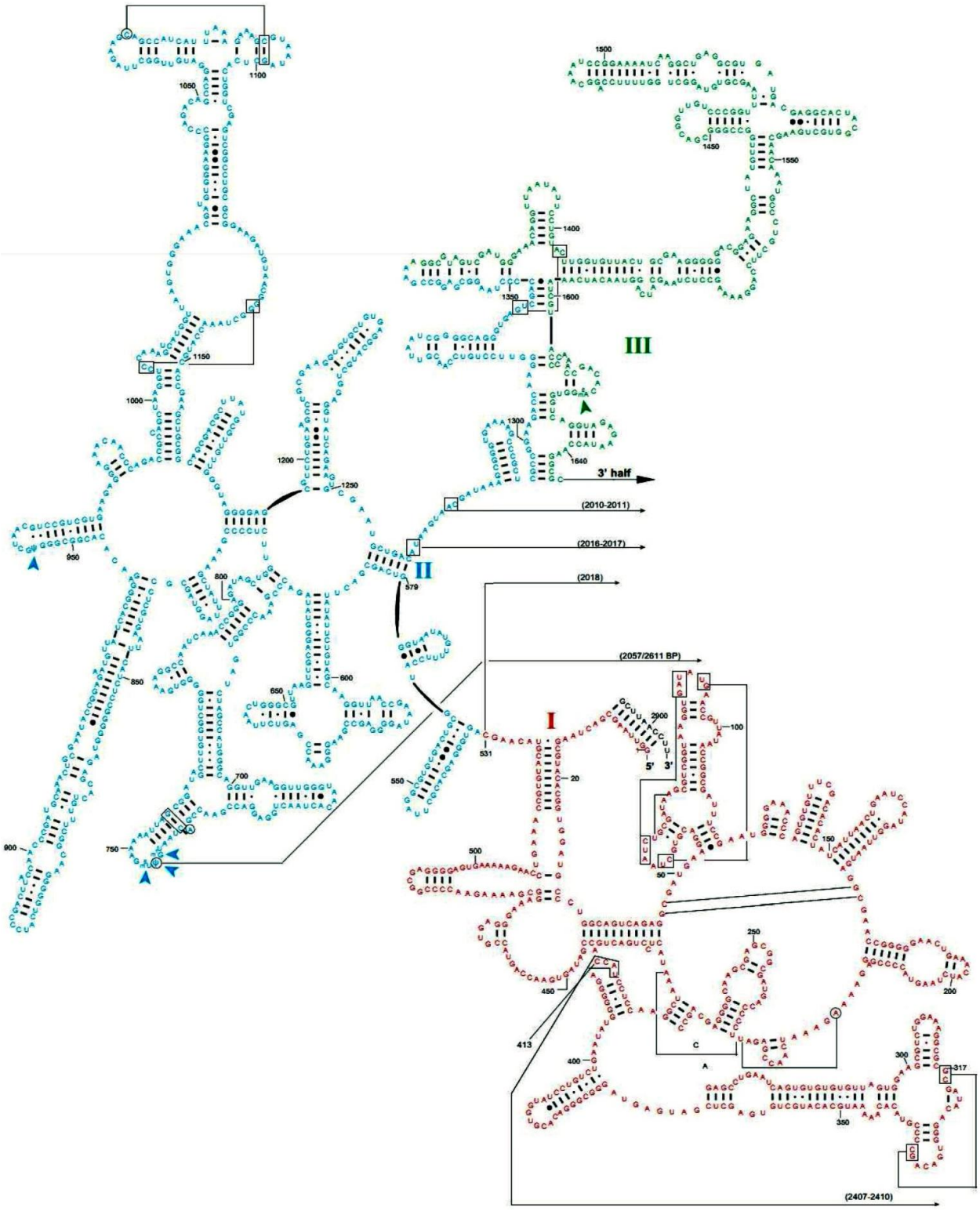

Figure 1.7 Secondary structure of *E. coli* 23S rRNA (shown in two pages).[14] Modified RNA nucleotides are labeled with arrows.

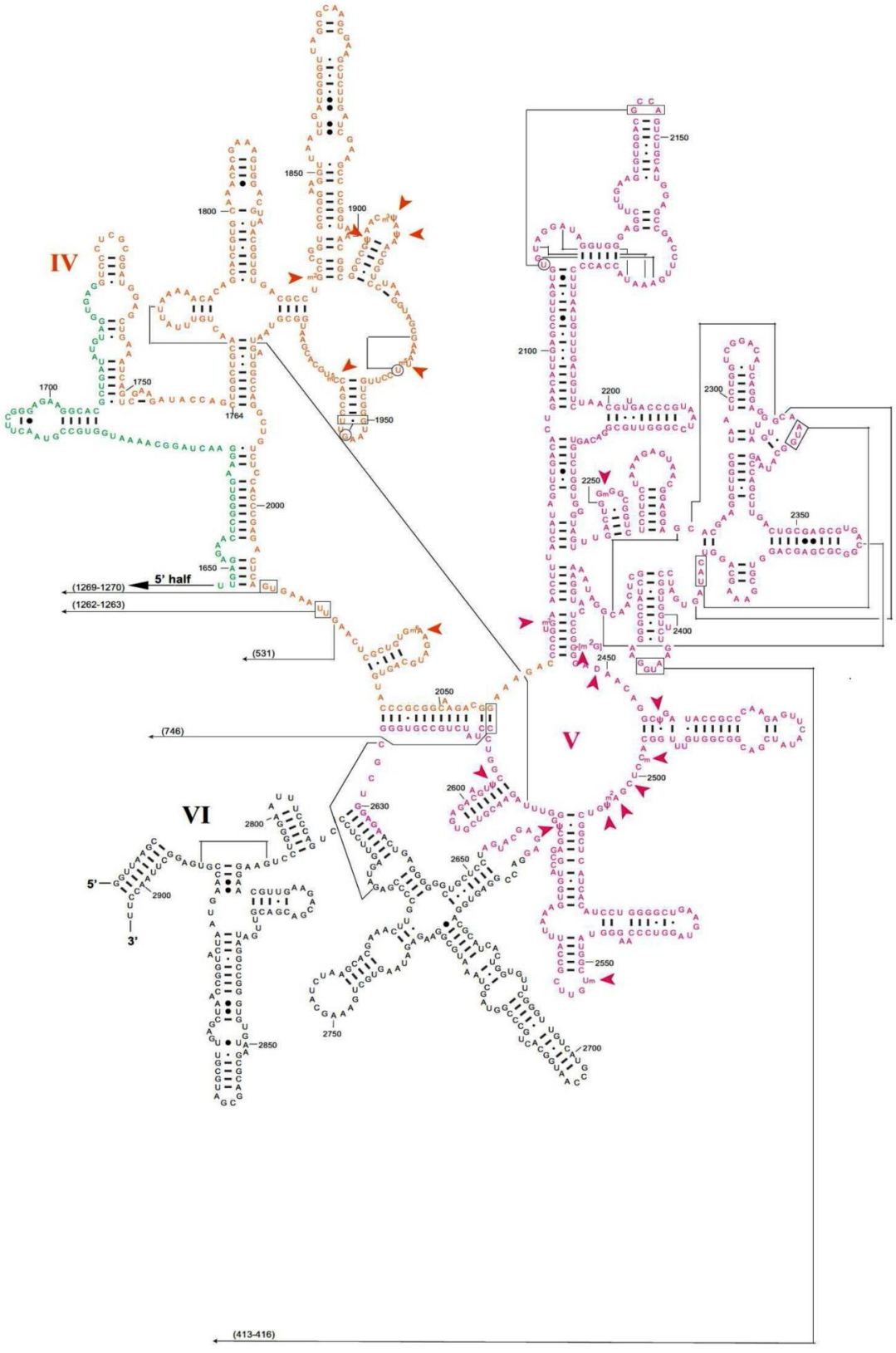

Figure 1.7 continued

Half of the currently available antibiotics target the functionally important regions of the bacterial ribosome.[132] Therefore, it would not be surprising if those rRNA modifications played an important role in mediating ribosome-antibiotic interactions. Modifications such as methylation in bacterial rRNA are known to confer resistance to antibiotics.[49] Therefore, post-transcriptional modifications appear to play an important role in modulating structure and function of rRNA.

1.5 The bacterial ribosome as a dug target

The key roles in protein biosynthesis, structural complexity, easy accessibility, and high abundance in the cell make the ribosome an ideal target for the development of antibacterial drugs.[132,133] Therefore, it is not surprising that half of the currently available antibiotics target the different functional centers within the bacterial ribosome. Based on the binding site in the ribosome, antibiotics can be classified into three major types: 1) the decoding-region antibiotics; 2) PTC and exit tunnel antibiotics; and 3) other types, including those targeting the translation-related protein factors.

1.5.1 Decoding-region targeting antibiotics

The decoding region of the ribosome involves mRNA translation and provides fidelity of codon-anticodon interactions during protein translation.[28,134] It is part of the bacterial A site and resides in the helix 44 (h44) region of the 30S ribosomal subunit. Aminoglycosides with a 2-deoxystreptamine ring (**Figure 1.8**) are known to inhibit protein translation by binding to the 30S ribosomal subunit.[135,136] Neomycin, paraomomycin, kanamycin, and gentamicin are some examples in this class. The initially identified primary binding site of this family of antibiotics is the decoding region, namely the intersubunit bridge B2a.[137-139] Upon binding to h44, aminoglycosides stabilize the A site in an extra-helical conformation. This conformational change shifts the position and dynamics of two universally conserved residues, A1492 and

A1493, which are responsible for recognition of the mRNA codon-aminoacyl-tRNA complex.[138,140,141] This stabilized conformational state leads to incorporation of incorrect aa-tRNAs, and decreased translation fidelity.[134,142] However, decreased translation fidelity alone has little effect on cell growth. Literature reports revealed that bacteria strains harbouring error-prone ribosomes are still viable.[143,144]Also, evidence of specific aminoglycosides inhibiting protein synthesis without exhibiting miscoding suggests that miscoding is not the only mechanism of action of aminoglycosides.[145] Furthermore, these combined observations suggest that aminoglycosides may interact with more than one functional site in the bacterial ribosome.

Interestingly, crystal structures have shown that neomycin, paramomycin, and gentamincin are able to interact with the major groove of helix 69 (H69) of 23S rRNA as well. [138,146,147] The interaction with H69 provides a possible mechanism for how aminoglycosides inhibit the recycling and translocation steps of protein synthesis.[33, 46] However, the bactericidal nature of 2-deoxystreptamine aminoglycoside antibiotics is still poorly understood despite decades of clinical use and biochemical studies. The emergence of strains with antibacterial resistance as well as impaired hearing and kidney functions at high doses of aminoglycosides make them less effective in clinical applications. Viomycin and capreomycin **(Figure 1.8)** are cyclic peptides belong to tuberactinomycin family antibiotics.[148] Recent studies have shown that these cyclic peptides target the bacterial ribosome. According to crystal structures, both cyclic peptides bind to the same site of the ribosome, which lies at the interface between h44 of the 30S and helix 69 (H69) of the 50S subunits. These peptide antibiotics are known to inhibit the translocation step of protein synthesis by stabilizing the tRNA in the A site in the pre-translocation state.[147,149]

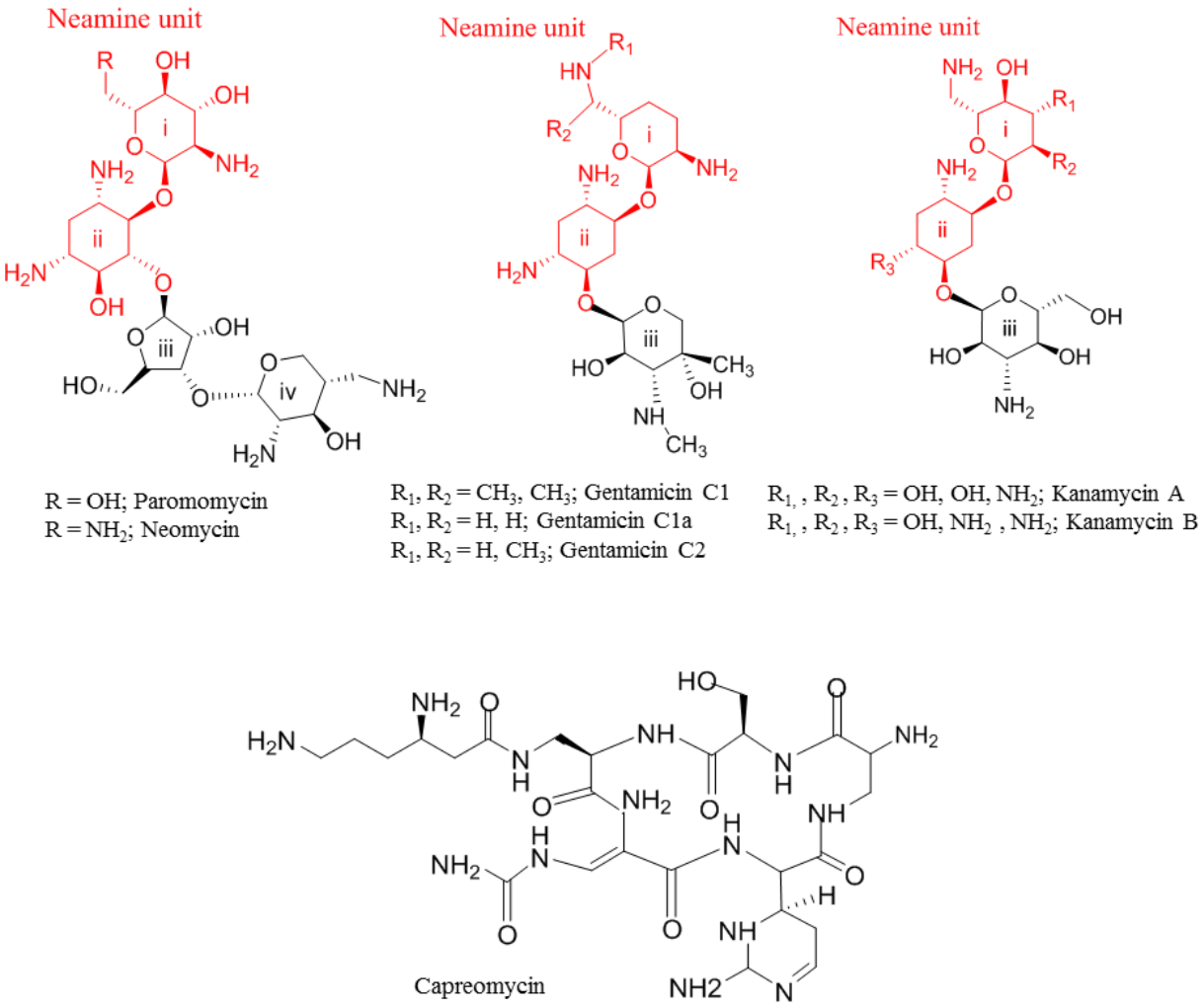

Figure 1.8 Aminoglycoside antibiotics. Chemical structures of the decoding-region targeting antibiotics are shown with the common 2-deoxystreptamine motif highlighted in red. The cyclic peptide capreomycin is shown for comparison.

1.5.2 Peptidyl-transferase center and exit-tunnel targeting antibiotics

The ribosomal PTC resides in the 50S subunit and catalyzes the two principle chemical reactions of protein translation, peptide bond formation and peptide release.[24] As the key functional domain of the ribosome, it is not surprising that different classes of antibiotics target this site on the ribosome. These antibiotics include clinically important antibiotics such as

macrolides, lincosamides, streptogramins, chloramphenicol, and the oxazolidinones.[17,132] Among these, macrolides are the clinically most important class of antibiotics. Macrolides are naturally occurring polyketide compounds that consist of a large macrocyclic lactone ring to which one or more deoxy sugars are attached.[150] Crystal structures of various macrolides bound to the 50S ribosomal subunit were solved.[150] According to the crystal structures, macrolides bind within the peptide exit tunnel, adjacent to the PTC. This binding sterically blocks the peptide exit channel, which in turn inhibits entrance of the nascent polypeptide chain and causes premature dissociation of the peptidyl-tRNA from the ribosome.[150,151] The binding sites of lincosamides and streptogramins overlap with macrolides and their mechanisms of action are proposed to be the same.[17,132] Even though the binding site overlaps, the mechanism of action of the oxazolidinones is different from all existing PTC-targeting antibiotics.[152,153] Recently, it was shown that oxazolidinones inhibit fMet-tRNA$_f^{Met}$ binding to the P site and inhibit the formation of initiation complex.[152,153] On the bacterial ribosome, chloramphenicol binds at the PTC in a position that overlaps with the amino-acyl moiety of the A-site tRNA and inhibits peptide-bond formation by blocking aa-tRNA binding this site.[154]

1.5.3 Other antibiotics

On the bacterial ribosome most of the antibiotic binding sites are clustered at or near the PTC region and the decoding center.[132] However, there are a few exceptions. Evernimicin (**Figure 1.9**), an oligosachcharide antibiotic isolated from *Micromonospora carbonaceae*, exclusively binds to the 50S subunit.[155] Although crystal structures of evernimicin bound to the ribosome are not available, chemical footprinting and mutagenic studies showed that the drug binds to the helix 89 and helix 92 regions of 23S rRNA[155]. Furthermore, evernimicin forms additional contacts with the ribosomal protein L16 as suggested by mutation studies.[156,157]

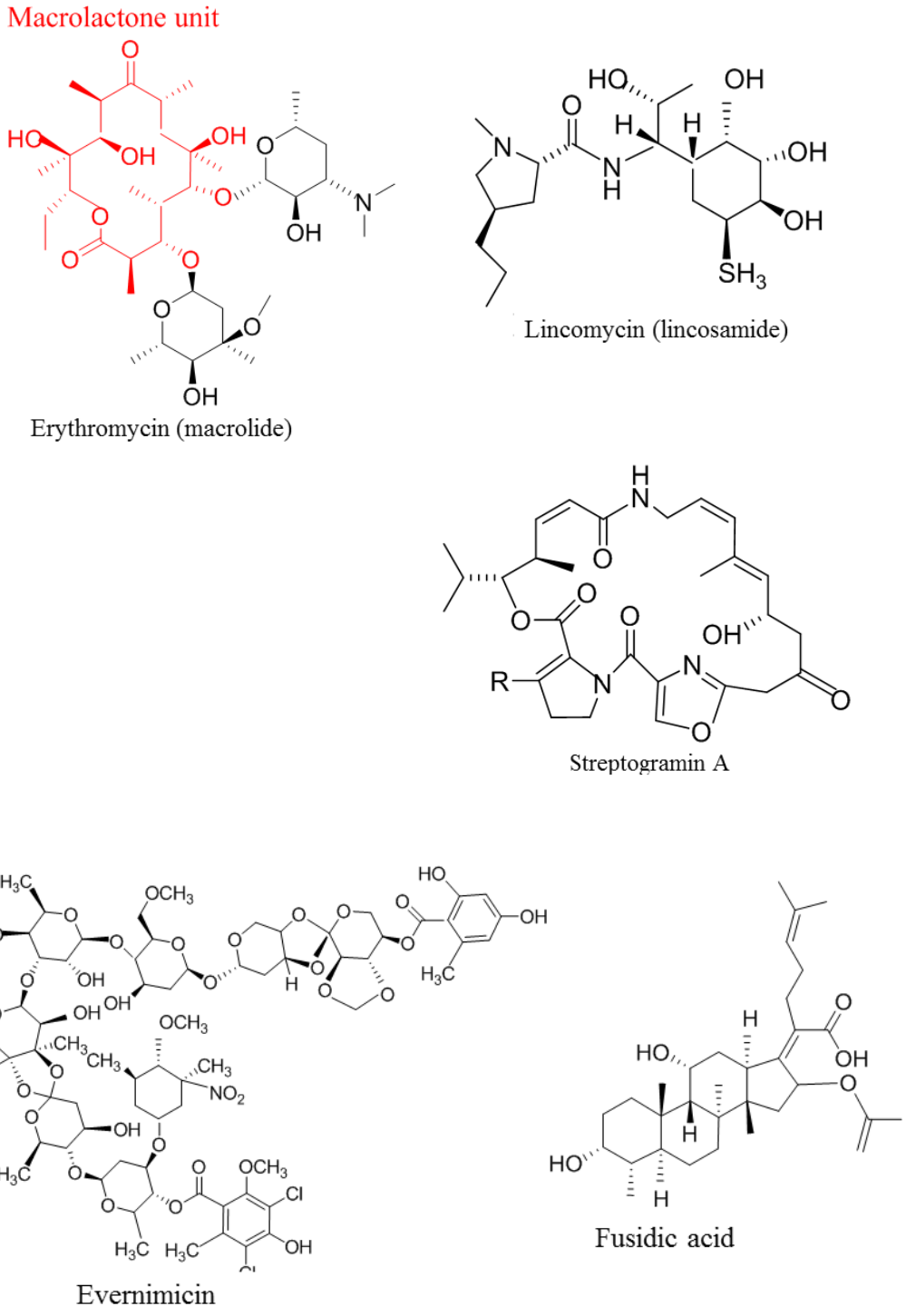

Figure 1.9 Peptidyl-transferase center and exit-tunnel targeting antibiotics. Chemical structures of the PTC and exit-tunnel targeting and other type of antibiotics are shown.

Interestingly, the binding site of evernimicin on the 50S subunit does not overlap with the binding site of other antibiotics, which may be the reason why cross-resistance is not prevalent with these clinical isolates. Thiostrepton is an antibiotic from the thiopeptide family. Biochemical and NMR studies showed that thiostrepton binds to 23S rRNA at the GTPase-associated domain of the 50S subunit.[158] The drug interacts with the ribosomal protein L11 and residues A1067 and A1095 of 23S rRNA.[158,159] Upon binding, thiostrepton interferes with EF-G binding to the ribosome and inhibits the ribosome translocation.[158,159] Fusidic acid is another antibiotic that is known to target EF-G. Upon binding to the protein, fusidic acid prevents its release from the ribosome after GTP hydrolysis.[159] As a result, the ribosome is trapped as the EF-G/GDP ribosome complex, which inhibits the next step of protein translation, namely the aa-tRNA selection step.[160]

1.6 The emergence of antibiotic resistance

Antibiotics have been used for the past 70 years to treat infectious diseases.[161,162] Although antibiotics were thought to be the perfect solution to bacterial infections, the emergence of resistance has become a global health issue.[132,163] The ability of bacteria to oppose the inhibitory effects of these drugs is known as antibiotic resistance. Antibiotic resistance is accelerated by overuse of antibiotics as well as poor infection prevention and control.[164] In 2013, the United States Center of Disease Control and Prevention reported that each year in the United States at least two million people become infected with bacteria and 23,000 people die as a result of these infections.[165,166] The World Health Organization (WHO) has named antibiotic resistance as one of the three most important public health threats of the 21st century.[163,165] Therefore, WHO has been leading multiple initiatives to address the problem of antibiotic resistance.[165,166] A global action plan on antibiotic resistance was endorsed at the World Health Assemble in May

2015.[163] The global action plan on antimicrobial resistance has five strategic objectives: 1) improve awareness and understanding of antimicrobial resistance; 2) strengthen surveillance and research; 3) reduce the incidence of infection; 4) optimize the use of antimicrobial medicines; and 5) ensure sustainable investment in countering antimicrobial resistance.[167,168] Antibiotic resistance is a global health problem requiring efforts from all nations and all levels of society to prevent and control.

1.7 Resistance mechanisms in bacteria

Understanding the underlying mechanisms of antibiotic resistance is essential for novel therapeutic development. There are three fundamental antibiotic resistance mechanisms in bacteria.[169] Modifications of the antibiotic molecules are some of the most effective resistance mechanisms. This can be a chemical alteration or destruction of the antibiotic molecule through the production and action of specific enzymes.[161] There are many types of modifying enzymes that catalyze acetylation (aminoglycosides, chloramphenicol, streptogramins), phosphorylation (aminoglycosides, chloramphenicol), and adenylation (aminoglycosides, lincosamides) of the antibiotic molecule.[161] The best examples are the aminoglycoside modifying enzymes that covalently modify the amino or hydroxyl groups of the aminoglycoside molecule.[161] Aminoglycoside modifying enzymes have become the predominant mechanism of aminoglycoside resistance worldwide.[170,171] The best example of deactivation of an antibiotic molecule is the mechanism shown by penicillin-resistance bacteria.[172] Penicillin is a β-lactam antibiotic that targets the bacterial cell wall. Production of the β-lactamase enzyme deactivates the antibiotic. The enzyme destroys the amide bond of the β-lactam ring, which is responsible for the antibiotic activity, therefore rendering the antibiotic ineffective.[173]

The next antibiotic resistance mechanism involves reduced antibiotic penetration or export of the drugs using efflux systems.[174,175] Most of the clinically used antibiotics have intracellular drug targets. Therefore, the drug must penetrate the outer membrane and accumulate inside bacterial cells in order to exert its antimicrobial activity. In gram-negative bacteria, the outer membrane acts as the first line of defense against the penetration of hydrophilic antibiotic molecules.[176,177] For example, vancomycin, a glycopeptide antibiotic, is not active against gram-negative bacteria due to its lack of penetration through the outer membrane.[178] Efflux-mediated antibiotic resistance is another common mechanism found in both gram-negative and gram-positive bacteria.[179,180] Bacterial efflux pumps are proteins that are localized in the plasma membrane. [180,181] The function of efflux pumps is to recognize and extrude toxic compounds out of the bacterial cell. Tetracycline resistance is one of the best examples of efflux-mediated resistance in gam-negative bacteria.[180,181] Gram-positive bacteria show efflux-mediated resistance to macrolides, lincosamides, and strepogramins.[180,182]

Target-site modification is the most common antibiotic resistance mechanism found in pathogenic bacteria, affecting almost all families of antibiotics.[132] Target alterations may consist of enzymatic modifications of the binding site (addition of methyl group) or point mutations in the genes encoding the target site. Macrolide resistance, which is caused by rRNA methylation, is a well-characterized example of target-site modification.[183] Methyltransferase Erm catalyzes methylation of the adenine residue at position A2058 of 23S rRNA.[184] As a result of this methyl modification, binding of the antibiotic molecule to its target is impaired. Expression of the erm genes confers resistance not only to macrolides, but also to lincosamides and streptogram B, since these antibiotics have overlapping binding sites on the 23S rRNA.[183,184] In the case of aminoglycoside antibiotics, methylation of the N7 position of G1405 or N1 position of A1408

confers resistance to the geneticin or neamine, respectively.[185,186] Besides enzymatic modifications, a site-specific mutation of the target site is enough to confer resistance to antibiotics. For example, A1408G mutation in 16S rRNA confers resistance to aminoglycosides such as neomycin.[187] Studies with model rRNA showed that the A1408G mutation reduces binding affinity of the antibiotic molecule to the A site, which causes antibiotic resistance.[188]

As mentioned earlier, half of the currently available antibiotics target the bacterial ribosome.[132] However, bacteria have developed resistance to most of these drugs.[132,189] Therefore, development of unique antibiotics targeting functionally important regions of rRNA is one promising way to overcome this issue. Most currently used antibiotics target key functional domains of the ribosome, such as the PTC and decoding center. Discovery of new drugs targeting these key functional domains is difficult, since a variety of resistance mechanisms involving these locations may already exist. Therefore, identification of novel druggable targets in the bacterial ribosome and discovery of compounds that selectively target those regions is a possible approach to combat antibiotic resistance.[190-193]

1.8 Helix 69 region of 23S rRNA as a novel drug target

Structural information obtained from x-ray crystallography has indicated that there are many key regions of ribosomal RNA (rRNA) that could serve as antibacterial drug targets.[132] The specific conserved region of the ribosome under investigation in this study is helix 69 (H69).[22] Helix 69 is a 19-nucleotide hairpin-loop structure that is located in domain IV of the 23S rRNA in the 50S subunit.[22,194] It interacts with helix 44 (h44) of the 16S rRNA to form intersubunit bridge B2a **(Figure 10)**, which plays significant roles in various ribosomal functions, including subunit association, translocation, peptide release, and ribosome recycling.[50,195] The nucleotide sequence of H69 contains three post-transcriptionally modified

nucleotides, or pseudouridines (Ψ), at positions 1911, 1915, and 1917 **(Figures 1.11** and **Figure 1.12)**.[196]

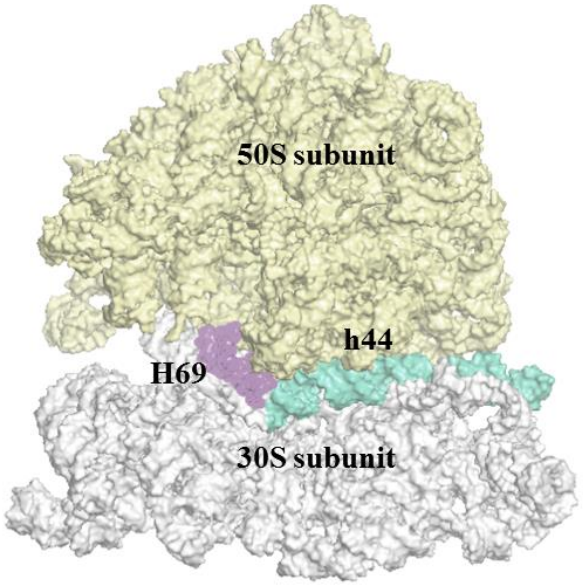

Figure 1.10 The location of H69 in the 70S full ribosome. H69 (in purple) is located at the junction between the 30S and 50S ribosomal subunits. It makes a direct interaction with helix 44 (h44), known as the aminoacyl tRNA site (A site) (in cyan), of the 30S subunit. Its proximity to essential translational machinery and at the interface of the two subunits makes H69 a potentially important antibacterial drug target. (PDB ID: 2AW4).[19,50]

The nucleotide sequence of H69 is highly conserved in bacteria, archaea, and eukaryotes.[22] However, there are some noticeable differences between the H69 sequences of bacteria (*E. coli*) and eukaryotes (*H. sapiens*) **(Figure 1.11).** The 1915 position of H69 in *E. coli* is a methylated Ψ, whereas in human it is unmethylated.[196,197] The nucleotide at the 3' end of the loop is an adenosine (A) in *E. coli* and guanosine (G) in *H. sapiens*.[22,198] Thirdly, the *H. sapiens* H69 has two extra Ψs in the stem region of the hairpin.[194] Considering the variety of functions of this motif in protein biosynthesis as well as the sequence conservation and key differences between bacterial and human H69, it is an attractive antibacterial drug target.

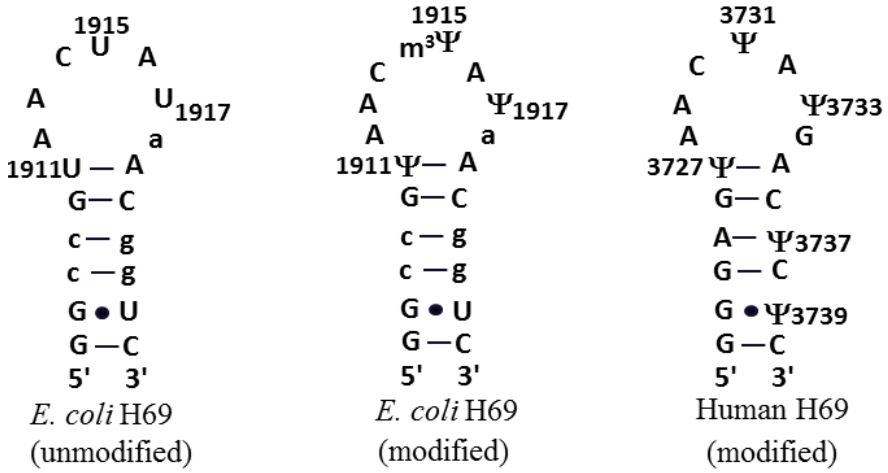

Figure 1.11 The secondary structures and sequences of modified and unmodified H69. The secondary structures of unmodified (UUU) and modified *E. coli* (Ψm^{3}ΨΨ) and modified human H69 show sequence differences (Ψ, pseudouridine; m^{3}Ψ, 3-methylpseudouridine). Nucleotides in upper case letters in the *E. coli* H69 sequence have >95% conservation and those in lower case have 88–95% conservation across phylogeny.[22]

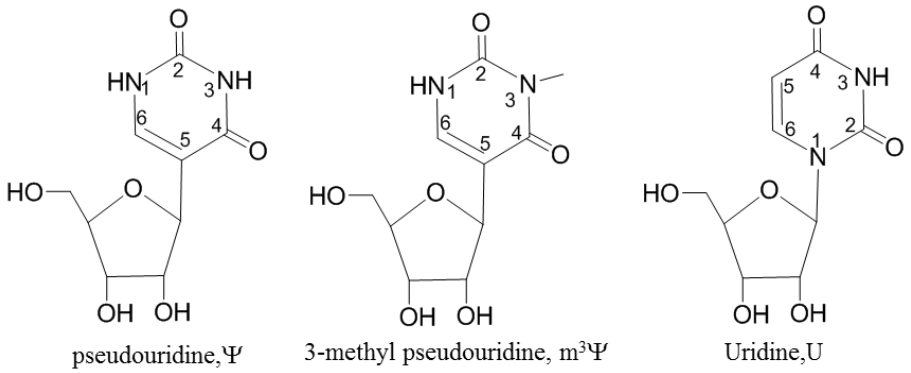

Figure 1.12 Chemical structures of pseudouridine, 3-methylpseudouridine, and uridine. Pseudouridine (Ψ, left) is a post-transcriptional modification of uridine (U, right). The difference between these two structures is a 120° rotation of the base in pseudouridine, forming a C–C glycosidic bond versus the canonical C–N glycosidic bond shown in uridine. Three-methylpseudouridine (m^{3}Ψ, middle) differs from Ψ only by a methylation on the 3-position of the base.

1.9 Antimicrobial peptide research

In order to provide effective treatments for future bacterial infections, innovative approaches to antimicrobial drug development are necessary, preferably with novel modes of

action or discovery of new drug classes. Recently, antimicrobial peptides (AMPs) have become promising compounds for drug development.[199-201] AMPs are essential components of the innate immune system.[199,202] Being "nature's antibiotics", AMPs form the first line of host defense against pathogenic infections.[202-204] During the past few decades, AMP research has grown rapidly in response to the demand for novel antibacterial agents to treat multi-drug resistance pathogens.[199,204] To date, the AMP database lists 2848 peptides with antimicrobial activity, which have been synthesized or discovered in natural sources.[205] This list includes AMPS from six kingdoms, three hundred and one peptides from bacteria (bacteriocins), four from archaea, eight from protista, thirteen from fungi, 343 from plants, and 2179 from animals.[205-207] AMPs are usually made up of between 12 to 50 amino acid residues and differ widely in their sequence and structure.[201,204] Most of the AMPs are polycationic and about 50% of their amino acids are hydrophobic.[200,207] The amphipathic nature enables AMPs to preferentially target the anionic bacterial membranes. Therefore, in contrast to small molecule antibiotics, most of the AMPs target the bacterial cell membrane and kill bacteria by lytic mechanisms.[203,208,209]

The bacterial cell membrane is an evolutionary conserved component of bacteria and rarely undergoes mutations. Therefore, AMPs are less likely to develop bacterial resistance. Interestingly, most of the AMPs are bactericidal and kill bacteria more rapidly than conventional small molecule antibiotics.[199] Compared to the bacterial cell membrane, the human cell membrane is dominated by phospholipids and cholesterols. The differences in membrane composition are the major reason for the selectivity of AMPs. However, the lytic activity of AMPs is a major concern when it comes to AMP-based therapeutic development. Higher peptide concentrations might cause toxic effects on mammalian cell membranes, which limit the clinical potential of the drug.[162,210] Therefore, during the past few decades, there have been efforts to

discover AMPs that kill bacteria by targeting intracellular processes rather than lytic mechanisms. Recent studies suggest that a number of AMPs are able to act on intracellular drug targets as their major mechanism of action.[211,212] For example, many cationic AMPs have been shown to interact with nucleic acids. Buforin II and indolicidin are well-characterized cationic AMPs that are known to interact with DNA.[213,214] Most recently, it was shown that proline-rich AMPs (PrAMPs) inhibit protein translation by strongly binding to the 70S ribosome.[215,216] The identification of intracellular targets of antimicrobial peptides provides more therapeutic options.

1.9.1 Peptides as ribosome-targeting ligands

The development of peptide ligands that specifically bind to higher-order structures of ribosomal RNA is one promising way to address the problem of antibiotic resistance. Since peptides are the natural building blocks of proteins, they do not identify as foreign invaders by the host immune system.[199,212,217] Therefore, compared to conventional antibiotics, the development of drug resistance would be harder with peptide antibiotics. In addition, peptides can be easily modified by incorporating additional functional groups or directly modifying the peptide backbone. Such modifications would enhance the structural stability, cell permeability, as well as affinity and selectivity of peptide antibiotics.

Viomycin and capreomycin are cyclic peptides that belong to the tuberactinomicin family of antibiotics **(Figure 1.8)**. These two cyclic peptides are among the most effective antibiotics against multi-drug resistance tuberculosis.[149] Recently, it was found that both of these cyclic peptides bind to the highly conserved intersubunit bridge B2a region of the ribosome and interact with H69 of the 50S subunit and h44 of the 30S subunit simultaneously.[148] These antibiotics are known to inhibit ribosome translocation by stabilizing the A-site-tRNA interaction.[149] Proline-rich antimicrobial peptides (PrAMPs) have attracted considerable attention in recent years as

promising candidates to combat multidrug resistance gram-negative pathogens.[210,215,218] Interestingly, recent studies in several laboratories showed that two insect-derived PrAMPs, oncocin and apidaecin, inhibit protein translation both *in vitro* and *in vivo* by strongly binding to the 70S ribosome.[215,216] Shortly afterwards, it was shown that a mammalian-derived PrAMP, bactenecin Bac7, also targets the 70S ribosome.[219,220] In 2015, the crystal structure of oncocin-bound *Thermus thermophilus* ribosome was solved.[221,222] According to the crystal structure, oncocin binds to the 50S ribosomal subunit where it blocks the PTC and destabilizes the initiation complex.[221-223] Further structural and biochemical studies indicate that PrAMPs inhibit the transition from the initiation to elongation phase of protein translation.[223] However, apidaecin-type peptides show a different translational inhibition mechanism by blocking assembly of the 50S subunit of the ribosome.[224,225] Several research groups and companies are optimizing PrAMPs as promising compounds to treat systemic infections caused by gram-negative bacteria.[226] More details about PrAMPs will be discussed in Chapter 2.

The binding sites of most of the newly discovered antimicrobial peptides overlap with the binding sites of conventional antibiotics.[199,210] For example, the binding site of PrAMPs on the 50S subunit overlaps with that of many clinically important antibiotics such as the macrolides, chloramphenicols, lincosamides, and pleuromutilins.[222,223] Therefore, the resistance mutations that arise against currently used antibiotics will also confer cross-resistance to these newly identified antimicrobial peptides. As such, the development of peptide ligands targeting novel druggable sites of the bacterial ribosome is a different strategy to overcome the problem of antibiotic resistance. Recent studies in several laboratories have identified short peptides targeting new sites of the bacterial ribosome.[190,216,221-223,227] In these studies, phage display was used to identify unique peptides against rRNA regions of interest. Short peptides with moderate

affinity (μM) and selectivity towards relatively unexplored regions of the bacterial ribosome such as helix 31 (970 loop) and h18 pseudoknot of 16S rRNA, or helix 69 of 23S rRNA were identified from random peptide libraries.[190-193] Some of these selected peptides showed inhibition of bacterial protein translation in cell-free translation systems and displayed desirable features for development as lead compounds for novel antimicrobials.[190,192,193] In fact, these selected peptides can be used as tools to validate novel antibiotic binding sites in the ribosome and to develop drug leads using peptidomimetic approaches.

1.9.2 The challenges and future of the antibiotic peptide research

AMPs display remarkable structural and functional diversity and rapidly attracted attention as novel antibiotic candidates. The broad spectrum of activity, low propensity to develop bacterial resistance, higher target specificity, and strong bactericidal activity make AMPs promising drug candidates. However, there are still some limitations in antibiotic peptide research that need to be addressed before AMPs can be applied clinically.

The poor correlation between *in vitro* antimicrobial activity and *in vivo* efficacy is one of the major obstacles that has limited the progression of AMP candidates towards clinical development.[162,228, 229] Most commonly, the identification of therapeutic peptides starts with *in vitro* screening of peptide libraries. This can be done with a random peptide library or peptide library derived from a known AMP.[191,215] For example, with the phage display technique, random phage-displayed peptide libraries are incubated with a target of interest to select for those specifically bind the target.[230] Typically, the target is immobilized on a solid support before addition of the phage library. However, in these *in vitro* screening techniques, the most crucial peptide-target interaction step occurs in a simulated environment, which is very different than the actual cellular environment.[228,229] This process also requires identification and synthesis or

isolation of the target prior to the experiment, as well as the assumption that the target is in its bioactive conformation under these *in vitro* conditions. Another important concern is that targets such as DNA, RNA, or proteins have numerous conformations *in vivo* that are influenced by their environment. Peptides are also highly sensitive to their environmental conditions, which results in discrepancies between their *in vitro* and *in vivo* activity. The development of *in vivo* peptide libraries would be an alternative approach to overcome the limitations of *in vitro* peptide library screens.[231-234]

Solid-phase peptide synthesis (SPPS) is the most commonly used method for chemical synthesis of therapeutic peptides. However, the relatively high cost of SPPS compared to bacterial production is considered as one of the major limitations in AMP research.[200,229,235] Recent evidence suggests that the production cost of a 5000 Da molecular mass peptide exceeds the production cost of a 500 Da molecular mass small molecule by more than 10-fold.[235] Therefore, the high cost of SPPS for clinical applications is a challenge in the AMP optimization process. After identifying an AMP from a natural source or from a peptide library screen, the next critical step is to obtain optimized structural analogs. Usually the optimization process is done by minimizing the peptide length and systematically substituting each amino acid residue.[235] This process is typically expensive and time consuming due to the need to employ SPPS. As a result of the above-mentioned limitations, out of thousands of identified AMPs, only a few have actually been studied in any great detail.

1.10 Objectives associated with this thesis work

The development of short peptides that specifically bind to higher-order structures of ribosomal RNA is one promising way to address the problem of antibiotic resistance. These peptides could potentially be developed into small molecule drugs. Recent studies in several

laboratories including ours have identified heptamer peptide sequences targeting rRNA motifs.[191,192,215,216,221-223] Most of these studies were confined to *in vitro* systems, including binding studies with small model rRNAs,[191,192] *in vitro* chemical footprinting studies with isolated ribosomes,[221] or elucidation of crystal structures of peptide-bound ribosomes.[221-223] The poor correlation between *in vitro* and in *vivo* activities of these peptides is one of the major limitations in antibiotic peptide research. Therefore, in contrast to these *in vitro* methods, one of the main objectives of my dissertation work was to utilize a plasmid-based system to *in vivo* express ribosome-targeting peptides and study their direct inhibitory effects on bacteria. There are some additional applications of the plasmid-based *in vivo* expression system. For example, we can utilize this system to *in vivo* probe peptide-ribosome interactions, express peptide mutants, generate peptide libraries, or study a variety of other biologically interesting peptides (*e.g.*, anti-freeze peptides).

In my dissertation research, the main focus was on helix 69 (H69) of the 50S subunit. Helix 69 is proposed to be a potential drug target based on its pivotal role in ribosome protein synthesis at multiple stages and its unique higher-order RNA structure. Helix 69 could potentially be targeted by small molecules such as peptides or DNA/RNA aptamers to interfere with the naturally occurring intersubunit interaction. In previous studies, the phage-display method was used to identify peptides that target the H69 region.[192,236] *In vitro* binding studies have shown that these selected peptides have moderate affinity towards H69.[191] In a second approach, peptide variants with higher affinity and enhanced selectivity were identified by doing alanine and arginine scans of the parent peptide sequence derived from phage display.[191] Specificity, stoichiometries and binding affinities of these peptides to H69 were determined by using *in vitro* methods. Our working hypothesis was that the selected peptides will bind to H69

and disrupt ribosome function. However, the *in vivo* activity of these peptides was not determined. Therefore, we hoped that *in vivo* expression of peptides would allow us to study the behavior of selected peptides in the actual cellular environment.

Another important type of small molecule considered in this thesis work is the aminoglycoside, a well-known antibiotic that targets the bacterial ribosome. The initially identified primary binding site of the 2-deoxystreptamine family of antibiotics is the h44 region of the small subunit adjacent to the decoding site.[132,139] Recent x-ray crystal structures have shown that neomycin, paromomycin, and gentamicin are able to interact with the major groove of H69.[138,140,146,147] However, the bactericidal nature of 2-deoxystreptamine aminoglycoside antibiotics is still poorly understood.[140,146] Previous work in our lab revealed that Ψ modifications are important for efficient binding of aminoglycosides to H69.[237,238 239] However, the effects of Ψ modifications on the bactericidal activity of aminoglycosides have not been examined. The work presented in the fourth chapter of this thesis discusses the effects of Ψs in H69 on the bactericidal nature of 2-deoxystreptamine aminoglycoside antibiotics. The information gained from these studies provides deeper insight into the underlying mechanism of action of aminoglycosides, which is important for the development of unique antibiotics that target the bacterial ribosome at novel sites such as H69.

In contrast to *in vitro* methods, most of the work I did for my dissertation is focused on the *in vivo* activity of antibacterial drugs targeting the bacterial ribosome. In fact, the methods I developed are not confined to ribosome-targeting drugs. We can expand this work to study the *in vivo* activity of other drugs as well. In order to achieve the main goals of my dissertation work, three specific aims were developed:

Aim 1) Optimized a specific plasmid system to *in vivo* express a ribosome-targeting peptide, oncocin, in bacteria and map its rRNA binding sites

The specific plasmid system I utilized for this study was developed by Dr. Phillip Cunningham's lab in the Department of Biological Sciences at Wayne State University.[231] In the Cunningham lab, they developed a series of plasmid systems to *in vivo* express random peptide libraries to identify inhibitory peptides. I optimized one of their plasmid systems to *in vivo* express the ribosome-targeting peptide oncocin (VDKPPYLPRPRPPRRIYNR) and its variants in bacteria. The interaction of the peptide with the bacterial ribosome was studied by doing *in vivo* chemical footprinting experiments.

Aim 2) Utilized the plasmid system to *in vivo* express H69-targeting peptides

The optimized-plasmid system was utilized to *in vivo* express H69-targeting peptides in bacteria. In the first approach, H69-targeting peptide were *in vivo* expressed as Green Fluorescent Protein (GFP)-tagged fusion peptides. In order to further characterize the selected peptides as potential drug leads, it is essential to determine their activity outside the context of the fusion protein. Therefore, in the second approach a different plasmid system was used to express H69-targeting peptides as free peptides in bacteria. The effects of these peptides on bacterial protein translation and growth were monitored through fluorescent intensities and optical densities of cultures expressing the peptides.

Aim 3) Evaluated the effects of pseudouridine modifications on the antibacterial activity of 2-deoxystreptamine class aminoglycosides

Minimum inhibitory concentration (MIC) studies were carried out with Ψ-deficient and wild-type *E. coli* strains using the broth micro dilution method. *E. coli* MC 415 *(*wild-type, ΨΨΨ) and *E. coli* MC 416 (RluD(–), UUU) were utilized in the study (Michael O'Connor's lab, University of Missouri). MIC experiments were carried out with a series of aminoglycosides that are known to target the H69 and A site of the ribosome.

CHAPTER 2 MOLECULAR BIOLOGICAL AND BIOCHEMICAL METHODS USED IN THE DISSERTATION WORK

2.1 Abstract

In contrast to *in vitro* methods, most of the work I did for my dissertation is focused on the *in vivo* activity of antibacterial drugs targeting the bacterial ribosome. The details of the molecular biological, microbiological, and biochemical methods I utilized in my dissertation work are discussed in this chapter. The main focus of **Chapter 3** and **4** is *in vivo* expression of antibacterial peptides in *E. coli*. In this work, specific plasmid systems developed in Dr. Phillip Cunningham's lab were utilized. Basic molecular cloning techniques and methods such as the polymerase chain reaction (PCR), ligation, transformation, colony PCR, and DNA sequencing were employed in this work. Activities of the peptides were assessed using bacterial growth assays. Moreover, an *in vivo* dimethyl sulfate footprinting technique was used to study peptide-ribosome interactions. The main focus of **Chapter 5** is evaluation of the effects of pseudouridine modifications on antibacterial activity of the 2-deoxystreptamine class aminoglycosides. In this work, a series of MIC experiments were carried out using the broth micro dilution method. A brief description of each experimental method followed by detailed protocols are summarized in this chapter. In fact, the methods described are not confined to ribosome-targeting drugs. We can expand this work to study the *in vivo* activity of other drugs.

2.2 *In vivo* expression of peptides in bacteria

Molecular cloning techniques were used to *in vivo* express peptides in *E. coli* (**Figure 2.1**). In the first approach, peptides were *in vivo* expressed as GFP-tagged fusion peptides (**Figure 2.2a**). In order to further characterize the selected peptides as potential drug leads, it is essential to determine their activities outside the context of the fusion protein. Therefore, in the second approach a different plasmid system was used to express free peptides in bacteria (**Figure**

2.2b). The effects of these peptides on bacterial protein translation and growth were monitored through fluorescent intensities and optical densities of cultures expressing the peptides.

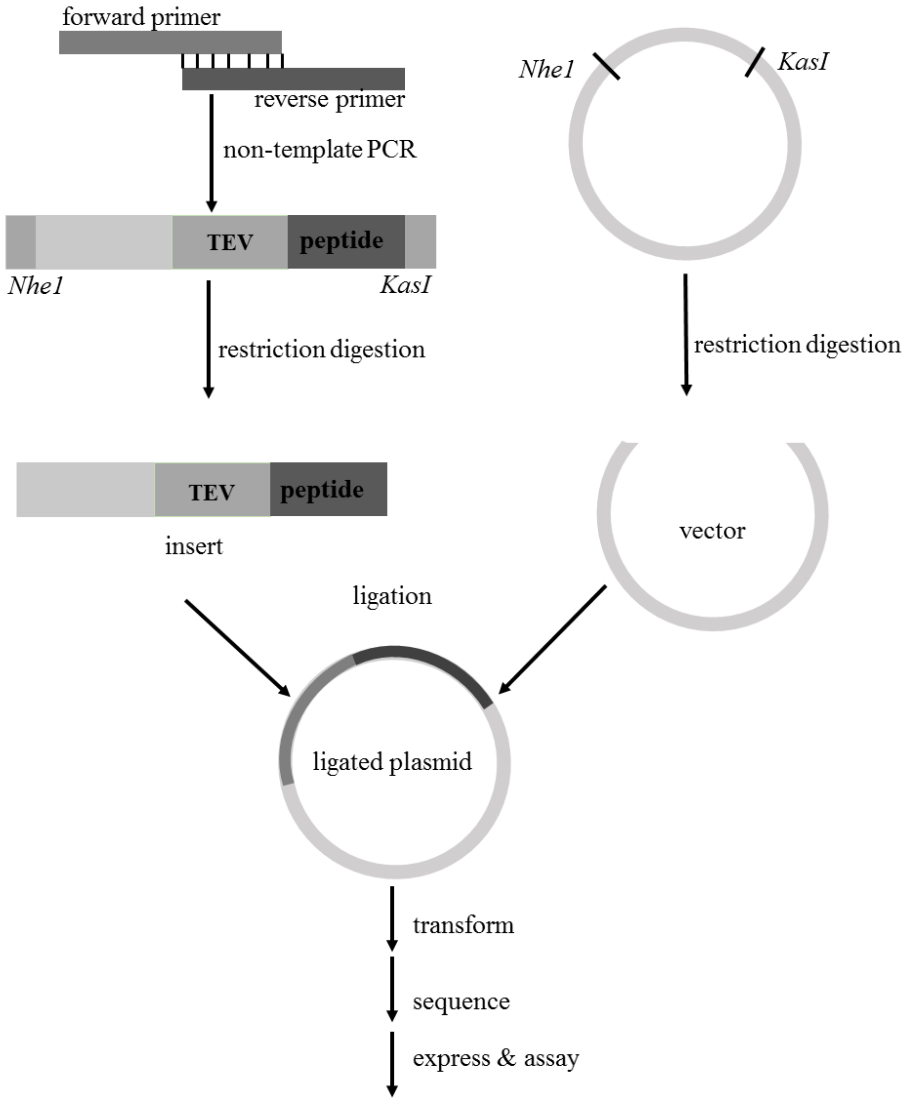

Figure 2.1 Cloning experiment. This schematic diagram illustrates the basic steps involved in the molecular cloning experiment. The DNA insert of peptide is synthesized using primer extension PCR. The insert and vector are digested with the appropriate restriction enzymes and then ligated. The ligated plasmid is electrotransformed into bacterial cells. The insertion is confirmed by DNA sequencing. Peptides are *in vivo* expressed by adding arabinose and utilized in bacterial growth assays.

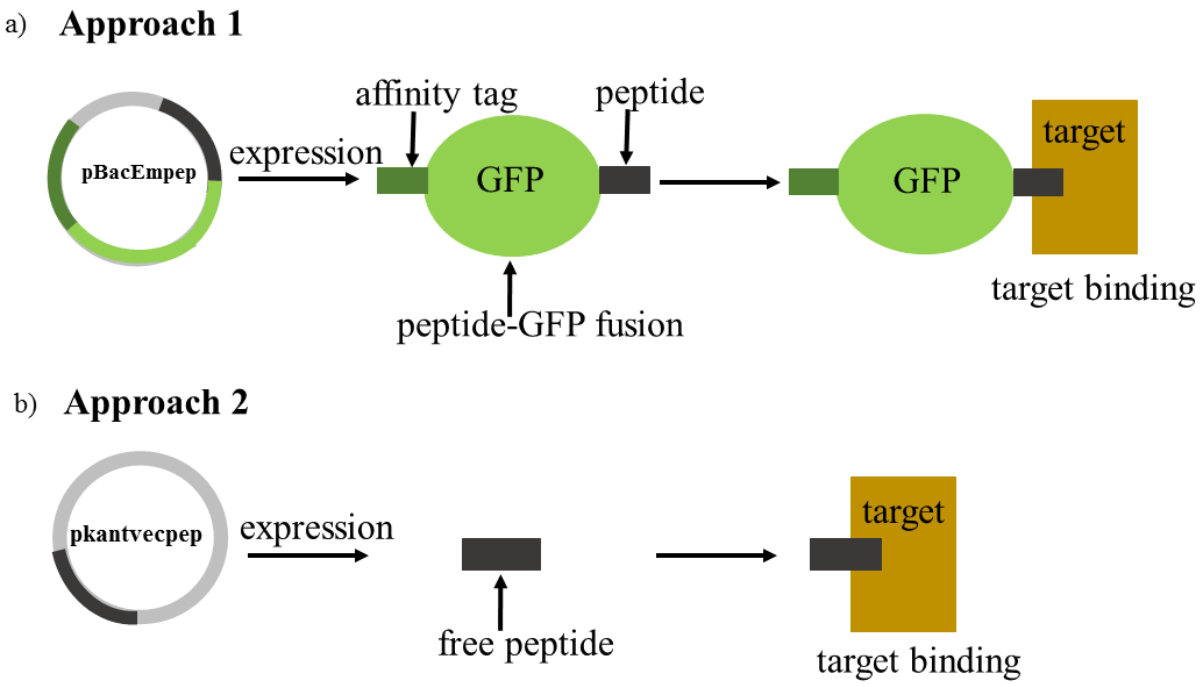

Figure 2.2 A schematic diagram of the two approaches used in the *in vivo* peptide expression methodology. a) In the first approach, peptides are cloned at the N-terminus of GFP and expressed as a fusion protein. The effects of peptides on bacterial growth and protein translation are monitored by measuring OD_{600nm} and fluorescence intensities of cultures expressing peptides. b) In the second approach, free peptides are expressed and the effects on bacterial growth are monitored by measuring OD_{600nm} of cultures expressing peptides.

2.2.1 Synthesis of the peptide DNA insert

In both GFP and free plasmid systems, primer extension PCR was used to generate the desired peptide DNA sequences. As illustrated in **Figure 2.3**, PCR to produce the peptide insert does not use a template, but the 3' ends of the two primers, universal forward and peptide-specific reverse, overlap to allow extension. During PCR, primers anneal with each other and extend to give the full-length DNA product. Restriction digestion of the PCR product with appropriate enzymes provides peptide inserts for the cloning experiments.

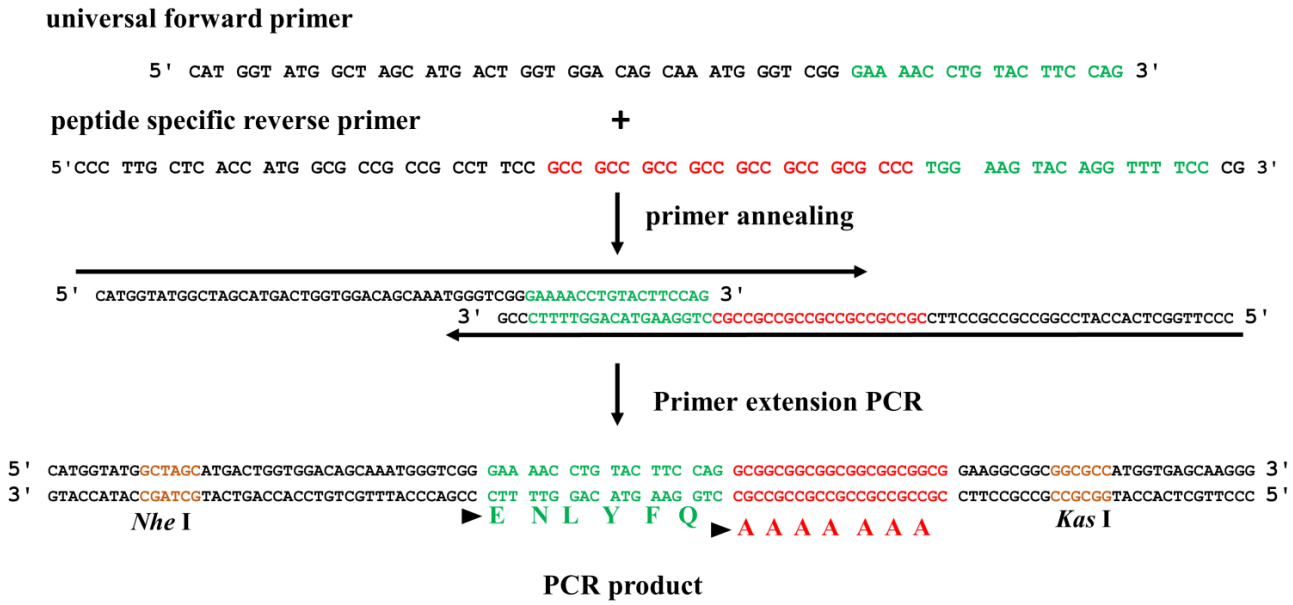

Figure 2.3 Peptide insertion by PCR. The design of the PCR experiment is shown. The nucleotide sequences of the universal forward and the peptide specific reverse primer sequence are shown. During PCR, the primers anneal with each other and extend to give the full-length DNA product. The nucleotides from the PCR product are shown with the restriction sites in orange. The amino acid sequences of the TEV protease recognition sequence, ENLYFQ (green) and the peptide, AAAAAAA (red), are in letters shown below the DNA sequence.

2.2.2 Cloning of peptides into the GFP plasmid system

The genes were cloned behind the P_{BAD} promoter of the plasmid such that the peptides could be expressed by inducing with L-arabinose. Dr. Wes Colangelo prepared the plasmid, pBacEmtvec3, for this experiment (**Figure 2.4**). The restriction enzyme sites *Kas* I and *Nhe* 1 were used to clone the peptide insert into the plasmid. In previous studies, it was shown that cloning of peptides at the N-terminus of the GFP gene shut down its own translation, and this could be overcome by cloning peptides a few amino acids away from the start codon.[193,231] Therefore, a normalizing sequence (g10 leader sequence) was added at the 5' end of the GFP gene and then a TEV (Tobacco Etch Virus) protease recognition sequence (ENLYFQG/S) was added after the normalizing sequence (**Figure 2.5**).

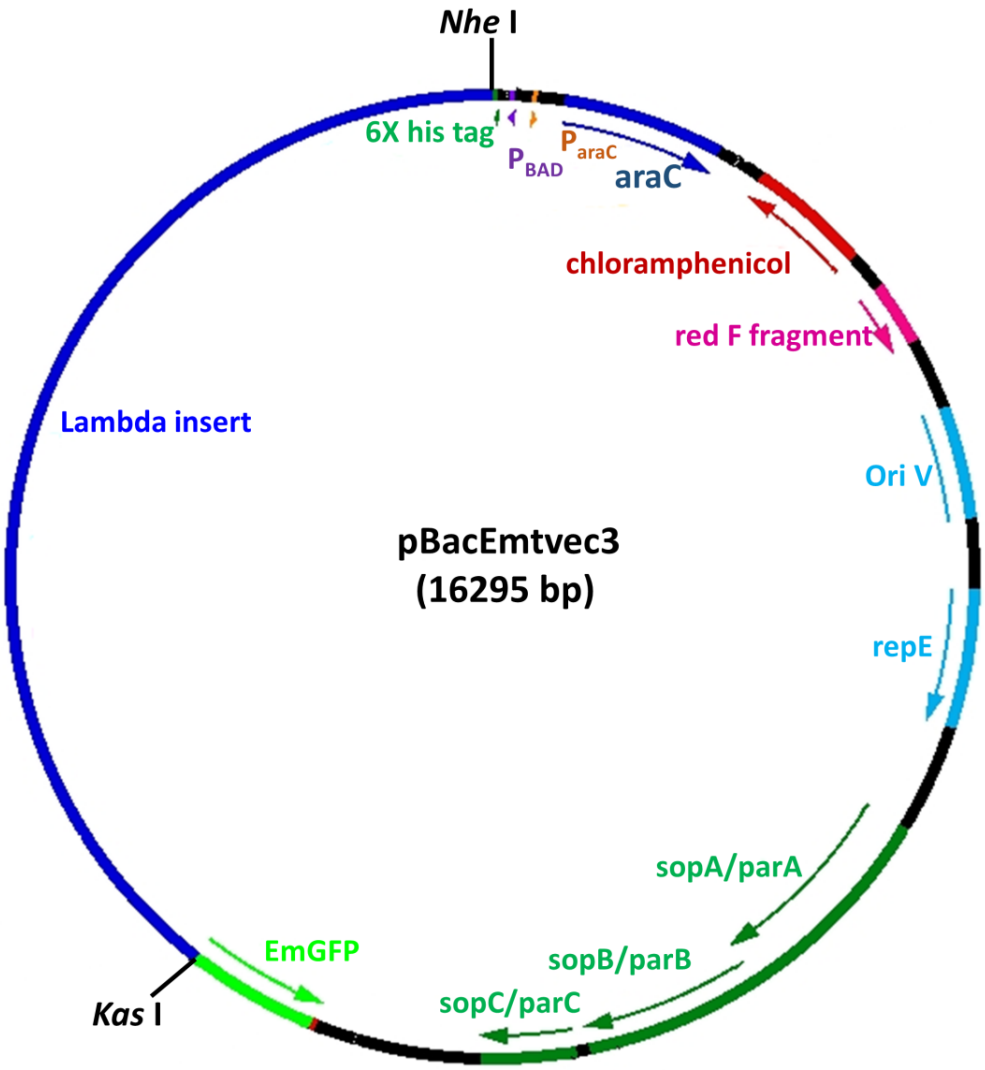

Figure 2.4 Plasmid map of pBACEmtvec3. pBACEmtvec3 is derived from the commercial plasmid pCC1BAC. The plasmid shows chloramphenicol resistance. The restriction enzyme sites *Nhe* I and *Kas* I are used to clone the peptide insert into the plasmid. Therefore, the lambda insert in the plasmid vector is replaced by the peptide sequence in the ligated plasmid. After insertion of the peptide sequence, its expression is controlled by the P_{BAD} and the P_{araC} promoters. The P_{BAD} promoter is adjacent to the P_{araC} promoter, which transcribes the *araC* gene in the opposite direction. The *araC* gene encodes AraC protein, which regulates activity of both the P_{BAD} and P_{araC} promoters.[240,241]

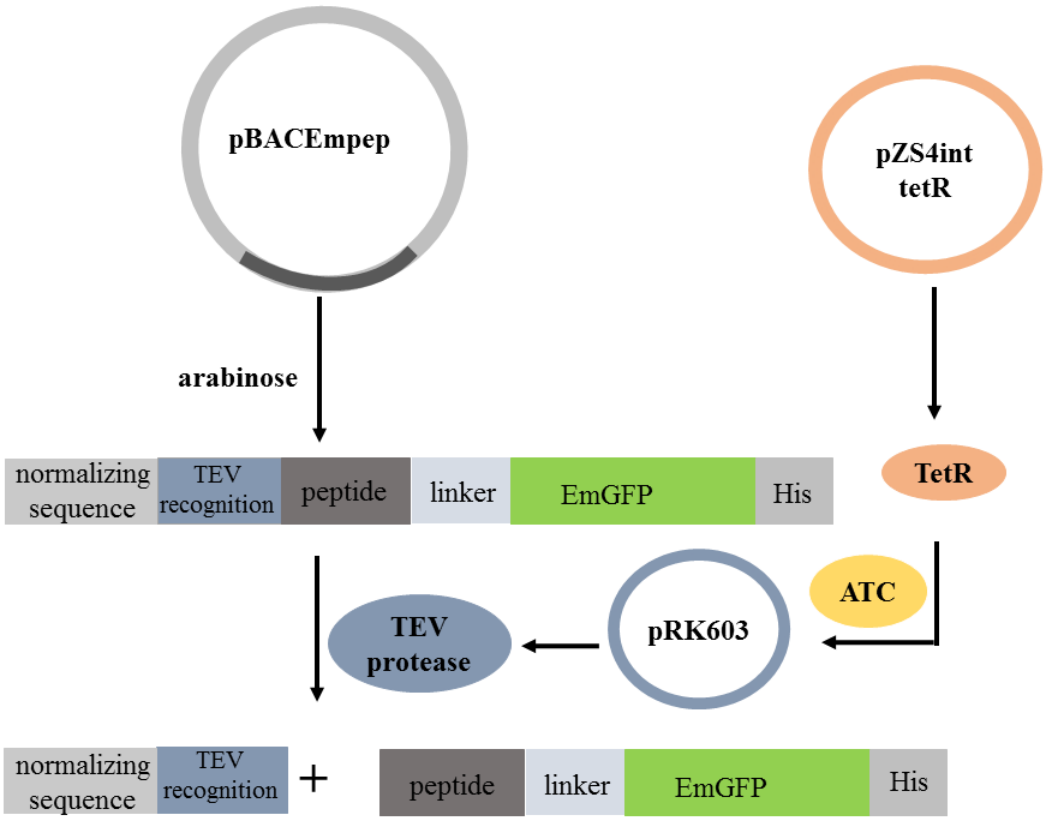

Figure 2.5 ***In vivo*** **expression of GFP-peptide fusion proteins.** A schematic diagram for the production of GFP-tagged peptides using the TEV protease expression system is shown. A normalizing sequence (g10 leader sequence) was added at the 5' end of the construct. The peptides are cloned behind the TEV protease recognition sequence. A peptide linker, EGGG, is placed before GFP to provide flexibility of the peptide. The expression of the peptide and TEV protease is induced by adding arabinose and anhydrotetracycline (ATC), respectively. Upon expression of TEV protease, the peptides are exposed at the N-terminus of GFP.

The expression of GFP tagged-peptides in the TEV protease system was carried out in *E. coli* strain EPI300. The ligated plasmids were electrotransformed into *E. coli* EPI300, which contained two plasmids for the expression of TEV protease and the tetracycline repressor protein (TetR). Therefore, the expression was done in a three-plasmid system (**Figure 2.5**) in which the first plasmid (pBacEmpep, chloramphenicol resistance) was used for expression of GFP-tagged peptides, the second (pRK603) for Tet-inducible TEV protease with kanamycin resistance, and the third (pZS4int-tetR, spectinomycin resistance) for constitutive tetracycline repressor protein

(TetR) expression.[242] **Figure 2.6** illustrates the mechanism that controls the *in vivo* expression of TEV protease from pRK603 in the presence and absence of the inducer, anhydrotetracycline (ATC). The expression of TEV protease from the pRK603 plasmid is under control of the P_{Tet} promoter. When co-transformed with pRK603, constitutive expression of TetR from pZS4int-tetR represses the expression of TEV protease from the P_{Tet} promoter by binding to its operator.

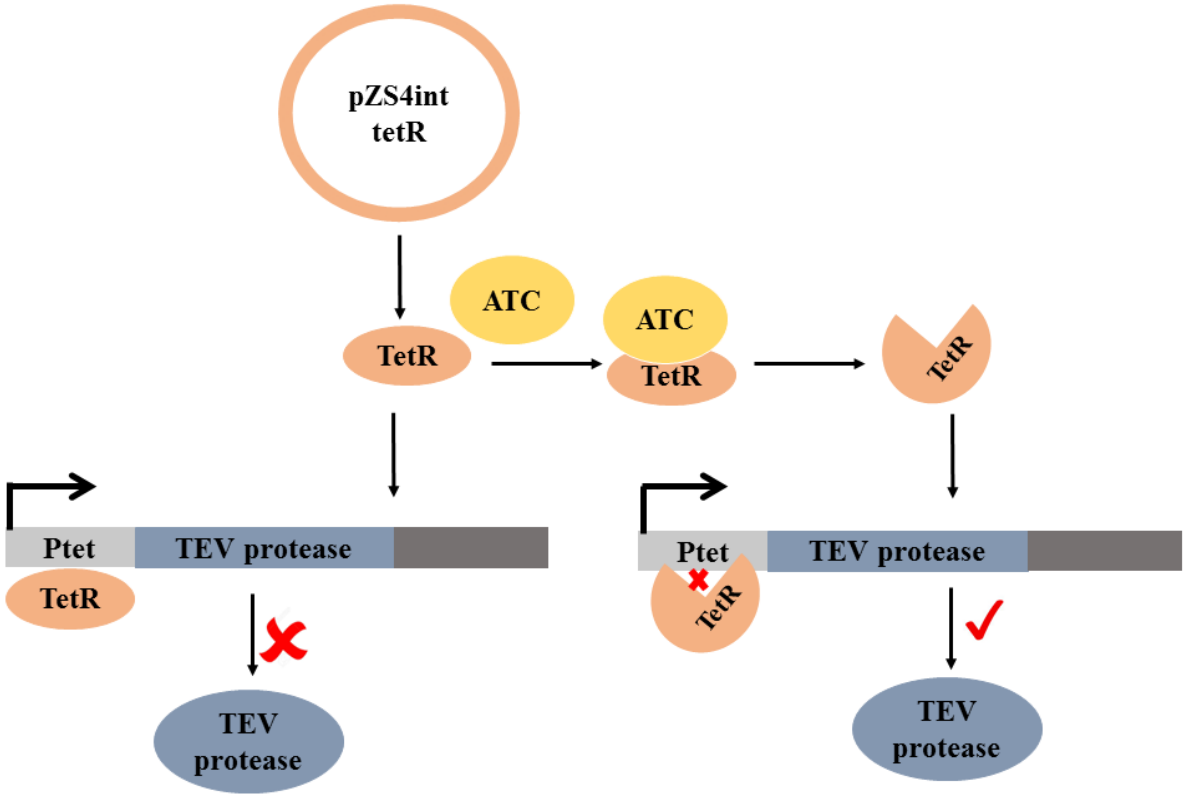

Figure 2.6 ***In vivo*** **expression of TEV protease.** A schematic diagram for the production of TEV protease is shown. The expression of TEV protease is under control of the P_{Tet} promoter. The binding of TetR to the promoter inhibits the expression of TEV protease. Upon the addition of ATC, it binds to TetR and causes a conformational change in the protein lowering its affinity for the P_{Tet}. With TetR removed, expression from P_{Tet} proceeds and produces TEV protease.

When ATC is added to a cell culture containing both plasmids, ATC binds to TetR and causes a conformational change in the protein lowering its affinity for the P_{Tet} operator. With TetR removed, expression from P_{Tet} proceeds and produces TEV protease. During the bacterial

growth assay, once the cells enter early log phase growth, ATC is added to induce TEV protease expression and allow it to accumulate in the cytoplasm. After an additional hour of incubation, L-arabinose was added to induce the expression of peptide-EmGFP fusion.

In this plasmid system, the peptide sequence was cloned behind the TEV protease recognition sequence. TEV protease is a 27-kDa catalytic domain of the Nuclear Inclusion a (NIa) protein encoded by the Tobacco Etch Virus.[243,244] Waugh's lab developed methods for *in vivo* processing of fusion proteins by this enzyme.[242,245] The expression of TEV protease from another plasmid in the same cell would lead to cleavage of the TEV recognition peptide sequence between residues Q and G, and the resulting peptide was exposed at the N-terminus of GFP.[242,245] TEV protease cleavage occurs between Q and G, leaving an extra glycine (G) at the N-terminus of the peptide sequence (**Figure 2.7**). Although the wild-type TEV protease recognition sequence is ENLYFQG/S, recent studies have shown that any amino acid after Q in the sequence could cleave efficiently such that the exact peptide sequence could be exposed after TEV cleavage.[231,242,246,247]

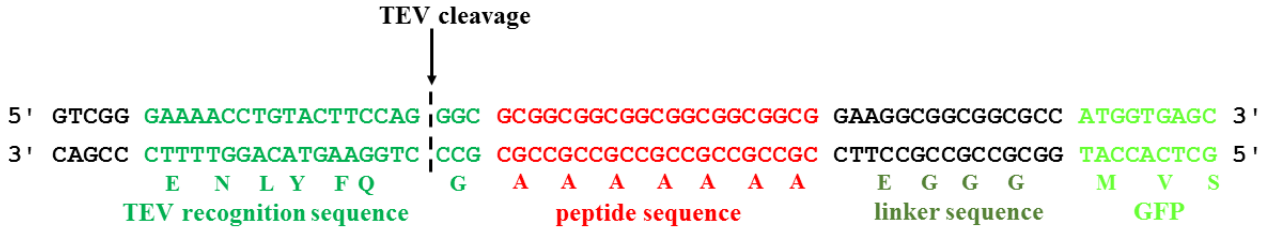

Figure 2.7 TEV cleavage site. The TEV protease has a 7 amino acid recognition sequence and cleaves between amino acids 6 and 7 (Q and G). This leaves a G residue attached to the desired peptide sequence, in this case producing GAAAAAAA at GFP end.

Therefore, later in this project peptide primers were designed excluding the codon corresponding to the C-terminus G residue. Therefore, after TEV protease cleavage the exact N-terminus sequence of the peptide is exposed. TEV cleavage of fusion proteins is typically more

efficient than thrombin or enterokinase. Furthermore, it is easy to overproduce and is resistant to many protease inhibitors.[246,247]

2.2.3 Free peptide expression system

In this approach, a single plasmid expression system pKan5tvVec (8243 bp) with an inducible P_{BAD} promoter and kanamycin resistance was used as the vector (**Figure 2.8**). Therefore, the peptides could be expressed by inducing with L-arabinose. The restriction enzyme sites *Hind* III and *Nhe* I were used to clone the peptide insert into the plasmid (**Figure 2.9**).

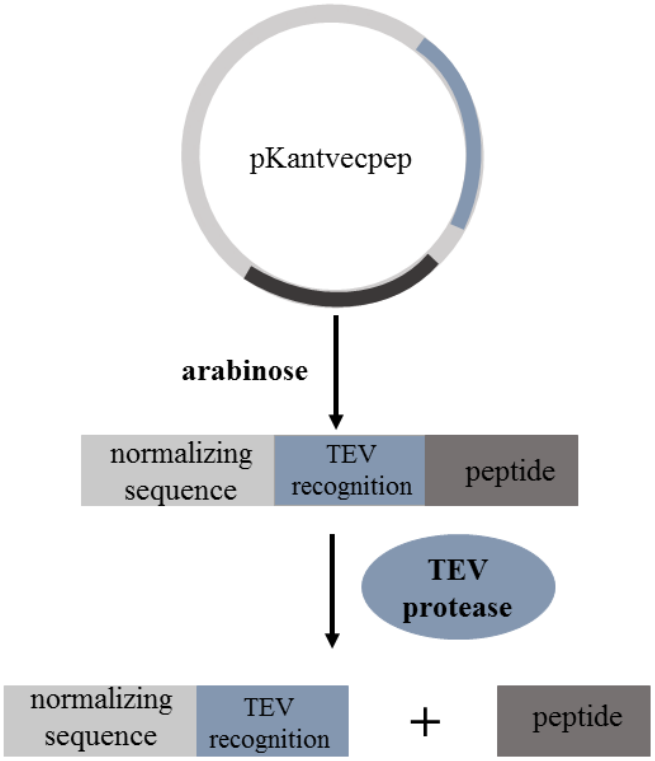

Figure 2.8 *In vivo* expression of free peptides. A schematic diagram for the production of free peptides using the TEV protease expression system is shown. The peptides are cloned behind the TEV protease recognition sequence and under control of the P_{BAD} promoter. Therefore, the expression of peptides and TEV protease is induced by adding arabinose. After TEV protease cleavage, free peptides are available in the cell.

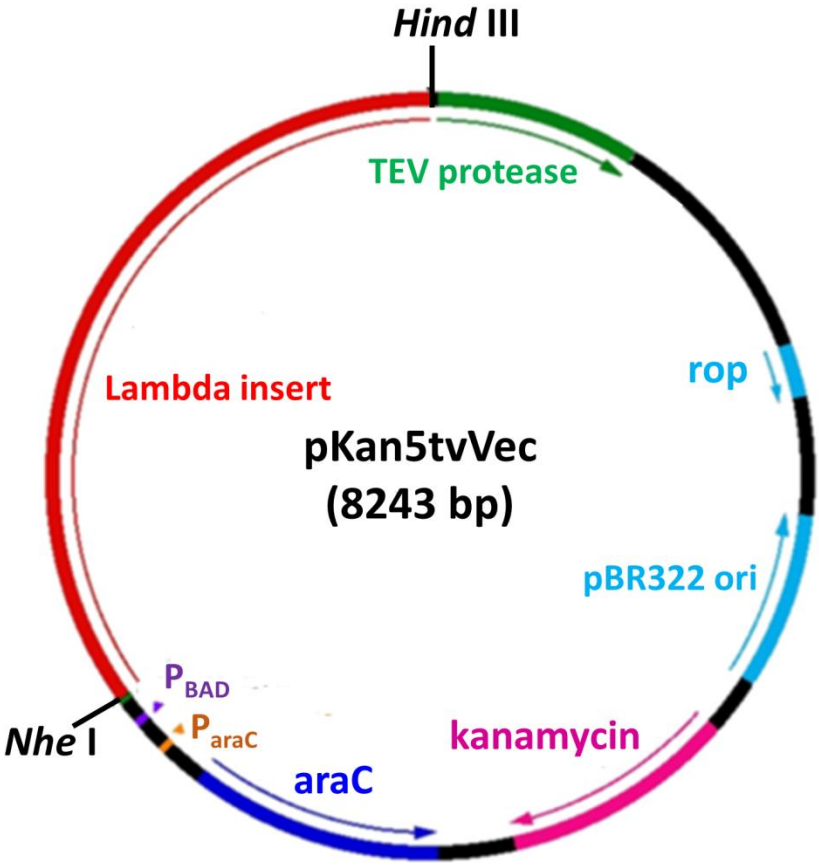

Figure 2.9 Plasmid map of pKan5tvVec. The restriction enzyme sites *Nhe* I and *Hind* III are used to clone the peptide insert into the plasmid. Therefore, the lambda insert in the plasmid vector is replaced by the peptide sequence in the ligated plasmid. The expression of the peptide and TEV-protease is controlled by the P_{BAD} and P_{araC} promoters. The plasmid shows kanamycin resistance.

The peptide insert was generated by using the non-template PCR method as described earlier (**Figure 2.3**). The ligated plasmids were transformed into *E.coli* DH5 cells. Expression of TEV protease from the same plasmid would cleave the TEV recognition peptide sequence leaving free peptides.

2.3 Materials and Methods

Materials

Plasmid maxi-prep purification was performed using a plasmid maxi-prep kit #12162 from Qiagen. Gotaq Green Master Mix (2×, #M712B) was purchased from Invitrogen (Carlsbad,

CA). NEB Buffer 2.1 restriction enzymes, *Hind* III, *Nhe* I, and *Kas* I, were obtained from New England Biolabs (lpswich. MA). Quantum Prep Freeze ‘N Squeeze DNA Gel Extraction Spin Columns were acquired from Bio-Rad Laboratories (Hercules, CA). OPTIZYME T4 DNA ligase is a product of Fisher BioReagents (Fair Lawn, NJ). Thermo Scientific (Lafayette, CO) manufactures the GeneJet Plasmid Miniprep Kit. *Escherichia coli* DH5, *Escherichia coli* EPI 301 cells, and plasmid vectors, pBACEmtvec3 and pKan5tvVec, were provided by the laboratory of Dr. Philip Cunningham. Lysogeny broth (LB) was purchased from Sigma-Aldrich (St. Louis, MO). All other chemicals used to make buffers were purchased from Sigma-Aldrich (St. Louis, MO) or Fisher BioReagents (Fair Lawn, NJ). DNA sequencing was done by the DNA Sequencing Lab Applied Genomics Technology Center at Wayne State University (Detroit, MI).

The PCR primers to generate the inserts, universal forward primers and reverse primers corresponding to each peptide sequence and sequencing primers were synthesized by Integrated DNA Technologies.

The list of primers used in the cloning experiments are as follows:

GFP-tagged peptide expression system

Universal forward primer

5'-CATGGTAT GCTAGCATGACTGGTGGACAGCAAATG GGTCGG GAAAACCTGTAC TTCCAGGGC-3'

RQVANHQ reverse primer

5'-CCCTTGCTCACCATGGCGCCGCCGCCTTCCTGGTGGTTCGCAACCTGACGCCCT GGAAGTACAGGTTTTCCCG-3'

TARHIY reverse primer

5'-CCCTTGCTCACCATGGCGCCGCCGCCTTCGTAGATGTGACGCGCGGTGCCCTG GAAGTACAGGTTTTCCCG-3'

NQAANHQ reverse primer

5'-CCCTTGCTCACCATGGCGCCGCCGCCTTCTGGTGGTTAGCCGCCTGGTTACCC
TGGAAGGTTTTCCCG-3'

AAAAAAAA reverse primer

5'-CCCTTGCTCACCATGGCGCCGCCGCCTTCGTAGATGTGACGCGCGGTGCCCTG
GAAGTACAGGTTTTCCCG-3'

Sequencing forward primer

5'-AACTCTCTACTGTTTCTCC-3'

Sequencing reverse primer

5'-GTGCAGATGAACTTCAGG-3'

Free peptide expression system

Universal forward primer

5'-CATGGTATGGCTAGCATGACTGGTGGACAGCAAATGGGTCGGGAAAACCTGTA
CTTCCAG-3'

AAA reverse primer

5'-TTAAAGTTAAAGCTTTTACGCCGCCGCCGCCGCCGCCGCACCCTGGAAGTACA
GGTTTTCCCGAC-3'

Oncocin reverse primer

5'-CTAAAGTTAAAGCTTTTAGCGGTTATAGATGCGGCGTGGTGGGCGTGGGCGT
GGCAGATATGGTGGCTTATCAACCTGGAAGTACAGGTTTTCCCGACCC-3'

Oncocin 3A reverse primer

5'-CTAAAGTTAAAGCTTTTAGCGGTTATAGATGCGGCGTGGTGGGCGTGGGCG
TGGCAGATATGGTGGCGCATCAACCTGGAAGTACAGGTTTTCCCGACCC-3'

Oncocin 6A reverse primer

5'-CTAAAGTTAAAGCTTTTAGCGGTTATAGATGCGGCGTGGTGGGCGTGGGCG
TGG CAGCGCTGGTGGCTTATCAACCTGGAAGTACAGGTTTTCCCGACCC-3'

Oncocin 7A reverse primer

5'-CTAAAGTTAAAGCTT TTAGCGGTTATAGATGCGGCGTGGGGGCGTGGGCGTGGCGCATA TGGTGGCTTATCAACCTGGAAGTACAGGTT TTCCCGACCC -3'

Oncocin 11A reverse primer

5'-CTAAAGTTAAAGCTTTTAGCGGTTATAGATGCGGCGTGGTGGCGCTGGGCGTGGCAGTAT GGTGGCTTATCAACCTGGAAGTACAGGTTTTCCCGACCC-3'

Oncocin 36711A reverse primer

5'-CTAAAGTTAAAGCTTTTAGCGGTTATAGATGCGGCGTGGTGGCGCTGGGCGTGGCGCC GCTGGTGGCGCATCAACCTGGAAGTACAGGTTTTCCCGACCC-3'

Sequencing forward primer

5'-CAACTCTCTACTGTTTCTCCATGC-3'

Sequencing reverse primer

5'-GCCCAAATCCAATACCATACACG-3'

Methods

All of the experimental methods used for the GFP and free plasmid system are the same except for the plasmid vector and the *E.coli* strain used in each system. Therefore, in this chapter, the experimental methods are explained in detail for the free plasmid system, which also applies to the GFP system. The specific information for each system is explained in detail in **Chapter 3** for the free plasmid and the **Chapter 4** for GFP system.

2.3.1 Preparation of *Escherichia coli* DH5 electrocompetent cells

E. coli DH5 cells were streaked from frozen stocks onto Luria-Bertani (LB) agar plates and incubated overnight at 37 °C. An overnight culture (3 mL) of LB broth was inoculated with a single isolated colony of the DH5 cells and incubated overnight (16 h) at 37 °C with shaking. In each of four flasks (2 L), 250 μL from a single overnight culture was added to 250 mL of preheated (37 °C) Super Optimal Broth (SOB) and incubated at 37 °C with vigorous shaking (350 rpm) until the OD_{550nm} = 0.8. The cultures were cooled to 4 °C on ice for 15 min before the

cultures were transferred to four Sorvall tubes (250 mL) on ice, then centrifuged (5000 rpm) at 4 °C for 15 min to harvest the cells. The supernatant was discarded and each pellet was washed with ice-cold 10% glycerol (250 mL) and the cells were centrifuged (5000 rpm) at 4 °C for 15 min. The wash and centrifugation steps were repeated a second time. The supernatant was decanted off and the cells were resuspended in the small volume (1 mL) of supernatant left in each tube. The cells were stored in 25 μL aliquots at -80 °C.

2.3.2 Preparation of pKan5tvVec vector

The vector DH5 strain for pKan5tvVec (8243 bp) was streaked from a frozen stock onto a fresh LB-agar plate with kanamycin (50 μg/mL) and incubated overnight at 37 °C. A single colony was used to inoculate a 5 mL culture using LB broth and kanamycin (50 μg/mL), which was incubated for 8 h at 37 °C with shaking (275 rpm). The 5 mL culture was added to LB broth (495 mL) with kanamycin (50 μg/mL) and incubated for 16 h overnight at 37 °C with shaking (275 rpm). The culture was divided into two Sorvall (250 mL) tubes and centrifuged (6000 rpm) at 4 °C for 15 min. The following steps were completed using a QIAGEN Plasmid Maxi Kit. The tubes were inverted to remove the media and the pellets were resuspended by swirling using buffer P1 (10 mL) with RNase A (10 mg/mL), and the resuspension was transferred to new Sorvall tubes. Lysis buffer P2 (10 mL) was added and the solution was mixed by inversion (6×), then incubated at room temperature for 5 min. Neutralization buffer P3 (10 mL, 4 °C) was added and mixed by inversion (6×), and the mixture was left on ice for 20 min. The mixture was centrifuged (13,000 rpm) at 4 °C for 30 min, and the supernatant was transferred to a new tube before a second centrifugation (13,000 rpm) at 4 °C for 15 min. To equilibrate the QIAGEN tip 500, buffer QBT (10 mL) was added to the column and emptied by gravity flow during centrifugation. All steps using the QIAGEN tip 500 empty by gravity flow. After centrifugation,

the supernatant was transferred to the column. The column was washed with buffer QC (2 × 30 mL). The plasmid DNA was eluted from the column using buffer QF (15 mL) and eluate was collected in a fresh tube. The DNA was precipitated by adding room temperature isopropanol (10.5 mL), which was mixing by inversion, then centrifuging (11,000 rpm) at 4 °C for 30 min. The supernatant was discarded. Two washes were carried out using 70% ethanol (5 mL) each time and centrifuging (11,000 rpm) at 4 °C for 15 min. After removing the ethanol, the pellet was allowed to air dry for 20 min. The DNA was resuspended in sterile ddH_2O (1 mL). The purity of DNA was checked by running it on an agarose gel.

2.3.3 Synthesis of DNA inserts of peptides

The non-template PCR method was used to generate constructs for the desired peptides. The following forward and reverse primers were used to amplify the PCR products. A universal forward primer (5 μM, 10 μL), reverse primer (5 μM, 10 μL), Gotaq-master mixture (2×, 50 μL), and ddH_2O (30 μL) were combined in a PCR tube. The PCR reaction was heated in a thermocycler to 95 °C for 5 min to denature, then 55 °C for 1.5 min to anneal the DNA, and 72 °C for 30 S to carry out extension. The reaction was held at 72 °C for 7 min after all 30 cycles were completed, and the sample was cooled to 4 °C. The PCR products were checked on an agarose gel and purified before restriction digestion.

2.3.4 Insert and vector digestion

To produce the peptide insert from the PCR product, 20 μL of the PCR product (1 μg) was combined with 1 μL *Hind* III (20 U/μL), 1 μL *Nhe* I (10 U/μL), 5 μL NEB Buffer 2.1 (10×), and sterile ddH_2O (23 μL). To digest the pKan5tvVec plasmid (8243 bp) to produce the vector DNA (5371 bp), 2.5 μL pKan5tvVec plasmid (1 μg) was combined with 1 μL *Hind* III (20

U/μL), 1μL *Nhe* I (10 U/μL), 5 μL NEB Buffer 2.1 (10×), and sterile ddH_2O (8 μL). The reactions were incubated overnight for 16 h at 37 °C.

2.3.5 DNA gel extraction with ethanol precipitation on digested products

Quantum Prep Freeze 'N Squeeze DNA Gel Extraction Spin Columns were used to purify the digested samples for both the vector and insert. The samples were separated by electrophoresis using TBE agarose 1% gels at 95 V, 1 h for the insert gel and 2 h for the vector gel. The gels were stained with 1 drop ethidium bromide (0.5 μg/ml) in water with shaking for 20 min. The insert band (78 bp) and vector band (5371 bp) were each excised from their respective gels using a scalpel, with sterile technique, sliced into small pieces, and placed into the individual filter cups. The filter cup was attached to the dolphin tube and the spin column was cooled in the -20 °C freezer for 5 min. The column was centrifuged (10,000 rpm) for 5 min at room temperature. The freeze and spin was repeated two more times in an identical manner. The DNA solution in the collection tube was transferred to a new microcentrifuge tube for each sample. The two DNA samples were concentrated using ethanol precipitation. For each 100 μL vector and insert sample, 100% ethanol (250 μL) was added with 3 M NaOAc (10 μL), and vortexed for 1 min. The samples were incubated on dry ice for 45 min then centrifuged (14,000 rpm) at 4 °C for 45 min. The supernatant was carefully removed. Ice cold 70% ethanol (100 μL) was added to the pellet and the mixture was incubated on dry ice for 30 min. After the final centrifugation (14,000 rpm) at 4 °C for 30 min, the pellet was dried in the Speedvac for 15 min. The DNA was resuspended in sterile ddH_2O (10 μL).

2.3.6 Ligation and electrotransformation

Ligation reactions were set up for the vector to insert (V:I) with ratios 1:2, 1:4 ,1:10, 1:100, and 1:250, with T4 DNA ligase (5 U/μL) enzyme, ligase buffer (10×) and sterile H_2O.

The reactions were incubated 1 h at room temperature and heat inactivated for 10 min at 70 °C. The ligation mixture (1.5 μL) was added to electrocompetent cells (25 μL) on ice and mixed gently by pipetting. Each sample was transferred into a pre-chilled electroporation chamber and electroporated. Each sample was used to inoculate LB broth (1 mL). Cultures were incubated 37 °C for 1 h with shaking. Samples were transferred to microcentrifuge tubes. Cells were pelleted (5000 rpm) at 4 °C for 10 min. The supernatant (800 μL) was removed carefully. Pelleted cells were resuspended in the remaining supernatant (200 μL) and plated on pre-warmed LB-agar plates with kanamycin (50 μg/mL).

2.3.7 Sequence confirmation

The peptide clones were confirmed by colony PCR and DNA sequencing. Several colonies from the plates of transformants were selected and used to streak a new master plate. A single colony from each master plate was used to inoculate 50 μL of sterile water in a PCR tube. The samples were boiled at 95 °C for 10 min in a thermocycler. The colony PCR reaction was prepared for each sample in a PCR tube using 2.5 μL of sequencing forward primer (5 μM), reverse primer (5 μM), 2.5 μL colony DNA mixture, 12.5 μL Gotaq Green Master mixture and 5 μL of sterile H_2O. The PCR reaction was run and products were checked on an agarose gel. Plasmids were isolated using a GeneJet Plasmid Miniprep kit and sent for DNA sequencing. Samples were sequenced by the Applied Genomics Technology Center DNA Sequencing Laboratory, Wayne State University.

2.3.8 Bacterial growth assay – free plasmid system

Ligated plasmids containing peptides were transformed into the *E. coli* DH5 strain. Cells were grown in LB/kanamycin medium to prepare an overnight culture. The culture was diluted 1:500 and incubated at 37 °C for 3-4 h until the optical density ($OD_{600\ nm}$) reached ~ 0.2. When

cells reached early log phase, ~200 min, L-arabinose was added to a final concentration of 0.2% (w/v) to induce the expression of free peptides. Control experiments were done without adding inducer. From each culture, 300 µL of cells were transferred to a 96-well plate. Optical densities (OD_{600nm}) of cultures were measured every 60 min until cells reached the stationary phase.

2.3.9 Bacteria growth and fluorescence assay

Ligated plasmids pep-GFP pBacEmtvec3 were transformed into the *E. coli* EPI300 strain. A single colony from each clone was grown in LB/chloramphenicol/kanamycin/spectinomycin medium to prepare an overnight culture. The culture was diluted 1:500 and incubated at 37 °C for 3-4 h until the optical density ($OD_{600\ nm}$) reached 0.1 (~ 200 min). Anhydrotetracyclin (ATC) was added to a final concentration of 250 ng/mL to induce TEV protease expression. When cells reached early log phase, ~240 min, L-arabinose was added to a final concentration of 0.2% (w/v) to induce the expression of GFP-tagged peptides. Control experiments were done without adding inducers to see the difference in cell growth in the presence or absence of GFP-tagged peptides. After induction of GFP-tagged peptides, the level of GFP expression in each culture was monitored by measuring fluorescence intensity at 60 min time intervals until cells reached the stationary phase. From each culture, 600 µL of cells were pipetted out into an Eppendorf tube and pelleted by centrifuging 2 min in a benchtop micro centrifuge. Cells were washed twice with 600 µL HN buffer (50 mM HEPES, pH 7.5, 150 mM NaCl). Two hundred µL of cells were transferred into each well of Costar, clear bottom 96-well black plate. The florescence intensity was measured at 487 nm (excitation) and 509 nm (emission). Optical density of cultures was measured at 600 nm.

2.3.10 Purification of the EmGFP-pep fusion protein

Ligated plasmids pep-GFP pBacEmtvec3 were transformed into the *E. coli* EPI300 strain. A single colony from each clone was grown in LB/chloramphenicol/kanamycin/spectinomycin medium to prepare an overnight culture. The culture was diluted 1:500 and incubated at 37 °C for 3-4 h until the optical density ($OD_{600\ nm}$) reached 0.1 (~ 200 min). Anhydrotetracyclin (ATC) was added to a final concentration of 250 ng/mL to induce TEV protease expression. When cells reached early log phase, ~240 min, L-arabinose was added to a final concentration of 0.2% (w/v) to induce the expression of GFP-tagged peptides. Bacteria culture was grown to 0.4 OD and the culture was centrifuged at 6,000 g for 20 min to pellet the cells. The pellet was resuspended in lysis buffer (50 mM Tris-Cl, pH 7.6, 300 mM NaCl, 10 mM imidazole, 1mM DTT, and 0.05% of Triton-X100) and lysed using a French Press. The lysate was centrifuged twice at 15,000 rpm for 30 min to remove cellular debris. The supernatant was collected. As previously described, the peptide construct was prepared in which His-tag was placed at the C-terminus of the EmGFP gene such that the peptide-GFP fusion protein could be purified using Ni-affinity chromatography. The column was packed with ~ 2 mL Ni-bound IMAC resin and equilibrated with 50 mM Tris-Cl, pH 7.6, 300 mM NaCl, 10 mM imidazole, 1 mM DTT, and 0.05% of Triton-X100. The equilibration of the column with 10 mM imidazole helps to remove cellular proteins having less affinity to nickel ions. To wash and elute of protein, 1× Tris-buffer (50 mM Tris-Cl, pH 7.6, 300 mM NaCl, 1 mM DTT, and 0.05% of Triton-X100) was used. The specific concentration of imidazole is mentioned in each step of purification. The crude protein was mixed with the resin and incubated for 30 min to allow binding. It was washed with 20 column volumes of equilibration buffer and then with five column volumes of 1× Tris-buffer with 20 mM imidazole. After washing with five column volumes of 1× Tris-buffer with 30 mM

imidazole, the protein was eluted with 1× Tris-buffer with 50 mM imidazole. The fractions were collected in 1.5 mL microcentrifuge tubes. The purity of eluted protein was checked by running the samples on a 12 % SDS-PAGE. After confirming the purity of protein, it was dialyzed against 50 mM Tris-Cl, pH 7.6, 300 mM NaCl, 1 mM DTT, and 0.05% of Triton X100 to remove the imidazole. Finally, the protein was quantified by using a standard Bradford assay. Isolated protein was characterized by matrix-assisted laser desorption ionization time-of-flight (MALDI-TOF) mass spectrometry.

2.4 Chemical probing of RNA structure

RNAs adopt highly structured biologically active scaffolds to carry out their functions. Therefore, identifying key RNA structural features at the nucleotide level is crucial for understanding their biological roles and to develop RNA-targeting therapeutics. Chemical probing is considered as a powerful technique to study RNA, including the nucleotide sequence, secondary and tertiary structures, and protein or drug interactions.[248-250] Applications of chemical probing for analyzing ribosome-tRNA interactions were reported by Moazed and Noller in the late 1980s.[39,251] In this work, they proposed the hybrid tRNA state during translocation based on chemical probing data.[39] Furthermore, they found that some clinically important antibiotics also interact with ribosomal RNAs at specific sites.[139] They demonstrated the power of chemical probing analysis and its broad potential to study RNA biomolecules. Many chemical reagents have been developed for the purpose of studying nucleic acid structures.[250,252] For example, dimethylsulfate (DMS), diethylpyrocarbonate (DEPC), and hydrazine were used to analyze RNA sequences and tertiary structures. In this dissertation work, DMS footprinting was employed to *in vivo* map the ribosome binding sites of peptide antibiotics. In the following section, the DMS footprinting technique will be discussed.

2.4.1 Dimethyl Sulfate (DMS) footprinting

DMS is one of the most versatile chemical reagents used to probe RNA structure.[249] DMS was introduced for RNA structure mapping in 1980 when Peattie and Gilbert adapted methods that had been used for sequencing DNA and RNA.[250,253,254] DMS can directly donate a methyl group to specific hydrogen-bond-accepting ring nitrogens on A, C, and G residues in RNA (**Figure 2.10**). DMS attacks the N1 position of A and the N3 position of C to produce 1-methyladenosine (m^1A) and 3-methylcytosine (m^3C), which inhibit Watson-Crick base-pair formation with the complementary base. DMS also attacks the N7 of G to produce 7-methylguanosine (m^7G) (**Figure 2.10**). In the case of A and C, the methylated base directly inhibits reverse transcriptase, because the methyl group alters the Watson-Crick face of the base. In order to map methylation at N7 of G, the RNA must be treated with aniline and borohydride to cleave the RNA backbone at the methylated Gs prior to reverse transcription (**Figure 2.11**). By comparing the pattern of modification-dependent reverse transcription stops to dideoxynucleoside triphosphate-generated stops using the same labeled primer, the sites of methylation can be mapped to the RNA sequence (**Figure 2.12**). Methylation-dependent stops occur one position before the corresponding dideoxynucleotide stop.

The DMS methylation reaction rate is relatively insensitive to changes in solution conditions such as pH and monovalent ion concentration and increases only mildly with increased temperature.[255-257] Therefore, the changes in DMS reactivity are typically due to structural changes rather than changes in reaction conditions. DMS footprinting has been used to monitor pH-dependent conformational changes in the ribosome, RNA structural changes in response to changes in ionic conditions or mutations, and to monitor protein binding to RNA.[239,255,258-262] This reagent has also been used to monitor binding of small ligands to RNAs,

notably the binding of antibiotics to the ribosomal complex.[139,239,263,264] If a particular base in RNA is involved in a secondary or tertiary RNA structure, or interacts with a protein or other ligand, it may have altered reactivity with DMS. For example, DMS reactivity at the N1 of A or N3 of C would be diminished when the nucleotide is involved in a Watson-Crick base pair.[249] A similar situation may occur during interactions with proteins or other ligands. If interactions reduce the reactivity of a particular nucleotide towards DMS, it can be identified by reduced band intensity on a gel compared to a DMS-only control (DMS protection) (**Figure 2.12**). If interactions with a ligand increase the reactivity of a nucleotide towards DMS, the corresponding gel band intensity increases compared to the DMS-only control (DMS exposed). The intensities of gel bands can be quantified using Image Quant Software. Therefore, normalized band intensities provide information about the interaction of ligands with RNA at the nucleotide level. In this manner, DMS reactivity can be used as a tool to monitor the RNA-ligand interactions.

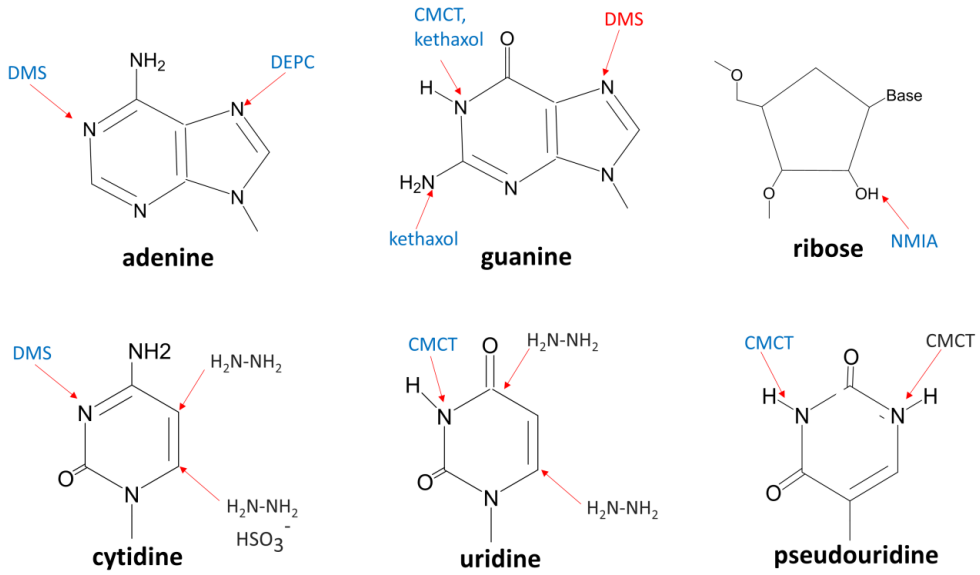

Figure 2.10 Types of chemical probing and target sites. DMS: dimethylsulfate; DEPC: diethylpyrocarbonate; NMIA: *N*-methylisatonic anhydride: CMCT: 1-cyclohexyl-(2-orpholinoethyl) carbodiimide metho-p-toluene sulfonate. The blue text shows chemical probing sites detected by direct reverse transcription analysis; red text shows modification sites detected after RNA strand scission by aniline treatment; and black text shows chemical probes used primarily for sequencing rather than structural analysis.

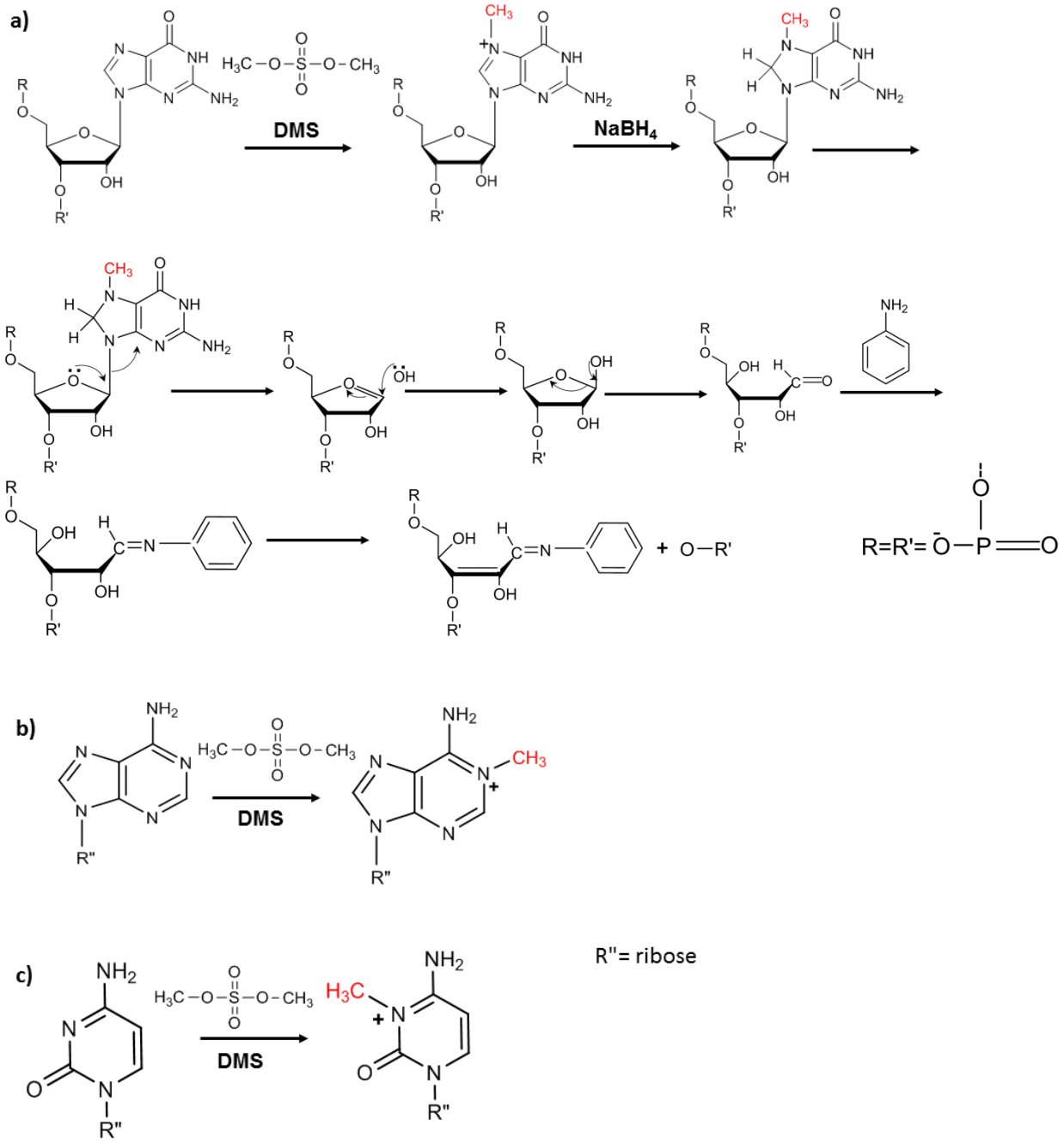

Figure 2.11 The use of dimethyl sulfate as a chemical probe. a) The general reaction scheme involves strand scission following DMS modification at G N7. b) Methylation of adenosine N1 by DMS and c) methylation of cytidine N3 by DMS are illustrated.[265]

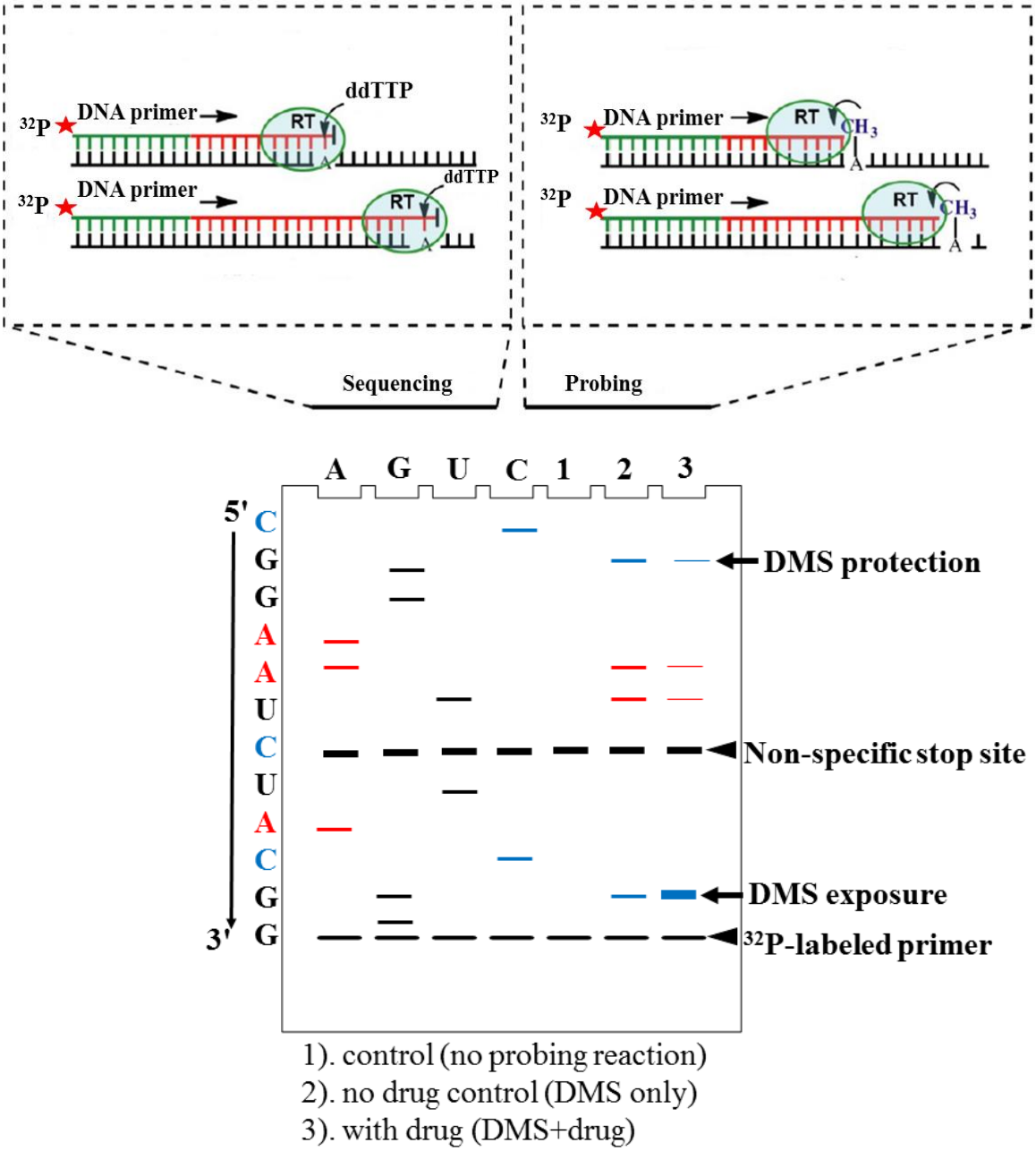

Figure 2.12 DMS footprinting gel schematic. This illustration shows a reverse transcription-based primer extension assay of RNA after DMS probing. The modified site on the gel is one nucleotide prior to the actual modified site because the dideoxy sequencing stops reverse transcription after incorporating a complementary base; the DMS modification stops reverse transcription without incorporation of the complementary base. Dideoxy sequencing lanes are labeled as C, U, G, and A (reverse transcription with ddGTP, ddATP, ddCTP, and ddTTP, respectively).

2.4.2 *In vivo* DMS footprinting

Since the folding of RNA might be different in a more complex environment such as living cells, it is highly important to study RNA structures *in vivo.* Methods and probes that are useful for studying RNA structure *in vivo* are limited. The most commonly used reagents are DMS, kethoxal, and lead (II).[265,266] Compared to other available chemical reagents, a major experimental convenience of DMS is its rapid penetration into all compartments of the cell.[267] This feature has allowed probing of RNA structure in a wide variety of cells, including gram negative and gram positive bacteria, yeast, protozoa, and plant, including the nucleus, nucleolus, and chloroplasts.[267-274] Since DMS readily penetrates cells without the need for extended permeabilization treatments, modification of RNA occurs under nearly *in vivo* conditions. Also, short incubation times at physiological temperatures allow for a quick snapshot of RNA structure *in vivo.* The method can be applied to many cultures simultaneously, facilitating direct determination of the effect of different mutations or treatments on folding of the target RNA. Using primers that are specific for a number of RNAs, the structures of multiple RNAs can be determined in the same sample. In this dissertation work, I optimized an *in vivo* DMS footprinting protocol to map the ribosome binding sites of a peptide antibiotic PrAMP, or oncocin. In the next section, the *in vivo* footprinting protocol will be discussed in detail.

2.5 Materials and Methods

Materials

Chemicals used in this experiment such as dimethyl sulfate (DMS), 2-mercaptoethanol (2-ME), sodium acetate (NaOAc), ethylenediammine tetraacetic acid (EDTA), 2-amino-2-hydroxymethylpropane-1,3-diol (Tris), phenol-chloroform-isoamyl alcohol (25:24:1) (PCI), urea, acrylamide, bisacrylamide, and isoamyl alcohol were purchased from Sigma-Aldrich (St. Louis,

MO) or Fisher Bioreagents (Fair Lawn, NJ). Lysogeny broth (LB) was purchased from Sigma-Aldrich (St. Louis, MO). Enzymes such as ImPromII reverse transcriptase (RT) and polynucleotide kinase (PNK) were purchased from Promega (Fitchburg, WI). Adenosine 5'-triphosphate γ-^{32}P (^{32}P-ATP) was purchased from Perkin Elmer Life Sciences Inc (Waltham, MA). DNA primers for primer extension (5'-GCTCAATGTTCAGTGTCA AGC-3' and 5'GAC ATCGAGGTGCCAAACAC-3') were synthesized by Integrated DNA Technologies (Coralville, IA).

Methods

2.5.1 *In vivo* DMS footprinting experiment

The DH5 strain containing ligated oncocin plasmid was streaked from a frozen stock onto a fresh LB-agar plate with kanamycin (50 μL/mL) and incubated overnight at 37 °C. A single colony was used to inoculate a 3 mL culture using LB broth and kanamycin (50 mg/mL), which was incubated overnight at 37 °C with shaking (250 rpm). From the overnight culture, 60 μL was added to LB broth (30 mL) with kanamycin (50 μL/mL) and incubated at 37 °C for 3-4 h until the optical density ($OD_{600\ nm}$) reached ~ 0.2. When cells reached early log phase, ~240 min, L-arabinose was added to a final concentration of 0.2% (w/v) to induce the expression of peptide. The incubation was continued for 1 h. The dimethyl sulfate (DMS) reaction was initiated by adding 100 μL of DMS, followed by incubation, with vigorous shaking for 5 min at 37 °C. The reaction was quenched by placing the tube on ice and adding β-mercaptoethanol (0.6 M, 5 mL) and water-saturated isoamyl alcohol (5 mL). After cooling on ice for 15 min, cells were pelleted at 5,000 rpm, at 4 °C for 30 min. The upper isoamyl alcohol phase and the lower aqueous phase was carefully removed from the pellet. The cell pellet was resuspended in β-mercaptoethanol (0.6 M, 5 mL) and centrifuged again (5000 rpm, at 4 °C for 30 min). The supernatant was

carefully removed and the cell pellet was washed with 1.5 mL ice-cold Tris-saline buffer (10 mM Tris-HCl, pH 8, 100 mM NaCl, 1 mM EDTA) and centrifuged again (5000 rpm, 10 min). Control experiments (no DMS, no drug) were carried out simultaneously. The cell pellet was used for the total RNA isolation as described below.

2.5.2 Total RNA isolation

The cell pellet was resuspended in 200 μL of AE buffer (50 mM sodium acetate pH 5.2, 10 mM EDTA). Sodium dodecyl sulfate (SDS) was added to a final concentration of 1%. An equal volume of phenol: isoamyl alcohol: chloroform (PCI) was added and the mixture was incubated at 65 °C for 4 min. The samples were immediately put in -20 °C freezer to cool down and allowed to thaw at room temperature. Samples were centrifuged (14,000 rpm at 4 °C for 10 min) and the supernatants were transferred to a new tube. The supernatant was subjected to phenol-chloroform extraction at least two times. Extracted RNA was isolated by doing ethanol precipitation. The purity of isolated total RNA was checked by agarose gel electrophoresis.

2.5.3 Radiolabeling of DNA at the 5' end

For the labeling of 50 pmol DNA, 10 μCi [γ^{32}P]–ATP and 10 units T4 polynucleotide kinase were reacted in T4 polynucleotide kinase buffer (50 mM Tris·HCl, pH 7.6, 10 mM $MgCl_2$, 5 mM DTT, 0.1 mM spermidine, and 0.1 mM EDTA). The total volume was adjusted to 50 μL with ddH_2O and the sample was incubated at 37 ^oC for 45 min. The labeled DNA was isolated by ethanol precipitation. The dried DNA pellet was redissolved in 50 μL of ddH_2O.

2.5.4 Reverse-transcription and primer extension reactions

The appropriate DNA primers were radiolabeled with [γ - ^{32}P] ATP at the 5' end as described earlier. RNA (500 ng) and 1 μL of radiolabeled primer (60,000-100,000 cpm) were incubated together at 80 °C for 3 min and then the mixture was cooled to room temperature for 5

min. The master mixture for a reverse transcription reaction was prepared by combining 24 units of ImProm-II reverse transcriptase enzyme, 1 μL of 5× reverse transcriptase reaction buffer, and 0.4 μL of 50 mM $MgCl_2$. To the primer-annealed platinated rRNA, 1.65 μL of the master mixture, 1 μL of dNTP (10 mM), and ddH_2O (total volume 5 μL) were added. Primer extension was carried out at 43 °C for 1 h. For sequencing, total RNA was used with the corresponding radiolabeled primer. For the sequencing reverse transcription reaction, 1 μL of dNTP: ddNTP 1:4 (0.5 mM:2 mM) was used instead of the dNTP mixture. Termination of the reactions was done by heating the reaction mixture at 95 °C for 2 min after adding 2 μL of denaturing loading dye (80% formamide, 1× TBE, 0.02% bromophenol blue, 0.02% xylene cyanol) and quickly placing on ice. Reactions (50,000 cpm per lane) were loaded onto 10% denaturing polyacrylamide gels (0.4 mm thick, acrylamide: bisacrylamide 19:1, 0.5× TBE, 7 M urea). Gels were run at 33 V/cm for approximately 3 h. Gels were exposed to a phosphor screen overnight and imaged on a Molecular Dynamics Phosphorimager and analyzed using ImageQuant software.

2.6 Evaluate the effects of pseudouridine (Ψ) modifications on the antibacterial activity of 2-deoxystreptamine aminoglycosides

The main focus of **Chapter 5** is evaluation of the effects of Ψ modifications in H69 on the antibacterial activity of the 2-deoxystreptamine class of aminoglycosides. The approach was to compare the susceptibilities of modified and unmodified bacterial strains to different aminoglycosides. In this work a series of MIC experiments was carried out using the broth micro dilution method. A brief description of the MIC methodology and details of the experimental protocol will be discussed in the following section.

2.6.1 Minimum inhibitory concentration (MIC) studies

Minimum inhibitory concentration (MIC) is defined as the lowest concentration of an antibiotic that will inhibit the visible growth of bacteria being investigated. MIC values are used to determine susceptibilities of bacteria to drugs and also to evaluate the activity of new antimicrobials agents. In clinical practice, this *in vitro* parameter is used to classify the tested microorganisms as clinically susceptible, intermediate, or resistant to the tested drug.[275,276] The interpretative standards for these classifications are published by different national organizations such as the Clinical and Laboratory Standards Institute (CLSI) in the USA and the European Committee on Antimicrobial Susceptibility Testing (EUCAST).[277,278] MIC determinations can be used for monitoring the development of antibiotic drug resistance. MIC wild-type distribution databases are available for relevant species-drug combinations. The highest MIC of the wild-type population is defined as the epidemiological cut-off value or the wild-type cutoff value. Organisms that acquired resistance can be easily identified by showing higher MIC values than the epidemicological cut-off value.[279-281] As even slight changes may become clinically relevant, the determination of MIC is a valuable means for resistance surveillance, as well as providing a valuable comparator for variants of a given antimicrobial agent and/or species with differential susceptibility. Indeed for new drug candidates, the MIC determination is one of the first steps to evaluate antimicrobial potential.

In this dissertation work, the MIC method was utilized as a tool to study the effects of rRNA modifications on the *in vivo* activities of antibiotics. In previous studies, the MIC method together with *in vitro* binding studies was employed to evaluate the effects of rRNA modifications on the antibacterial activity of aminoglycosides. For example, in one study it was shown that mutations in 16S rRNA distrupt *in vitro* binding of aminoglycosides.[282] In this work,

in vitro binding studies were done by chemical probing experiments with mutant and wild-type ribosomes. In the same study, *in vivo* activity was measured by MIC experiments with mutant and wild-type bacterial strains. In this manner, altered drug interactions with the target can be implied if the *in vitro* data correlate with resistance observed *in vivo*. Binding studies are often carried out with model RNAs or isolated ribosomes and therefore confined to *in vitro* systems. In contrast, MIC data allow direct effects of rRNA modifications on the antibacterial activities of drug to be assessed. Higher MIC values may indicate that rRNA modifications cause drug resistance, whereas lower MIC values indicate that rRNA modifications increase susceptibility of bacteria to the drugs. Therefore, it is important to carry out *in vitro* binding and MIC studies together to evaluate the effects of rRNA modifications on drug activity.

2.6.2 Agar and broth dilution methods

Agar and broth dilution are the most commonly used techniques to determine the MIC values of antimicrobial agents.[275,276,283] For agar dilution, solutions with defined numbers of bacterial cells are spotted directly onto the nutrient agar plates that have incorporated different antibiotic concentrations. After incubation, the presence of bacterial colonies on the plate indicates growth of the organism. Broth dilution uses liquid growth media containing geometrically increasing concentrations (typically a two-fold dilution series) of the antimicrobial agents, which is inoculated with a defined number of bacteria cells. The final volume of the test defines whether the method is termed macro dilution, (< 2 mL), or micro dilution (microtiter plates using > 500 µL per well) (**Figure 2.13**).

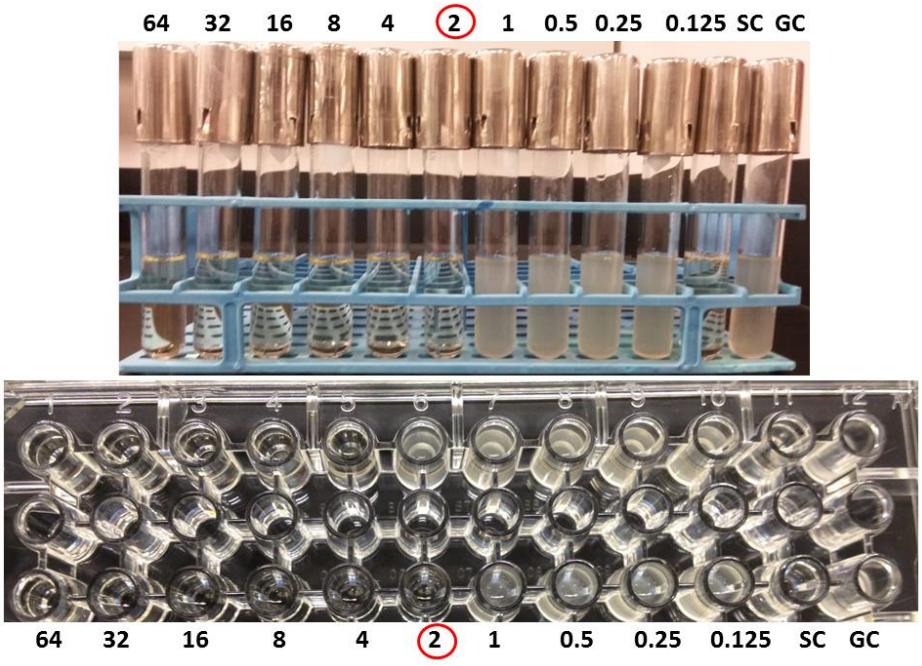

Figure 2.13 Broth dilution methods. a) Broth macro dilution and b) broth micro dilution results are shown for neomycin as an example. The MIC value is represented by a red circle in each experiment. SC is the sterility control and GC is the growth control.

After incubation, the presence of turbidity indicates growth of the organism. In both agar and broth dilution approaches, the MIC is defined as the lowest concentration (in mg/L) of the antimicrobial agent that prevents visible growth of a microorganism under defined conditions. Broth macro dilution method has been widely used to determine MIC.[283] However, the tedious procedure and need for large amounts of drugs make the macro dilution method undesirable for studying expensive compounds such as antimicrobial peptides.[283,284] Therefore, the broth micro dilution method has become the most common and popular and practical method for MIC experiments. In this dissertation work, broth micro dilution was employed to determine the MIC of different antibiotics. The protocol was adapted from a standard protocol for antimicrobial susceptibility testing that was published by CLSI.[275,277]

2.7 Materials and Methods

Materials

Mueller Hinton broth (MHB) was purchased from Becton, Dickinson, and Company. All of the antibiotics used in the study, neomycin sulfate, paromomycin sulfate, kanamycin sulfate capreomycin sulfate, gentamicin, streptomycin sulfate, spectinomycin sulfate, and carbenicillin were purchased from Sigma-Aldrich (St. Louis, MO). Clear bottom 96-well plates were purchased from Sigma-Aldrich (St. Louis, MO). *E. coli* MC415 *(*wild-type, ΨΨΨ) and *E. coli* MC416 RluD(–), UUU) were provided by Professor Michael O'Connor's lab, University of Missouri (Kansas City, MO).

Methods

2.7.1 Preparation of the bacterial suspension

Bacterial isolates to be tested were streaked from a frozen stock onto LB-agar plates without antibiotics to obtain single colonies. Plates were incubated overnight at 37 °C. Mueller Hinton broth (3 mL) was inoculated with a single colony of bacteria. The inoculated broth was incubated for 4 to 6 h at 37 °C in a shaker at 225 rpm until it reached a visible turbidity. The turbidity of the bacterial suspension was verified by measuring the absorbance of the suspension spectrophotometrically ($OD_{600\ nm}$ at 0.08 to 0.13). The bacterial suspension was adjusted to 1×10^8 cfu/mL and diluted by a factor of 1:100 by adding 200 µL bacterial suspension to 19.8 mL sterile Muller Hinton broth. After turbidity adjustment, the bacterial suspension was used within 30 min, as the cell number might otherwise change.

2.7.2 Broth micro dilution method

Antibiotic dilutions were prepared in sterile Mueller Hinton broth 96-well plate. Antibiotic concentrations ranged from 43 to 0.02 mg/L. As the antibiotic solution was inoculated

with an equal amount of bacteria in broth, the dilutions were prepared at a concentration twice the desired level. Each well of the microtiter plate was labeled with the respective antibiotic concentration. The sterility and growth control wells were filled with 100 and 50 μL, respectively, of the sterile broth. After turbidity adjustment of the bacteria suspension, the microtiter plate was inoculated by adding 50 μL of bacteria to each well (with the exception of negative control). The optical density ($OD_{600\ nm}$) of bacteria was taken after initial treatment. The plate was incubated at 37 °C for 24 h. The bacterial growth was monitored by measuring optical density ($OD_{600\ nm}$). Percent inhibition of bacterial growth in the presence of different drug concentrations was calculated and normalized to the growth control using formula below.[285]

$$\%\ \text{inhibition of growth} = 100 - \left[\frac{(OD_{600nm\ 24\ h} - OD_{600nm\ initial})_{drug}}{(OD_{600nm\ 24\ h} - OD_{600nm\ initial})_{growth\ control}} \times 100 \right]$$

CHAPTER 3 *IN VIVO* EXPRESSION AND RIBOSOME MAPPING OF A PROLINE-RICH ANTIMICROBIAL PEPTIDE, ONCOCIN, IN *ESCHERICHIA COLI*

3.1 Abstract

The development of short peptides that specifically bind to higher-order structures of ribosomal RNA is one promising way to address the problem of antibiotic resistance. Recent studies in several laboratories, including ours, have identified short peptide sequences targeting the bacterial ribosome.[191,192,215,216,221-223] The poor correlation between *in vitro* and in *vivo* activities of these peptides is one of the major questions in antibiotic peptide research. Therefore, one of the main objectives of my dissertation work was to utilize a plasmid-based system to *in vivo* express ribosome-targeting peptides and study their direct inhibitory effects on bacteria. In this chapter, the main focus is oncocin, a proline-rich antimicrobial peptide known to target the bacterial ribosome.[215,221-223,225] A specific plasmid system was optimized to *in vivo* express oncocin and its variants in bacteria. The direct inhibitory effects of *in vivo*-expressed peptides were measured by doing bacterial growth assays. Our data show that the *in vivo*-expressed-peptide completely inhibits bacterial growth and displays bactericidal activity. According to previous biochemical and structural data, oncocin is known to inhibit bacteria by targeting the bacterial ribosome.[221,223,225] Since our system allows us to *in vivo* express the bioactive peptide, it is of interest to probe its interactions with the ribosome in an actual cellular environment. The dimethyl sulfate (DMS) footprinting protocol was optimized to *in vivo* map the ribosome binding sites of oncocin. Our footprinting data revealed interactions of oncocin with the PTC region of the bacterial ribosome. To the best of our knowledge, this is the first effort to use DMS footprinting to *in vivo* probe peptide-ribosome interactions.

3.2 Introduction

Antimicrobial peptides (AMPs) are essential components of the innate immune system.[199,202] Being "nature's antibiotics", AMPs form the first line of host defense against pathogenic infections.[202-204] During the past few decades, AMP research has grown rapidly in response to the demand for novel antibacterial agents to treat multi-drug resistance pathogens.[199,204] Although most of these AMPs inhibit bacteria by permeabilizing the membrane, the action of AMPs is not limited to the surface of pathogens.[212] Recently, subclasses of AMPs have been identified that inhibit bacterial growth by targeting fundamental intracellular processes.[286] The proline-rich AMPs (PrAMPs) belong to one such subclass that targets the ribosome and interferes with protein translation in bacteria.[218,222,225] The activity of PrAMPs against gram-negative bacteria was discovered more than 25 years ago with the isolation of apidaecins from honey bee (*Apis melifera*)[287] and bactenecins from cattle (*Bos taurus*)[288] in the late 1980s. Initially, PrAMPs were found in mammals and insects. They include cathelicidin-derived peptides bactenecin and PR-39 from mammals and oncocin, drosocin, pyrrhocoricin, and apidaecin from insects. Subsequently, they were also found in other animal species, such as crustaceans, amphibians, and molluscs.[218] Even though PrAMPs have different origins, all of them are characterized as cationic AMPs with a high content of proline (typically 25 to 50%) and arginine, often arranged in conserved patterns (**Table 3.1**).

Oncocin (VDKPPYLPRPRPPRRIYNR) is a PrAMP derived from *Oncopeltus fasciatus* (milkweed bug),[215,289] which has been optimized to be effective against gram-negative human pathogens.[215] Interestingly, recent studies have shown that PrAMPs such as oncocin target the bacterial ribosome and inhibit protein translation.[216,221] Most recently, two groups independently identified the binding site of oncocin to the 50S subunit of the *Thermus thermophilus* 70S

ribosome, where it blocks the peptidyl transferase center (PTC) and destabilizes the initiation complex.[222,223] These structures reveal peptide binding to the PTC region of the ribosome (**Figure 3.1**). Upon binding to the upper region of the peptide exit tunnel, oncocin interferes with binding of the aminoacyl-tRNA in the A site. Although it allows formation of the initiation complex, the steric occlusion caused by the 19-mer peptide destabilizes the initiation complex and causes dissociation.[216,222,223] Therefore, oncocin inhibits protein translation by inhibiting the transition from initiation to elongation (**Figure 3.2**).[216,222,223]

Table 3.1 Amino acid sequences of some selected PrAMPs

Peptide	Sequence	References
Bac7	**RRIRPRPPRLPRPRPRPLPFPRPGPRPIPRPLPFP**	**219**
Pyrrhocoricin	**VDKGSYLPRPTPPRPIYNRN**	**290**
Metalnikowin	**VDKPDYRPRPRPPNM**	**291**
Oncocin	**VDKPPYLPRPRPPRRIYNR**	**215,292**
Oncocin112	**VDKPPYLPRPRPPRrIYNr**	**223,289**
Oncocin72	**VDKPPYLPRPRPPROIYNO**	**216,289**

r =D - Arg ; O = Ornithine
The conserved residues of selected PrAMPs are highlighted in blue. The underlined residues correspond to the common core region.

Previous structural and biochemical data suggest that the N-terminal residues of oncocin are responsible for targeting this peptide to the ribosome.[216,223] The positively charged amino acid residues distributed along the entire peptide sequence are necessary for efficient cellular uptake of the peptide.[221,223] The inner membrane protein SbmA, which is a part of the ABC transporter system, is responsible for the cellular uptake of oncocin. SbmA transporters are specific to gram-negative bacteria.[293] Therefore, oncocin does not penetrate through mammalian cell membranes, which makes it non-toxic to mammalian cells even at high concentrations.[170,210]

Recent studies have shown that PrAMPs such as oncocin can be shuttled into mammalian cells by cell-penetrating peptide penetratin.[294]

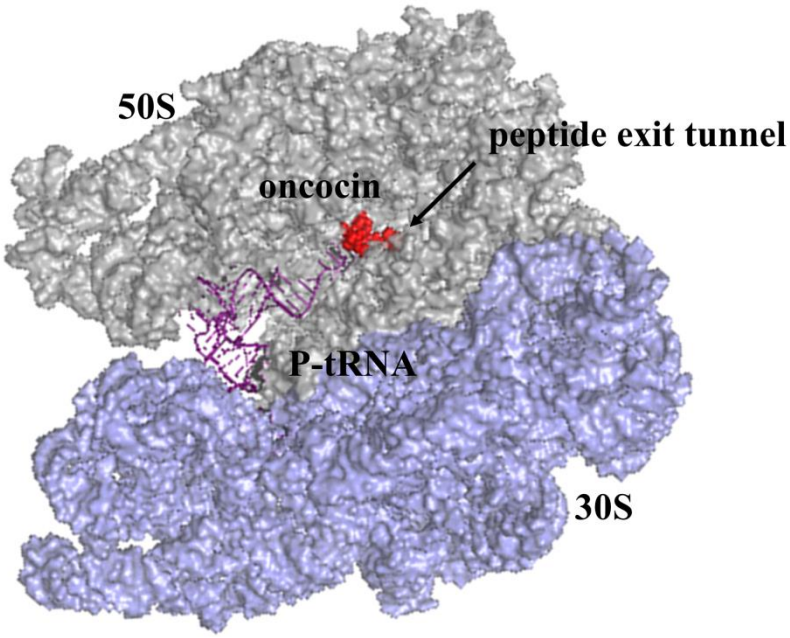

Figure 3.1 A crystal structure of the oncocin-ribosome complex. The structure of oncocin (red) and the P-site $tRNA^{fMet}$ (purple) bound to the 70S ribosome (PDB: 5HCR) is shown.[221] The 50S and 30S subunits are shown in grey and blue, respectively.

Oncocin was optimized to treat gram-negative pathogens such as *Escherichia coli, Pseudomonas aeruginosa,* and *Acinetobacter baumannii.*[215] Its minimal inhibitory concentrations range from 0.125 to 8 μg/mL for 34 different strains and clinical isolates from *Escherichia coli, Pseudomonas aeruginosa,* and *Acinetobacter baumannii.*[215] The amino acid sequence of oncocin was optimized to produce derivatives with improved antibacterial activity and stability. Onc112 and Onc72 are examples of optimized oncocin derivatives (**Table 3.1**).[289] The pharmacokinetic profiles explain the high *in vivo* efficacies in models of systemic infection and indicate the potential use of these oncocin derivatives for the treatment of urinary tract infections.[295]

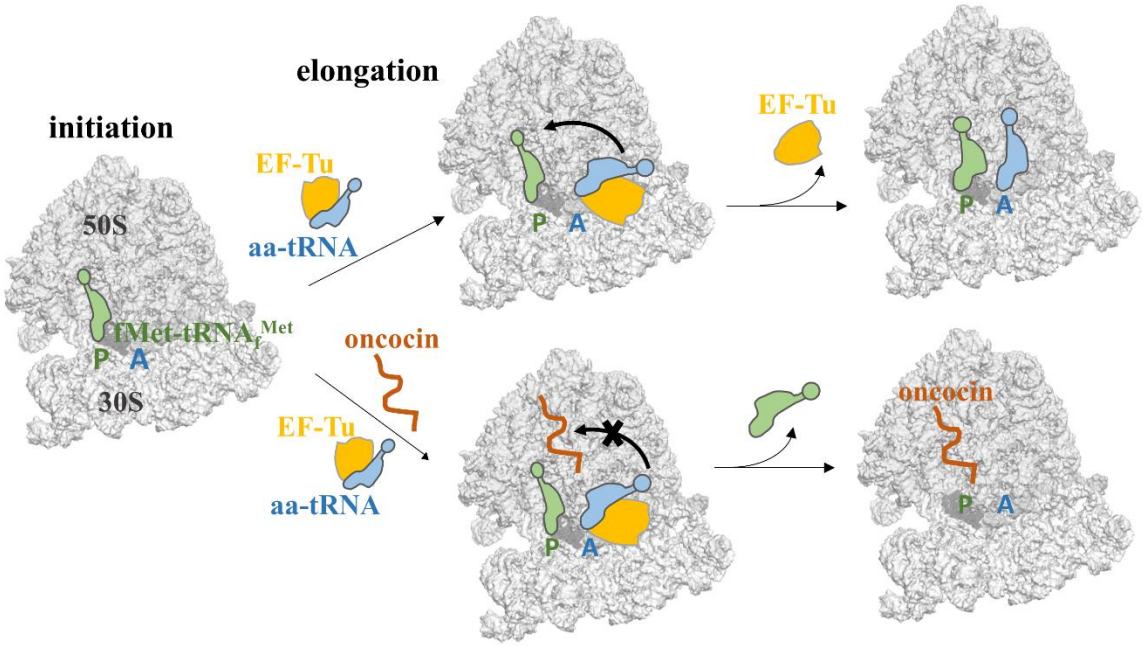

Figure 3.2 Inhibition of protein synthesis by oncocin. a) Model for the mechanism of action of oncocin is shown. The upper panel shows the main steps involved in canonical translation in the absence of protein synthesis inhibitors. Translation begins with initiator tRNA (green) binding to the ribosomal P site. During elongation, the aa-tRNA is delivered by EF-Tu to the A site, followed by tRNA accommodation into the A site on the large subunit and subsequent departure of EF-Tu. In the presence of PrAMPs, such as oncocin, aminoacyl tRNA (aatRNA) delivery can occur, but the aa-tRNA accommodation step is blocked. The initiation complex is destabilized, thus leading to dissociation from the P site.

In 2015, two groups independently identified the binding site of oncocin 112 to the 50S subunit of the *Thermus thermophilus* 70S ribosome, where it blocks the PTC and destabilizes the initiation complex.[222,223] According to the crystal structure, the binding site of oncocin within the ribosomal exit tunnel overlaps with the binding site of many clinically important classes of antibiotics such as the macrolides (*e.g.*, erythromycin), which aborts translation by interfering with movement of the nascent polypeptide chain through the ribosomal exit tunnel.[221-223] Chloramphenicols, pleuromutilins (*e.g.*, tiamulin), and lincosamides (*e.g.*, clindamycin) sites also overlap; these compounds inhibit peptide-bond formation by preventing correct positioning of the tRNA substrates.[221-223] Even though it is very promising for the development of novel

antibiotics, it is unclear whether resistance mutations that arise against currently used antibiotics will also confer cross-resistance against oncocin. The development of novel antimicrobial compounds based on PrAMPs such as oncocin is a possible approach to overcome multi-drug resistant pathogenic bacteria.

3.3 Objectives of this project

The poor correlation between *in vitro* and *in vivo* activities of antimicrobial peptides is one of the major questions in antibiotic peptide research. Therefore, in contrast to *in vitro* methods, the main objectives of my dissertation work were to develop a biological approach for in-cell synthesis of peptide antibiotics. I optimized a specific plasmid system to *in vivo* express the ribosome-targeting peptide oncocin and studied its direct inhibitory effects on bacteria. Since the system allows us to synthesize peptides inside bacteria, it has several other downstream applications **(Figure 3.3)**. The system was utilized to *in vivo* express oncocin variants and study their inhibitory activities. Furthermore, *in vivo* DMS footprinting experiments were carried out to map the ribosome binding sites of oncocin. The objective of this chapter is to emphasize the different applications and advantages of the *in vivo* peptide expression approach using oncocin as a model peptide. The *in vivo* peptide expression approach provides important information about the biological function and peptide-target interactions in actual cellular environment.

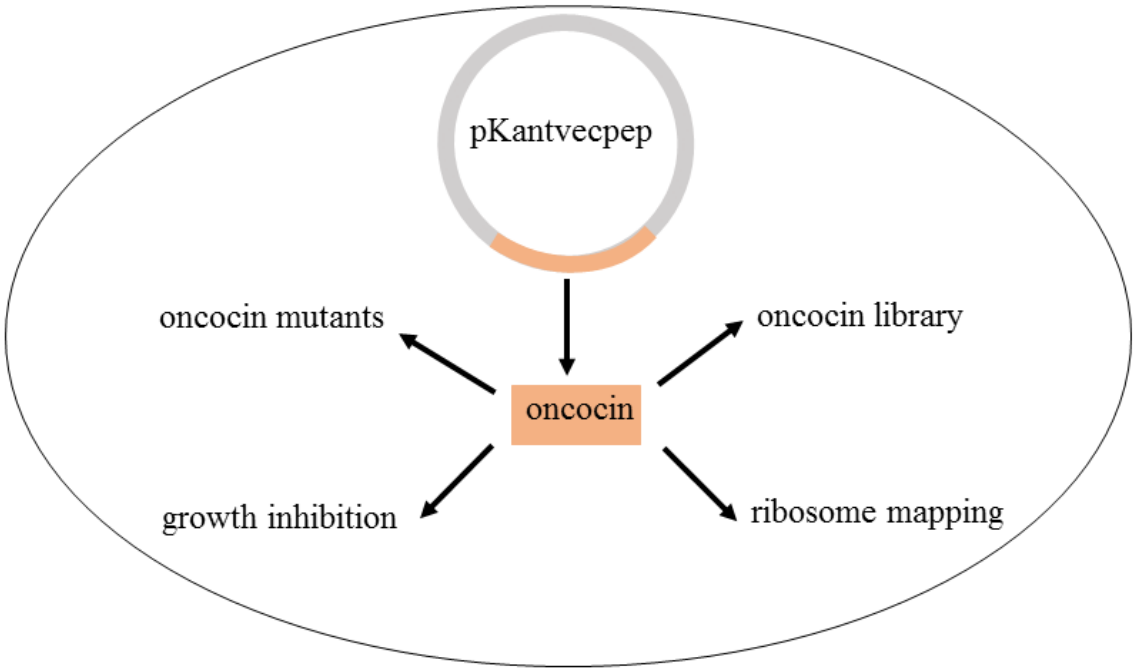

Figure 3.3 Different applications of *in vivo* peptide expression in bacteria. As explained in Chapter 2, the pKantvec plasmid system was utilized to *in vivo* express oncocin as a free peptide in bacteria. After expression, its direct inhibitory effects on bacterial growth were measured by doing growth assays. Oncocin-ribosome interactions were determined by doing *in vivo* DMS footprinting experiments. An *in vivo* alanine scan was carried out by expressing alanine mutants of oncocin followed by growth assays. In order to identify oncocin-derived AMPs, an oncocin-based *in vivo* peptide library was constructed.

3.4 Results and discussion

3.4.1 Cloning of oncocin peptide into the plasmid system

The proline-rich antimicrobial peptide oncocin was chosen for this study. A single plasmid expression system, pKan5tvVec (8243 bp) with an inducible P_{BAD} promoter and kanamycin resistance, was used as the vector. Dr. Wesley Colangelo (Cunningham lab) prepared the plasmid for this experiment. The restriction enzyme sites *Hind* III and *Nhe* I were used to clone the peptide insert into the plasmid. As explained in the experimental methods section in Chapter 2, the primer extension PCR method was used to generate the corresponding DNA sequences that code for the desired peptide sequences. The size of the DNA product

corresponding to 19-mer peptide sequence is 135 bp. The PCR product was checked on an agarose gel before the restriction digestion (**Figure 3.4**).

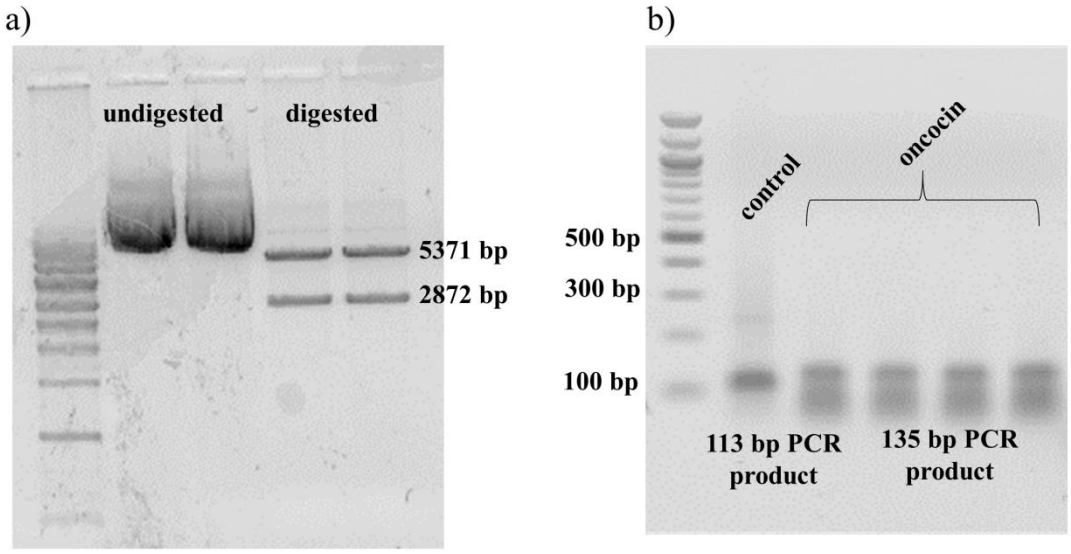

Figure 3.4 Plasmid vector and peptide-insert preparation. a). Plasmid pkan5tvec (8243 bp) was digested using *Nhe* I and *Hind* III restriction enzymes and the gel band corresponding to the desired vector fragment (5371 bp) was purified before ligation. b) The insert was synthesized using the non-template PCR method and purified before and after restriction digestion. The size of the PCR prodcut of oncocin is 135 bp. The control lane contains a 113 bp DNA product for comparison.

The DNA products were gel purified and ligated to obtain the new plasmid pPep-oncocin (5485 bp) (**Figure 3.5**). The genes were cloned behind the P_{BAD} promoter of the plasmid pKan5tvVec such that the peptides could be expressed by inducing with L-arabinose. The ligated plasmid was transformed into *E. coli* DH5 electrocompetent cells. The sequence of the peptide clone was confirmed by doing DNA sequencing (**Figure 3.6**).

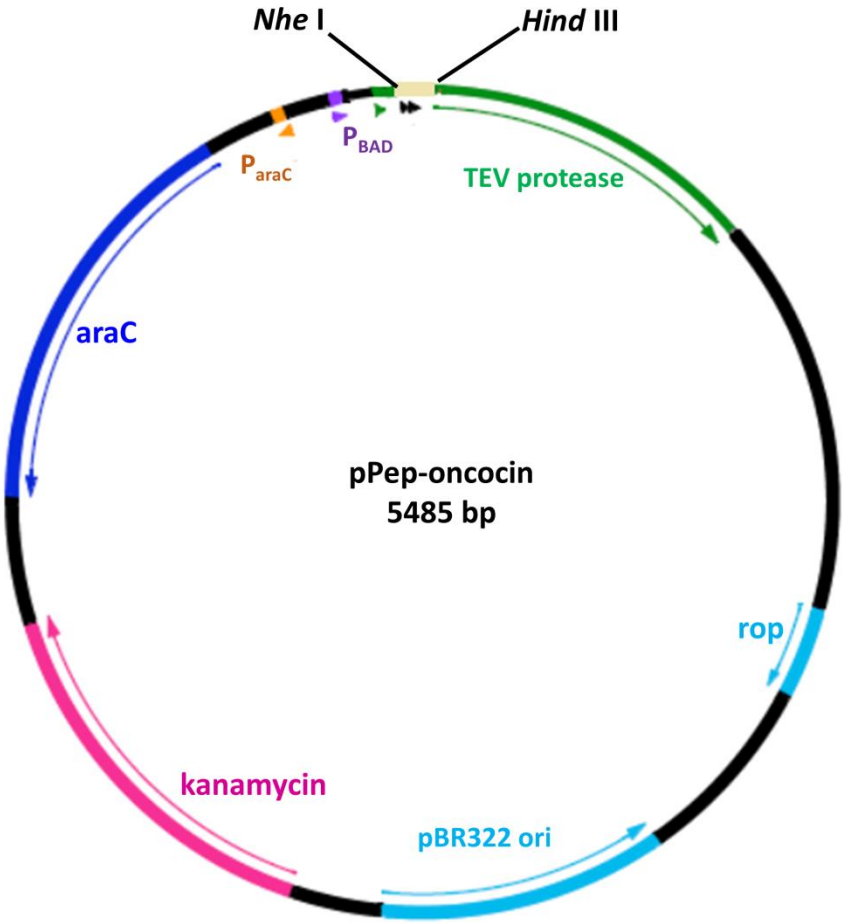

Figure 3.5 Plasmid map of pPep-oncocin. The restriction enzyme sites *Nhe* I and *Hind* III were used to clone the peptide insert into the plasmid. The expression of the peptide and TEV-protease was controlled by the P_{BAD} promoter. The plasmid shows kanamycin resistance.

In a previous study, it was shown that cloning of the peptide sequence right after the start codon completely inhibited translation of the peptide.[193] Therefore, in this study the peptide sequence was cloned behind the TEV (Tobacco Etch Virus) protease recognition sequence (ENLYFQG/S). The protease enzyme specifically cleaves between residues Q and G/S of its recognition sequence, resulting in an extra G or S amino acid at the N-terminus of the peptide sequence.[242,245] Although the wild-type TEV protease recognition sequence is ENLYFQG/S, studies have shown that any amino acids after Q in the ENLYFQ/S sequence could cleave efficiently such that the exact peptide sequence is exposed after TEV cleavage.[231,242,243,246]

Therefore, a primer was designed that excluded the codon corresponding to the C-terminal G residue of the oncocin peptide. Therefore, after TEV protease cleavage the exact N-terminus sequence of the oncocin peptide would be exposed (**Figure 3.7**).

a)

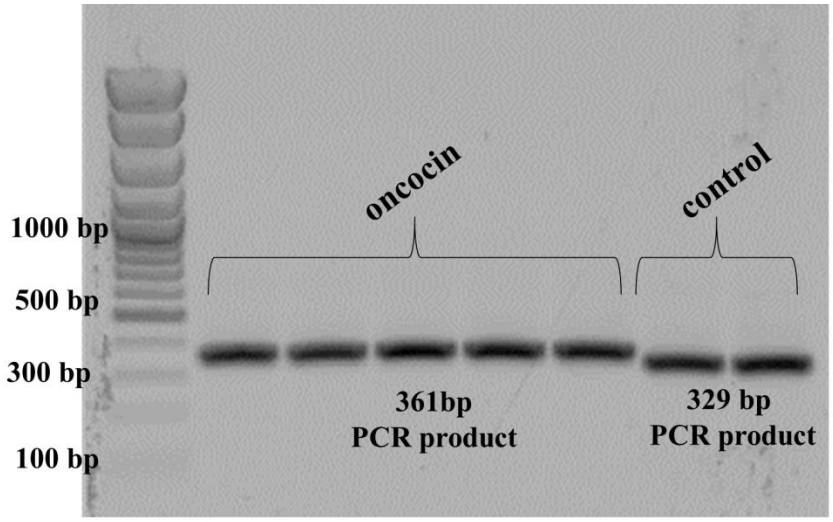

b)

Figure 3.6 Peptide sequence confirmation. a) The peptide clones were confirmed by doing colony PCR, which gave 361 bp PCR products for the 19-mer peptide in colony PCR. Control lanes contain a 329 bp DNA product for comparison. b) The sequence alignment of ligated plasmid pPep-oncocin. The full alignment is 1020 bp, whereas this section only shows the nucleotide sequence of the TEV recognition sequence in the first box (green) with the amino acid sequence labeled in green. The amino acid sequence of oncocin is shown in red and the corresponding nucleotides are in box 2 (red).

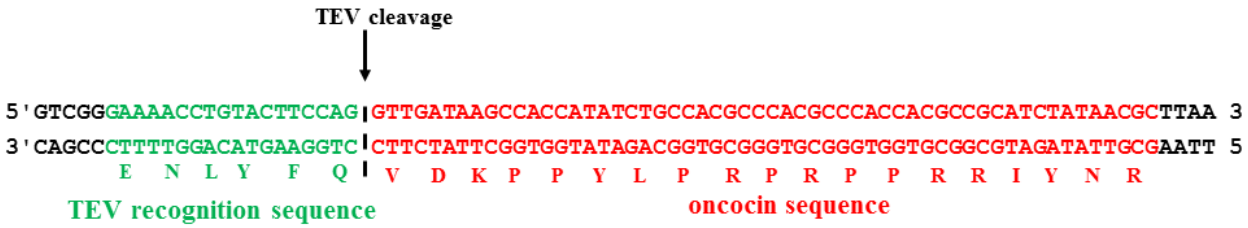

Figure 3.7 TEV cleavage site. Oncocin primers were designed excluding the C-terminal G residue of the wild-type TEV recognition sequence (ENLYFQG). Therefore, TEV protease cleavage occurs between Q and V, resulting in the exact oncocin peptide sequence.

3.4.2 Study the effects of oncocin on bacterial growth (bacterial growth assay)

After confirming the sequence of each peptide clone, they were used in bacterial growth assays as described earlier. Bacteria were grown in LB/kanamycin medium. When cells reached late lag phase or OD_{600nm} = 0.2, (~200 min), L-arabinose was added to induce the expression of peptides. Cell growth was measured with and without adding inducer. The bacterial growth was monitored by measuring the optical density of all bacteria cultures every 60 min (**Figure 3.8**). In growth assays, DH5 strain CSL011 from the Cunningham lab, which expresses peptide KGTRAFATTNSH, was utilized as a positive control. In previous studies in the Cunningham lab, this 12-mer peptide inhibited bacterial growth.[231] The 7-mer peptide AAAAAAA was used as a negative control, and did not show growth inhibition in previous experiments. All of the induced cultures, including the controls, showed slower growth rates as compared to the un-induced cultures (**Figure 3.8a**). This effect was likely due to the high stress on cells created by the over-expressed mRNA or proteins. Compared to the negative control peptide GAAAAAAA, complete inhibition of bacterial growth was observed in the cultures that expressed oncocin (**Figure 3.8a**).

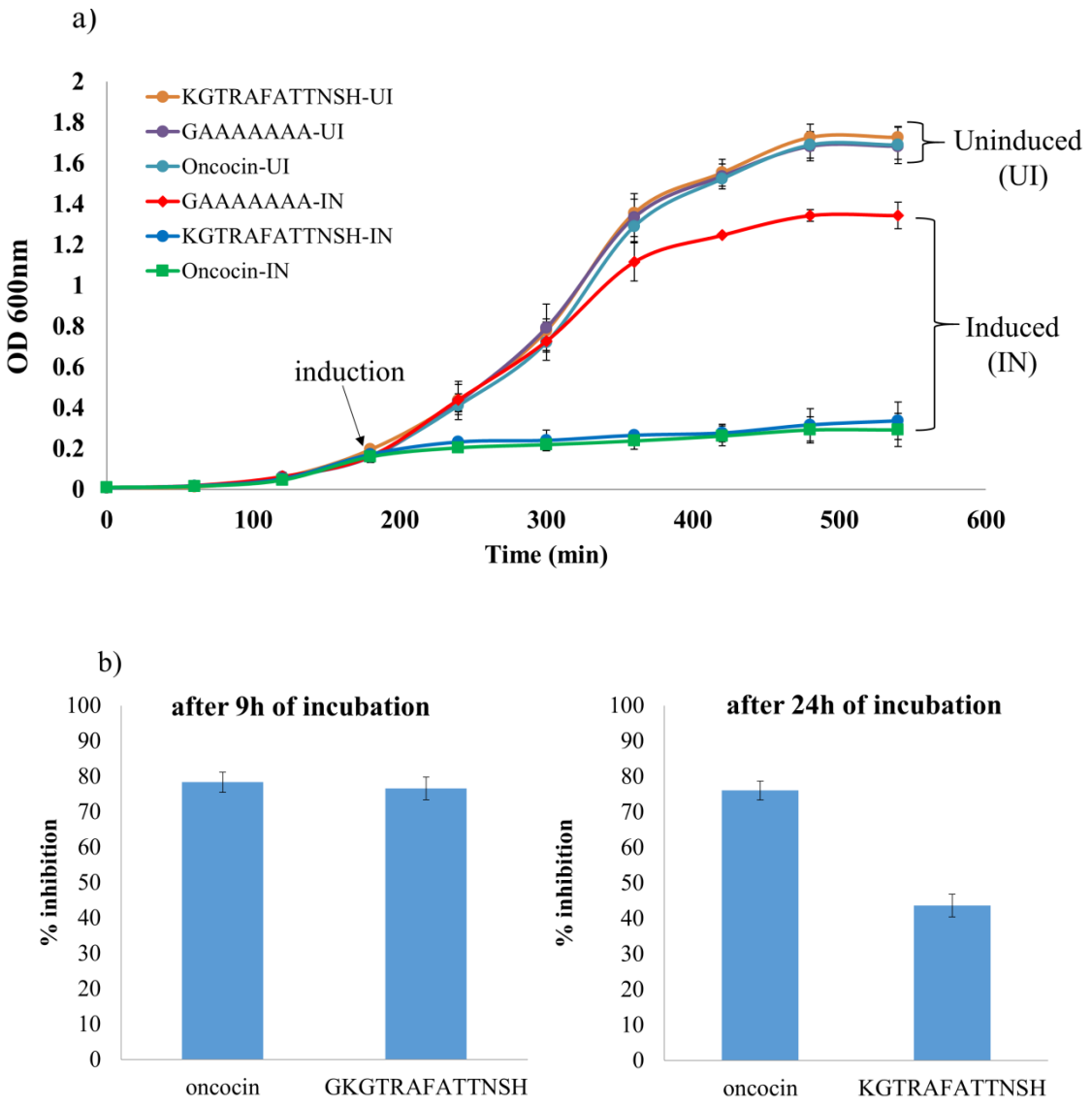

Figure 3.8 Oncocin impacts on growth assay. a) Effects of the expression of different peptides on bacterial cell growth were assessed. Oncocin-UI is the uninduced growth curve for the pPep-oncocin plasmid, whereas, Oncocin-IN is its induced partner. Peptide-induced cultures show slower growth compared to the uninduced cultures. b) Percent inhibition of bacterial growth after 540 min (9 h) (left), or 24 h (right) upon expression of different peptides was measured and normalized to the negative control (induced GAAAAAAA). All growth assays were performed at least three times independently and results were averaged.

After 540 min (9 h) of incubation, both oncocin and the positive control peptide showed ~ 80% inhibition of growth (**Figure 3.8b**). Interestingly, even after overnight incubation oncocin showed complete inhibition of bacterial growth, which was not observed with the positive

control peptide. This behavior suggests strong bactericidal activity of oncocin compared to the positive control peptide. After 9 h of incubation, 50 μL of bacteria was taken out and plated in LB/agar medium and incubated at 37 °C. After overnight incubation, we did not observe colonies on plates incubated with bacteria expressing oncocin. However, an average of 60 colonies were observed on plates incubated with bacteria expressing the positive control peptide. This observation demonstrated the bactericidal activity of oncocin directly compared to the positive control peptide. Therefore, our data are in a good agreement with the previously reported information about oncocin as an antimicrobial peptide.[221,289] Furthermore, our data suggest that the plasmid-based system can be utilized to identify *in vivo* antibacterial activities of peptides. In previous studies, this system was utilized to *in vivo* express only 7-mer peptides.[193,231] However, by *in vivo* expressing oncocin, we showed that the system can be used for the recombinant expression of even larger peptides.

After optimizing the plasmid system to *in vivo* express peptides, we considered the possible applications of the plasmid system. The *in vivo* peptide expression approach could be useful in AMP optimization processes. After identifying an AMP from a natural source or from a peptide library screen, the next critical step is to obtain optimized structural analogs. Usually the optimization process is done by minimizing the peptide length and systematically substituting each amino acid residue.[235] This process is typically expensive and time consuming due to the need to employ solid-phase peptide synthesis (SPPS).[235] For example, the bioactive oncocin peptide sequence we utilized in this study was obtained after a very long optimization process.[215] Oncocin is the optimized peptide sequence of Oncopeltus antibacterial peptide 4, which was originally isolated from *Oncopeltus fasciatus* (milkweed bug) together with three other AMPs.[292] Since, the original peptide sequence isolated from milkweed bug did not show considerable

antimicrobial activity, its sequence was optimized to obtain a bioactive peptide sequence.[215] In this process, peptide variants were chemically synthesized using SPPS and utilized in MIC studies with different bacteria strains. Finally, they came up with the bioactive 19-mer peptide sequence of oncocin (VDKPPYLPRPRPPRRIYNR-NH_2), which was found to be active against 37 different isolates of *E. coli*, *K. pneumoniae*, *P. aeruginosa*, *A. baumannii*, *E. cloacae*, and *Proteus vulgaris*.[215] Despite the favorable antibacterial spectrum of AMPs, there are multiple obstacles to be overcome in their further development for therapeutic consideration.

Recently, one research group in Germany used rational design to optimize the oncocin sequence. In this work, they found several oncocin derivatives with improved protease stability and antibacterial activity.[289] The relatively high cost of SPPS compared to bacterial production is considered as one of the major limitations in AMP research. Recent evidence suggests that the production cost of a 5000 Da peptide exceeds the production cost of a 500 Da small molecule by more than 10-fold.[235] Therefore, the high cost of SPPS for clinical applications is a challenge in the AMP optimization process.[200,229] This *in vivo* peptide expression approach has several advantages in AMP optimization. The bacterial production of peptides is cost effective and less time consuming compared to SPPS. On the other hand, *in vivo* approaches allow the study of peptide activities in actual cellular environments which is not possible with *in vitro* experiments. Considering these facts, one of the possible applications of this plasmid system is *in vivo* expression of AMP variants and the study of their *in vivo* activities. In this dissertation work, an *in vivo* alanine scan experiment of oncocin was carried out. The main focus of the next section of this chapter is *in vivo* expression and evaluation of the activities of the alanine mutants of oncocin.

3.4.3 *In vivo* expression of alanine mutants of oncocin

Previous structural and biochemical data suggested that the N-terminal residues of oncocin are responsible for targeting this peptide to the ribosome, whereas the positively charged amino acid residues distributed along the entire peptide sequence are necessary for efficient cellular uptake of the peptide.[216,221,223] After the discovery of oncocin, scientists were curious to study the role of each amino acid residue of oncocin. In one study, a positional alanine scan was carried out to identify critical residues for antibacterial activity. In this work, all possible 19 peptides resulting from a positional alanine scan were chemically synthesized and utilized in MIC studies.[289] In this work, they showed that alanine substitutions at positions 3, 6, 7, and 11 completely abolished the antibacterial activity.

According to previous structural and biochemical data, Lys3, Tyr6, Leu7, and Arg11 of oncocin are critical for the ribosome binding and antibacterial activity of oncocin.[216,289] However, all of these studies were confined to *in vitro* systems and entirely depended on SPPS. Therefore, it was of interest to examine the activities of oncocin mutants in an actual cellular environment. Each critical amino acid residue of oncocin was substituted with alanine to obtain four single alanine mutants of oncocin (oncK3A, oncY6A, onc7LA, oncR11A). In addition, all four positions were substituted with alanine to obtain the onc3KAY6AL7AR11A mutant. DNA inserts corresponding to each alanine mutant (**Figure 3.9a**) were cloned into the plasmid vector and transformed into DH5α cells as described in Chapter 2 (Methods section). The ligation was confirmed by doing colony PCR (**Figure 3.9b**), and individual peptide clones were confirmed by DNA sequencing. The bacterial growth assays were carried out with oncocin and alanine mutants to evaluate the antibacterial activities.

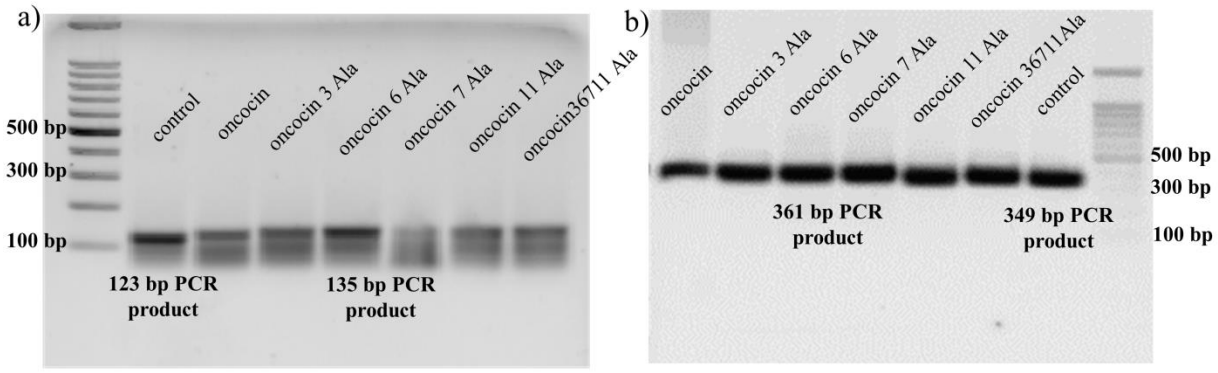

Figure 3.9 Cloning of alanine mutants of oncocin. a) The peptides inserts were generated using the non-template PCR method and gel purified before and after restriction digestion. The size of the 19-mer peptide PCR product was 135 bp. The control lane contains a PCR product of a 15-mer peptide (123 bp) for comparison. b) The peptide clones were confirmed by doing colony PCR, which gave 361 bp PCR products. The control lane contains a colony PCR product of a 15-mer peptide (349 bp) for the comparison

Figure 3.10 shows the growth curves for the oncK3AY6AL7AR11A mutant and wild-type oncocin. When all four amino acid residues were substituted with alanine, a complete loss of antibacterial activity was observed. After 540 min (9 h) of incubation, more than 80% inhibition was observed with wild-type oncocin, whereas only 3% growth inhibition was observed in the cultures expressing the mutant peptide. After 9 h of incubation, 50 μL of bacteria was taken out and plated in LB/agar medium and incubated at 37 °C. After overnight incubation, we did not observe colonies on plates incubated with bacteria expressing oncocin. However, more than 100 colonies were observed in plates incubated with bacteria expressing the alanine mutant. This observation demonstrated the bactericidal activity of oncocin directly compared to the mutant peptide. According to our *in vivo* data, substitution of Lys3, Tyr6, Leu7, and Arg11 with alanine led to complete loss of the antimicrobial activity of oncocin. This observation is consistent with one or more of these residues being critical for the antibacterial activity of oncocin.

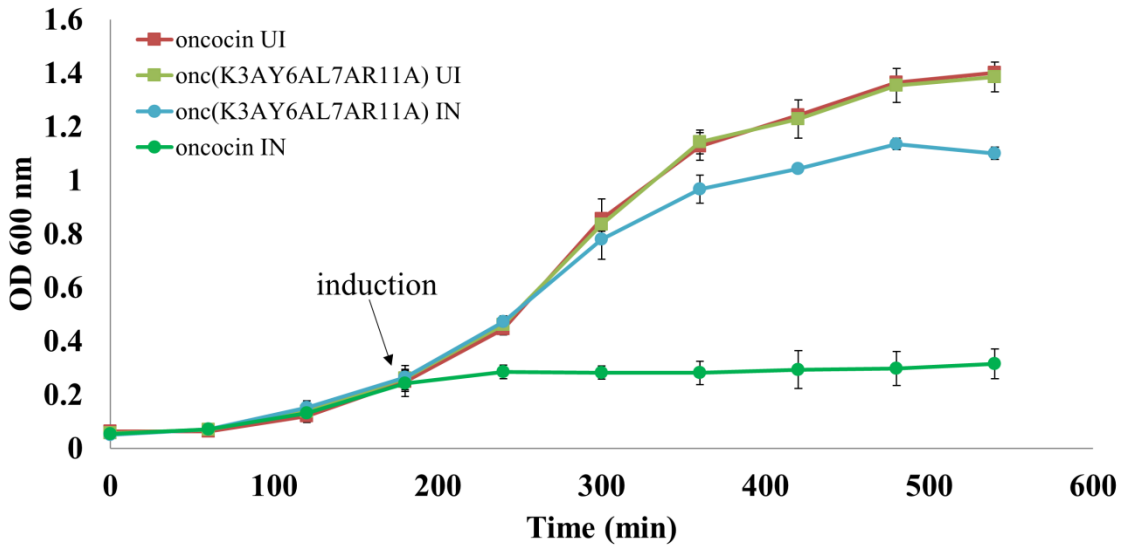

Figure 3.10 OncK3AY6AL7AR11A mutant growth assay. Effects of expression of the OncK3AY6AL7AR11A mutant on bacterial cell growth compared to the wild-type oncocin. Peptide uninduced growth curves are shown as UI, whereas its induced partner is shown as IN. The growth inhibition is completely abolished for the alanine muatant compared to oncocin (induced). All growth assays were performed at least three times independently and results were averaged.

Our *in vivo* data are in a good agreement with previous observations for the mutant peptide onc3KA6YA7LAR11A. Previously, it was shown that alanine substitution of Lys3, Tyr6, Leu7, and Arg11 severely reduced the antimicrobial activity of oncocin and decreased its binding affinity to the 70S ribosome by more than 30-fold.[216,296] Altogether, previous *in vitro* data with chemically synthesized mutant peptides and our data with *in vivo* expressed mutant peptides support Lys3, Tyr6, Leu7, and Arg11 as critical residues for the antibacterial activity of oncocin.

In the next step, we wanted to look at the contributions of individual amino acid residues on the antibacterial activity of oncocin. Therefore, single alanine mutants of oncocin (oncK3A, oncY6A, onc7LA, and oncR11A) were expressed and utilized in bacterial growth assays as explained previously. In this experiment, onc3AY6AL7AR11A and wild-type oncocin were used for comparison as inactive and active variants, respectively. Previous structural and biochemical

data suggested that N-terminal residues of oncocin were responsible for targeting this peptide to the ribosome.[222,223] Previous mutational studies also showed that substitution of Val1, Asp2, and especially Lys3, by alanine in oncocin led to a loss of antimicrobial activity. The effect was significant with the Lys3 substitution.[216] Therefore, we examined the *in vivo* activity of the oncK3A mutant.

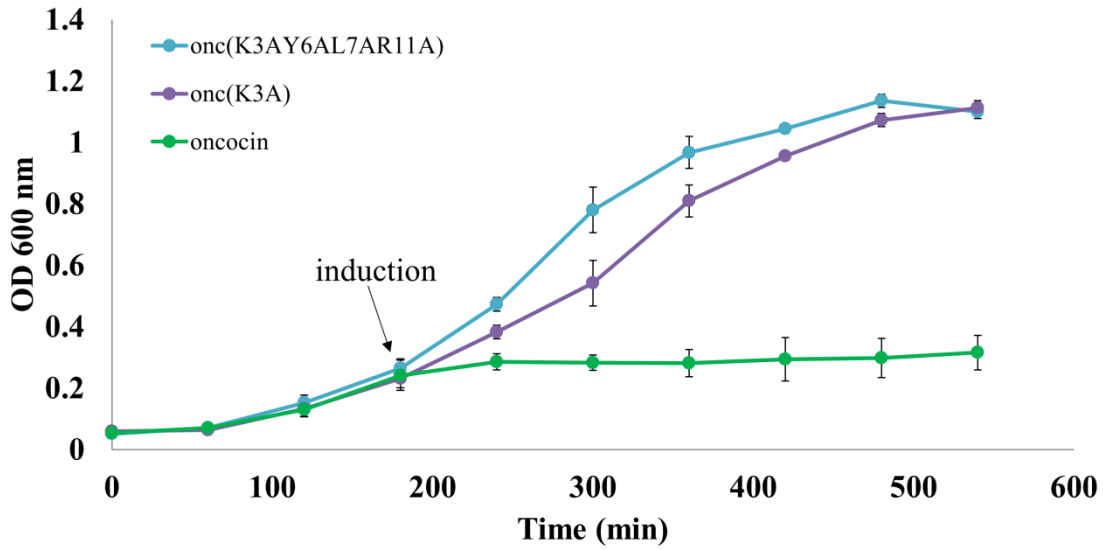

Figure 3.11 OncK3A mutant growth assay. Effect of the expression of oncK3A mutant on bacterial growth compared to the wild-type oncocin and oncK3AY6AL7AR11A mutant peptides. All growth assays were performed at least three times independently and results were averaged.

In growth assays with the K3A mutant, we observed a loss of antimicrobial activity compared to oncocin. However, compared to the mutant peptide, K3AY6AL7AR11A, complete loss of activity was not observed at shorter times (**Figure 3.11**). For example, after 3 h of induction (at 360 min), oncK3A showed 22% inhibition, whereas oncocin showed 77% inhibition. However, after 6 h of induction (at 540 min) oncK3A showed complete loss of antibacterial activity (no inhibition), and oncocin showed more than 80% growth inhibition. In previous studies with the oncK3A mutant peptide, it was shown that upon alanine substitution, the MIC value for the mutant peptide increased by 10-fold compared to the wild-type peptide. In

the same study, it was shown by fluorescence polarization method that ribosome binding of the mutant peptide decreased 5-fold compared to the wild-type peptide sequence.[216] Collectively, previous *in vitro* data and our *in vivo* data suggest that Lys3 of oncocin is important for antibacterial activity.

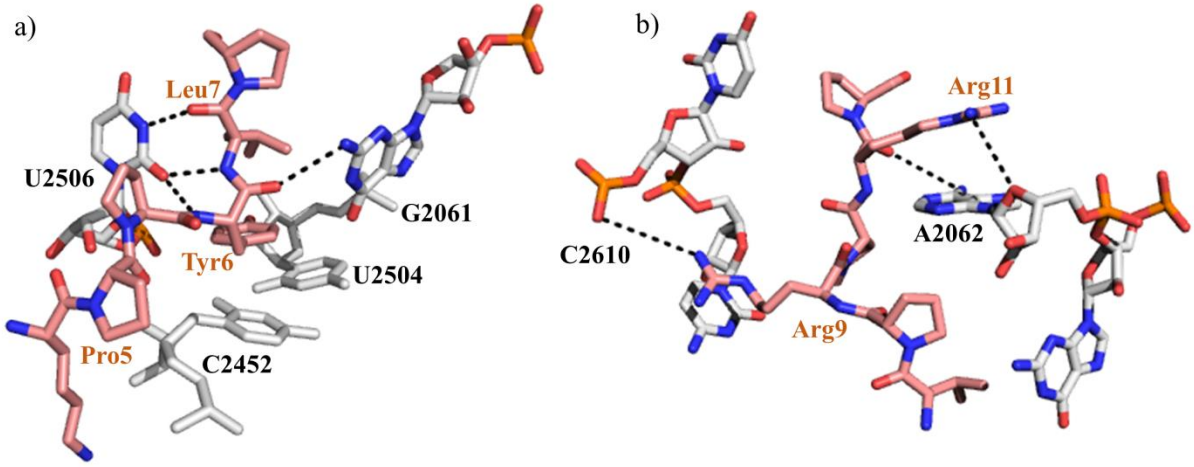

Figure 3.12 Interactions of oncocin within the PTC. a) The middle part of oncocin occupies the A-site cleft in the PTC. Residues Leu7 and Tyr6 form a three-layer stack with the nucleotide base of C2452. b) Interactions of the C-terminus of oncocin with the peptide exit tunnel are shown. Arg9 and Arg11 form a stacking interaction with the nucleotide bases of C2610 and A2062, respectively (PDB ID: 5HCR).[221]

The second set of oncocin-ribosome interactions involves the side chains of Tyr6 and Leu7. According to a crystal structure,[221] the aromatic side chain of Tyr6 establishes a π-stacking interaction with C2452 of the 23S rRNA (**Figure 3.12a**). The backbone of Leu7 forms two hydrogen bonds with U2506. The compact hydrophobic core formed by Tyr6 and Leu7 is likely to be key in anchoring the peptide to the exit tunnel. Previous mutagenesis experiments showed that alanine substitution of either residue in oncocin reduced the ribosome binding affinity by a factor of 7 and resulted in a complete loss of inhibitory activity on *in vitro* translation.[216] In order to look at *in vivo* activities, a bacterial growth assay was performed with oncY6A and oncL7A mutants. Complete loss of antibacterial activity with both mutant peptides was observed compared to the wild-type oncocin (**Figure 3.13**).

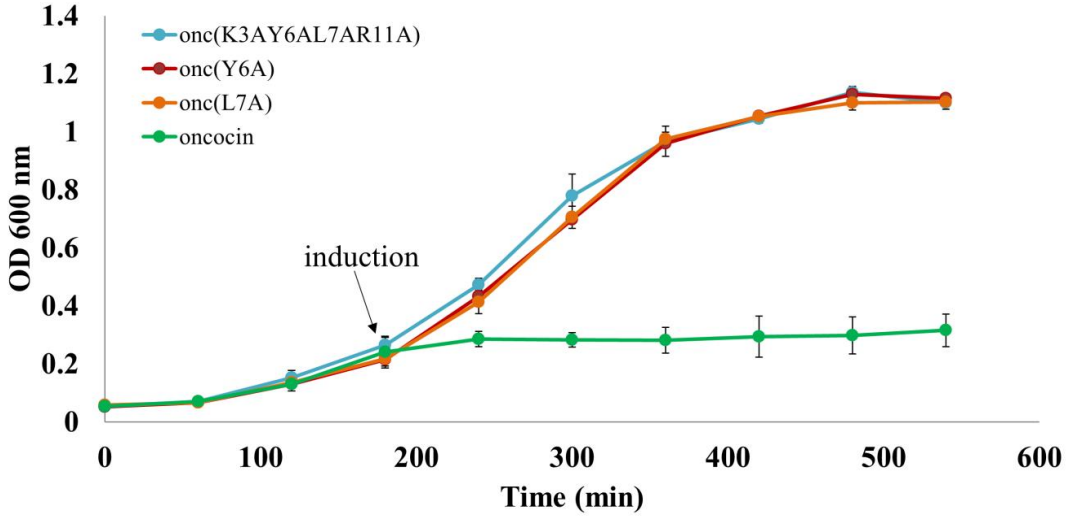

Figure 3.13 OncY6A and oncL7A mutants growth assay. Effects of the expression of mutant peptides on bacterial cell growth compared to the wild-type oncocin. The growth inhibition is completely abolished upon the induction of alanine muatant compared to oncocin. All growth assays were performed at least three times independently and results were averaged.

After 3 h of induction (at 360 min), the growth curves of both mutant peptides overlapped with the negative control peptide, onc3KAY6AL7AR11A and showed complete loss of antibacterial activity. Our data are in a good agreement with previous observations of these mutant peptides in *vitro* and support roles for Tyr6 and Leu7 in the antibacterial activity of oncocin. In addition to the above-mentioned interactions, the crystal structure revealed that the C-terminal PRPRP motif of oncocin interacts with 23S rRNA.[221-223] This includes π-stacking interactions between the guanidino groups of Arg9 and Arg11 with nucleotides of 23S rRNA (**Figure 3.13b**). Previous mutagenesis experiments showed that substitution of Arg11 with alanine in oncocin reduced the ribosome binding affinity by a factor of 6 and increased the MIC and IC_{50} of the peptide by 8- and 14-fold, respectively. [216] Therefore, it was of interest to examine the *in vivo* activity of the onc11A mutant. In the growth assay, loss of antibacterial activity was observed with onc11A cultures compared to oncocin-expressing bacterial cultures (**Figure 3.14**). However, onc11A did not show complete loss of activity as did

onc3KAY6AL7AR11A peptide. After 3 h of induction (at 540 min) compared to the onc3KAY6AL7AR11A mutant, oncR11A showed only 24% inhibition.

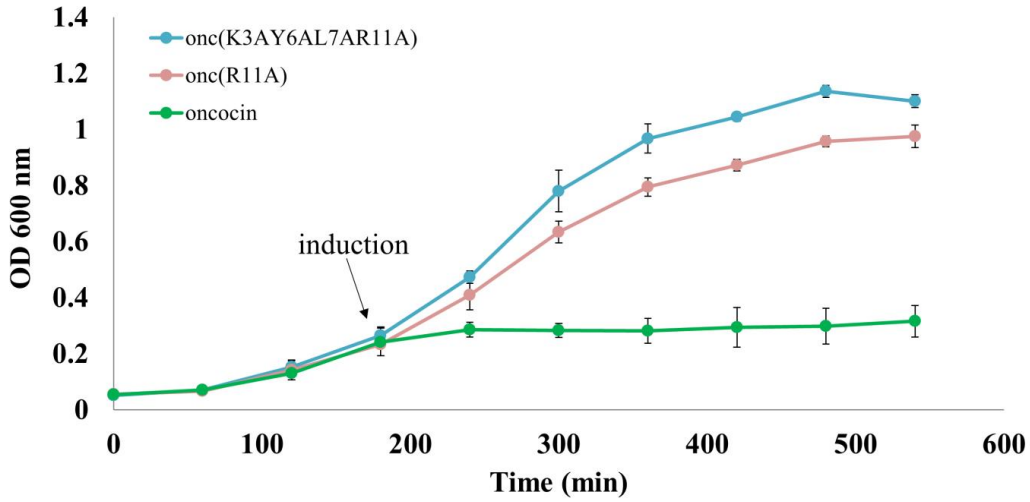

Figure 3.14 OncR11A mutant growth assay. Effects of the expression of the oncR11A mutant on bacterial cell growth compared to the wild-type oncocin. All growth assays were performed at least three times independently and results were averaged.

Therefore, the antibacterial activity of the mutant peptide was retained to a certain extent even with the alanine substitution. From our alanine scanning experiment, it appears that all four residues, Lys3, Tyr6, Leu7, and Arg11, are important for the antibacterial activity of oncocin. Out of them, Tyr6 and Leu7 seem to be the most important, because the growth of Y6A and L7A mutants was similar to the K3AY6AL7AR11A mutant. Our observations with the oncocin alanine mutants are in good agreement with previously observed *in vitro* activities of these mutants.[216,221,223] The purpose of this alanine scan experiment was to determine whether we can utilize the plasmid-based system as a tool to study the *in vivo* activities of peptide variants. The *in vivo* activities of oncocin mutants correlated well with the previously observed *in vitro* activities of these peptides. Therefore, our *in vivo* approach has promising applications in peptide optimization processes. However, there are some limitations. Since the peptides are expressed in an actual cellular environment, there is a possibility for them to undergo proteolytic degradation

by bacteria proteases. However, we have the same issue when chemically synthesized peptides are utilized in MIC experiments, since peptides act inside bacterial cells. The advantage of the *in vivo* approach is the overexpression of the peptide. Although some amount of peptide undergoes degradation, the cell can produce enough peptide to show activity. In-cell synthesis can also help to overcome cell permeability issues associated with short peptides. With our data, we propose that for the initial optimization process of an AMP (such as alanine scanning), the plasmid-based system could be used as an alternative to SPPS and MIC studies. It saves both money and time during the initial optimization process. At later stages of AMP optimization, *in vivo* approaches can be used together with *in vitro* experiments to obtain more information about the behavior of selected peptide variants. Similarly, mutants can be chemically modified by SPPS following sequence optimization.

3.4.4 *In vivo* probing of oncocin-ribosome interactions

In 2015, two research groups independently solved the x-ray crystal structures of onc112-bound *Thermus thermophilus* ribosomes.[221,223] According to these crystal structures, the peptide binds to the PTC region and interferes with binding of the aminoacyl-tRNA in the A site. Furthermore, these x-ray crystal structures reveal that several 23S rRNA nucleotides in the PTC region undergo different conformation changes upon peptide binding. X-ray crystallography is a powerful technique for understanding the structures, biological functions and ligand interactions, of many biomoleules. A major use of this technology is the identification and study of drug targets. For example, in the ribosome research field, x-ray crystallography is a commonly use technique. Crystal structures represent time and space averages of all molecules present within the crystal lattice and often exhibit significant conformational variations in their structures.[297]

Despite their utility, crystal structures of ribosome complexes show that some regions of the ribosome are dynamic, and these motifs can have significantly different conformations in the crystal from those in solution.[298] The intrinsic dynamics of the ribosome in solution could lead to alternative or additional binding modes.[262] Even though high-resolution crystal structures of oncocin bound ribosome are available, in order to better understand the rRNA-oncocin interactions it is important to look at the rRNA dynamics in solution. Chemical footprinting is a commonly used biochemical tool to examine such conformational changes of rRNA nucleotides upon drug binding.[139,263] Alterations in reactivities of rRNA nucleotides towards chemical modifications provide valuable information about the rRNA-drug interactions.[139,239,263] In a previous study, *in vitro* chemical footprinting was employed to study ribosome-oncocin interactions in solution.[221] In this study, the authors observed that several nucleotides in the PTC region were protected by oncocin from chemical modifications. These observations in *in vitro* probing experiments were consistent with binding of oncocin to the PTC region. Even though it provided information about rRNA dynamics in solution, the experiment was confined to an *in vitro* system. In *in vitro* footprinting experiments, the most crucial peptide-target interaction step occurs in a simulated environment, which is very different than the actual cellular environment.[228,229] This process also requires synthesis or isolation of the target prior to the experiment, as well as the assumption that the target is in its bioactive conformation under these *in vitro* conditions. For example in previous studies, the fooprinting experiment was carried out with isolated ribosomes and it was not clear if they used activated ribosomes for the experiment. Another important concern is that targets such as DNA, RNA, or proteins have numerous conformations *in vivo* that are influenced by their environment. Peptides are also highly sensitive to environmental conditions, which may result in discrepancies between their *in vitro* and *in vivo*

activity. Considering these facts, it is of interest to probe the ribosome-peptide interactions in actual cellular environments.

The development of a tool that could monitor ongoing rRNA conformational states in actual cellular environments would be significant. Since this plasmid system allows us to produce AMPs inside bacteria, it was of interest to *in vivo* probe the binding sites of oncocin and confirm its interactions with the PTC region of the bacterial ribosome. In this dissertation work, I optimized an *in vivo* DMS footprinting protocol to map the ribosome binding sites of oncocin. The details of the *in vivo* DMS footprinting technique and the experimental protocols are described in Chapter 2. In this *in vivo* footprinting experiment, oncocin-expressing bacterial cells were treated with DMS, followed by isolation of chemically modified RNA. In order to look at ribosome-oncocin interactions, reverse transcription-based primer extension analysis of the PTC region was performed by using of 5'-^{32}P-labeled DNA primers. The objective of our experiment was to identify oncocin-ribosome interactions under *in vivo* conditions and compare with previously reported *in vitro* data.[221] The *in vivo* footprinting provides additional information regarding altered binding interactions of oncocin with the ribosome relative to *in vitro* conditions. To the best of our knowledge, this is the first effort to use *in vivo* DMS footprinting to study ribosome-drug interactions. Unlike most known antibiotics, a single oncocin molecule interacts with not just one, but with two adjacent functional sites of the ribosome. Its N-terminus binds near the PTC of the 50S subunit, where it interferes with the A-site tRNA and the peptidyl-tRNA in the P site.[222,223] The other portion of oncocin interacts with the peptide exit tunnel of the 50S subunit and blocks it completely.[221,223] We carried out two DMS footprinting experiments to monitor 23S rRNA nucleotides in the peptide exit tunnel and the PTC region.

3.4.4.1 Interactions of oncocin in the peptide exit tunnel region

Previous structural and biochemical data revealed that several nucleotides in the upper chamber of the peptide exit tunnel undergo conformational changes upon oncocin binding.[218,221] Nucleotide A2062 adopts a conformation that allows the base to form a favorable stacking interaction with Arg11 of oncocin. A similar interaction was also observed between Arg9 and C2610 (**Figure 3.15**).[222,223] The binding site of oncocin in the peptide exit tunnel overlaps with the binding sites of macrolide antibiotics, erythromycin and azithromycin.[223] Interestingly, a crystal structure of the macrolide antibiotic erythromycin bound to ribosomes revealed that nucleotide A2062 undergoes different conformational changes upon drug binding.[299-301] Previous studies showed that mutations of A2062 and C2610 substantially reduced antibiotic-dependent ribosome stalling.[302,303] Moreover, alanine scan experiments showed that substitution of Arg11 in oncocin with alanine decreased its binding affinity to the ribosome by about 6-fold.[216] For this dissertation work, I performed an *in vivo* alanine scan experiment and observed loss of antimicrobial activity upon substitution of Arg11 with alanine (data explained in Section 3.4.3). These observations explained the important role of A2062 in oncocin-ribosome interactions.

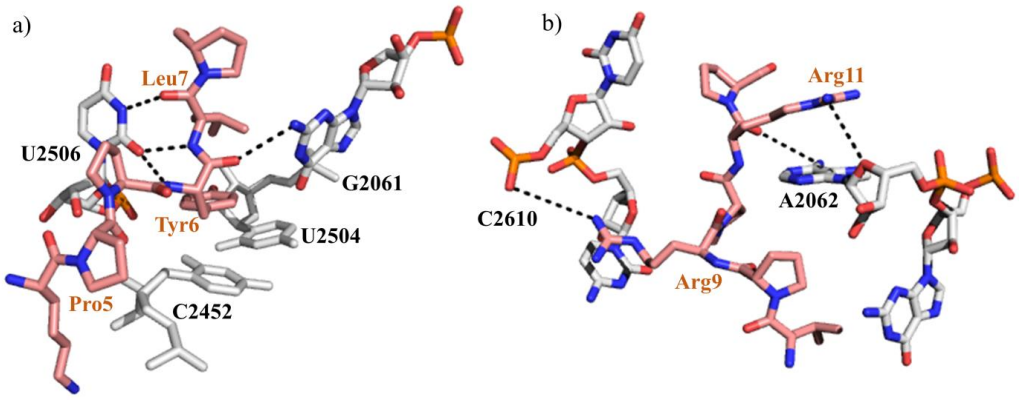

Figure 3.15 Interactions of oncocin within the PTC. a) The middle part of oncocin occupies the A-site cleft in the PTC. Residues Leu7 and Tyr6 form a three-layer stack with the nucleotide base of C2452. b). Interactions of the C-terminus of oncocin with the peptide exit tunnel are shown. Arg9 and Arg11 form a stacking interaction with the nucleotide bases of C2610 and A2062, respectively. (PDB ID: 5HCR).[221]

In *in vivo* footprinting experiments, strong protection of A2062 by oncocin is observed (**Figure 3.16**). This observation is consistent with A2062 undergoing a conformational change upon oncocin binding. In addition to A2062, strong DMS protection is observed at A2058 and A2059, which was not previously observed by *in vitro* oncocin footprinting experiments.[221]

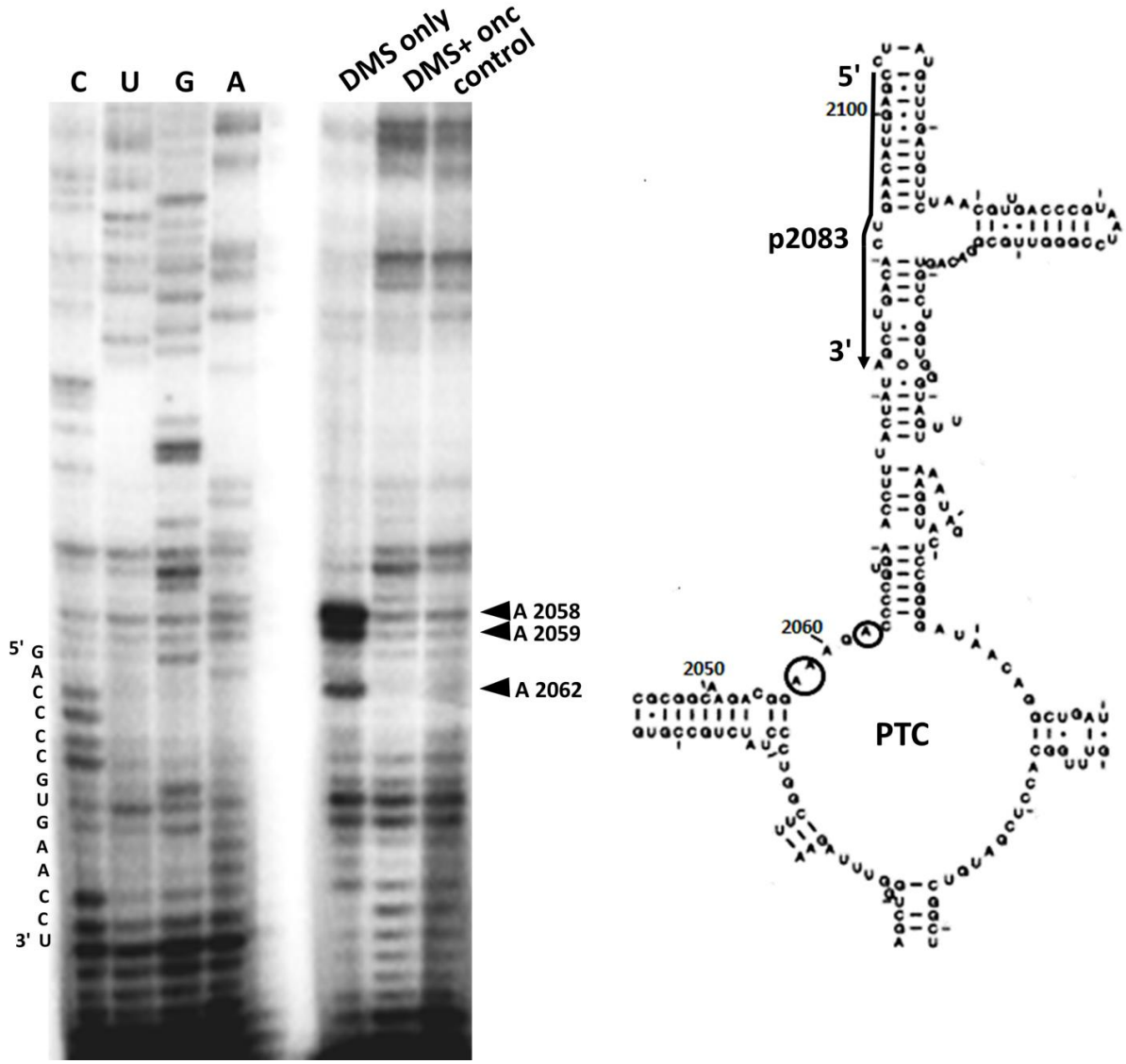

Figure 3.16 ***In vivo*** **DMS footprinting of oncocin-PTC interactions.** The autoradiogram (left) shows reverse transcription mapping of oncocin binding sites in the peptide exit tunnel region. Dideoxy sequencing lanes are labeled as C, U, G, and A (reverse transcription with ddGTP, ddATP, ddCTP, and ddTTP, respectively). The strong DMS reactive sites are labeled with black arrows and circled on the secondary structure map of the PTC region (right). The primer site is indicated with p2083.

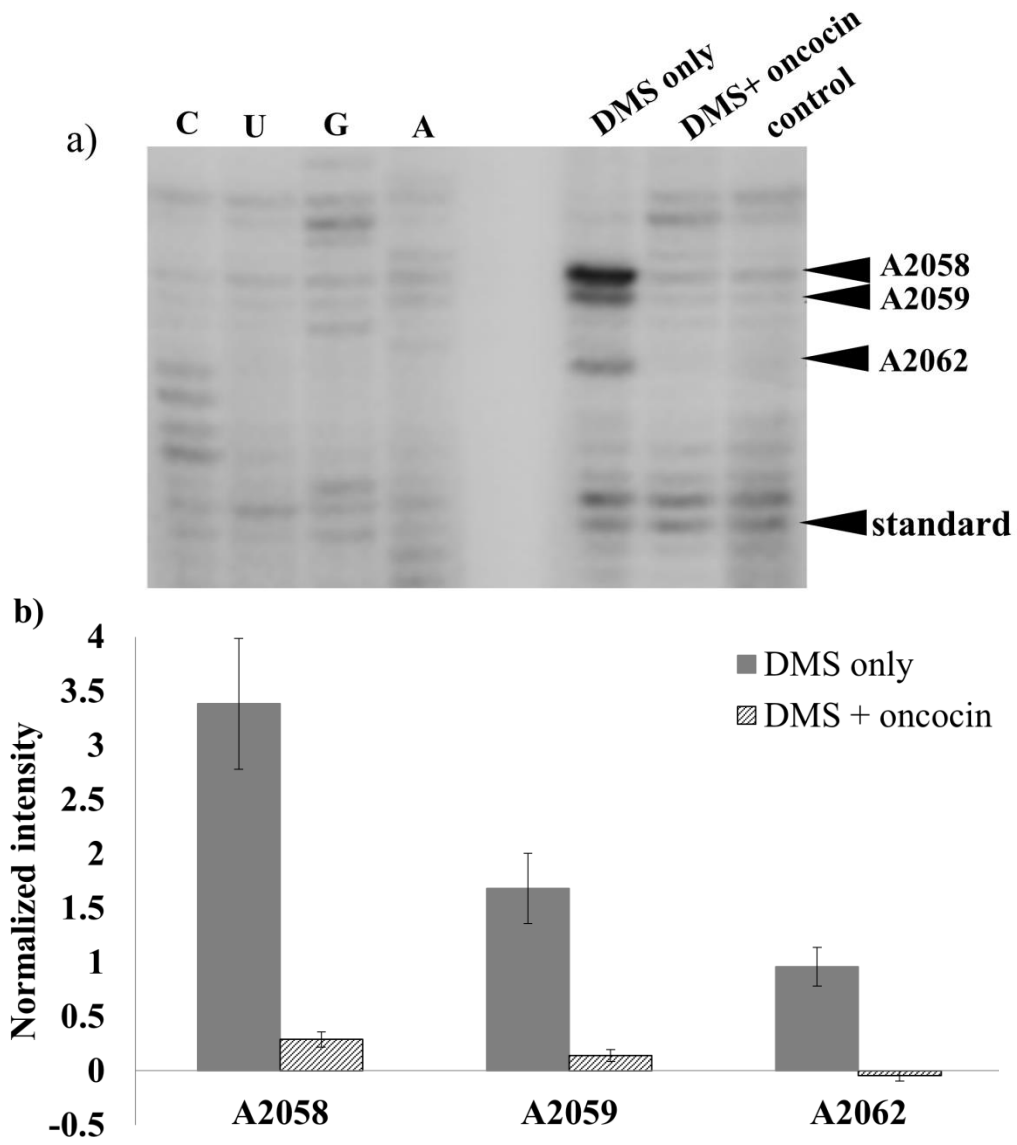

Figure 3.17 ***In vivo*** **DMS footprinting analysis of oncocin-PTC interactions.** a) Autoradiogram for DMS footprinting followed by primer extension analyses of oncocin binding to peptide exit tunnel. Reverse transcription stops before the DMS modification site, so the product mobility differs from the sequencing lane by one nucleotide. b) Quantification of DMS reactivity of each nucleotide in the presence and absence of oncocin is shown. Band intensities were normalized to a non-specific stop site labeled as the standard. Three independent footprinting experiments were carried out and results were averaged.

The reduced band intensities of the reverse transcription stop sites compared to the DMS-only control indicate low DMS reactivity of these nucleotides in the presence of oncocin. The gel bands were quantified using Image Quant software, and normalized intensities were determined (**Figure 3.17b**). Compared to the no drug control, 20-fold decreased DMS reactivity was

observed for A2062, with 12-fold decreased reactivity for both A2058 and A2059. The DMS protection of A2058 and A2059 by oncocin was not observed in previous *in vitro* footprinting studies.[221] In addition, the oncocin-ribosome crystal structure did not show any direct interactions of the peptide with either A2058 or A2059.[222,223] Despite lack of interactions with oncocin, all currently available crystal structures of 14-membered-ring macrolide-ribosome complexes revealed significant interactions with A2058 and A2059 of 23S rRNA (**Figure 3.18**).[304-306] These two nucleotides are recognized as the main constituents of the macrolide-binding pocket. The high binding affinities of macrolides originate mainly from hydrophobic interactions of their lactone rings and hydrogen bonds of their desosamine sugars with nucleotides A2058 and A2059.[306]

A crystal structure of erythromycin bound to ribosomes indicated that nucleotide 2058 plays a key role in macrolide binding and selectivity, the base component is an adenine in eubacteria and a guanine in eukaryotes.[305] Furthermore, the prominent macrolides-lincosamides-streptograminB (MLS) resistance mechanisms, an A to G substitution or *erm*-gene methylation, are related to the increasing size of A2058.[17,305,307] Moreover, previous *in vitro* DMS footprinting studies with erythromycin showed strong DMS protections of A2058 and A2059.[305] In this previous study, the footprinting experiments were done with ribosomes isolated from four different species, archaea (*H. halobium*) and three different bacterial species (*D. radiodurans, E. coli, or S. aureus*), and in all cases strong DMS protection was observed at A2058 and A2059. Collectively, these data indicate that A2058 and A2059 play crucial roles in macrolide antibiotic binding to the PTC region. Therefore, it was not surprising that we observed strong protection of A2058 and A2059 by oncocin. The extended arginine side chains of oncocin span across the peptide exit tunnel and completely block the upper chamber. Even though in x-ray structures the

peptide did not show direct interactions with A2058 and A2059, Leu7 of oncocin forms H-bonding interactions with the neighboring nucleotide G2061, which provides additional stabilization of the peptide inside the peptide exit tunnel (**Figure 3.15**).[222] This indirect interaction may induce conformational changes of A2058 and A2059, nucleotides which could reduce their reactivity towards DMS.

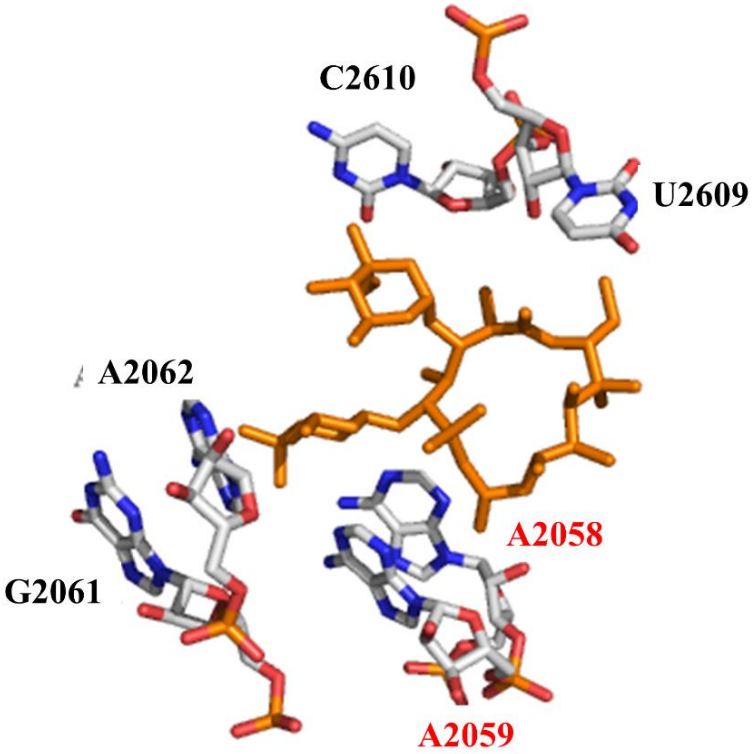

Figure 3.18 Crystal structure of macrolide antibiotic bound ribosomes. Macrolide, antibiotic erythromycin (shown in orange) binds to the PTC. Nucleotide positions at which mutation confers resistance for erythromycin are labeled in red (PDB ID: 4V7Y).[50]

Crystal structures of ribosome complexes are static and some regions of the ribosome could have significantly different conformations in the crystal from those in solution.[298] The intrinsic dynamics of the ribosome in solution, especially in the more complex cellular environment, could lead to alternative or additional binding modes.[262] This could be a possible

explanation for the observed DMS protection of A2058 and A2059 nucleotides in the *in vivo* footprinting experiment. With these data, we can argue that compared to *in vitro* probing studies, antibiotic footprinting in cellular environments provides additional information about AMP-ribosome interactions.

3.4.4.2 Interactions of the oncocin N-terminus with the ribosome

The structures of Pr-AMP bound ribosomes revealed that the N-terminus of peptides form several interactions with helix 92 (H92), which forms the A loop of 23S rRNA.[221-223] According to a crystal structure, the first three amino acids of oncocin (VDK) form multiple interactions with H92 (**Figure 3.19**).[222]

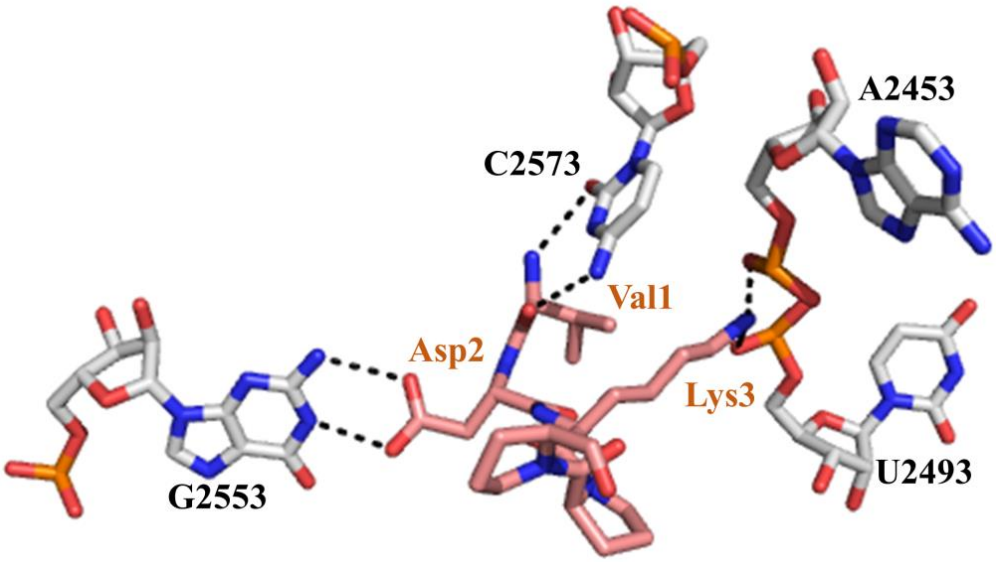

Figure 3.19 Interactions of the N-terminus of oncocin with 23S rRNA. The side chain of Asp2 forms two H-bonding interactions with G2553, a residue located helix H92 (H92) of 23S rRNA, termed the A loop (PDB ID: 5HCR).[221]

The main chain peptide backbone of Val1 forms two H-bonding interactions with C2573 (**Figure 3.19**). In addition to that, the side chain of Asp2 also forms H-bonding interactions with G2553.[221] The nucleotide G2553 is part of the A loop and forms a Watson-Crick base pair with C75 of the aa-tRNA.[308] The interactions of oncocin with H92 interfere with binding of the CCA

end of aa-tRNA in the PTC region. Although a crystal structure is available, it was of interest to examine the interactions of H92 nucleotides with oncocin in the cellular environment, which would provide additional insight into the oncocin-ribosome interaction and mechanism of action of oncocin.

In our *in vivo* footprinting experiment, we observed that several nucleotides in the H92 region undergo conformational changes upon oncocin binding (**Figure 3.20**). Nucleotide C2556 located in the loop region (A loop) of H92 shows strong DMS protection upon drug binding. Compared to the DMS-only control, a 50-fold decrease in DMS reactivity is observed (**Figure 3.21b**). In addition, C2551 in the loop and A2560 and C2559 in the stem region of H92 are also protected by oncocin from DMS modification. According to the crystal structure, none of these nucleotides have direct interactions with oncocin.[222] However, the direct interaction of G2553 with Asp2 of oncocin might cause indirect structural effects on neighboring nucleotides. According to the crystal structure, Val1 of oncocin also forms two H-bonding interactions with C2573 (**Figure 3.19**). This interaction may cause conformational changes of C2573, which leads to changes in DMS reactivity of this nucleotide. Consistent with that report, our footprinting experiment reveals DMS protection at nucleotide C2573. Compared to the DMS-only control, we observe a 12-fold reduced DMS reactivity at this residue (**Figure 3.21b**). This observation supports the interaction of C2573 with oncocin *in vivo*.

The goal of our *in vivo* footprinting experiment was to evaluate the oncocin-ribosome interactions in a cellular environment. Collectively, our *in vivo* footprinting analysis supported the interaction of oncocin with the PTC region of the bacterial ribosome. Our data are in good agreement with previous observations regarding oncocin-ribosome interactions. Under *in vivo* conditions, we observed additional binding information in the PTC, which was not obtained from

in vitro experiments. With these data, it is apparent that our plasmid system can provide important contact identification of ribosome-peptide interactions by *in vivo* probing. To the best of our knowledge, this is the first effort to use DMS footprinting method to *in vivo* probe drug-ribosome interactions.

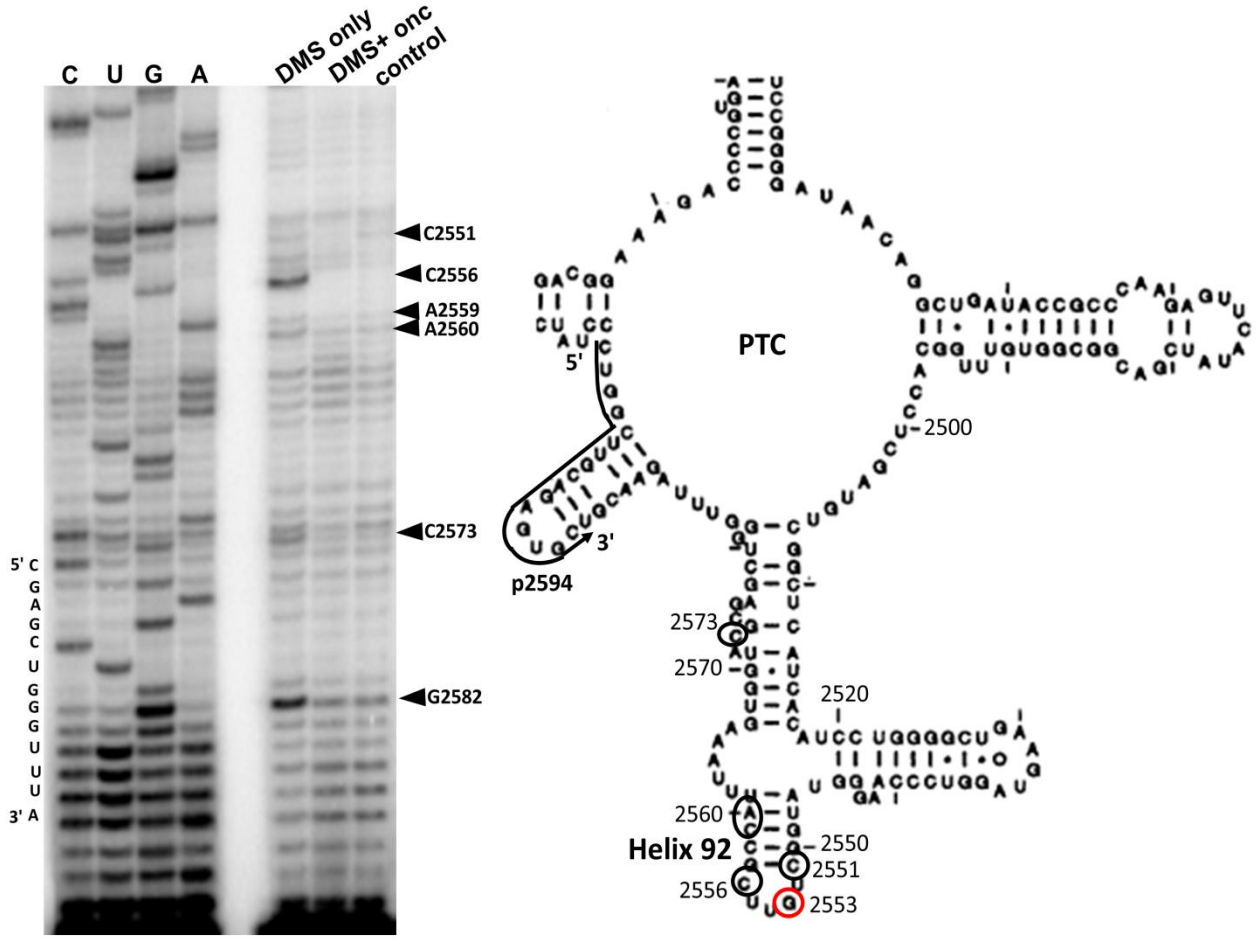

Figure 3.20 *In vivo* DMS footprinting of oncocin-H92 interactions. The autoradiogram (left) shows reverse transcription mapping of oncocin binding sites in the H92 region of 23S rRNA. Dideoxy sequencing lanes are labeled as C, U, G, and A (reverse transcription with ddGTP, ddATP, ddCTP, and ddTTP, respectively).. The corresponding reactive sites are labeled with black arrows and circled in the secondary structure map of the PTC region (right). Nucleotide G2553 of the A loop is shown in red. The primer site is indicated with p2594.

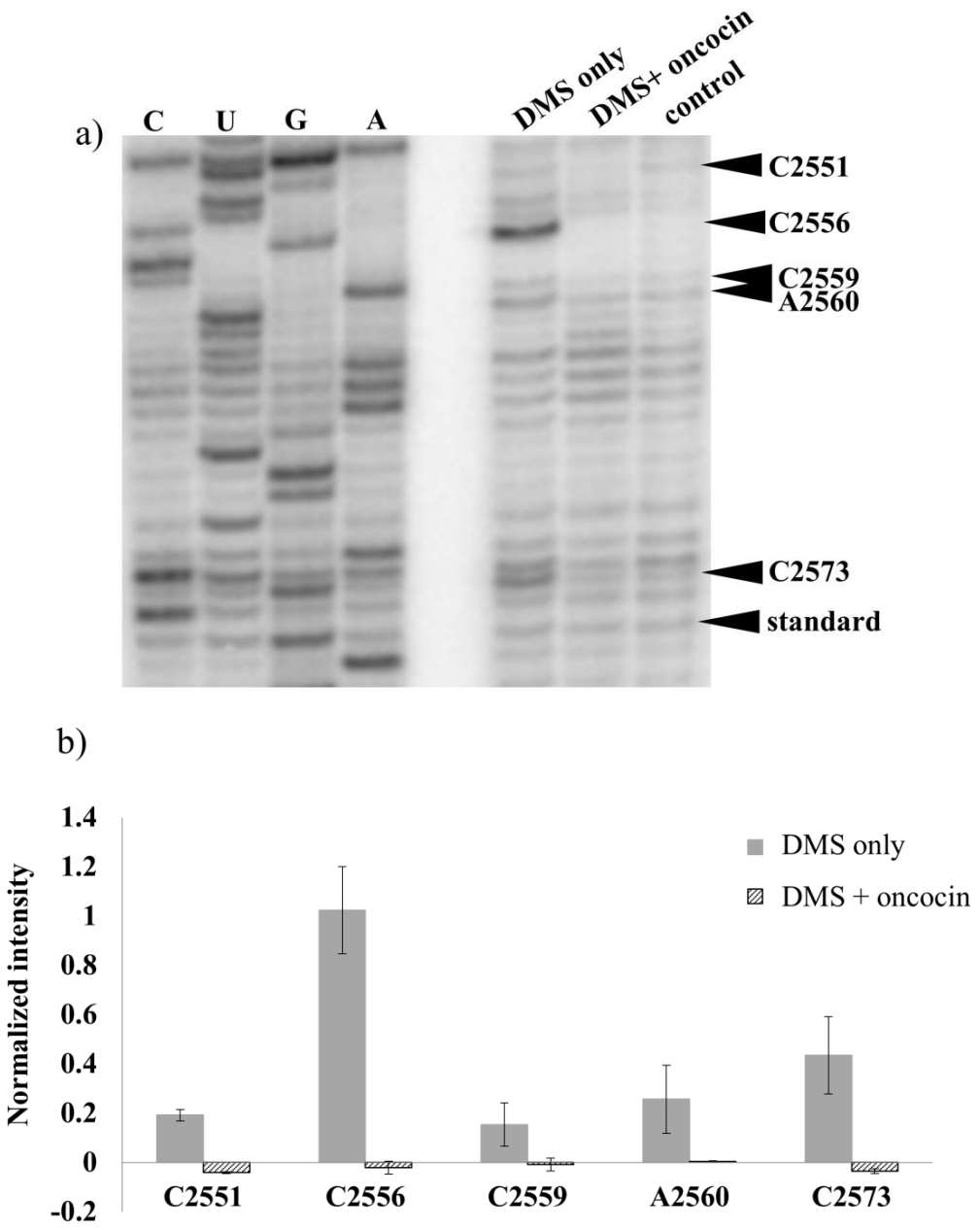

Figure 3.21 ***In vivo*** **DMS footprinting analysis of oncocin-PTC interactions.** a) Autoradiogram for DMS footprinting followed by primer extension analyses of oncocin binding to PTC. Reverse transcription stops before the DMS modification site, so the product mobility differs from the sequencing lane by one nucleotide. b) Quantification of DMS reactivity of each nucleotide in the presence and absence of oncocin is shown. Band intensities were normalized to a non-specific stop site labeled as the standard. Three independent footprinting experiments were carried out and results were averaged.

3.5 Summary and conclusions

The development of short peptides that specifically bind to higher-order structures of ribosomal RNA is one promising way to address the problem of antibiotic resistance.[191] However, the poor correlation between *in vitro* and *in vivo* activities of peptides is one of the major limitations in antibiotic peptide research. Therefore, in contrast to *in vitro* methods, one of the main objectives of my dissertation work was to utilize a plasmid-based system to *in vivo* express ribosome-targeting peptides and to study their direct inhibitory effects on bacteria. In this chapter, the main focuses was *in vivo* expression of the PrAMP oncocin, and study its direct inhibitory effects on bacterial growth. The 19-mer oncocin peptide sequence was cloned into a plasmid vector and *in vivo* expressed as a free peptide. The antibacterial activity of the peptide was confirmed by doing bacterial growth assays. After induction of the peptide, complete inhibition of bacterial growth (~ 80%) was observed. Data for our growth assays confirmed the strong antibacterial activity of oncocin.

Since this system allows us to produce peptides inside bacterial cells, there are some additional applications of the plasmid-based *in vivo* expression system. For example, we utilized the system to *in vivo* express alanine mutants of oncocin. According to previous structural and biochemical data, Lys3, Tyr6, Leu7, and Arg11 of oncocin are critical for ribosome binding and antibacterial activity of oncocin.[216,289] However, all of these studies were confined to *in vitro* systems and based on tedious SPPS and individual peptide testing. Therefore, we carried out an *in vivo* alanine scan experiment. Each critical amino acid residue of oncocin was substituted with alanine to obtain four single alanine mutants of oncocin (oncK3A, oncY6A, onc7LA, oncR11A). At the same time, all four positions were substituted with alanine to obtain the oncK3AY6AL7AR11A mutant. According to our *in vivo* data, substitution of Lys3, Tyr6, Leu7,

and Arg11 with alanine leads to loss of antimicrobial activity of oncocin. The effect was significant with the oncK3AY6AL7AR11A mutant. Results of our *in vivo* alanine scan experiment supported the critical roles of Lys3, Tyr6, Leu7, and Arg11 residues of oncocin in ribosome binding and antibacterial activity.

Even though crystal structures of the ribosome complexed with prAMPS such as oncocin are available, molecular details of the peptide-rRNA interactions on the full ribosome were still unclear, especially in solution. On the other hand, the folding of RNA might be different in a more complex environment such as living cells. Therefore, it is important to study ribosome-peptide interactions *in vivo*. One additional application of our plasmid system is *in vivo* probing of ribosome-peptide interactions. *In vivo* chemical footprinting studies were carried out using dimethyl sulfate (DMS) as the probe to monitor oncocin-ribosome interactions. Our *in vivo* footprinting experiments identified several nucleotides in the peptide exit tunnel that undergo conformational changes upon oncocin interactions. Residues A2058, A2059, and A2062 of the peptide exit channel were protected by oncocin from DMS modification. Nucleotides A2058 and A2059 are the main constituents in the macrolide binding pocket.[305,306] Even though literature reports suggested that oncocin overlaps with the macrolide binding site, under *in vitro* footprinting conditions DMS protection was not observed at A2058 and A2059.[221] In contrast, our *in vivo* footprinting analysis showed strong protection at both A2058 and A2059. In addition, our *in vivo* footprinting analysis revealed that several nucleotides in the H92 region were also protected by oncocin. Together these data support the interaction of oncocin with the PTC region of the ribosome. Collectively, we showed in this work that there are several advantages for *in vivo* peptide expression compared to *in vitro* approaches that are entirely dependent on SPPS. However, there are some limitations to the *in vivo* method such as possible proteolytic

degradation of the short peptides. Therefore, further experiments such as mass analysis of the cell lysate need to be done to confirm the presence of intact peptides inside cells. In this study, we used oncocin as an example to explore the different applications of our plasmid system. However, we can expand our plasmid system to study a variety of other AMPs. There are some additional applications of the plasmid-based *in vivo* expression system. For example, we can utilize this system to generate peptide libraries, or study a variety of other biologically interesting peptides (*e.g.*, anti-freeze peptides).

CHAPTER 4 *IN VIVO* EXPRESSION OF HELIX 69-TARGETING PEPTIDES IN *ESCHERICHIA COLI*

4.1 Abstract

The specific region of the bacterial ribosome under investigation of this study is helix 69 (H69).[22] H69 is a multifunctional and highly conserved hairpin-loop structure that is located in domain IV of the 23S rRNA in the 50S ribosomal subunit.[22] In previous studies, the phage-display method was used to identify peptides that target the H69 region. *In vitro* binding studies have shown that these selected peptides have moderate affinity towards H69.[192] In a second approach, peptide variants with higher affinity and enhanced selectivity were identified by doing alanine and arginine scans of the parent peptide sequence selected in the phage-display method.[191] However, the *in vivo* activities of these peptides were not determined in this initial study. In contrast to the *in vitro* methods, the objective of the current study was to *in vivo* express the selected peptides in bacteria and study their inhibitory effects on bacterial protein translation and growth. Plasmid-based, *in vivo* expression systems were used to express GFP-tagged as well as free H69 peptides inside bacteria. However, our bacterial growth assays revealed that the selected peptide sequences do not have considerable antibacterial activity. Proteolytic degradation of short peptides could be a possible reason for this behavior. Out of the different peptide sequences we studied, we found out that NQAANHQ peptide shows better inhibition compared to other H69-targeting peptides. Based on our *in vivo* and *in vitro* data, we can consider NQAANHQ as a potential drug lead that would need further development and improvement in activity.

4.2 Introduction

The development of peptide ligands that specifically bind to higher-order structures of rRNA is one promising way to address the problem of antibiotic resistance.[190-192,221] Structural

information obtained from x-ray crystallography has indicated that there are many significant regions of rRNA that could serve as antibacterial drug targets.[132] The specific conserved region of the ribosome under investigation in this study is H69. Helix 69 is a 19-nucleotide hairpin-loop structure that is located in domain IV of the 23S rRNA in the 50S subunit.[22] It interacts with helix 44 (h44) of the 16S rRNA to form intersubunit bridge B2a **(Figure 4.1)**, which plays significant roles in various ribosomal functions, including subunit association, translocation, peptide release, and ribosome recycling.[50,195] The nucleotide sequence of H69 contains three post-transcriptionally modified nucleotides, or pseudouridines (Ψ), at positions 1911, 1915, and 1917 [196] **(Figures 4.2** and **Figure 4.3)**.

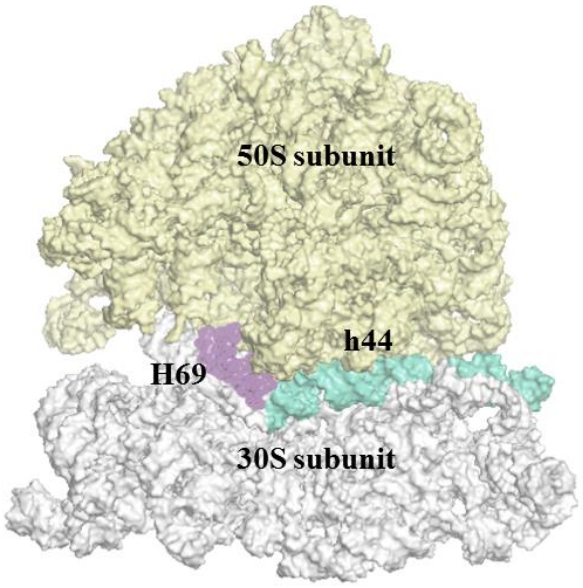

Figure 4.1 The location of H69 in the 70S full ribosome. H69 (in purple) is located at the junction between the 30S and 50S ribosomal subunits. It makes direct interactions with helix 44 (h44), known as the aminoacyl tRNA site (A site) (in cyan), of the 30S subunit. Its proximity to essential translational machinery and at the interface of the two subunits makes H69 a potentially important antibacterial drug target. (PDB ID: 2AW4).[19,50]

The nucleotide sequence of H69 is highly conserved in bacteria, archaea, and eukaryotes.[22] However, there are some noticeable differences between the H69 sequences of bacteria (*E. coli*) and eukaryotes (*H. sapiens*) **(Figure 4.2).** The 1915 position of H69 in *E. coli* is a methylated Ψ, whereas in human it is unmethylated.[196,197] The nucleotide at the 3' end of the loop is an adenosine (A) in *E. coli* and guanosine (G) in *H. sapiens*.[22,198] Thirdly, the *H. sapiens*

H69 has two extra Ψs in the stem region of the hairpin.[194] Considering the variety of functions of this motif in protein biosynthesis as well as the sequence conservation and key differences between bacterial and human H69, it is an attractive antibacterial drug target.

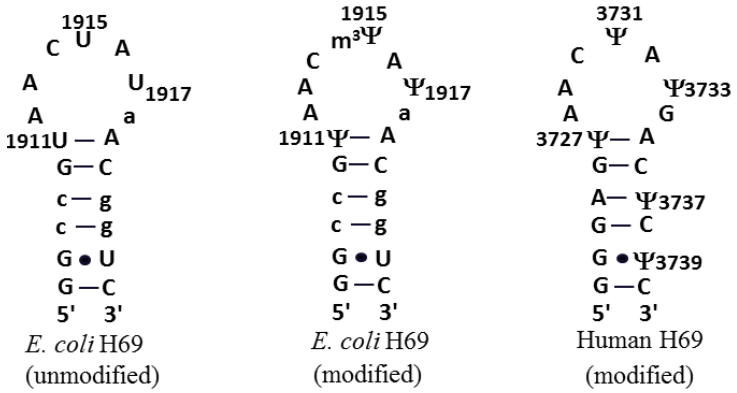

Figure 4.2 The secondary structures and sequences of modified and unmodified H69. The secondary structures of unmodified (UUU) and modified *E. coli* (Ψm^{3}ΨΨ) and modified human H69 show sequence differences (Ψ, pseudouridine; m^{3}Ψ, 3-methylpseudouridine). Nucleotides in upper case letters in the *E. coli* H69 sequence have >95% conservation and those in lower case have 88–95% conservation across phylogeny.[22]

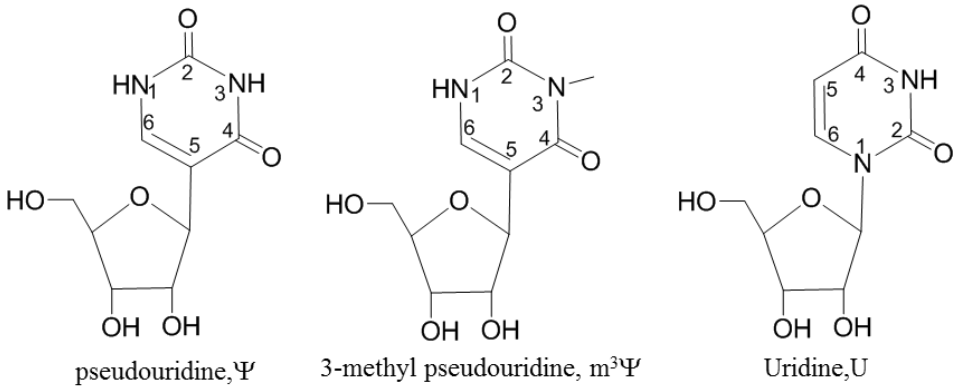

Figure 4.3 Chemical structures of pseudouridine, 3-methylpseudouridine, and uridine. Pseudouridine (Ψ, left) is a post-transcriptional modification of uridine (U, right). The difference between these two structures is a 120° rotation of the base in pseudouridine, forming a C–C glycosidic bond versus the canonical C–N glycosidic bond shown in uridine. Three-methylpseudouridine (m^{3}Ψ, middle) differs from Ψ only by a methylation on the 3-position of the base.

4.3 Objectives of the study

Helix 69 could potentially be targeted by small molecules such as peptides or DNA/RNA aptamers to interfere with the naturally occurring intersubunit interaction. In previous studies, the phage-display method was used to identify peptides that target the H69 region.[192] *In vitro* binding studies have shown that these selected peptides have moderate affinity towards H69. In the second approach peptide variants with higher affinity and enhanced selectivity were identified by doing alanine and arginine scans of the parent peptide sequence selected in the phage-display method.[191] The working hypothesis is that the selected peptides will bind to H69 selectively and disrupt ribosome function. Specificity, stoichiometry and binding affinity of these peptides to H69 were determined by using *in vitro* methods.[191,192] However, the *in vivo* activity of these selected peptides was not determined in this initial study. Therefore, some of the selected peptide sequences were chemically synthesized using solid-phase peptide synthesis and utilized in minimum inhibitory concentration (MIC) studies to determine their antibacterial activity. Data in MIC studies suggested that the peptides likely have penetration problems and cannot cross cell walls.

In contrast to these *in vitro* methods, the objective of the current study is to utilize a plasmid-based system to *in vivo* express these selected peptides in bacteria and study their inhibitory effects on bacterial protein translation and growth. In the first approach, H69-targeting peptide were *in vivo* expressed as Green Fluorescent Protein (GFP)-tagged fusion peptides (**Figure 4.4a**). In order to further characterize the selected peptides as potential drug leads, it is essential to determine their activity outside the context of the fusion protein. Therefore, in the second approach a different plasmid system was used to express H69-targeting peptides as free peptides in bacteria (**Figure 4.4a**). The effects of these peptides on bacterial protein translation

and growth were monitored through fluorescent intensities and optical densities of cultures expressing the peptides. Therefore, we hoped that *in vivo* expression of peptides would allow us to study the behavior of selected peptides in the actual cellular environment.

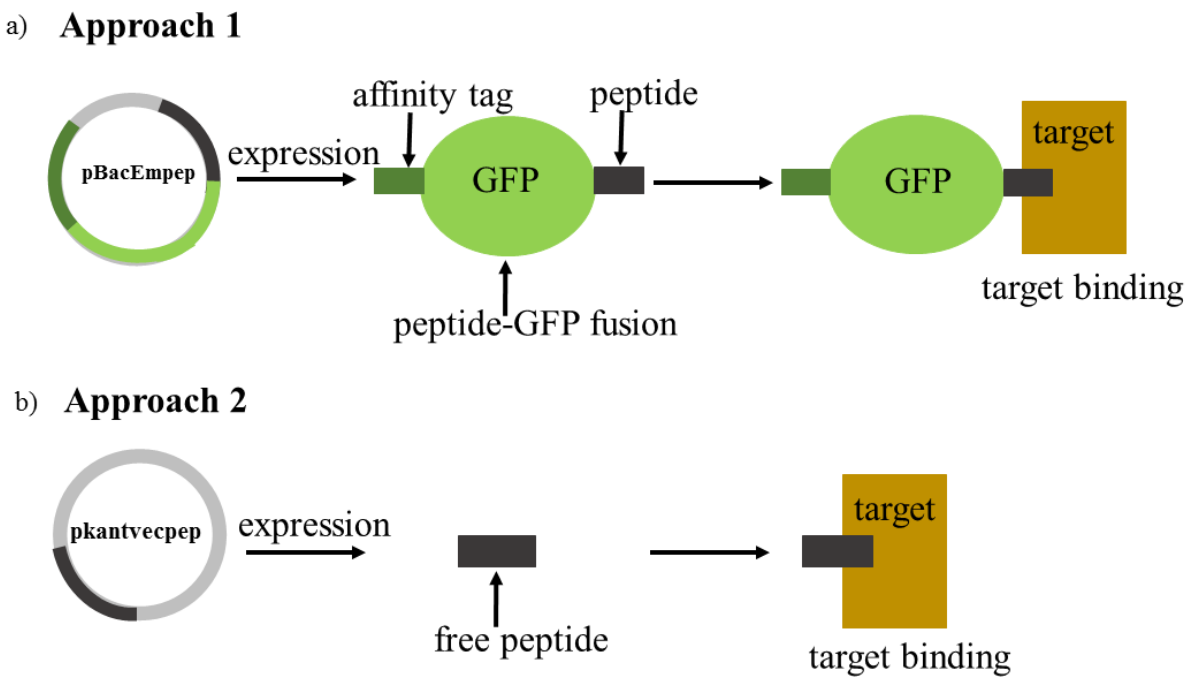

Figure 4.4 A schematic diagram of the two approaches used in the *in vivo* peptide expression methodology. a) In the first approach, peptides were cloned at the N-terminus of GFP and expressed as a fusion protein. The effects of peptides on bacterial growth and protein translation were monitored by measuring OD_{600nm} and fluorescence intensities of cultures expressing peptides. b) In the second approach, free peptides were expressed and the effects on bacterial growth were monitored by measuring OD_{600nm} of cultures expressing peptides.

4.4 Results and discussion

4.4.1 *In vivo* expression of GFP-tagged H69 peptides

4.4.1.2 Cloning of H69-peptides into the GFP plasmid system

Three peptide sequences (RQVANHQ, TARHIY, and NQAANHQ) were chosen for these studies. The details of the molecular cloning experiment is explained in the Experimental Method Section in Chapter 2. Dr. Wesley Colangelo prepared the plasmid vector pBacEmtvec3 for this experiment. The restriction enzyme sites *Kas* I and *Nhe* I were used to clone the peptide

insert into the plasmid. Therefore, the peptide insert and the plasmid vector were digested using *Kas* I *and Nhe* I enzymes (**Figure 4.5**). The primer extension PCR method was used to generate the corresponding DNA sequences that code for the desired peptides. The size of the DNA product corresponding to the 7-mer peptide sequence is 113 pb. The PCR product was checked on an agarose gel before the restriction digestion (**Figure 4.5b**).

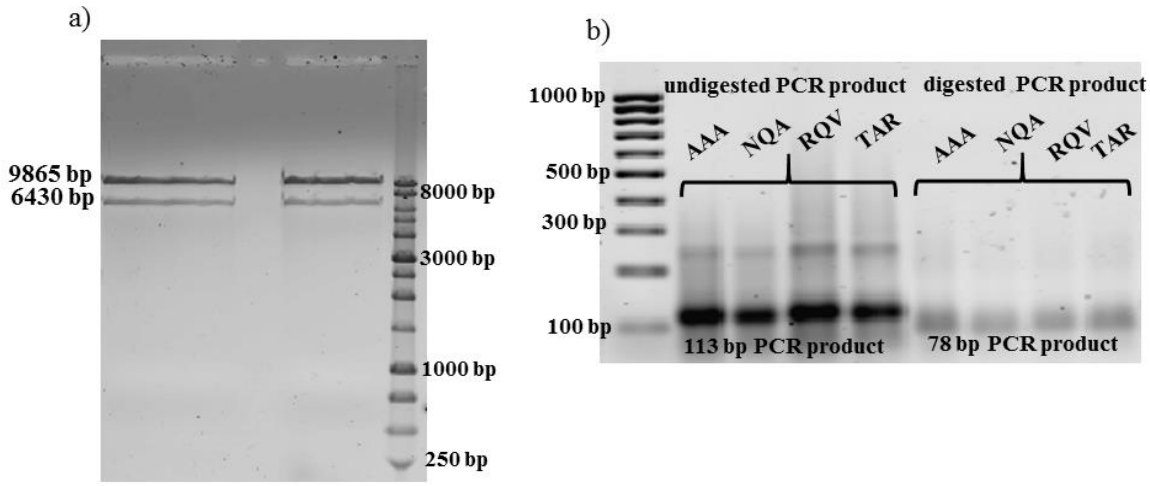

Figure 4.5 Plasmid vector and peptide insert preparation. a). Plasmid pBacEmtvec (16, 295 bp) was digested using *Nhe* I and *Kas* I restriction enzymes and the gel band corresponding to the desired vector fragment (9865 bp) was purified before ligation. b) The insert was synthesized using the non-template PCR method and purified before and after restriction digestion. The size of the PCR product corresponding to the 7-mer peptide sequence is 113 bp.

The DNA products were gel purified and ligated to obtain the new plasmid pBacEmGH-pep (9943 bp). The genes were cloned behind the P_{BAD} promoter of the plasmid such that the peptides could be expressed by inducing with L-arabinose. The ligated plasmids were electrotransformed into *E. coli* EPI300, which contained two other plasmids for the expression of TEV protease. Therefore, the peptide expression was done in a three-plasmid system. The details of the TEV-protease plasmid system is explained in chapter 2. The correct ligation was confirmed by doing colony PCR (**Figure 4.6a**). The sequence of the peptide clones were confirmed by doing DNA sequencing (**Figure 4.6b**).

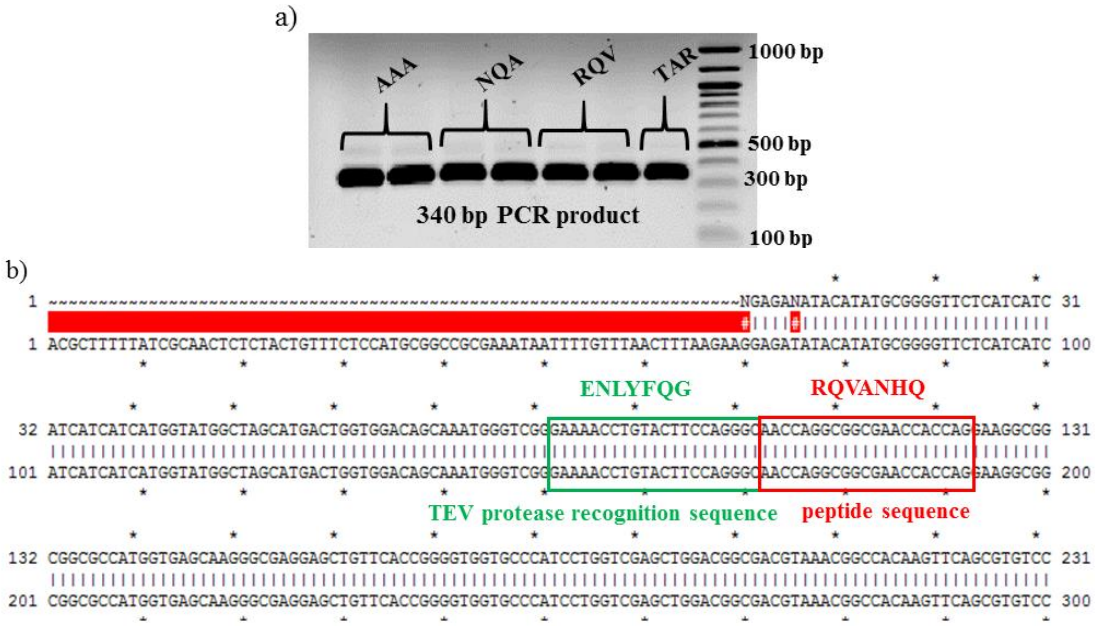

Figure 4.6 Peptide sequence confirmation. a) The peptide clones were confirmed by doing colony PCR, which gave a 340 bp PCR product for the 7-mer peptide in colony PCR. b) The sequence alignment of ligated plasmid. The full alignment is 1040 bp, whereas this section only shows the nucleotide sequence of the TEV recognition sequence in the first box (green) with the amino acid sequence labeled in green. The amino acid sequence of 7-mer peptide, RQVANHQ, is shown in red and the corresponding nucleotides are in box 2 (red).

In this plasmid system, the peptide sequence was cloned behind the TEV protease recognition sequence. The expression of TEV protease from another plasmid in the same cell would lead to cleavage of the TEV recognition peptide sequence between residues Q and G, and the resulting peptide was exposed at the N-terminus of GFP.[243,245] TEV protease cleavage occurs between Q and G, leaving an extra glycine (G) at the N-terminus of the peptide sequence (**Figure 4.7**). Although the wild-type TEV protease recognition sequence is ENLYFQG/S, recent studies have shown that any amino acid after Q in the sequence could cleave efficiently such that the exact peptide sequence could be exposed after TEV cleavage.[243,246,247] However, at the beginning of this project peptide primers were designed without excluding the codon corresponding to the C-terminus G residue. Therefore, TEV protease cleavage occurs between Q

and G, leaving an extra glycine (G) at the N-terminus of the peptide sequence (**Figure 4.7**). Therefore, all of the peptide sequences we expressed had an extra G-residue at the N-terminus.

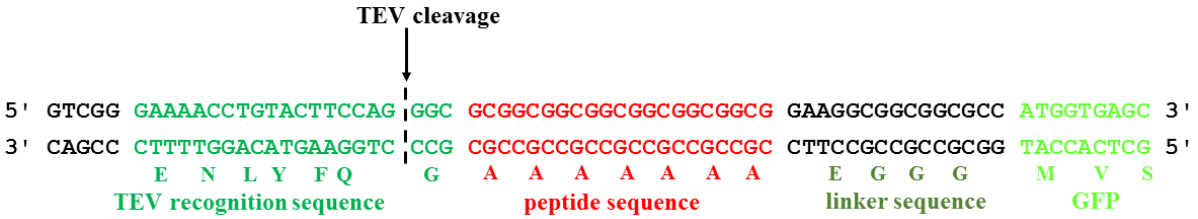

Figure 4.7 The TEV cleavage site. The TEV protease has a 7 amino acid recognition sequence and cleaves between amino acids 6 and 7 (Q and G). This leaves a G residue attached to the desired peptide sequence, in this case producing GAAAAAAA at the GFP end.

4.4.1.3 Study the effects of H69-targeting peptides on bacterial growth

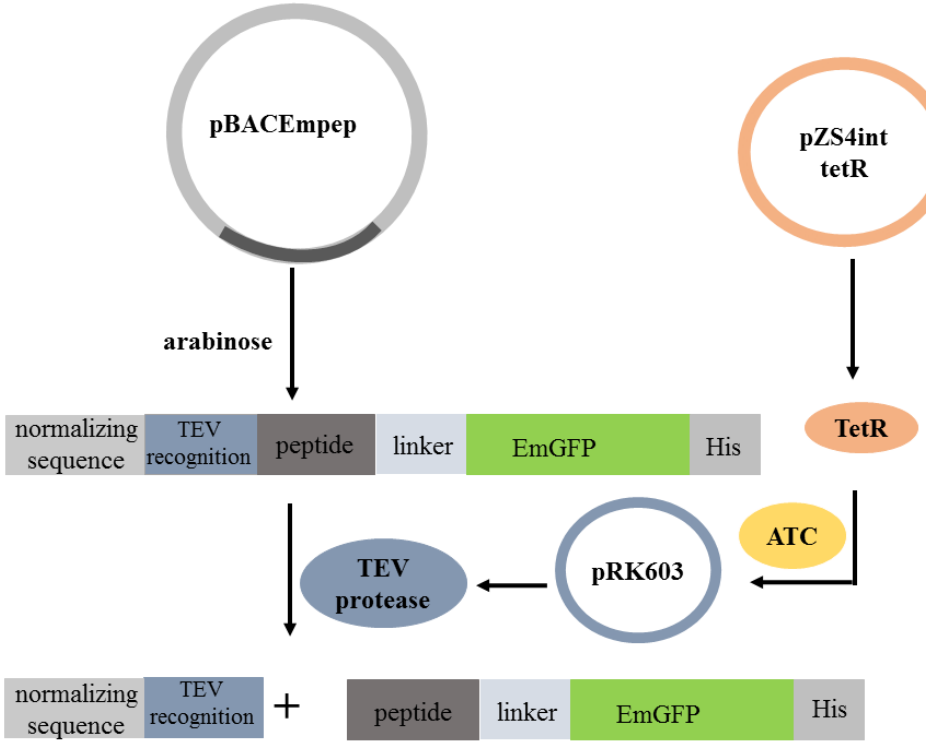

Figure 4.8 *In vivo* expression of GFP-peptide fusion proteins. A schematic diagram for the production of GFP-tagged peptides using the TEV protease expression system is shown. A normalizing sequence (g10 leader sequence) was added at the 5' end of the construct. The peptides were cloned behind the TEV protease recognition sequence. A peptide linker, EGGG, was placed before GFP to provide flexibility of the peptide. The expression of the peptide and TEV protease was induced by adding arabinose and anhydrotetracycline (ATC), respectively. Upon expression of TEV protease, the peptides were exposed at the N-terminus of GFP.

After confirming the sequence of each peptide clone, they were used in bacterial growth assays. As explained in Chapter 2 the expression was done in a three-plasmid system in which the first plasmid (pBacEmpep, chloramphenicol resistance) was used for expression of GFP-tagged peptides, the second (pRK603) for Tet-inducible TEV protease with kanamycin resistance, and the third (pZS4int-tetR, spectinomycin resistance) for constitutive tetracycline repressor protein (TetR) expression [242] (**Figure 4.8)**.

Bacteria were grown in LB medium containing three antibiotics, chloramphenicol, kanamycin, and spectinomycin. When cells reached late lag phase (~210 min), anhydrotetracycline (ATC) was added to induce the expression of TEV protease from the pRK603 plasmid. The L-arabinose was then added (~240 min) to induce the expression of GFP-tagged peptides.

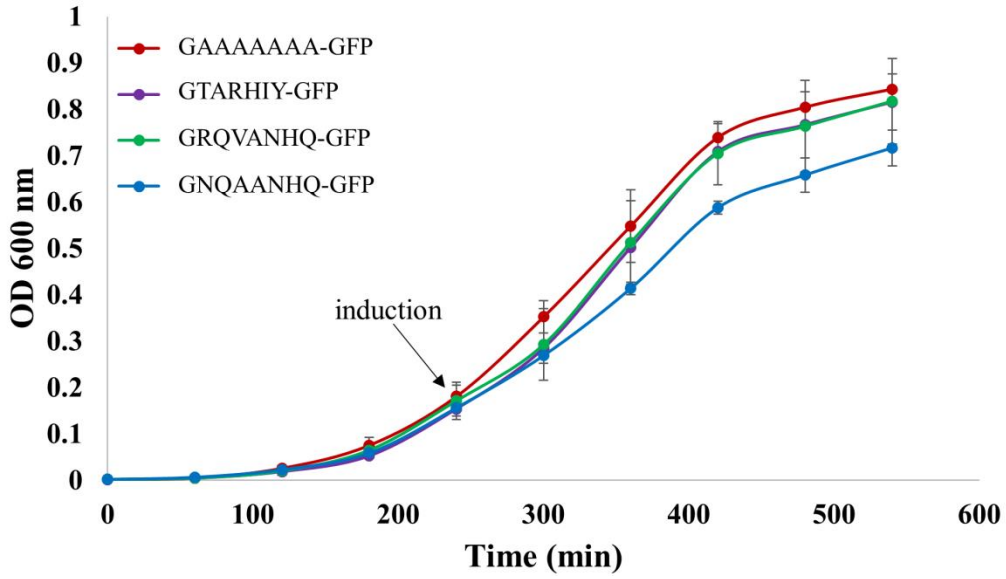

Figure 4.9 Bacterial growth assay. Measurement of *E. coli* growth upon the expression of peptide-GFP and TEV protease is shown. Optical density ($OD_{600\ nm}$) of cultures expressing different peptides were measured at every 60 min. Compared to the negative control GAAAAAAA-GFP, slightly reduced growth was observed in cultures expressing the GNQAANHQ-GFP.

Cell growth was measured with and without adding inducers. The bacterial growth was monitored by measuring the optical density of all bacteria cultures every 60 min (**Figure 4.5**). In growth assays, the 7-mer peptide GAAAAAAA-GFP fusion was used as a negative control, which did not show growth inhibition in previous experiments. Compared to the negative control fusion protein GAAAAAAA-GFP, we could observe some level of growth inhibition of the cells bearing GNQAANHQ-GFP, GRQVANHQ-GFP, and GTARHIY-GFP peptide-fusion proteins (**Figure 4.9**).

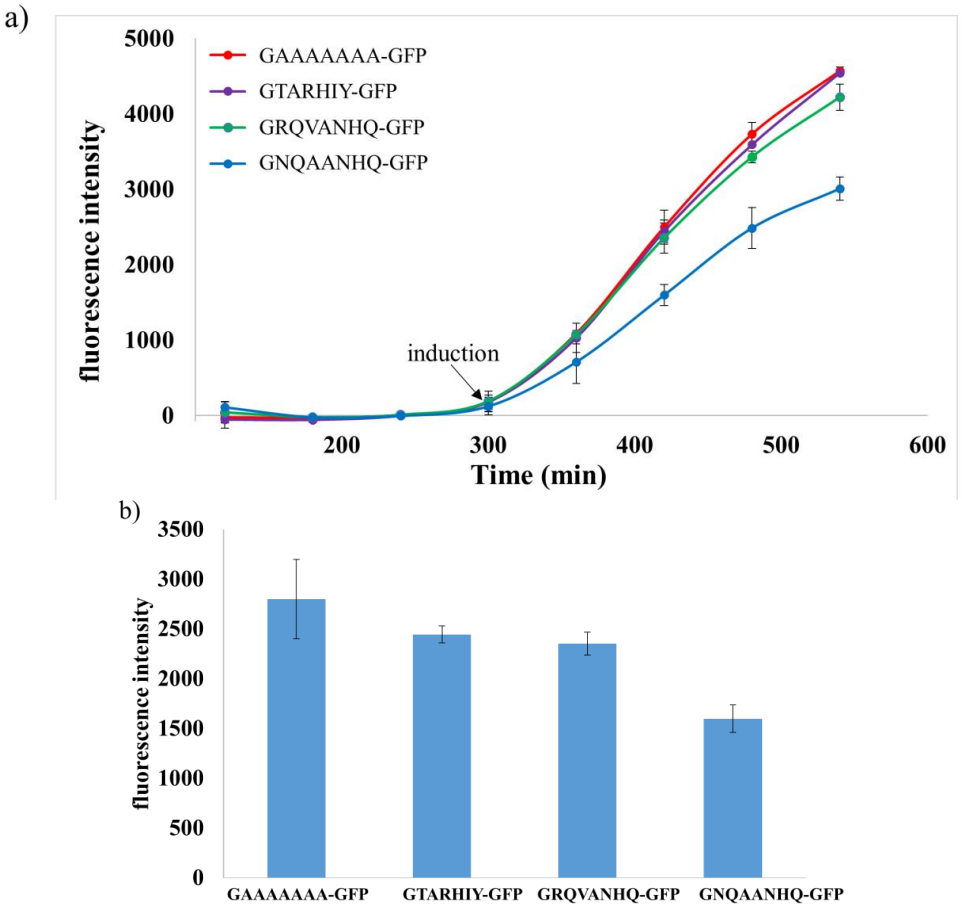

Figure 4.10 GFP translation assay. a) The level of GFP translation by different peptides in the TEV protease system is shown. The GFP fluorescence was measured for different peptides at different time intervals after induction. b) Compared to the control (GAAAAAAA-GFP), a modest decrease in fluorescence intensity was observed in the cultures expressing GNQAANHQ-GFP, GRQVANHQ-GFP, and GTARHIY-GFP fusion proteins. All growth assays were performed at least three times independently and results were averaged.

The amount of GFP translation in the presence of different peptides was monitored by measuring the fluorescence intensity (excitation at 487 nm and emission at 509 nm) at 60 min time intervals. The fluorescence intensity was divided by the optical density of the bacteria culture at each time point to calculate florescence intensity per cell and plotted against the time (min) (**Figure 4.10**). The presence of peptides did not completely inhibit GFP translation; however, compared to the negative control peptide, GNQAANHQ, GRQVANHQ, and GTARHIY showed 24, 7, and 5% inhibition of GFP translation, respectively. From the results of growth and fluorescence inhibition, we conclude that the *in vivo* expression of GNQAANHQ showed comparatively better inhibition of growth and protein translation of bacteria.

4.4.1.4 Purification of the EmGFP-pep fusion protein

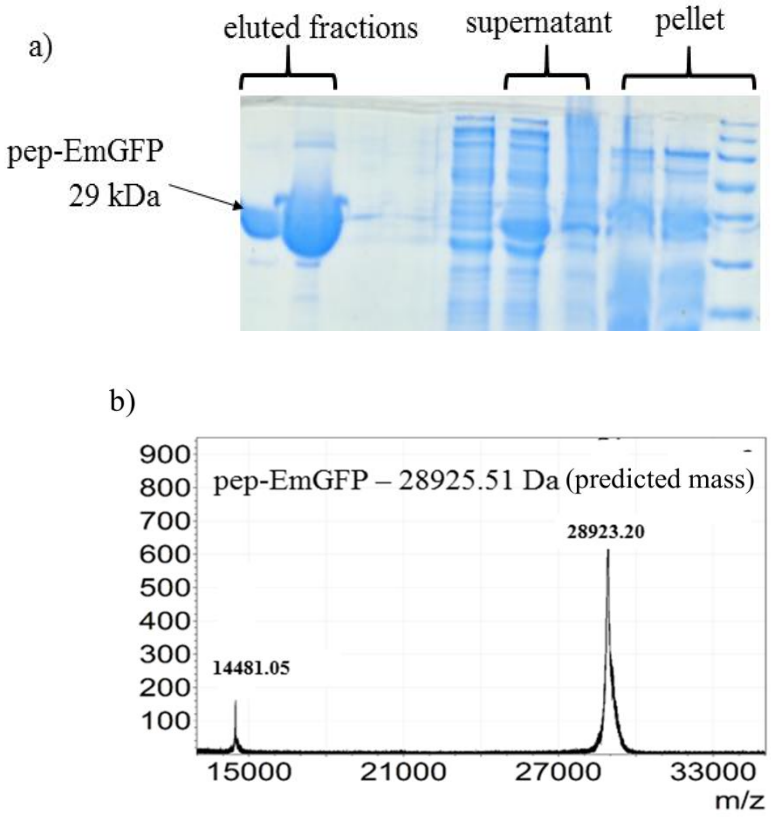

Figure 4.11 Protein purification and characterization. a) A 12 % SDS polyacrylamide gel shows the purified EmGFP-peptide fusion protein. b) The MALDI spectrum of the purified EmGFP-peptide fusion protein is given.

We could successfully utilize this TEV-protease-based, three-plasmid system to *in vivo* express H69 peptides as EmGFP fusion proteins. As previously described, the peptide construct was prepared in which a His-tag was placed at the C-terminus of the EmGFP gene such that the peptide-GFP fusion protein could be purified for further experiments.

The proteins were purified by Ni-affinity chromatography and the product was checked by running SDS-PAGE (**Figure 4.11a**). Isolated protein was characterized by Matrix-assisted laser desorption ionization time-of-flight (MALDI-TOF) mass spectrometry (**Figure 4.11b**). Purified GFP-tagged peptides can be used in *in vitro* binding experiments such as surface plasmon resonance (SPR) to further characterize the binding affinity and specificity of peptides to the H69 target.

4.4.2 *In vivo* expression of free peptides

In the first approach, we utilized a TEV-protease based plasmid system to *in vivo* express H69 targeting peptides as GFP fusion proteins in bacteria cells. In this system, the display protein EmGFP serves numerous functions such as stabilizing the structure, reducing proteolysis and producing a visible means of quantification. However, in order to further characterize selected peptides as potential drug leads, it is essential to determine their activity outside the context of the fusion protein. Therefore, in the second approach we utilized a different plasmid system to express H69- targeting peptides as free peptides in bacterial cells (**Figure 4.12**). The H69 targeting peptides NQAANHQ, RQVANHQ, and TARHIY were selected for the study.

4.4.2.1 Cloning of H69 peptides into pKantvec plasmid system

In this approach, a single plasmid expression system pKan5tvVec (8243 bp) with an inducible P_{BAD} promoter and kanamycin resistance was used as the vector. Therefore, the peptides could be expressed by inducing with L-arabinose (**Figure 4.12**).

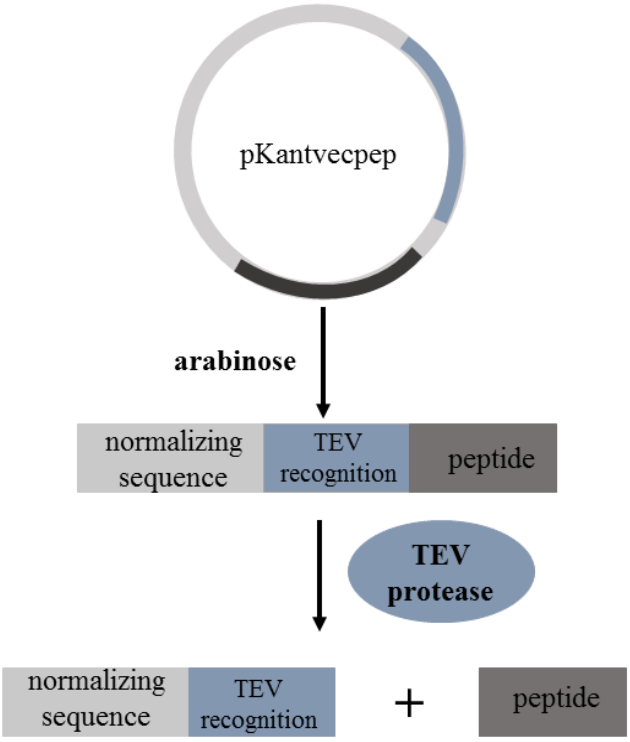

Figure 4.12 *In vivo* expression of free peptides. A schematic diagram for the production of free peptides using the TEV protease expression system is shown. The peptides were cloned behind the TEV protease recognition sequence and under control of the P_{BAD} promoter. Therefore, the expression of peptides and TEV protease was induced by adding arabinose. After TEV protease cleavage, free peptides would be available in the cell.

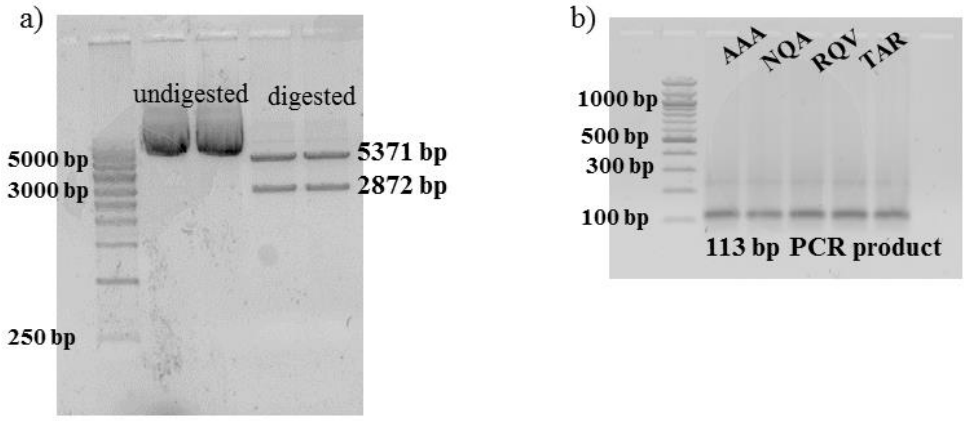

Figure 4.13 Plasmid vector and peptide insert preparation. a). Plasmid pkan5tvec (8243 bp) was digested using *Nhe* I and *Hind* III restriction enzymes and the gel band corresponding to the desired vector fragment (5371 bp) was purified before ligation. b) The peptide inserts were synthesized using the non-template PCR method and gel purified before and after restriction digestion. The size of the PCR product corresponding to the 7-mer peptide sequence was 113 bp.

The details of the pKan5tvVec plasmid system are explained in Chapter 2, Section 2.2.3. The peptide inserts were generated by using the non-template PCR method as described earlier. The size of the DNA product corresponding to the 7-mer peptide sequence was 113 pb. The PCR product was checked on an agarose gel before the restriction digestion (**Figure 4.13b**). The restriction enzyme sites *Hind* III and *Nhe* I were used to clone the peptide insert into the plasmid. Therefore, the peptide insert and plasmid vector were digested using *Hind* III *and Nhe* I enzymes (**Figure 4.13**). The DNA products were gel purified and ligated to obtain the new plasmid pKantvec-pep (5459 bp). The ligated plasmids were electrotransformed into *E. coli* DH5 cells. The correct ligation was confirmed by doing colony PCR (**Figure 4.14a**). The sequences of the peptide clones were confirmed by doing DNA sequencing (**Figure 4.14b**).

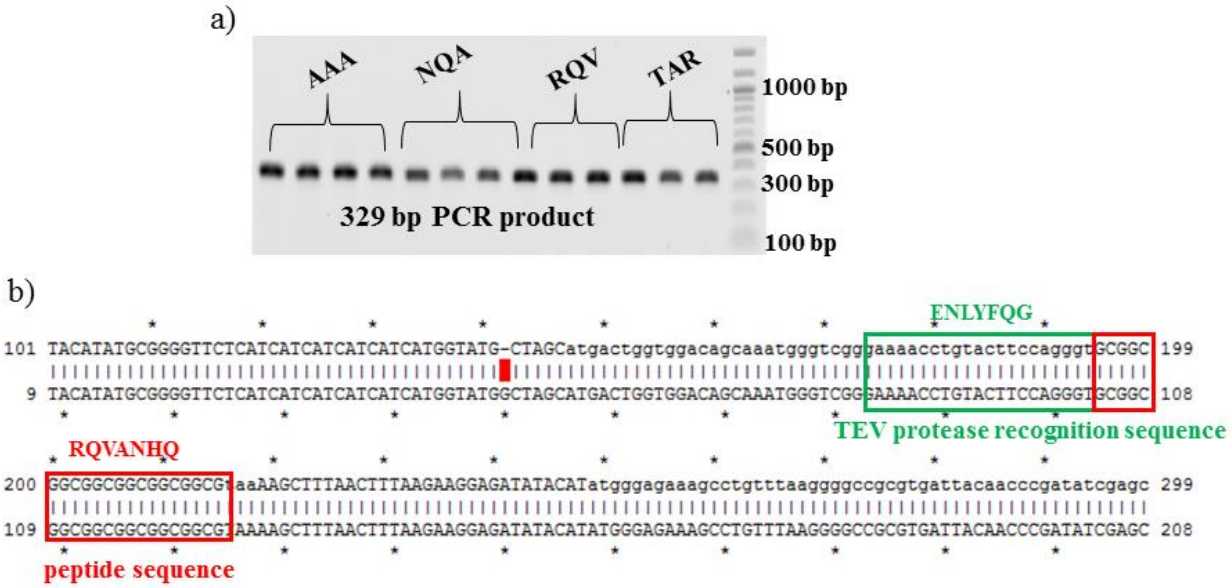

Figure 4.14 Peptide sequence confirmation. a) The peptide clones were confirmed by doing colony PCR, which gave a 329 bp PCR product for the 7-mer peptide in colony PCR. b) The sequence alignment of ligated plasmid is given. The full alignment was 1020 bp, whereas this section only shows the nucleotide sequence of the TEV recognition sequence in the first box (green) with the amino acid sequence labeled in green. The amino acid sequence of 7-mer peptide, RQVANHQ is shown in red and the corresponding nucleotides are in box 2 (red).

4.4.2.2 Study the effects of H69-targeting peptides on bacterial growth

After confirming the sequence of each peptide clone, they were used in bacterial growth assays as described in Chapter 2, Section 2.3.8. Bacteria were grown in LB/kanamycin medium. When cells reached late lag phase with OD_{600nm} = 0.2, (~200 min), L-arabinose was added to induce the expression of peptides. The bacterial growth was monitored by measuring the optical density of all bacterial cultures every 60 min (**Figure 4.15**). In growth assays, DH5 strain CSL011 from the Cunningham lab, which expresses peptide KGTRAFATTNSH, was utilized as a positive control. In previous studies in the Cunningham lab, this 12-mer peptide inhibited bacterial growth. The 7-mer peptide AAAAAAA with an N-terminus G was used as a negative control, and did not show growth inhibition in previous experiments. Compared to the negative control peptide GAAAAAAA, we did not see much difference between the growth curves and the inhibition profiles of the H69-targeting peptides.

Compared to the negative control peptide, the GNQAANHQ peptide showed only slightly more inhibition at 360 min. The percent inhibition of growth was calculated and normalized to the negative control peptide (**Figure 4.15b**). According to our results, 18, 14, and 7% inhibition was observed with the GNQAANHQ, GRQVANHQ, and GTARHIY peptides, respectively. In contrast to H69-peptides, the positive control peptide showed complete inhibition of growth right after induction. Throughout the incubation period it showed more than 80% inhibition of bacterial growth. The growth inhibition with the positive control peptide support that the peptides can have activities inside bacteria without undergoing proteolytic degradation or efflux.

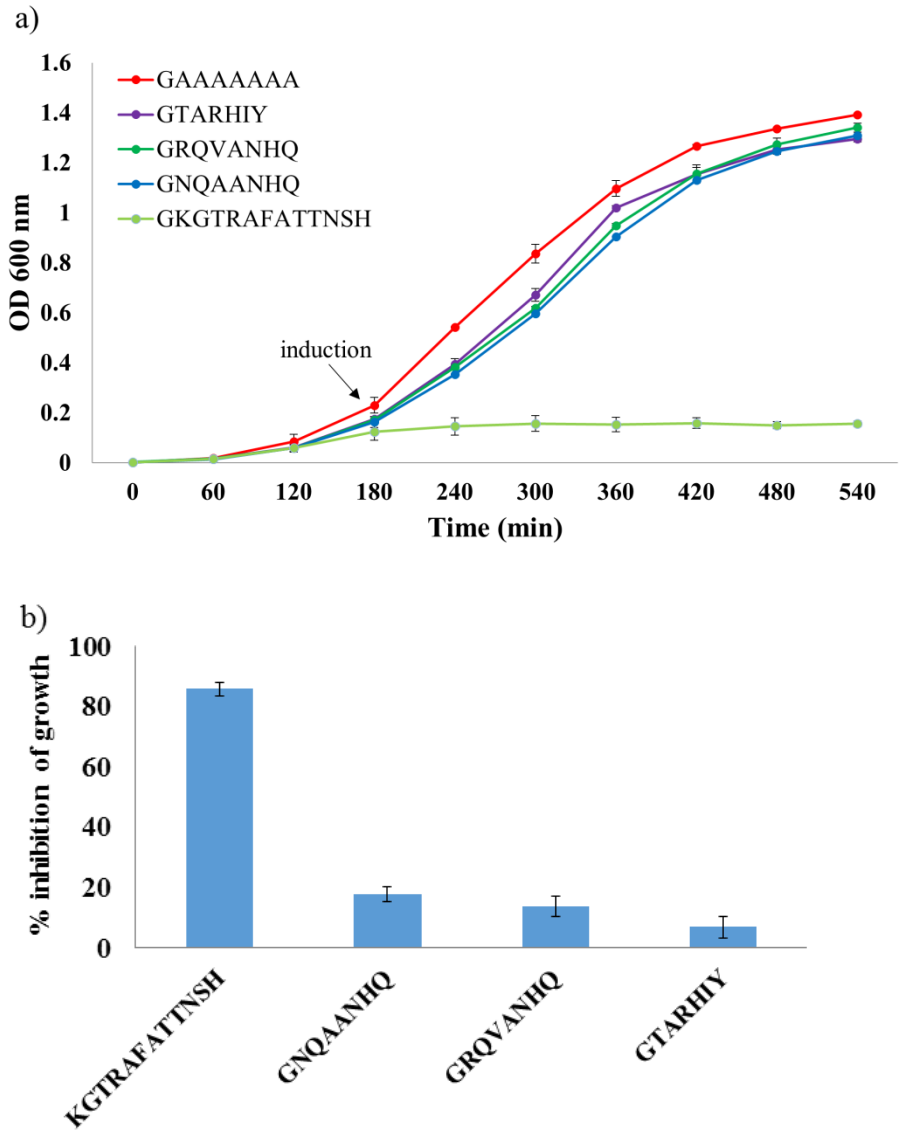

Figure 4.15 Effects of H69-targeting peptides on bacterial growth. a) Measurement of *E. coli* growth upon the expression of free peptides and TEV protease is shown. b) Percent inhibition of growth after 360 min of incubation was calculated and normalized to the negative control, GAAAAAAA. All growth assays were performed at least three times independently and results were averaged.

The peptides are overexpressing, but may undergo some level of undergoes degradation. However; our results suggest that the cell can produce enough peptide to reach the MIC. Therefore, growth inhibition appears to depend on the MIC of each peptide. The peptides with lower MICs would achieve cell death faster and display complete inhibition of growth. This idea

is supported by the complete inhibition by the 12-mer positive control peptide and oncocin discussed in Chapter 3. Therefore, we can conclude that MICs of the H69-targeting peptides are much higher than the 12-mer positive control peptide. By *in vivo* expressing the positive control peptide and a proline-rich AMP oncocin, we showed that our system can be used as a tool to *in vivo* express short peptide sequences and study their antibacterial activity. As mentioned before, in this TEV-protease-based plasmid system we cloned the 7-mer peptide sequence behind the TEV protease recognition sequence (ENLYFQG/S). Since TEV protease cleavage occurs between Q and G, an extra glycine (G) is left at the N-terminus of the peptide sequence. Therefore, all of the peptide sequences that were expressed have an extra G at the N-terminus. This may be a possible reason for the lower antibacterial activity of our peptides. However, it is not known if this small difference in the peptide sequence would affect the potency of the original peptide. One approach to test this would be to reclone the peptide sequences without G of the TEV protease recognition sequence. If the peptide sequences are cloned with the altered TEV protease recognition sequence, then completely free unaltered peptides will be produced inside bacterial cells. Another approach to test the effect of the extra glycine would be to clone the 7-mer peptide sequence in front of the TEV protease cleavage site. This approach would give the peptide with extra G at the C-terminus, NQAANHQG. If this arrangement of peptides shows enhanced activity, it would confirm that the N-terminus of the peptide is important for its antibacterial activity. Further cloning experiments with the above-mentioned approaches will provide a better understanding of the antibacterial activities of H69-targeting peptides as potential drug leads.

4.5 Overall summary and conclusions

The poor correlation between *in vitro* and in *vivo* activities of peptides is one of the major questions in antibiotic peptide research. In this work, we successfully utilized a plasmid-based systems to *in vivo* express H6-targeting peptides in bacteria. In the first approach peptides were expressed as GFP-fusion proteins, and in the second approach they were expressed as free peptides. However, bacterial growth assays revealed that selected peptide sequences do not have any significant antibacterial activity. The dynamic nature of H69 of differing conformations in the actual cellular environment compared to *in vitro* peptide selection conditions may also be a factor. Therefore, peptides or RNA may not find the active conformations that favor binding. Proteolytic degradation of these short peptides by bacterial proteases could be another possible reason for this behavior. In both systems, we found that GNQAANHQ peptide shows better inhibition compared to other H69-targeting peptides. Based on *in vivo* and *in vitro* data, we can consider NQAANHQ as a potential drug lead, but it will need considerable modifications or alterations to improve its activity. Further cloning experiments with the above-mentioned approaches may provide a better understanding of the antibacterial activity of H69-targeting peptides as potential drug leads.

CHAPTER 5 EFFECTS OF PSEUDOURIDINE MODIFICATION ON ANTIBACTERIAL ACTIVITY OF THE 2-DEOXYSTREPTAMINE AMINOGLYCOSIDES

5.1 Abstract

Aminoglycosides with a 2-deoxystreptamine (2-DOS) motif are known to inhibit protein translation by binding to the helix 44 (h44) region of the small subunit adjacent to the decoding site. However, recent x-ray crystal structures have shown that neomycin, paromomycin, and gentamicin are able to interact with the major groove of the helix 69 region (H69). Previous work in our lab revealed that Ψ modifications are important for efficient binding of aminoglycosides to H69. However, the effects of Ψ modifications on bactericidal activity of aminoglycosides have not been examined. Therefore, the objective of this work was to evaluate the effects of Ψ modification on the antibacterial activities of 2-DOS class aminoglycosides. Antibacterial activities were assessed by performing minimum inhibitory concentration (MIC) studies using wild-type and Ψ-deficient bacterial strains. Our data reveal that loss of Ψ modifications confers resistance to 4,6-linked-2-DOS aminoglycosides, gentamicin and kanamycin, whereas the effect was not significant with 4,5-linked-2-DOS aminoglycosides, neomycin and paromomycin. However, bacterial strains carrying partially defective RF2 show resistance to neomycin and paromomycin in the RluD(–) background. The observed results could be a combined effect of loss of Ψs and defective RF2 that perturbs the ribosome-drug interactions. The information gained from these studies provides deeper insight into the underlying mechanism of action of aminoglycosides, which is important for the development of unique antibiotics to target the bacterial ribosome at novel sites such as H69.

5.2 Introduction

The key roles in protein biosynthesis, structural complexity, easy accessibility, and high abundance in the cells, make the bacterial ribosome an obvious target for antibacterial drug development.[133,309,310] Most of known antibiotics target functional regions within the bacterial ribosome.[17,132] Aminoglycosides belong to a class of compounds effective against gram-negative bacteria.[311,312] These antibiotics inhibit the bacterial ribosome by interacting with rRNA.[135,140,313]

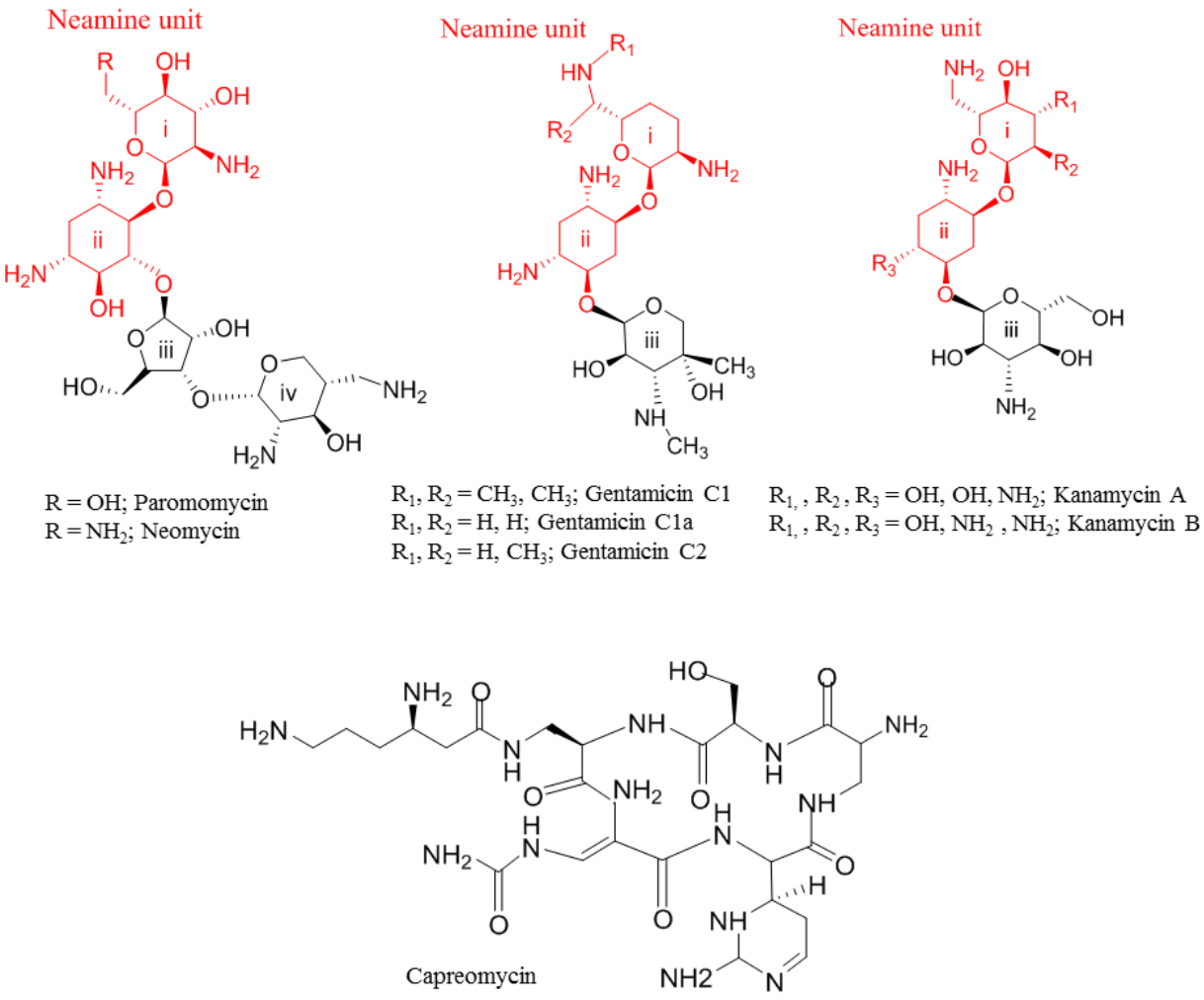

Figure 5.1 Aminoglycoside antibiotics. Chemical structures of the decoding-region-targeting antibiotics are shown with the common 2-DOS motif (highlighted in red). The cyclic peptide capreomycin is shown for comparison.

Aminoglycosides with a 2-deoxystreptamine (2-DOS) motif (**Figure 5.1**) are known to inhibit protein translation by binding to the 30S ribosomal subunit.[135,136] Neomycin, paraomomycin, kanamycin, and gentamicin are some examples in this class. The initially identified primary binding site of this family of antibiotics is the decoding region, involving the intersubunit bridge B2a.[137-139] Upon binding to helix 44 (h44), aminoglycosides stabilize the A site in an extra-helical conformation.[28] This conformational change shifts the position and dynamics of two universally conserved residues, A1492 and A1493, which are responsible for recognition of the mRNA codon-aminoacyl-tRNA complex.[138,140,141] This stabilized conformational state leads to incorporation of incorrect aa-tRNAs, and decreased translation fidelity.[134,142] However, decreased translation fidelity alone has little effect on cell growth. Literature reports revealed that bacteria strains harboring error-prone ribosomes are still viable.[143,144] Also, evidence of specific aminoglycosides inhibiting protein synthesis without exhibiting miscoding suggests that miscoding is not the only mechanism of action of aminoglycosides.[145] Furthermore, these combined observations suggest that aminoglycosides may interact with more than one functional site in the bacterial ribosome.

Interestingly, crystal structures have shown that neomycin, paramomycin, and gentamicin are able to interact with the major groove of helix 69 (H69) of 23S rRNA as well (**Figure 5.2**).[138,146,147] The interaction with H69 provides a possible mechanism for how aminoglycosides inhibit the recycling and translocation steps of protein synthesis.[33, 46] However, the bactericidal nature of 2-DOS aminoglycoside antibiotics is still poorly understood despite decades of clinical use and biochemical studies. The emergence of strains with antibacterial resistance as well as impaired hearing and kidney functions at high doses of aminoglycosides make them less effective in clinical applications.[314] Therefore, it is necessary to develop new and more specific

drugs to combat bacterial infections. Understanding the underlying mechanism of action of this class of antibiotics is significant for the development of unique antibiotics that target the bacterial ribosome.

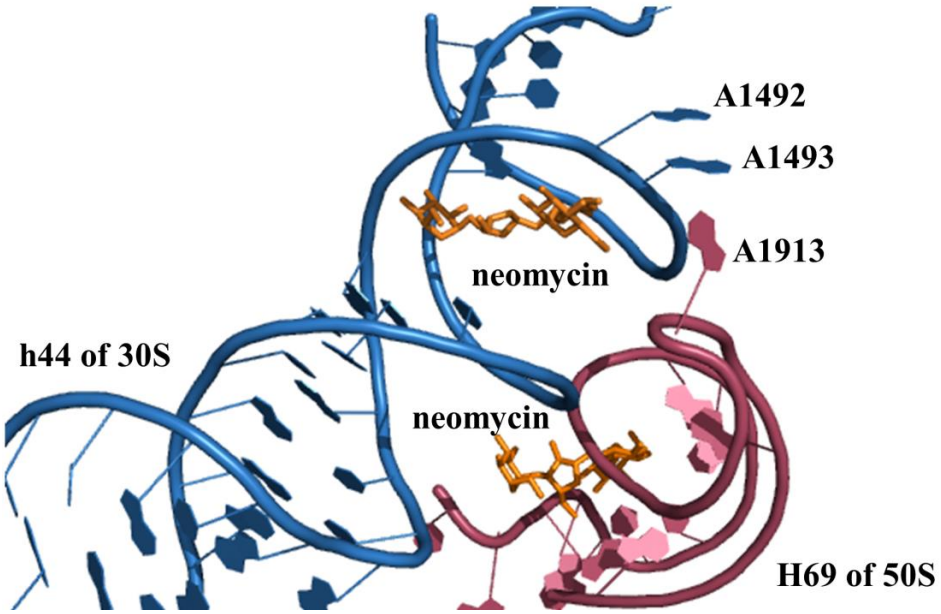

Figure 5.2 Binding of neomycin at the h44 and H69 regions of the ribosome. Neomycin binds at the decoding site of h44 and major groove of H69. Drug binding induces conformational changes of residues A1492 and A1493 of h44 and A1913 of H69 (PDB ID: 4V52).[147]

5.3 Objectives

The *E. coli rluD* gene encodes a pseudouridine synthase responsible for the Ψ modifications at positions 1911, 1915, and 1917 in H69 of 23S rRNA[196] (**Figure 5.3**). These Ψ modifications are important for ribosome function and modulation of the loop structure.[25] Previous work in our lab revealed that Ψ modifications are important for efficient binding of aminoglycosides to H69.[237,239] It was also shown that structurally similar aminoglycosides had different structural impacts on the modified and unmodified H69 RNAs.[237]

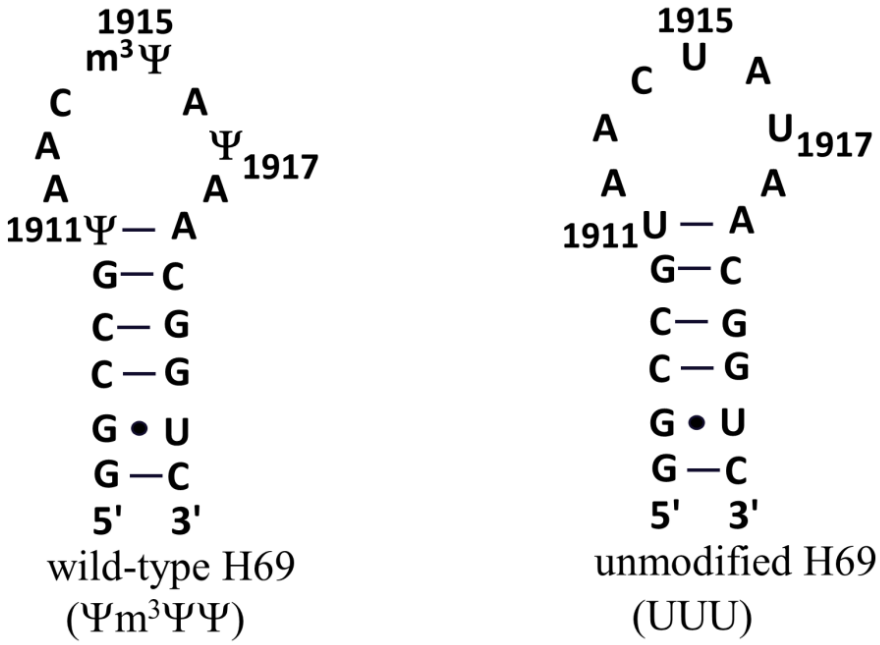

Figure 5.3 Pseudouridylation of H69. Secondary structures and nucleotide sequences of modified and unmodified H69 rRNA.

Previous observations with H69 model systems were further confirmed by doing antibiotic footprinting studies in the context of modified and unmodified full ribosome.[239] However, the effects of Ψ modifications on the bactericidal activity of aminoglycosides have not been examined. Considering previous observations, we hypothesized that lack of Ψ modifications would affect the antibacterial activity of aminoglycosides. Therefore, the objective of the current study was to investigate the effects of Ψ modifications of H69 on the bactericidal activity of the 2-DOS class of aminoglycosides.

5.4 Results and discussion

5.4.1 Background information on the different *E. coli* strains

Four different strains of *E. coli* were utilized in our MIC experiments (**Figure 5.4**). First, a brief background on the different bacterial strains used in the current study will be given.

E. coli K-12 MG1655 RluD(–) strain

Most of the previously reported genetic and biochemical analyses of rluD function have been carried out with *E. coli* K-12 strain MG1655.[102,315] It was reported previously that deletion of the *rluD* gene in *E. coli* K-12 strains led to extremely slow growth, increased read through of stop codons, and defects in 50S ribosomal subunit assembly and subunit association.[102,315] However, recent studies revealed that the RluD(–) mutant phenotype can be rescued by an additional mutation in RF2 at a site adjacent to H69-interacting residues.[316,317] Further genetic analysis revealed that the slow growth and other defects associated with inactivation of *rluD* in *E. coli* K-12 strains were due to a defective RF2 protein, with a threonine at position 246, which is in contrast to the more typical alanine found at this position in most bacterial RF2s.[318]

E. coli K-12 MC415 (wild-type) and MC416 (RluD(–)) strains

The suppressor mutations of RF2 link H69 residues with the termination phase of protein synthesis.[316,317] However, the role of Ψ modifications in the translation termination process was questionable. In order to study the role of Ψ modifications of H69, several *E. coli* K-12 strains with fully functional RF2 were generated by Michael O'Connor's lab.[317] In *E. coli* strain MC415, the K-12 *prfB* allele was replaced with the *E. coli B prfB*. Therefore, the strain has fully functional RF2 (alanine at 246). Deletion of the *rluD* gene in the MC415 strain produces *E. coli* strain MC416.[317] O'Connor's lab showed that deletion of the *rlud* gene did not affect growth or subunit association in these strains. This observation further confirmed that previously observed slow growth and other defects associated with inactivation of *rluD* in *E. coli* K-12 strains are due to a defective RF2 protein.[315] These observations suggest that inactivation of RluD pseudouridine synthase has minimal effects on bacterial growth and ribosome function. However, the highly conserved nature of H69 pseudouridylation suggests that it plays a

significant role in bacteria.[196] Previous *in vitro* studies showed that Ψ modifications play a role in aminoglycoside binding to H69.[237,239,319] Therefore, it was of interest to evaluate aminoglycoside suceptibilities of wild-type and Ψ-deficient strains. *E. coli* MC415 *(*wild-type, $\Psi m^3\Psi\Psi$) and *E. coli* MC 416 (RluD(–), Um^3UU) from O'Connors's lab were utilized in this study. The only genetic variation of these two strains is the deletion of *rlud* gene in MC416.[317] Therefore, direct comparisons of MICs of these two strains indicate the effects of modifications on the antibacterial activities of the drugs we studied.

***E. coli* MRE600**

MRE600 is an *E. coli* strain that was originally identified for its low RNase I activity.[320-322] The architecture of the MRE600 genome is distinct from that of *E. coli* K-12. However, the MRE600 translational machinery is similar to that of *E. coli* K-12. The MRE600 strain carries modified H69 with three Ψ modifications in the loop region (1911, 1915 and 1917).[321] Also, in contrast to *E. coli* K-12 strain, MRE600 has an alanine at position 246 of RF2.[323] Comparative analyses between MRE600 and *E. coli* K-12 showed that these two strains exhibit nearly identical ribosomal proteins, ribosomal RNAs, and highly homologous tRNA species.[321] Considering these similarities, MRE600 and K-12 MG1655 RluD(–) were used in our previous aminoglycoside footprinting experiments to isolate modified and unmodified ribosomes.[239] However, the growth of these strains with aminoglycosides was not assessed. Therefore, the four different *E. coli* strains were utilized in MIC experiments with a series of aminoglycosides that are known to target H69 and the A site of ribosomes. MIC experiments were carried out simultaneously with the four different strains and at least three independent experiments were carried out with each antibiotic.

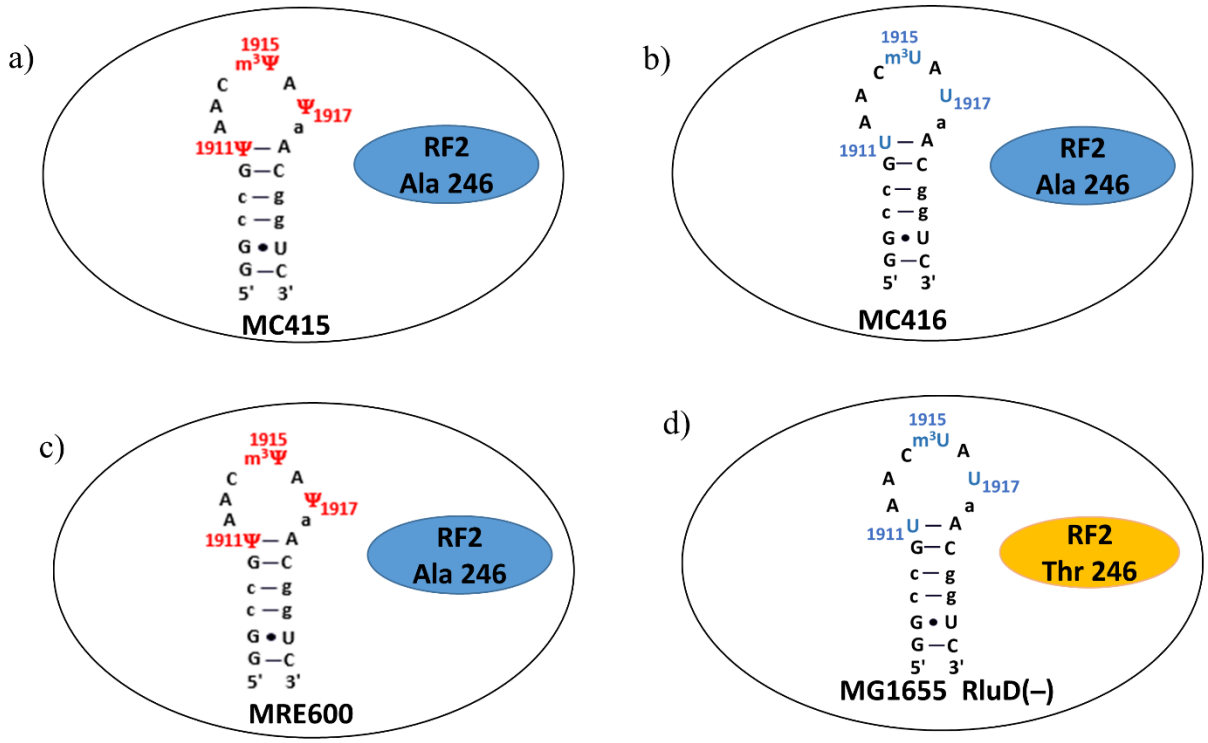

Figure 5.4 *E. coli* strains used in the study. a) *E. coli* strain MC415 has modified H69 and RF2 with alanine at position 246. b) *E. coli* strain MC416 is the RluD(–) version of MC415. c) *E. coli* strain MRE600 has modified H69 and RF2 with alanine at position 246. d) *E. coli* MG1655 RluD(–) strain has unmodified H69 and defective RF2 with threonine at position 246.

5.4.2 Comparison of MICs with different bacterial strains

MC415 vs. MC416

MC416 is the RluD(–) version of MC415 (**Figure 5.4a & b**). Other than absence of the *rluD* gene in MC416, these two strains are genetically similar.[317] Therefore, we can do direct comparison of the MICs of these two strains. If there is any difference in MICs, we can consider it as a consequence of the Ψ modifications in H69.

MC416 vs. MG1655 RluD(–)

Both of these RluD(–) strains are derived from *E. coli* K-12. However, MC416 has fully functional RF2 with alanine at 246 position, whereas MG1655 has defective RF2 with threonine

at position 246.[318] Previous studies showed that loss of Ψ modifications affect RF2-ribosome interactions and the effect is significant in *E. coli* K-12 strains carrying defective RF2.[315] However, until now we did not know how defects in RF2-ribosome interactions affected drug binding or antibacterial activities of aminoglycosides. Therefore, comparison of the MIC values of MC416 and MG1655 RluD(–) strains reveals the effects of perturbed RF2-ribosome interactions on the antibacterial activities of aminoglycosides.

MRE600 vs. MC415

Although both of these strains carry modified H69, we cannot do a direct comparison of the MIC values because they are two different strains of *E. coli*. MRE600 is a divergent *E. coli* strain that displays features of the closely related genus Shigella, whereas MC415 is an *E. coli* K-12 strain derived from *E. coli* MG1655.[321,323] However, comparative analyses between MRE600 and K-12 revealed that these two strains exhibit nearly identical ribosomal proteins, ribosomal RNAs, and highly homologous tRNA species.[321] Therefore, we hypothesized that these two strains would show similar inhibition profiles for ribosome-targeting antibiotics. A recent study investigating the genomes of 20 *E. coli* strains identified a total of 17,838 distinct genes, with only 1,976 being common to all. Such genomic variation contributes to each strain's distinct physiological properties, such as their varied abilities to metabolize sugars, resistance to particular antibiotics, and growth rate-temperature profiles.[321,324] Therefore, in addition to drug-target interactions, genomic variations of each bacteria strain would affect the *in vivo* potency of the drug. This would give rise to unique inhibition and resistance profiles to these structurally similar aminoglycosides.

5.4.3 Neomycin shows better inhibition than paromomycin

Neomycin and paramomycin are structurally similar 4, 5-linked-2-DOS aminoglycosides. Paromomycin differs chemically from neomycin at a single position in ring 1 (**Figure 5.1**). Neomycin has a primary amine at the 6' position, whereas it is a hydroxyl group in paromomycin. Recently, the crystal structures of neomycin and paromomycin bound with *E. coli* 70S ribosomes were solved. According to these crystal structures, both neomycin and paromomycin interact with the major groove of h44 and H69, namely the intersubunit bridge B2a region.[146,147] However, crystal structures revealed that paromomycin induces a different H69 loop conformation compared to neomycin.[140,146] These *in vitro* observed structural and binding differences could affect the *in vivo* potency of the drug and this would give rise to unique inhibition and resistance profiles to these aminoglycosides despite their structurally similarities.

Literature reports that neomycin is the most potent and toxic member of 4,5-linked aminoglycoside class.[325] This is in good agreement with the higher affinty binding of neomycin to bacterial A site as well as H69 compared to paramomycin.[319,326] The reported K_d values of neomycin and paramomycin for the A site RNA range from 60 nm to 0.02 μM, depending on the method and conditions.[319,326] Previous biophysical studies showed that unmodified H69 has a more than 10-fold higher affinity for neomycin (K_d = 0.3 (± 0.1) μM) than paramomycin (5.4 (± 1.1) μM).[319] In our MIC experiments, neomycin showed better bactericidal activity compared to paramomycin in both wild-type (MRE 600 and MC415) and Ψ-deficient (RluD**(–)**) strains (MG1655 and MC416) (**Table 5.1 and Figure 5.5**). For both wild-type strains, neomycin showed ~2-fold lower MIC value compared to paramomycin. For the RluD**(–)** strains, neomycin showed ~4-fold lower MIC values compared to paramomycin (**Table 5.1**).

Table 5.1 Comparison of the observed MIC values for different antibiotics tested.

	Wild-type		RluD(–)	
Antibiotic	**MRE600**	**MC415**	**MG1655**	**MC416**
Neomycin	> 0.7 mg/L	> 0.7 mg/L	> 11 mg/L	> 0.7 mg/L
Paromomycin	> 1.4 mg/L	> 1.4 mg/L	> 43 mg/L	> 2.8mg/L
Gentamicin	> 0.7 mg/L	> 0.045 mg/L	> 0.7 mg/L	> 0.7 mg/L
Kanamycin	> 1.4 mg/L	> 0.045 mg/L	> 1.4 mg/L	> 1.4 mg/L
Capreomycin	> 43 mg/L	> 43 mg/L	> 43 mg/L	> 43 mg/L
Carbenicillin	> 0.35 mg/L	> 0.35 mg/L	> 0.35 mg/L	> 0.35 mg/L

MIC experiments were carried out simultaneously with the four different strains and at least three independent experiments were carried out with each antibiotic.

Similar MIC values were observed for both wild-type strains, MRE600 and MC415, for both aminoglycosides, despite the fact that they are two distinct strains of *E. coli*. The MRE600 genome is distinct from that of *E. coli* K-12, however, their translational machinery is similar to that of *E. coli* K-12.[321] Comparative analyses between MRE600 and *E. coli* K-12 show that these two strains exhibit nearly identical ribosomal proteins, ribosomal RNAs, and highly homologous tRNA species.[321] Therefore, we can assume that these two strains would show similar inhibition profiles to ribosome-targeting antibiotics. Indeed, the observed MIC values for the wild-type *E. coli* strains are similar to literature reported values for neomycin and paramomycin.[189,327] Therefore, our MIC data are in a good agreement with the literature, with greater activity of neomycin compared to paromomycin. The inhibition profiles of neomycin and paromomycin for three *E. coli* K-12 strains, MC415, MC416 and MG1655 RluD(–), are shown in **Figure 5.5**.

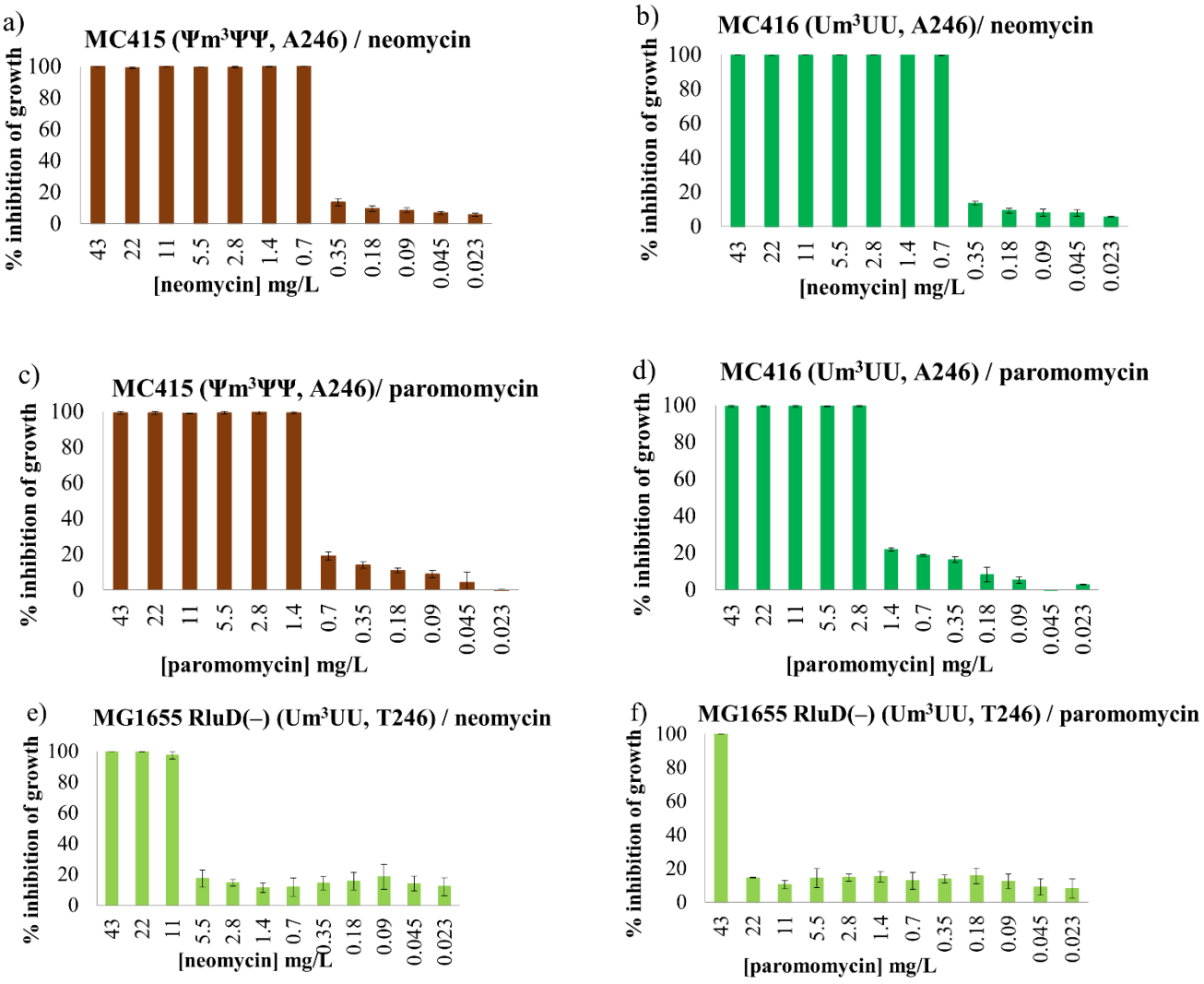

Figure 5.5 Growth inhibition profiles of neomycin and paromomycin in *E. coli* K-12. Inhibition data for the MIC experiments done with neomycin and paromomycin in a) & c) MC415 (wild-type,$\Psi m^3\Psi\Psi$), b) and d) MC416 (RluD(–),Um^3UU) and e) and f) MG1655 RluD(–). Percent inhibition of bacterial growth in the presence of different drug concentrations was calculated and normalized to the growth control as described in **Chapter 2,** Methods, Section 2.6.

5.4.4 Loss of pseudouridylation of H69 confers resistance to paromomycin compared to neomycin

The main objective of the current study was to evaluate the effects of Ψ modifications on the antibacterial activity of 2-DOS-class aminoglycosides, which are known to target H69. Previous studies suggested that Ψ modifications are important for modulation of H69 loop

structure.[328,329] Previous studies also showed that structurally similar aminoglycosides had different structural impacts on the modified and unmodified H69 RNAs.[237] These observations with H69 model systems were further confirmed by doing antibiotic footprinting studies on modified and unmodified ribosomes.[239] However, the effects of Ψ modifications on the bactericidal activity of aminoglycosides had not been examined. Considering previous observations, we hypothesized that lack of Ψ modifications would affect the antibacterial activity of aminoglycosides.

For direct comparison of the effects of *rlud* gene deletions on the antibacterial activities, two strains of *E. coli* K-12, generated by Michael O'Connor's lab, MC415 (wild-type, $\Psi m^3\Psi\Psi$) and MC416 (RluD(–), Um^3UU), were utilized in MIC experiments. Although typical *E. coli* K-12 strains have defective RF2 with an Ala246Thr mutation, the two strains utilized in this study have corrected RF2 with alanine at position 246. For neomycin, the observed MIC values for wild-type and RluD(–) strains were both > 0.7 mg/L (**Figures 5.5 a &b, Table 5.1**). In contrast, for paromomycin the observed MIC value for the RluD(–) strain was 2-fold higher than that of the wild-type strain (**Figures 5.5 c & d, Table 5.1**). These data indicate that the Ψ modifications on H69 affect the antibacterial activity of paromomycin, but not neomycin. Considering the structural similarities of these aminoglycosides, it was surprising to observe such different behavior in the RluD(–) strain. To understand this result, we examined the crystal structures of neomycin and paromomycin bound to 70S ribosomes. According to crystal structures, both neomycin and paromomycin interact with the major groove of h44 and H69, namely the intersubunit bridge B2a region.[147] However, the crystal structures revealed that paromomycin induces a different H69 loop conformation compared to neomycin. According to these structures, residue A1913 located at the apical tip of H69 forms hydrogen bonding interactions with the 6'

hydroxyl group of paramomycin (**Figure 5.6**), which was not observed with neomycin.[140] Further single-molecule FRET studies revealed that neomycin and paromomycin drive subunit rotation in opposite directions, which may be the result of differing interactions with H69.[146]

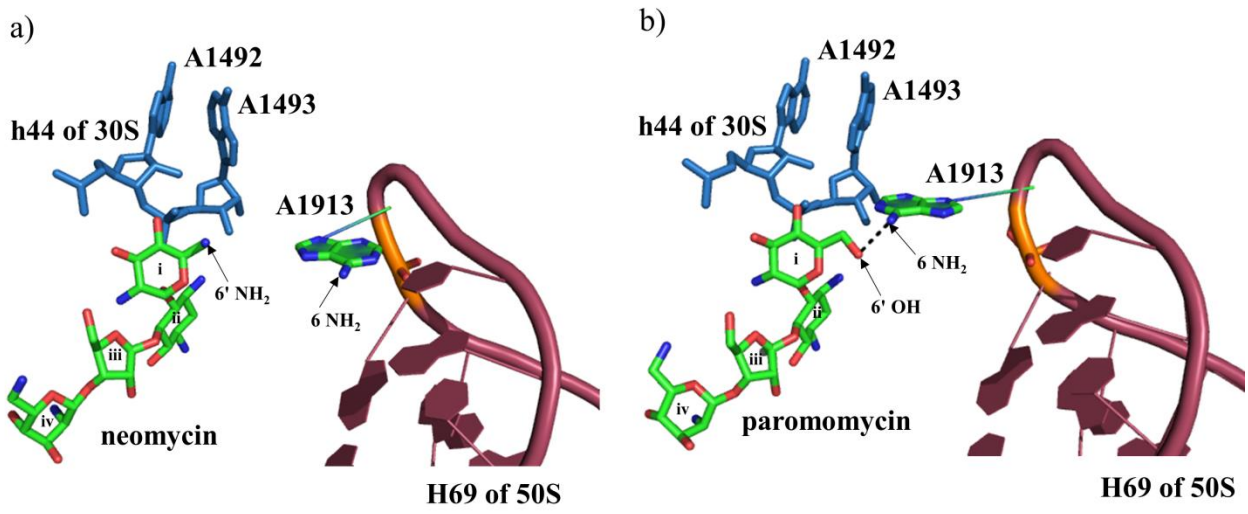

Figure 5.6 Crystal structures of 70S *E. coli* ribosomes bound a) neomycin (PDB ID: 4V9C)[140] and b) paromomycin (PDB ID: 4WOI).[146] Neomycin and paromomycin induce distinct H69 loop conformation. In contrast to neomycin, paromomycin bound within the h44-decoding site contacts the apical tip of H69 via ring I (6'-OH) and the universally conserved base A1913 (N6) of H69 from its canonical h44 site of binding. The potential formation of a H-bonding interaction is shown in black dotted lines.

Information from crystal structures and single-molecule FRET studies suggests that A1913 remains dynamic when neomycin is bound and relatively static when paromomycin is bound.[140,146] It is interesting that previous biochemical studies in our lab also suggested similar behavior of H69 with neomycin and paromomycin.[237] Previous work using H69 model systems as well as antibiotic footprinting experiments in the context of full ribosomes revealed that neomycin and paromomycin induce different structural impacts on the ribosome despite their structural similarity.[237,239] It was also shown that these structural impacts are influenced by Ψ modifications. The different conformational changes induced by neomycin would help to

maintain its strong binding interactions with the ribosome, and it is not affected as greatly by the perturbations caused by the loss of Ψ modifications. In contrast, paromomycin was more susceptible to H69 perturbations caused by the loss of Ψs. Therefore, we concluded at this point that different binding patterns within the ribosome give unique inhibition and resistance profiles to paromomycin and neomycin, despite their structural similarities as 4,5-linked aminoglycosides.

5.4.5 Defective RF2 in RluD(–) confer resistance to both neomycin and paromomycin

Previous studies have shown that the H69 is indispensable for efficient termination by RFs and its conformational dynamics are likely to be important to facilitate a stable RF interaction with the ribosome.[330-332] However, the role of Ψ modifications in H69 in the translation termination process is questionable. Recent studies revealed that the RluD(–) mutant phenotype in *E. coli* K-12 can be rescued by an additional mutations in RF2 at a site adjacent to H69-interacting residues.[316] This suppressor mutation links H69 Ψ residues with the termination phase of protein synthesis. However, the role of H69-RF2 interactions in translation termination is still not understood clearly. In another study, Kipper and co-workers investigated the role of H69 Ψs in peptide release by class 1 release factors in an *in vitro* system consisting of purified components of the *E. coli* translation apparatus.[333] In this study, they showed that lack of all three Ψs compromised the activity of RF2, but did not affect the activity of RF1.[333] Altogether these previous observations suggest that H69-RF2 interactions play an important role in translation termination. Therefore, it is of interest to see how defective RF2 affects the RF2-H69 interaction. Residue 246 in *E. coli* RF2 is threonine in strain K12, whereas it is a conserved alanine or serine in other known bacterial sequences of RF2, including other strains of *E. coli*.[318]

Amino acid residue 246 in RF2 is four positions towards the N-terminus, and very close to the universally conserved GGQ motif (**Figure 5.7**).[318,323]

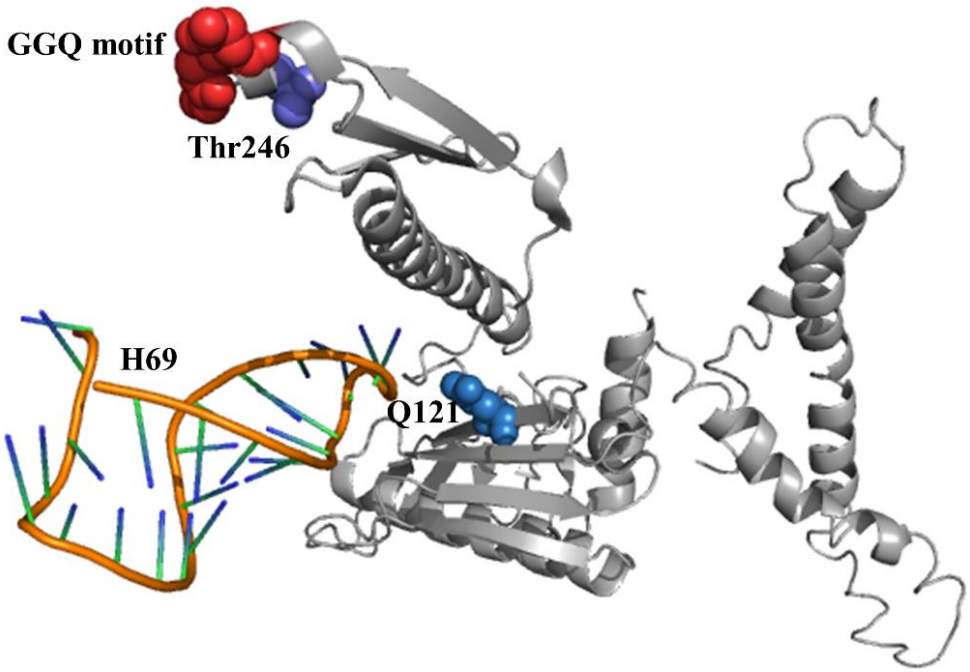

Figure 5.7 Crystal structure of RF2 bound ribosome. Residue 246 is in close proximity to the universally conserved GGQ motif. Q121 of RF2 is within H-bonding distance to C1914 and U1915 of the loop region of H69 (PDB ID: 4V5E).[334]

Previous studies revealed that amino acid residue 246 plays a crucial role in stop codon recognition and polypeptide release during translation termination.[318] In these studies, it was shown that Thr246 decreases RF2-dependent translation termination efficiency compared with Ala246.[318,323] Further studies revealed that effects of decrease in translation efficiency are significant in RluD(–) bacterial strains.[317] From these observations, it is clear that pseudouridylation and Ala246 play important roles in the H69-RF2 interaction. Moreover, work in the O'Connor lab revealed that inactivation of the *rluD* gene in *E. coli* strains containing the *prfB* allele from *E. coli* B or in *Salmonella enterica*, both carrying a fully functional RF2 (with Ala246), had negligible effects on growth, termination, or ribosome function.[317] According to the

crystal structure, residue 246 of RF2 does not have direct interactions with the H69 region (**Figure 5.7**).[334,335] However, an Ala246Thr mutation might cause indirect effects on the H69-RF2 interaction, which might be enhanced in the RluD(–) background since H69 has a less ordered loop conformation.[329]

The 2-DOS class of aminolglycosides is known to target the H69 region and inhibit the ribosome recycling step.[147] Since ribosome recycling and termination are sequential steps in the translation process, defects in the termination step may affect drug binding as well as the inhibition profiles of these drugs. On the other hand, it is still not clearly understood how the *E. coli* K-12 strain with defective RF2 (Thr246) would respond to aminoglycosides compared to strains with fully functional RF2. In addition to decreased translation termination efficiency, defective RF2 may play a role in antibiotic resistance, specially under an RluD(–) background. Considering these facts we thought it would be of interest to compare the inhibition profiles of MG1655 RluD(–) (UUU, Thr246) and MC416 (UUU, Ala246) strains. Both of these strains are *E. coli* K-12 strains and the only genetic variation is the single mutation in RF2, which results in fully functional RF2 in MC416 and defective RF2 in MG1655. Comparison of the inhibition profiles of MG1655 RluD(–) with MC416 could reveal the importance of the fully functional RF2 on the antibacterial activity. For the MG1655 RluD(–) strain, the observed MICs for neomycin and paromomycin are 11 and 43 mg/L, respectively. The observed MICs are 16-fold higher than those with the MC416 strain (**Figure 5.5 b, e & d, f)**. This result indicates that the defective RF2 in MG1655 confers resistance to both neomycin and paromomycin. From these data, we suggest that RF2-H69 interactions may play direct or indirect roles in drug binding and antibacterial activities of these structurally related aminoglycosides. With these observations, we propose that bacterial strains carrying partially defective RF2 show resistance to neomycin and

paromomycin in the RluD(–) background. Further, we suggest that aminoglycoside resistance could arise through defects in pseudouridylation or RF2 mutations. The observed results could be a combined effect of defective RF2 and loss of Ψs on MG1655 strain that perturbs the RF2-H69 interactions.

5.4.6 Loss of Ψ modifications confers resistance to 4, 6-substituted 2-DOS aminoglycosides

Kanamycin and gentamicin have a 4,6-substituted 2-DOS moiety instead of the 4,5-substituted 2-DOS found in neomycin and paromomycin (**Figure 5.1**). Both of these antibiotics are known to bind the A site of the 30S ribosomal subunit and inhibit protein synthesis.[147] However, crystal structures revealed that gentamicin also interacts with the H69 region as a secondary binding site.[147] Considering their different binding modes with H69, it was of interest to see how pseudouridylation affects the antibacterial activities of these drugs. Previous biochemical data showed that structural differences of gentamicin impact the binding to H69.[237,239] For example, previous antibiotic footprinting studies in our lab revealed that at the higher concentrations, gentamicin appears to have a secondary binding site on H69 or an altered binding mode that leads to different interactions with H69 compared to neomycin and paromomycin.[239] Similar differences were obtained previously with A-site RNA constructs, in which the 4,6-linked aminoglycoside displayed binding stoichiometries greater than 1:1.[141] Since Ψ modifications in the H69 loop region are associated with modulation of the conformational states, studies were carried out previously to see how the modifications affect the binding of gentamicin to H69. In previous antibiotic footprinting experiments, a lower level of DMS protection at G1922 of unmodified H69 compared to the wild-type suggested that Ψ modifications play a role in aminoglycoside binding to H69.[239] However, the level of protection by gentamicin was much lower compared to neomycin and paromomycin. These data also

supported that gentamicin has different binding interactions with H69, and Ψ modifications are important for those interactions. Even though gentamincin and kanamycin are structurally related aminoglycosides, kanamycin targets the h44 region and has not been shown to interact with H69.[336] Therefore, despite their structural similarity, kanamycin might recognize different RNA structural motifs. In this study, MIC experiments were carried out with the 4,6-linked aminoglycosides and wild-type (MC415, $\Psi m^3\Psi\Psi$) and RluD(–) strains (MC416 (Um^3UU) (**Figure 5.8**).

As mentioned previously, both strains have fully functional RF2 (Ala 246) and the only genetic variation is the *rluD* gene deletion in MC416.[317] For gentamicn, the observed MICs for wild-type and RluD(–) strains are 0.045 mg/L and 0.7 mg/L, respectively (**Figure 5.8a & b**). Interestingly, the RluD(–) mutant shows a 16-fold higher MIC value compared to the wild-type strain with modified H69. This observation is in good agreement with our antibiotic footprinting studies with unmodified RNA and gentamicin.[239] Interestingly, we observed similar behavior for the structurally-related kanamycin. (0.045 mg/L and 1.4 mg/L for wild-type and RluD(–) strains (**Figure 5.8c & d**). Compared to wild-type the RluD(–) strain showed a ~30-fold higher MIC for kanamycin. Considering the close proximity of h44 and H69 in the 70S ribosome, we hypothesize that modifications on H69 could affect the mechanism of action of A-site binding antibiotics.

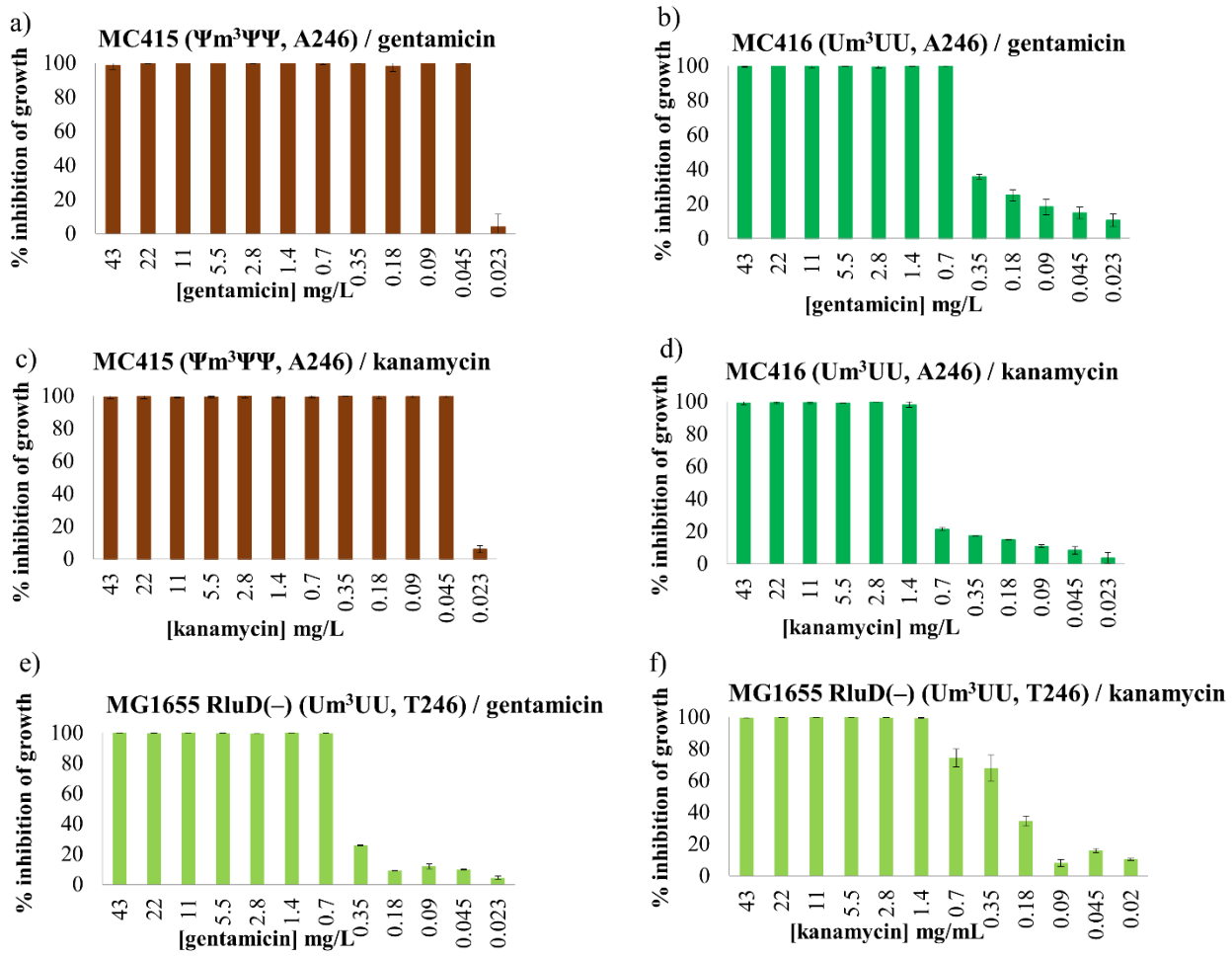

Figure 5.8 Effects of H69 pseudouridylation on antibacterial activity of 4,6-linked aminoglycosides. Inhibition data for the MIC experiments done with gentamicin and kanamycin in a) and c) wild-type MC415 and in b) and d) RluD(–) MC416 strains and e) and f) MG1655 RluD(–). Percent inhibition of bacterial growth in the presence of different drug concentrations was calculated and normalized to the growth control as described in **Chapter 2**, Methods, Section 2.6.

Our data with kanamycin suggest that conformational changes of H69 upon loss of modifications could affect the binding and/or antibacterial activity of kanamycin, although we cannot determine whether this effect is direct (H69 binding) or indirect (h44 binding). Altogether our data indicate that absence of pseudouridylation confers resistance to 4,6-linked-2-DOS

aminoglycosdies. Future structure studies may reveal how these different binding interactions might lead to the differing inhibition and resistance profiles of these aminoglycosides.

5.4.7 Defective RF2 in RluD(–) does not confer resistance to 4,6-linked-2-DOS aminoglycosides

We also determined MICs of gentamicin and kanamycin in the MG1655 RluD(–) strain, which lacks fully functional RF2. Comparison of the MIC values of MC416 and MG1655 RluD(–) strains reveals the effects of perturbed RF2-ribosome interactions on the antibacterial activities of aminoglycosides. In contrast to our observations with neomycin and paromomycin (Section 5.4.5), we did not observe any differences in MICs in the MG1655 strain compared to MC416 with fully functional RF2 (**Figure 5.8e & f**). The different trends with structurally similar aminoglycosides, 4,5- vs. 4,6-linked, are consistent with their different binding interactions with the ribosome.[147,336] From these observations, we conclude that perturbations caused by defective RF2 and lack of Ψs do not equally affect all aminoglycosides. Perhaps the H69 conformational changes induced by Ψ or RF2 do not affect or are not significant enough to impact the *in vivo* activities of 4,6-linked aminoglycosides, but are important for the 4,5-linked compounds. These results provide further evidence for the secondary role of H69 in aminoglycoside antibiotic activity.

5.4.8 Loss of Ψ modifications do not affect the antibacterial activity of peptide antibiotic capreomycin

Capreomycin is a cyclic peptide antibiotic that belongs to the tuberactinomycin family.[148] Viomycin was the first peptide antibiotic identified in this family. However, the second-generation drug capreomycin is the only member being clinically used for *Mycobacterium tuberculosis* infections.[148,149] These cyclic peptide antibiotics do not effectively inhibit *E. coli* cell growth and their mechanism of action is not clearly understood. Such peptide antibiotics are proposed to inhibit ribosome translocation by stabilizing the A-site tRNA binding interaction,

while allowing EF-G binding and GTP hydrolysis.[337] Capreomycin was recently found to bind at the interface of the ribosomal subunits and interact with H69 of the 50S subunit and h44 of the 30S subunit simultaneously (**Figure 5.9**).[149]

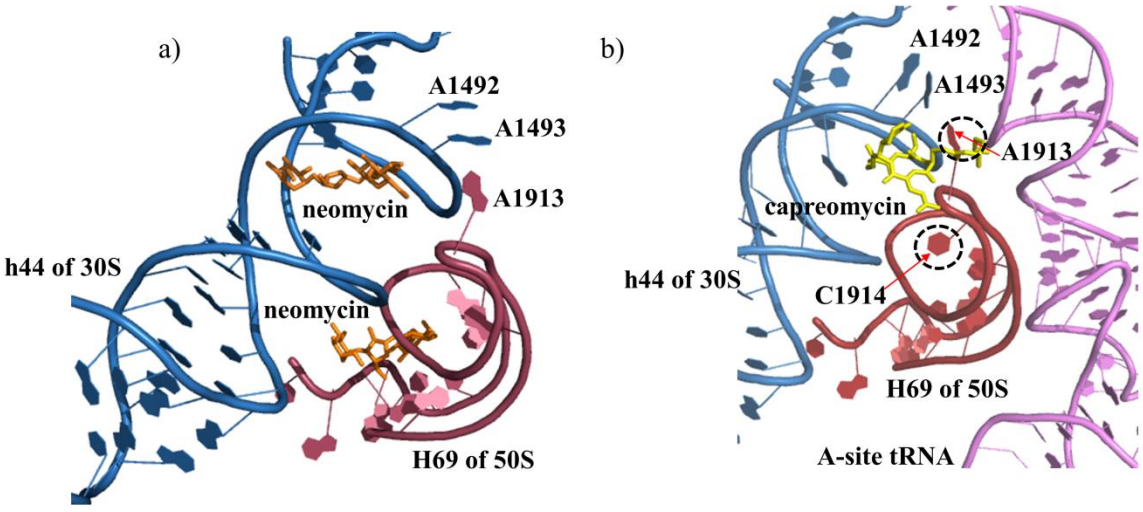

Figure 5.9 Crystal structures of a) neomycin (PDB ID: 4V9C)[140] and b) capreomycin (PDB ID: 4V7M)[149] bound 70S ribosomes. Capreomycin bind at the interface of the ribosomal subunits and interact with H69 of the 50S subunit and h44 of the 30S subunit simultaneously. In contrast, two neomycin molecules bind at the decoding site of h44 and major groove of H69.

Capreomycin binds to a site that lies between the large and small subunit in a cleft formed between h44 of the 16S rRNA and the tip of H69 of 23S rRNA. According to a crystal structure, the binding mode of capreomycin to H69 is different than aminoglycoside antibiotics.[149] This was further confirmed in antibiotic footprinting studies, in which capreomycin did not show any interactions with H69.[239] Considering its different binding mode with H69 compared to aminoglycosides, it was of interest to examine the effect of H69 pseudouridylation on the antibacterial activity of capreomycin.

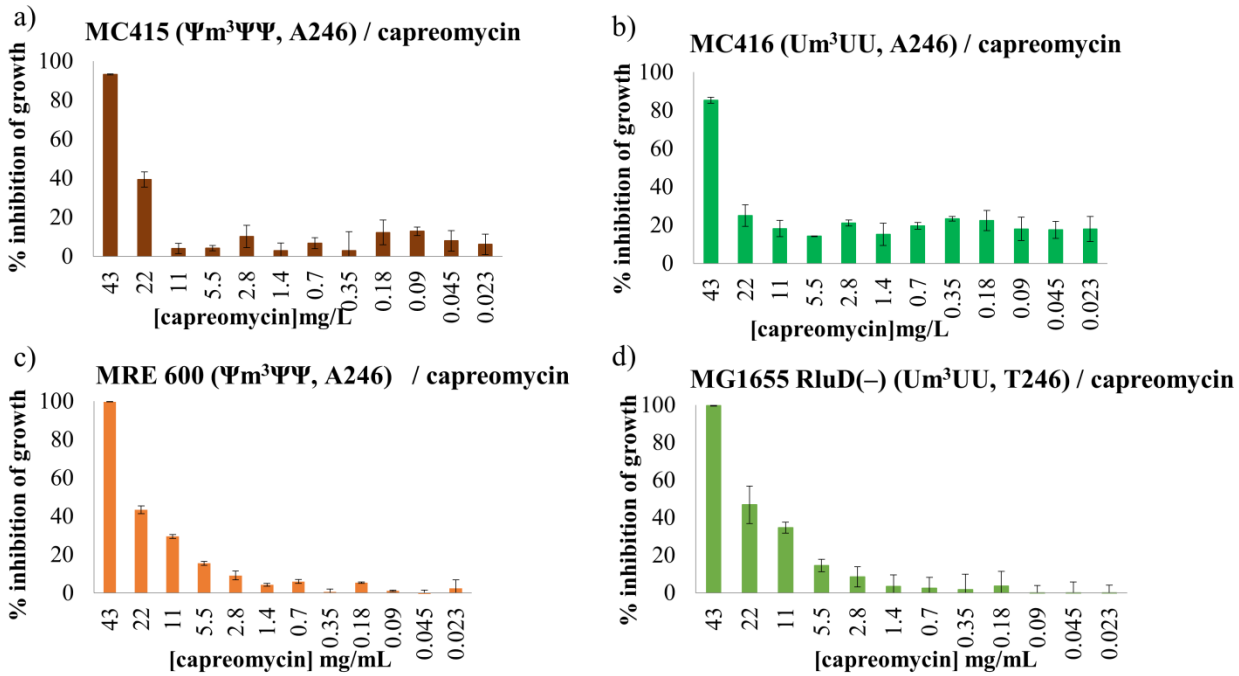

Figure 5.10 Effect of H69 pseudouridylation on antibacterial activity of peptide antibiotic, capreomycin. Inhibition data for the MIC experiments done with capreomycin in a) a) wild-type MC415, b) RluD(–) MC416 c) MRE600 and d) MG1655 RluD(–) strains. Percent inhibition of bacterial growth in the presence of different drug concentrations was calculated and normalized to the growth control, as described in **Chapter 2**, Methods, Section 2.6.

Previously it was proposed that the 2'-OH methylation at C1409 of h44 and C1920 of H69 are important for the antimicrobial activity of peptide antibiotics. Since these modifications are naturally absent in *E. coli* strains, these cyclic peptide antibiotics do not effectively inhibit *E. coli* cell growth.[148] For capreomycin, the observed MIC is 43 mg/L for both wild-type and RluD(–) strains (**Figure 5.10**). The higher MIC value of capreomycin is consistent with its poor activity against *E. coli* strains. In addition, our result indicates that loss of Ψ modificatons on the H69 loop does not affect the already poor bactericidal activity of capreomycin. We observed the same trend with the *E. coli* MRE600 and *E. coli* K-12 RluD(–) strains (**Figure 5.10 c & d**), which were previously used in antibiotic footprinting experiments. Because of the weak binding of capreomycin to *E. coli* H69, the bactericidal activity of the drug may result from interactions

with h44. Therefore, changes in H69 may not have significant effect on the bactericidal activity of capreomycin. The close proximity of H69 and h44 in the ribosome suggests that structural changes of H69 caused by modifications may have impacts on h44 as well. Our *in vivo* data suggest this could be impacting aminoglycosides binding differently than capreomycin. We also determined the MIC of capreomycin in the MG1655 RluD(–) strain, which lacks fully functional RF2. Comparison of the MIC values of MC416 and MG1655 RluD(**–**) strains reveals the effects of perturbed RF2-ribosome interactions on the antibacterial activities of capreomycin. However, we did not observe any differences in MICs in the MG1655 strain compared to MC416 with fully functional RF2 (**Figure 5.9d**). From these observations, we can conclude that perturbations caused by defective RF2 and lack of Ψs does not affect the antibacterial activity of capreomycin. Perhaps the H69 conformational changes induced by Ψs or RF2 do not affect or are not significant enough to impact the *in vivo* activities of peptide antibiotic capreomycin. These results provide further evidence for the existence of a distinct mechanism of action of peptide antibiotics compared to .aminoglycosides.

5.4.9 Wild type and RluD(–) strains showed similar suceptibility to non-ribosomal targeting antibiotics

To determine whether wild-type and RluD(–) *E. coli* strains have similar or different suceptibilities to other antibiotics, we did MIC experiments with the non-ribosomal targeting antibiotc carbenicillin as a control experiment. Carbenicillin is a bectericidal antibiotic that targets bacteria cell wall synthesis. It belongs to the carboxypenicillin subgroup of β-lactam antibiotics.

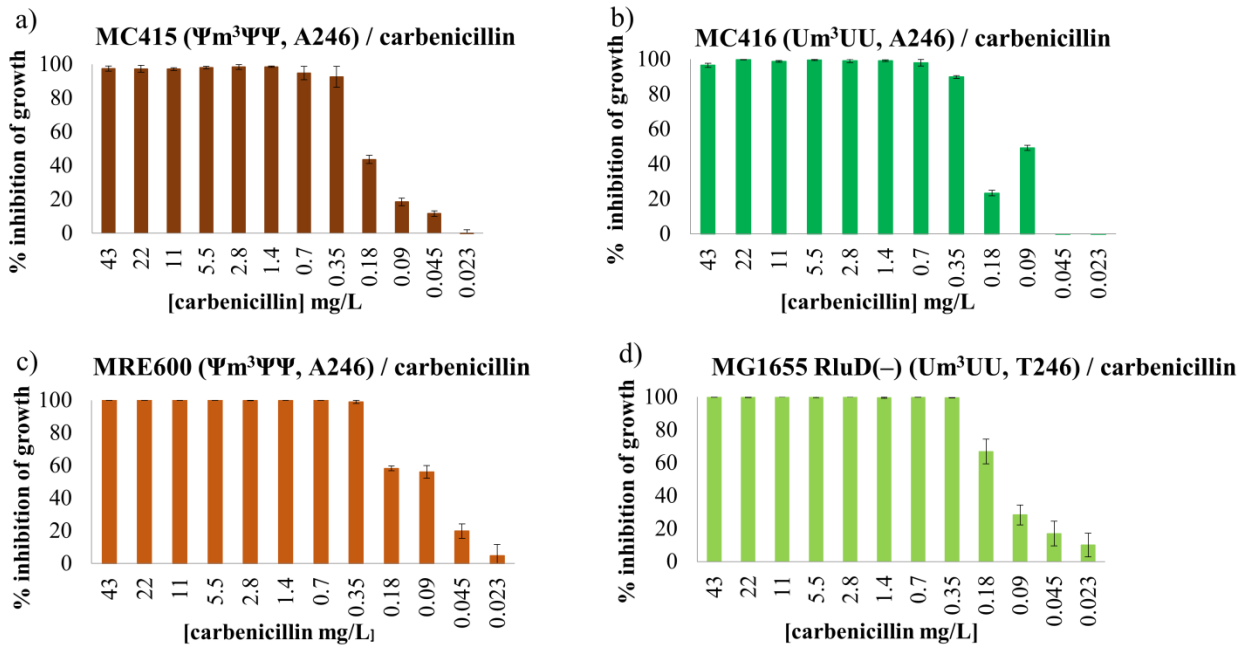

Figure 5.11 Effects of H69 pseudouridylation on antibacterial activity of the non-ribosome targeting antibiotic carbenicillin. Inhibition data for the MIC experiments done with carbenicillin in a) wild-type MC415, b) RluD(–) MC416, c) MRE600 and d) MG1655 RluD(–) strains. Percent inhibition of bacterial growth in the presence of different drug concentrations was calculated and normalized to the growth control as described in **Chapter 2**, Methods.

The only genetic variation between MC415 ($\Psi m^3\Psi\Psi$) and MC416 (Um^3UU) is abscence of the *rlud* gene in MC416.[317] Previous studies in the O'Connor lab showed that these two strains have similar growth rates despite absence of the *rlud* gene. In this work, *E. coli* MC415 and MC416 displayed the same MIC values and similar inhibition profiles with carbenicillin (**Figure 5.11a & b**). This observation suggests that the unique inhibition profiles observed with aminoglycosides with wild-type (MC415) and Ψ-deficient (MC416) strains results from interactions of the drug with the ribosome. Although we cannot do direct comparisons of MICs of MRE600 (ΨΨΨ) and MG1655 (UUU) strains, it was satisfying that these two strains showed the same MIC value and similar inhibition profiles with carbenicillin (**Figure 5.5c & d**).

5.5 Overall summary and conclusions

Aminoglycosides are one of the most clinically important classes of antibiotics, which inhibit bacterial protein translation by targeting the 70S ribosome.[311] Aminoglycosides with a 2-DOS motif are known to inhibit protein translation by binding to the h44 region of the small subunit adjacent to the decoding site.[137,139] However, recent x-ray crystal structures have shown that neomycin, paromomycin, and gentamicin are able to interact with the major groove of H69 of 23S rRNA as well. [138,146,147] The observed interactions with H69 provide a possible mechanism for how aminoglycosides inhibit the recycling and translocation steps of protein synthesis. [147] However, the bactericidal nature of 2-DOS aminoglycoside antibiotics is still poorly understood despite decades of clinical use and biochemical studies. The emergence of resistance strains to prevailing aminoglycoside antibiotics and impaired hearing and kidney functions at high doses made them less effective in clinical applications.[314] Therefore, understanding the underlying mechanism of action of this class of antibiotics is important for the development of unique antibiotics that target the bacterial ribosome. Pseudouridylation is the most frequent single-base modification in ribosomal RNA. Helix 69 contains three Ψs at positions 1911, 1915, and 1917.[196] Previous work showed that these Ψ modifications are important for ribosome function and modulation of the loop structure.[237,239] However, few studies were done previously to understand the role of Ψs in aminoglycoside-ribosome interactions.[237,239,319] Previous work in our lab revealed that Ψ modifications are important for efficient binding of some aminoglycosides to H69.[237,239] This work also showed that structurally similar aminoglycosides have different structural impacts on the modified and unmodified H69 RNAs. However, all of these previous studies were confined to *in vitro* systems. In contrast, the main goal of the work

presented in this thesis was to investigate the effects of Ψ modifications in H69 on the bactericidal activity of 2-DOS class aminoglycosides.

Data from our MIC experiments with wild-type (MC415, $\Psi m^3\Psi\Psi$) and Ψ-deficient (MC416, Um^3UU) bacterial strains revealed that loss of Ψ modifications conferred resistance to paromomycin with much smaller impacts on neomycin activity despite its structural similarity to paromomycin. This effect might be due to the different binding interactions of neomycin with H69 compared to paromoycin, which was previously reported.[146] Interestingly, the observed antibiotic resistance was even higher for gentamicin and kanamycin, which belong to the 4,6-linked aminoglycoside class.

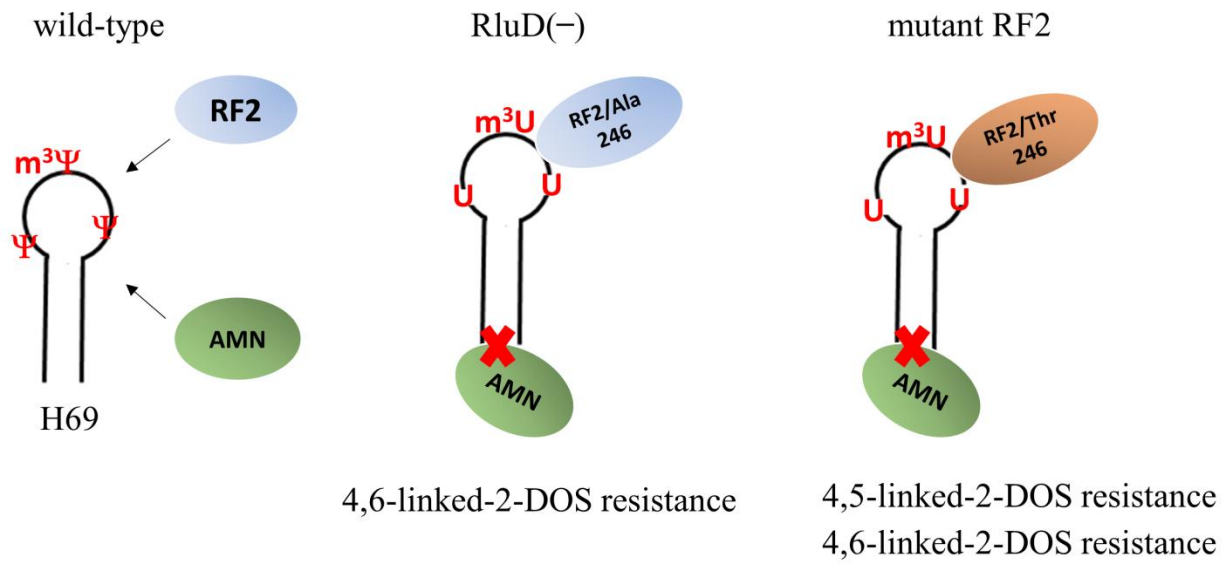

Figure 5.12 Loss of pseudouridylation and defective RF2 (Thr246) confer resistance to 2-DOS aminoglycosides. The most notable finding of this chapter is the aminoglycoside resistance showed by MG1655 strain. This might be a combined effect of defective RF2 and loss of Ψs on MG1655 strain that perturb RF2-H69 interactions, which may cause decreased ribosome-aminoglycoside (AMN) binding leading to drug resistance.

Compared to wild-type, the Ψ-deficient strain showed ~2, ~16, and ~30-fold higher MIC values, respectively, for paromomycin, gentamicin, and kanamycin. Moreover, our data showed

that H69-pseudouridylation did not affect antibacterial activity of the peptide antibiotic capreomycin, in which we observed the same MIC values for wild-type and Ψ-deficient strains. In addition, comparison of the inhibition profiles of MC416 (RF2, Ala246) and MG1655 (RF2, Thr246) strains gave us the opportunity to evaluate the effects of defective RF2 (Thr246) protein on the antibacterial activities of aminoglycosides in an RluD(–) background (summarized in **Figure 5.12**). Our data reveal that defective RF2 (Thr246) confers resistance to 4,5-linked-2-DOS-aminoglycosides neomycin and paromomycin in the RluD(–) background. For both neomycin and paromomycin, the observed MIC values in the RluD(–) strain (MC416) increased by 16-fold in RluD(–) and Ala246Thr double mutant strain (MG1655). This might be a combined effect of defective RF2 and loss of Ψs on MG1655 strain that perturb RF2-H69 interactions. However, we did not see this behavior with 4,6-linked-2-DOS aminoglycosides gentamicin and kanamycin or peptide antibiotic capreomycin.

Previous observations suggest that H69-RF2 interactions play an important role in translation termination. It was also shown that Thr246 decreases RF2-dependent translation termination efficiency compared with Ala246.[318,323] However, it is still not clearly understood the exact role of Ala246Thr mutation in *E. coli* K-12 strain. In addition to decreased translation termination efficiency, defective RF2 may play a role in antibiotic resistance, specially under an RluD(–) background. The 2-DOS class of aminoglycosides is known to target the H69 region and inhibit the ribosome recycling step.[147] Since ribosome recycling and termination are sequential steps in the translation process, defects in the termination step may affect drug binding as well as the inhibition profiles of these drugs. Although neomycin, paromomycin, gentamicin, and capreomycin are known to interact with H69, crystal structures revealed that each of these antibiotics has unique binding interactions with H69. Our in *vivo* data suggest that, these

different interaction patterns of antibiotics with H69 play a role in the *in vivo* potency of the drug, giving rise to unique inhibition and resistance profiles to these structurally similar aminoglycosides. The information gained from these studies provides deeper insight into the underlying mechanism of action of aminoglycosides, which is important for the development of unique antibiotics that target the bacterial ribosome at novel sites such as H69.

CHAPTER 6 OVERALL CONCLUSIONS AND FUTURE DIRECTIONS

6.1 Overall conclusions

Antibiotics have been used for the past 70 years to treat infectious diseases.[161] Although antibiotics were thought to be the perfect solution to bacterial infections, the emergence of resistance has become a global health issue.[132,163] The development of short peptides that specifically bind to higher-order structures of ribosomal RNA is one promising way to address the problem of antibiotic resistance. These peptides could potentially be developed into small molecule drugs. Recent studies in several laboratories including ours have identified short peptide sequences targeting rRNA motifs.[191,192,215,216,221-223] Most of these studies were confined to *in vitro* systems, including binding studies with small model rRNAs,[191,192] *in vitro* chemical footprinting studies with isolated ribosomes,[221] or elucidation of crystal structures of peptide-bound ribosomes.[221-223] The poor correlation between *in vitro* and in *vivo* activities of these peptides is one of the major questions in antibiotic peptide research. Therefore, in contrast to these *in vitro* methods, one of the main objectives of my dissertation work was to utilize a plasmid-based system to *in vivo* express ribosome-targeting peptides and study their direct inhibitory effects on bacteria.

In **Chapter 3**, I optimized a specific plasmid system to *in vivo* express a proline-rich AMP oncocin and studied its direct inhibitory effects on bacteria. The 19-mer, oncocin peptide sequence was cloned into a plasmid vector and *in vivo* expressed as a free peptide. The antibacterial activity of the peptide was confirmed by doing a bacterial growth assay. After induction of the peptide complete inhibition of (< 80%) bacterial growth was observed. Data of our growth assay supported the strong antibacterial activity of oncocin. Since the system allows us to synthesize peptides inside bacteria it has several other downstream applications. The system was utilized to *in vivo* express alanine mutants of oncocin and study their inhibitory

activities. Results of our *in vivo* alanine scan experiment are in a good agreement with previously reported structural and biochemical data and support the critical roles of Lys3, Tyr6, Leu7, and Arg11 residues of oncocin in ribosome binding and antibacterial activity. One additional application of our plasmid system is *in vivo* probe ribosome-peptide interactions. *In vivo* chemical footprinting studies were carried out using dimethyl sulfate (DMS) as the chemical probe to study the oncocin-ribosome interactions. Data of our footprinting experiments confirmed the interaction of oncocin with the PTC region of the ribosome. To the best of our knowledge this is the first effort to use *in vivo* DMS footprinting technique to study ribosome-peptide interactions.

In my dissertation research, the main focus was on H69 of the 50S subunit. H69 is proposed to be a potential drug target based on its pivotal role in ribosome protein synthesis at multiple stages and its unique higher-order RNA structure.[50,195,196] In previous studies, the phage-display method was used to identify peptides that target the H69 region.[192,236] *In vitro* binding studies have shown that these selected peptides have moderate affinity towards H69.[191,192] In a second approach, peptide variants with higher affinity and enhanced selectivity were identified by doing alanine and arginine scans of the parent peptide sequence derived from phage display.[191] Specificity, stoichiometries, and binding affinities of these peptides to H69 were determined by using *in vitro* methods. Our working hypothesis was that the selected peptides will bind to H69 and disrupt ribosome function. However, the *in vivo* activity of these peptides was not determined. In **Chapter 4** of this dissertation work, we utilized the optimized-plasmid system to *in vivo* express H69-targeting peptide sequences, NQAANHQ, TARHIY, and RQVANHQ. We hoped that *in vivo* expression of these peptides would allow us to study their behavior of selected peptides in the actual cellular environment. In the first approach, peptides

were expressed as GFP fusion proteins, and in the second approach they were expressed as free peptides. In both systems, we found that the NQAANHQ peptide had slightly better inhibition compared to other H69-targeting peptides. Based on *in vivo* and *in vitro* data, we can consider NQAANHQ as a potential drug lead, but it will need considerable modifications or alterations to improve its activity.

Another important type small molecule considered in this thesis work is the aminoglycoside, a well-known antibiotic that targets the bacterial ribosome. The previously identified primary binding site of the 2-deoxystreptamine (2-DOS) family of antibiotics was h44 of the small subunit adjacent to the decoding site.[132,139] Recent x-ray crystal structures have shown that neomycin, paromomycin, and gentamicin are able to interact with the major groove of H69.[138,140,146,147] However, the bactericidal nature of 2-DOS aminoglycoside antibiotics is still poorly understood.[140,146] Previous work in our lab revealed that Ψ modifications are important for efficient binding of aminoglycosides to H69.[237,238] [239] However, the effects of Ψ modifications on the bactericidal activity of aminoglycosides have not been examined. The work presented in the **Chapter 5** of this thesis discusses the effects of Ψs in H69 on the bactericidal nature of 2-DOS aminoglycoside antibiotics. Antibacterial activities were assessed by performing minimum inhibitory concentration (MIC) studies using wild-type and Ψ-deficient bacterial strains. Our data reveal that loss of Ψ modifications in the MC416 strain confer resistance to 4,6-2-DOS-linked aminoglycosides, gentamicin and kanamycin, whereas the effect was not significant with 4,5-2-DOS-linked aminoglycosides, neomycin and paromomycin. In addition, comparison of the inhibition profiles of MC416 (RF2, Ala246) and MG1655 (RF2, Thr246) strains gave us the opportunity to evaluate the effects of defective RF2 (Thr246) protein on the antibacterial activities of aminoglycosides in an RluD(–) (pseudouridine-deficient)

background. Our data reveal that defective RF2 (Thr246) confers resistance to 4,5-linked-2-DOS-aminoglycosides, neomycin and paromomycin. However, we did not see this behavior with 4,6-linked-2DOS aminoglycosides, gentamicin and kanamycin, or peptide antibiotic capreomycin. With this observation, we suggest that bacterial strains carrying partially defective RF2 show resistance to 4,5-linked-2-DOS aminoglycosides and this might be a combined effect of defective RF2 and loss of Ψs on the MG1655 strain, which likely perturb RF2-H69 interactions. Altogether our data confirm that *in vitro* observed structural and binding differences affect the *in vivo* potency of the drug and give rise to unique inhibition and resistance profiles to these structurally similar aminoglycosides. The information gained from these studies provides deeper insight into the underlying mechanism of action of aminoglycosides, which is important for the development of unique antibiotics that target the bacterial ribosome at novel sites such as H69. In contrast to *in vitro* methods, most of the work that I did for my dissertation is focused on the *in vivo* activity of antibacterial drugs targeting the bacterial ribosome. In fact, the methods that I developed are not confined to ribosome-targeting drugs. We can expand this work to study the *in vivo* activity of other peptide-based as well as other classes of drugs.

6.2 Future directions

6.2.1 *In vivo* expression of peptide libraries

The poor correlation between *in vitro* antimicrobial activity and *in vivo* efficacy is one of the major obstacles that has limited the progression of AMP candidates towards clinical development.[228,229] Most commonly, the identification of therapeutic peptides starts with *in vitro* screening of peptide libraries. This can be done with a random peptide library or peptide library derived from a known AMP.[191,215] For example, with the phage display technique, random phage-displayed peptide libraries are incubated with a target of interest to select for those

specifically binding to the target.[230] Typically the target is immobilized on a solid support before addition of the phage library. However, in these *in vitro* screening techniques, the most crucial peptide-target interaction step occurs in a simulated environment, which is very different than the actual cellular environment.[228,229] This process also requires identification and synthesis or isolation of the target prior to the experiment, as well as the assumption that the target is in its bioactive conformation under these *in vitro* conditions. Another important concern is that targets such as DNA, RNA, or proteins have numerous conformations *in vivo* that are influenced by their environment. Peptides are also highly sensitive to their environmental conditions, which results in discrepancies between their *in vitro* and *in vivo* activity. On the other hand *in vitro* peptide library screens entirely depend on SPPS, which is expensive and time consuming. Therefore, the development of *in vivo* peptide libraries would be an alternative approach to overcome the limitations of *in vitro* peptide library screens.[231-234]

In a recent study, an oncocin-based *in vitro* peptide library was synthesized in order to identify analogs with improved antibacterial activity against gram-positive bacterial strains.[338] A library of singly substituted oncocin analogs was produced by replacing each residue with all 20 canonical amino acids, yielding a set of 361 individual peptides. In this work, a peptide array technology was employed to synthesize monosubstituted oncocin analogs on cellulose membranes using cleavable linkers to release the free individual peptides for further antimicrobial tests.[338] Thirteen substitutions appeared promising and their improved antibacterial activities were confirmed for different bacterial strains after larger scale synthesis of these analogs. By combining two favorable substitutions into one peptide, they finally obtained an oncocin analog that was ten times more active against *P. aeruginosa* and even 100-fold more active against *S. aureus* compared to the original oncocin peptide. However, these kind of studies

are entirely dependent on SPPS. In addition, the chemical synthesis of proline-containing peptides is difficult because of the low reactivity of secondary amines. Therefore, the *in vivo* peptide expression approach will have several advantages over SPPS. Considering these facts, as the next immediate step of this project, we have already expressed an oncocin-based *in vivo* peptide library in our laboratory. The ultimate goal of this project is to identify oncocin analogs with improved antibacterial activity. Our system is not confined to AMPs. Therefore, we can utilize our plasmid system to generate peptide libraries, or study a variety of other biologically interesting peptides (*e.g.,* anti-freeze peptides).

6.2.2 *In vivo* and *in vitro* chemical footprinting studies with H69-targeting peptides

In **Chapter 3** of this dissertation work, I optimized an *in vivo* DMS footprinting protocol to study oncocin-ribosome interactions. Our data in this footprinting experiment are in good agreement with previously reported information on oncocin-ribosome interactions. This implies that the *in vivo* footprinting protocol that I optimized is useful for studying peptide-ribosome interactions in cellular environments. Therefore, we can use this optimized protocol to study a variety of other ribosome-targeting peptides. Since the H69-targeting peptide NQAANHQ showed comparatively higher inhibitory activity in our bacterial growth assays, it is of interest do *in vivo* as well as *in vitro* DMS footprinting experiments with our H69-targeting peptides to confirm their interactions with H69 region. In addition, we are currently using the *in vivo* DMS footprinting technique to examine h31-targeting peptide-ribosome interactions.

6.2.3 Synthesis of peptide-aminoglycoside conjugates with enhanced antibacterial activity.

Based on our *in vivo* and *in vitro* data, we can consider NQAANHQ as a potential drug lead, but it will need considerable modifications or alterations to improve its activity. Since 2-DOS aminoglycosides also target the H69 region, a fragment-based drug design approach for

producing peptide-aminoglycoside conjugates would be an interesting approach to improve the antibacterial activity of H69-targeting peptides. There are several previous reports on aminoglycoside-peptide conjugates.[339-341] In most of these studies, click-chemistry was used to synthesize the aminoglycoside-peptide conjugates, and the new classes of compounds showed enhanced antibacterial activities against aminoglycoside-resistant bacterial strains.[339,340] Docking studies using PDB files of known crystal structures of the bacterial ribosome can be used to study possible conjugation profiles between the neamine core of aminoglycosides and H69-targeting peptides. This modeling approach could provide the best information for synthesizing compounds containing peptide and aminoglycoside compounds.

6.2.4 Chemical footprinting studies with 2-DOS aminoglycosides

The work presented in **Chapter 5** of this thesis focused on the effects of Ψs in H69 on the bactericidal nature of 2-DOS aminoglycoside antibiotics. The antibacterial activities of different antibiotics in wild-type (MC415,ΨΨΨ) and RluD(–) (MC416, UUU) bacteria strains were assessed by performing MIC studies. Even though MIC is a very good indication of the *in vivo* activities of antibiotics, it does not entirely depend on the drug-target interaction. Therefore, in order to gain further information about aminoglycoside-H69 interactions it is of interest to do *in vitro* chemical footprinting experiments with 2-DOS aminoglycosides. Chemical footprinting is considered as a powerful technique to study RNA-drug interactions.[248-250] The chemical footprinting technique was explained in detail in **Chapter 2**. However, for footprinting experiments we have to isolate modified and unmodified ribosomes from MC415 and MC416 strains, respectively. Comparison of the antibiotic footprinting patterns of modified and unmodified ribosomes will provide more information about the effects of Ψ modifications on the binding of aminoglycosides. Previous studies in our laboratory had employed ribosomes with a

mutant RF2 (Thr 246). The information gained from these studies in conjunction with the wild-type RF2 protein will provide deeper insight into the underlying mechanism of action of aminoglycosides, which is important for the development of unique antibiotics that target the bacterial ribosome at novel sites such as H69.

REFERENCES

(1) Crick, F. *Nature* **1970**, *227*, 561.

(2) Ramakrishnan, V. *Cell* **2002**, *108*, 557

(3) Palade, G. E. *Biophys. Biochem. Cytol.* **1955**, *1*, 59.

(4) Microsomal Particles and Protein Synthesis. In *Microsomal Particles and proteyn Synthesis*, Roberts, R. B., Ed. Pergamon Press, Inc.: New York, **1958**.

(5) Palade, G. E. "The Nobel Prize in Physiology or Medicine 1974". Nobelprize.org.Nobel Media AB 2013. Web. 30 May 2014. <http://www.nobelprize.org/nobel_prizes/medicine/laureates/1974/>.

(6) Carl Woese, The genetic code., 1967.

(7) Kruger, K.; Grabowski, P. J.; Zaug, A. J.; Sands, J.; Gottschling, D. E.; Cech, T. R. *Cell* **1982**, *31*, 147.

(8) Guerrier-Takada, C.; Gardiner, K.; Marsh, T.; Pace, N.; Altman, S. *Cell* **1983**, *35*, 849.

(9) Noller, H. F. *Annu. Rev. Biochem.* **1991**, *60*, 191.

(10) Noller, H. F. *Int J Bacteriol.* **1993**, *175*, 5297.

(11) Mitchell, P.; Osswald, M.; Brimacombe, R. *Biochemistry* **1992**, *31*, 3004.

(12) Gutell, R. R. *Nucleic Acids Res.* **1994**, *22*, 3502.

(13) Selmer, M.; Dunham, C. M.; Murphy, F. V. t.; Weixlbaumer, A.; Petry, S.; Kelley, A. C.; Weir, J. R.; Ramakrishnan, V. *Science* **2006**, *313*, 1935.

(14) Ban, N.; Nissen, P.; Hansen, J.; Moore, P. B.; Steitz, T. A. *Science* **2000**, *289*, 905.

(15) Tocilj, A.; Schlunzen, F.; Janell, D.; Gluhmann, M.; Hansen, H. A.; Harms, J.; Bashan, A.; Bartels, H.; Agmon, I.; Franceschi, F.; Yonath, A. *Proc. Natl. Acad. Sci.* **1999**, *96*, 14252.

(16) Taylor, M. M.; Glasgow, J. E.; Storck, R. *Proc. Natl. Acad. Sci.* **1967**, *57*, 164.

(17) Poehlsgaard, J.; Douthwaite, S. *Nat. Rev. Microbiol.* **2005**, *3*, 870.

(18) Steitz, T. A. *Nat. Rev. Mol. Cell Biol.* **2008**, *9*, 242.

(19) Schuwirth, B. S.; Borovinskaya, M. A.; Hau, C. W.; Zhang, W.; Vila-Sanjurjo, A.; Holton, J. M.; Cate, J. H. *Science* **2005**, *310*, 827.

(20) Wilson, D. N.; Doudna Cate, J. H. *Cold Spring Harb Perspect Biol.* **2012**, *4*, a011536.

(21) Ben-Shem, A.; Garreau de Loubresse, N.; Melnikov, S.; Jenner, L.; Yusupova, G.; Yusupov, M. *Science* **2011**, *334*, 1524.

(22) Cannone, J. J.; Subramanian, S.; Schnare, M. N.; Collett, J. R.; D'Souza, L. M.; Du, Y.; Feng, B.; Lin, N.; Madabusi, L. V.; Muller, K. M.; Pande, N.; Shang, Z.; Yu, N.; Gutell, R. R. *BMC Bioinformatics.* **2002**, *3*, 2.

(23) Shine, J.; Dalgarno, L. *Biochem. J.* **1974**, *141*, 609.

(24) Schmeing, T. M.; Ramakrishnan, V. *Nature* **2009**, *461*, 1234.

(25) Antoun, A.; Pavlov, M. Y.; Lovmar, M.; Ehrenberg, M. *Mol. Cell.* **2006**, *23*, 183.

(26) Grigoriadou, C.; Marzi, S.; Pan, D.; Gualerzi, C. O.; Cooperman, B. S. *J Mol Biol.* **2007**, *373*, 551.

(27) Milon, P.; Konevega, A. L.; Gualerzi, C. O.; Rodnina, M. V. *Mol. Cell.* **2008**, *30*, 712.

(28) Ogle, J. M.; Brodersen, D. E.; Clemons, W. M., Jr.; Tarry, M. J.; Carter, A. P.; Ramakrishnan, V. *Science* **2001**, *292*, 897.

(29) Ogle, J. M.; Murphy, F. V.; Tarry, M. J.; Ramakrishnan, V. *Cell* **2002**, *111*, 721.

(30) Valle, M.; Sengupta, J.; Swami, N. K.; Grassucci, R. A.; Burkhardt, N.; Nierhaus, K. H.; Agrawal, R. K.; Frank, J. *EMBO J.* **2002**, *21*, 3557.

(31) Berk, V.; Zhang, W.; Pai, R. D.; Cate, J. H. D. *Proc. Natl. Acad. Sci.* **2006**, *103*, 15830.

(32) Brunelle, J. L.; Youngman, E. M.; Sharma, D.; Green, R. *RNA* **2006**, *12*, 33.

(33) Youngman, E. M.; Brunelle, J. L.; Kochaniak, A. B.; Green, R. *Cell* **2004**, *117*, 589.

(34) Weinger, J. S.; Parnell, K. M.; Dorner, S.; Green, R.; Strobel, S. A. *Nat. Struct. Mol. Biol.* **2004**, *11*, 1101.

(35) Villa, E.; Sengupta, J.; Trabuco, L. G.; LeBarron, J.; Baxter, W. T.; Shaikh, T. R.; Grassucci, R. A.; Nissen, P.; Ehrenberg, M.; Schulten, K.; Frank, J. *Proc. Natl. Acad. Sci.* **2009**, *106*, 1063.

(36) Korostelev, A.; Ermolenko, D. N.; Noller, H. F. *Curr. Opin. Chem. Biol.* **2008**, *12*, 674.

(37) Agirrezabala, X.; Lei, J.; Brunelle, J. L.; Ortiz-Meoz, R. F.; Green, R.; Frank, J. *Mol. Cell.* **2008**, *32*, 190.

(38) Ermolenko, D. N.; Majumdar, Z. K.; Hickerson, R. P.; Spiegel, P. C.; Clegg, R. M.; Noller, H. F. *J Mol Biol.* **2007**, *370*, 530.

(39) Moazed, D.; Noller, H. F. *Nature* **1989**, *342*, 142.

(40) Frank, J.; Agrawal, R. K. *Nature* **2000**, *406*, 318.

(41) Kisselev, L.; Ehrenberg, M.; Frolova, L. *EMBO J.* **2003**, *22*, 175.

(42) Nakamura, Y.; Ito, K. *Trends Biochem. Sci.* **2003**, *28*, 99.

(43) Pavlov, M. Y.; Freistroffer, D. V.; MacDougall, J.; Buckingham, R. H.; Ehrenberg, M. *EMBO J.* **1997**, *16*, 4134.

(44) Monro, R. E.; Marcker, K. A. *J Mol Biol.* **1967**, *25*, 347.

(45) Noller, H. F.; Hoffarth, V.; Zimniak, L. *Science* **1992**, *256*, 1416.

(46) Woese, C. R.; Magrum, L. J.; Gupta, R.; Siegel, R. B.; Stahl, D. A.; Kop, J.; Crawford, N.; Brosius, J.; Gutell, R.; Hogan, J. J.; Noller, H. F. *Nucleic Acids Res.* **1980**, *8*, 2275.

(47) Xu, Z.; Culver, G. M. *RNA* **2010**, *16*, 1990.

(48) Wriggers, W.; Agrawal, R. K.; Drew, D. L.; McCammon, A.; Frank, J. *Biophys. J.* **2000**, *79*, 1670.

(49) Decatur, W. A.; Fournier, M. J. *Trends Biochem. Sci.* **2002**, *27*, 344.

(50) Yusupov, M. M.; Yusupova, G. Z.; Baucom, A.; Lieberman, K.; Earnest, T. N.; Cate, J. H.; Noller, H. F. *Science* **2001**, *292*, 883.

(51) Chow, C. S.; Lamichhane, T. N.; Mahto, S. K. *ACS Chem Biol.* **2007**, *2*, 610.

(52) Lesnyak, D. V.; Osipiuk, J.; Skarina, T.; Sergiev, P. V.; Bogdanov, A. A.; Edwards, A.; Savchenko, A.; Joachimiak, A.; Dontsova, O. A. *J Biol Chem.* **2007**, *282*, 5880.

(53) Sergiev, P. V.; Lesnyak, D. V.; Bogdanov, A. A.; Dontsova, O. A. *J Mol Biol.* **2006**, *364*, 26.

(54) Bujnicki, J. M.; Rychlewski, L. *BMC Bioinformatics.* **2002**, *3*, 10.

(55) Sergeeva, O. V.; Prokhorova, I. V.; Ordabaev, Y.; Tsvetkov, P. O.; Sergiev, P. V.; Bogdanov, A. A.; Makarov, A. A.; Dontsova, O. A. *RNA* **2012**, *18*, 1178.

(56) Nishimura, K.; Hosaka, T.; Tokuyama, S.; Okamoto, S.; Ochi, K. *Int J Bacteriol.* **2007**, *189*, 3876.

(57) Benitez-Paez, A.; Villarroya, M.; Armengod, M. E. *RNA* **2012**, *18*, 795.

(58) Mikheil, D. M.; Shippy, D. C.; Eakley, N. M.; Okwumabua, O. E.; Fadl, A. A. *J. Antibiot.* **2012**, *65*, 185.

(59) Sunita, S.; Purta, E.; Durawa, M.; Tkaczuk, K. L.; Swaathi, J.; Bujnicki, J. M.; Sivaraman, J. *Nucleic Acids Res.* **2007**, *35*, 4264.

(60) Tscherne, J. S.; Nurse, K.; Popienick, P.; Ofengand, J. *J Biol Chem.* **1999**, *274*, 924.

(61) Basturea, G. N.; Dague, D. R.; Deutscher, M. P.; Rudd, K. E. *J Mol Biol.* **2012**, *415*, 16.

(62) Bujnicki, J. M. *FASEB J.* **2000**, *14*, 2365.

(63) Gu, X. R.; Gustafsson, C.; Ku, J.; Yu, M.; Santi, D. V. *Biochemistry* **1999**, *38*, 4053.

(64) Foster, P. G.; Nunes, C. R.; Greene, P.; Moustakas, D.; Stroud, R. M. *Structure* **2003**, *11*, 1609.

(65) Weitzmann, C.; Tumminia, S. J.; Boublik, M.; Ofengand, J. *Nucleic Acids Res.* **1991**, *19*, 7089.

(66) Kimura, S.; Suzuki, T. *Nucleic Acids Res.* **2010**, *38*, 1341.

(67) Motorin, Y.; Helm, M. *Wiley Interdiscip. Rev. RNA.* **2011**, *2*, 611.

(68) Boehringer, D.; O'Farrell, H. C.; Rife, J. P.; Ban, N. *J Biol Chem.* **2012**, *287*, 10453.

(69) Desai, P. M.; Culver, G. M.; Rife, J. P. *Biochemistry* **2011**, *50*, 854.

(70) Connolly, K.; Rife, J. P.; Culver, G. *J Mol Microbiol.* **2008**, *70*, 1062.

(71) O'Farrell, H. C.; Scarsdale, J. N.; Rife, J. P. *J Mol Biol.* **2004**, *339*, 337.

(72) Poldermans, B.; Bakker, H.; Van Knippenberg, P. H. *Nucleic Acids Res.* **1980**, *8*, 143.

(73) Poldermans, B.; Roza, L.; Van Knippenberg, P. H. *J Biol Chem.* **1979**, *254*, 9094.

(74) Basturea, G. N.; Rudd, K. E.; Deutscher, M. P. *RNA* **2006**, *12*, 426.

(75) Basturea, G. N.; Deutscher, M. P. *RNA* **2007**, *13*, 1969.

(76) Wrzesinski, J.; Bakin, A.; Nurse, K.; Lane, B. G.; Ofengand, J. *Biochemistry* **1995**, *34*, 8904.

(77) Conrad, J.; Niu, L.; Rudd, K.; Lane, B. G.; Ofengand, J. *RNA* **1999**, *5*, 751.

(78) Sivaraman, J.; Sauvé, V.; Larocque, R.; Stura, E. A.; Schrag, J. D.; Cygler, M.; Matte, A. *Nat. Struct. Mol. Biol.* **2002**, *9*, 353.

(79) Green, R.; Noller, H. F. *RNA* **1996**, *2*, 1011.

(80) Gustafsson, C.; Persson, B. C. *Int J Bacteriol.* **1998**, *180*, 359.

(81) Das, K.; Acton, T.; Chiang, Y.; Shih, L.; Arnold, E.; Montelione, G. T. *Proc. Natl. Acad.*

Sci. **2004**, *101*, 4041.

(82) Liu, M.; Novotny, G. W.; Douthwaite, S. *RNA* **2004**, *10*, 1713.

(83) Sergiev, P. V.; Bogdanov, A. A.; Dontsova, O. A. *Nucleic Acids Res.* **2007**, *35*, 2295.

(84) Lesnyak, D. V.; Sergiev, P. V.; Bogdanov, A. A.; Dontsova, O. A. *J Mol Biol.* **2006**, *364*, 20.

(85) Kimura, S.; Ikeuchi, Y.; Kitahara, K.; Sakaguchi, Y.; Suzuki, T.; Suzuki, T. *Nucleic Acids Res.* **2012**, *40*, 4071.

(86) Wang, K. T.; Desmolaize, B.; Nan, J.; Zhang, X. W.; Li, L. F.; Douthwaite, S.; Su, X. D. *Nucleic Acids Res.* **2012**, *40*, 5138.

(87) Sirum-Connolly, K.; Mason, T. L. *Science* **1993**, *262*, 1886.

(88) Purta, E.; Kaminska, K. H.; Kasprzak, J. M.; Bujnicki, J. M.; Douthwaite, S. *RNA* **2008**, *14*, 2234.

(89) Sunita, S.; Tkaczuk, K. L.; Purta, E.; Kasprzak, J. M.; Douthwaite, S.; Bujnicki, J. M.; Sivaraman, J. *J Mol Biol.* **2008**, *383*, 652.

(90) Motorin, Y.; Lyko, F.; Helm, M. *Nucleic Acids Res.* **2010**, *38*, 1415.

(91) Purta, E.; O'Connor, M.; Bujnicki, J. M.; Douthwaite, S. *J Mol Microbiol.* **2009**, *72*, 1147.

(92) Sergiev, P. V.; Serebryakova, M. V.; Bogdanov, A. A.; Dontsova, O. A. *J Mol Biol.* **2008**, *375*, 291.

(93) Kaminska, K. H.; Purta, E.; Hansen, L. H.; Bujnicki, J. M.; Vester, B.; Long, K. S. *Nucleic Acids Res.* **2010**, *38*, 1652.

(94) Boal, A. K.; Grove, T. L.; McLaughlin, M. I.; Yennawar, N. H.; Booker, S. J.; Rosenzweig, A. C. *Science* **2011**, *332*, 1089.

(95) Kehrenberg, C.; Schwarz, S.; Jacobsen, L.; Hansen, L. H.; Vester, B. *J Mol Microbiol.*

2005, *57*, 1064.

(96) Giessing, A. M.; Jensen, S. S.; Rasmussen, A.; Hansen, L. H.; Gondela, A.; Long, K.; Vester, B.; Kirpekar, F. *RNA* **2009**, *15*, 327.

(97) Yan, F.; LaMarre, J. M.; Rohrich, R.; Wiesner, J.; Jomaa, H.; Mankin, A. S.; Fujimori, D. G. *J. Am. Chem. Soc.* **2010**, *132*, 3953.

(98) Yan, F.; Fujimori, D. G. *Proc. Natl. Acad. Sci.* **2011**, *108*, 3930.

(99) Shisler, K. A.; Broderick, J. B. *Curr Opin Struct Biol.* **2012**, *22*, 701.

(100) Hamilton, C. S.; Greco, T. M.; Vizthum, C. A.; Ginter, J. M.; Johnston, M. V.; Mueller, E. G. *Biochemistry* **2006**, *45*, 12029.

(101) Hoang, C.; Chen, J.; Vizthum, C. A.; Kandel, J. M.; Hamilton, C. S.; Mueller, E. G.; Ferre-D'Amare, A. R. *Mol. Cell.* **2006**, *24*, 535.

(102) Raychaudhuri, S.; Niu, L.; Conrad, J.; Lane, B. G.; Ofengand, J. *J Biol Chem.* **1999**, *274*, 18880.

(103) Wright, J. R.; Keffer-Wilkes, L. C.; Dobing, S. R.; Kothe, U. *RNA* **2011**, *17*, 2074.

(104) McDonald, M. K.; Miracco, E. J.; Chen, J.; Xie, Y.; Mueller, E. G. *Biochemistry* **2011**, *50*, 426.

(105) Desmolaize, B.; Fabret, C.; Bregeon, D.; Rose, S.; Grosjean, H.; Douthwaite, S. *Nucleic Acids Res.* **2011**, *39*, 9368.

(106) Huang, L.; Ku, J.; Pookanjanatavip, M.; Gu, X.; Wang, D.; Greene, P. J.; Santi, D. V. *Biochemistry* **1998**, *37*, 15951.

(107) Conrad, J.; Sun, D.; Englund, N.; Ofengand, J. *J Biol Chem.* **1998**, *273*, 18562.

(108) Mizutani, K.; Machida, Y.; Unzai, S.; Park, S. Y.; Tame, J. R. *Biochemistry* **2004**, *43*, 4454.

(109) Ero, R.; Leppik, M.; Liiv, A.; Remme, J. *RNA* **2010**, *16*, 2075.

(110) Purta, E.; O'Connor, M.; Bujnicki, J. M.; Douthwaite, S. *J Mol Biol.* **2008**, *383*, 641.

(111) Agarwalla, S.; Kealey, J. T.; Santi, D. V.; Stroud, R. M. *J Biol Chem.* **2002**, *277*, 8835.

(112) Sivaraman, J.; Iannuzzi, P.; Cygler, M.; Matte, A. *J Mol Biol.* **2004**, *335*, 87.

(113) Del Campo, M.; Ofengand, J.; Malhotra, A. *RNA* **2004**, *10*, 231.

(114) Ero, R.; Peil, L.; Liiv, A.; Remme, J. *RNA* **2008**, *14*, 2223.

(115) Gutgsell, N. S.; Del Campo, M.; Raychaudhuri, S.; Ofengand, J. *RNA* **2001**, *7*, 990.

(116) Gutgsell, N. S.; Deutscher, M. P.; Ofengand, J. *RNA* **2005**, *11*, 1141.

(117) Vaidyanathan, P. P.; Deutscher, M. P.; Malhotra, A. *RNA* **2007**, *13*, 1868.

(118) Lee, T. T.; Agarwalla, S.; Stroud, R. M. *Cell* **2005**, *120*, 599.

(119) Lee, T. T.; Agarwalla, S.; Stroud, R. M. *Structure* **2004**, *12*, 397.

(120) Persaud, C.; Lu, Y.; Vila-Sanjurjo, A.; Campbell, J. L.; Finley, J.; O'Connor, M. *Biochem. Biophys. Res. Commun.* **2010**, *392*, 223.

(121) Del Campo, M.; Kaya, Y.; Ofengand, J. *RNA* **2001**, *7*, 1603.

(122) Pan, H.; Ho, J. D.; Stroud, R. M.; Finer-Moore, J. *J Mol Biol.* **2007**, *367*, 1459.

(123) Hager, J.; Staker, B. L.; Jakob, U. *Int J Bacteriol.* **2004**, *186*, 6634.

(124) Caldas, T.; Binet, E.; Bouloc, P.; Costa, A.; Desgres, J.; Richarme, G. *J Biol Chem.* **2000**, *275*, 16414.

(125) Bugl, H.; Fauman, E. B.; Staker, B. L.; Zheng, F.; Kushner, S. R.; Saper, M. A.; Bardwell, J. C.; Jakob, U. *Mol. Cell.* **2000**, *6*, 349.

(126) Hager, J.; Staker, B. L.; Bugl, H.; Jakob, U. *J Biol Chem.* **2002**, *277*, 41978.

(127) Corollo, D.; Blair-Johnson, M.; Conrad, J.; Fiedler, T.; Sun, D.; Wang, L.; Ofengand, J.; Fenna, R. *Acta Crystallogr.* **1999**, *55*, 302.

(128) Feder, M.; Pas, J.; Wyrwicz, L. S.; Bujnicki, J. M. *Gene* **2003**, *302*, 129.

(129) Sunita, S.; Zhenxing, H.; Swaathi, J.; Cygler, M.; Matte, A.; Sivaraman, J. *J Mol Biol.* **2006**, *359*, 998.

(130) Alian, A.; DeGiovanni, A.; Griner, S. L.; Finer-Moore, J. S.; Stroud, R. M. *J Mol Biol.* **2009**, *388*, 785.

(131) Ofengand, J.; Malhotra, A.; Remme, J.; Gutgsell, N. S.; Del Campo, M.; Jean-Charles, S.; Peil, L.; Kaya, Y. *Cold Spring Harb. Symp. Quant Biol.* **2001**, *66*, 147.

(132) Hermann, T. *Curr Opin Struct Biol.* **2005**, *15*, 355.

(133) Auerbach-Nevo, T.; Baram, D.; Bashan, A.; Belousoff, M.; Breiner, E.; Davidovich, C.; Cimicata, G.; Eyal, Z.; Halfon, Y.; Krupkin, M.; Matzov, D.; Metz, M.; Rufayda, M.; Peretz, M.; Pick, O.; Pyetan, E.; Rozenberg, H.; Shalev-Benami, M.; Wekselman, I.; Zarivach, R.; Zimmerman, E.; Assis, N.; Bloch, J.; Israeli, H.; Kalaora, R.; Lim, L.; Sade-Falk, O.; Shapira, T.; Taha-Salaime, L.; Tang, H.; Yonath, A. *Antibiotics* **2016**, *5*, 24.

(134) Ogle, J. M.; Ramakrishnan, V. *Annu. Rev. Biochem.* **2005**, *74*, 129.

(135) Davies, J.; Gorini, L.; Davis, B. D. *Mol. Pharmacol.* **1965**, *1*, 93.

(136) Edelmann, P.; Gallant, J. *Cell* **1977**, *10*, 131.

(137) Recht, M. I.; Douthwaite, S.; Puglisi, J. D. *EMBO J.* **1999**, *18*, 3133.

(138) Fourmy, D.; Recht, M. I.; Blanchard, S. C.; Puglisi, J. D. *Science* **1996**, *274*, 1367.

(139) Moazed, D.; Noller, H. F. *Nature* **1987**, *327*, 389.

(140) Wang, L.; Pulk, A.; Wasserman, M. R.; Feldman, M. B.; Altman, R. B.; Cate, J. H.; Blanchard, S. C. *Nat. Struct. Mol. Biol.* **2012**, *19*, 957.

(141) Wong, C. H.; Hendrix, M.; Priestley, E. S.; Greenberg, W. A. *J. Biol. Chem.* **1998**, *5*, 397.

(142) Rodnina, M. V.; Wintermeyer, W. *Annu. Rev. Biochem.* **2001**, *70*, 415.

(143) Jorgensen F, *FEMS Microbiol. Lett.* **1987**, *40*, 43.

(144) O'Connor, M.; Goringer, H. U.; Dahlberg, A. E. *Nucleic Acids Res.* **1992**, *20*, 4221.

(145) Perzynski, S.; Cannon, M.; Cundliffe, E.; Chahwala, S. B.; Davies, J. *Eur. J. Biochem.* **1979**, *99*, 623.

(146) Wasserman, M. R.; Pulk, A.; Zhou, Z.; Altman, R. B.; Zinder, J. C.; Green, K. D.; Garneau-Tsodikova, S.; Cate, J. H.; Blanchard, S. C. *Nat. Commun.* **2015**, *6*, 7896.

(147) Borovinskaya, M. A.; Pai, R. D.; Zhang, W.; Schuwirth, B. S.; Holton, J. M.; Hirokawa, G.; Kaji, H.; Kaji, A.; Cate, J. H. *Nat. Struct. Mol. Biol.* **2007**, *14*, 727.

(148) Johansen, S. K.; Maus, C. E.; Plikaytis, B. B.; Douthwaite, S. *Mol. Cell.* **2006**, *23*, 173.

(149) Stanley, R. E.; Blaha, G.; Grodzicki, R. L.; Strickler, M. D.; Steitz, T. A. *Nat. Struct. Mol. Biol.* **2010**, *17*, 289.

(150) Hansen, J. L.; Ippolito, J. A.; Ban, N.; Nissen, P.; Moore, P. B.; Steitz, T. A. *Mol. Cell.* **2002**, *10*, 117.

(151) Schlunzen, F.; Zarivach, R.; Harms, J.; Bashan, A.; Tocilj, A.; Albrecht, R.; Yonath, A.; Franceschi, F. *Nature* **2001**, *413*, 814.

(152) Patel, U.; Yan, Y. P.; Hobbs, F. W., Jr.; Kaczmarczyk, J.; Slee, A. M.; Pompliano, D. L.; Kurilla, M. G.; Bobkova, E. V. *J Biol Chem.* **2001**, *276*, 37199.

(153) Swaney, S. M.; Aoki, H.; Ganoza, M. C.; Shinabarger, D. L. *Antimicrob. Agents Chemother.* **1998**, *42*, 3251.

(154) Long, K. S.; Porse, B. T. *Nucleic Acids Res.* **2003**, *31*, 7208.

(155) McNicholas, P. M.; Najarian, D. J.; Mann, P. A.; Hesk, D.; Hare, R. S.; Shaw, K. J.; Black, T. A. *Antimicrob. Agents Chemother.* **2000**, *44*, 1121.

(156) Adrian, P. V.; Zhao, W.; Black, T. A.; Shaw, K. J.; Hare, R. S.; Klugman, K. P.

Antimicrob. Agents Chemother. **2000**, *44*, 732.

(157) Arenz, S.; Juette, M. F.; Graf, M.; Nguyen, F.; Huter, P.; Polikanov, Y. S.; Blanchard, S. C.; Wilson, D. N. *Proc. Natl. Acad. Sci.* **2016**, *113*, 7527.

(158) Egebjerg, J.; Douthwaite, S.; Garrett, R. A. *EMBO J.* **1989**, *8*, 607.

(159) Cameron, D. M.; Thompson, J.; Gregory, S. T.; March, P. E.; Dahlberg, A. E. *Nucleic Acids Res.* **2004**, *32*, 3220.

(160) Bodley, J. W.; Zieve, F. J.; Lin, L. *J Biol Chem.* **1970**, *245*, 5662.

(161) Munita, J. M.; Arias, C. A. *Microbiol. Spectr.* **2016**, *4*, 10.1128/microbiolspec.VMBF.

(162) Guilhelmelli, F.; Vilela, N.; Albuquerque, P.; Derengowski Lda, S.; Silva-Pereira, I.; Kyaw, C. M. *Front Microbiol.* **2013**, *4*, 353

(163) Ventola, C. L. *Pharm. Ther.* **2015**, *40*, 277.

(164) Bush, K. *Clin. Microbiol. Infect.* **2004**, *10 Suppl 4*, 10.

(165) CDC. Active Bacterial Core Surveillance Report, 2013

(166) http://www.cdc.gov/abcs/ 2013

(167) Bloom, G.; Merrett, G. B.; Wilkinson, A.; Lin, V.; Paulin, S. *BMJ Glob. Health.* **2017**, *2*, e000518.

(168) Yevutsey, S. K.; Buabeng, K. O.; Aikins, M.; Anto, B. P.; Biritwum, R. B.; Frimodt-Moller, N.; Gyansa-Lutterodt, M. *BMC Public Health* **2017**, *17*, 896.

(169) Walsh, C. *Nature* **2000**, *406*, 775.

(170) Wilson, D. N. *Nat. Rev. Microbiol.* **2014**, *12*, 35.

(171) Ramirez, M. S.; Tolmasky, M. E. *Drug Resist. Updat.* **2010**, *13*, 151.

(172) Philippon, A.; Labia, R.; Jacoby, G. *Antimicrob. Agents Chemother.* **1989**, *33*, 1131.

(173) Paterson, D. L.; Bonomo, R. A. *Clin. Microbiol. Rev.* **2005**, *18*, 657.

(174) Paulsen, I. T.; Brown, M. H.; Skurray, R. A. *Microbiol. Rev.* **1996**, *60*, 575.

(175) Levy, S. B. *Antimicrob. Agents Chemother.* **1992**, *36*, 695.

(176) Wu, M.; Maier, E.; Benz, R.; Hancock, R. E. *Biochemistry* **1999**, *38*, 7235.

(177) Silhavy, T. J.; Kahne, D.; Walker, S. *Cold Spring Harb Perspect Biol.* **2010**, *2*, a000414.

(178) Hancock, R. E.; Brinkman, F. S. *Annu. Rev. Cell Dev. Microbiol.* **2002**, *56*, 17.

(179) McGowan, J. E., Jr. *Am. J. Infect. Control* **2006**, *34*, S29.

(180) Poole, K. *J. Antimicrob. Chemother.* **2005**, *56*, 20.

(181) McMurry, L.; Petrucci, R. E.; Levy, S. B. *Proc. Natl. Acad. Sci.* **1980**, *77*, 3974.

(182) Singh, K. V.; Weinstock, G. M.; Murray, B. E. *Antimicrob. Agents Chemother.* **2002**, *46*, 1845.

(183) Leclercq, R.*Clin. Infect. Dis.* **2002**, *34*, 482.

(184) Weisblum, B. *Antimicrob. Agents Chemother.* **1995**, *39*, 577.

(185) Beauclerk, A. A.; Cundliffe, E. *J Mol Biol.* **1987**, *193*, 661.

(186) Thompson, J.; Skeggs, P. A.; Cundliffe, E. *Mol. Gen. Genet.* **1985**, *201*, 168.

(187) Prammananan, T.; Sander, P.; Brown, B. A.; Frischkorn, K.; Onyi, G. O.; Zhang, Y.; Bottger, E. C.; Wallace, R. J., Jr. *J. Infect. Dis.* **1998**, *177*, 1573.

(188) Pfister, P.; Hobbie, S.; Vicens, Q.; Bottger, E. C.; Westhof, E. *Chembiochem.* **2003**, *4*, 1078.

(189) Zhou, Y.; Gregor, V. E.; Sun, Z.; Ayida, B. K.; Winters, G. C.; Murphy, D.; Simonsen, K. B.; Vourloumis, D.; Fish, S.; Froelich, J. M.; Wall, D.; Hermann, T. *Antimicrob. Agents Chemother.* **2005**, *49*, 4942.

(190) Llano-Sotelo, B.; Klepacki, D.; Mankin, A. S. *J Mol Biol.* **2009**, *391*, 813.

(191) Dremann, D. N.; Chow, C. S. *Bioorganic Med. Chem.* **2016**, *24*, 4486.

(192) Kaur, M.; Rupasinghe, C. N.; Klosi, E.; Spaller, M. R.; Chow, C. S. *Bioorganic Med. Chem.* **2013**, *21*, 1240.

(193) Lamichhane, T. N.; Abeydeera, N. D.; Duc, A. C.; Cunningham, P. R.; Chow, C. S. *Molecules* **2011**, *16*, 1211.

(194) Ofengand, J. *FEBS Lett.* **2002**, *514*, 17.

(195) Harms, J.; Schluenzen, F.; Zarivach, R.; Bashan, A.; Gat, S.; Agmon, I.; Bartels, H.; Franceschi, F.; Yonath, A. *Cell* **2001**, *107*, 679.

(196) Bakin, A.; Ofengand, J. *Biochemistry* **1993**, *32*, 9754.

(197) Kowalak, J. A.; Bruenger, E.; Hashizume, T.; Peltier, J. M.; Ofengand, J.; McCloskey, J. A. *Nucleic Acids Res.* **1996**, *24*, 688.

(198) Sumita, M.; Desaulniers, J. P.; Chang, Y. C.; Chui, H. M.; Clos, L., 2nd; Chow, C. S. *RNA* **2005**, *11*, 1420.

(199) Baltzer, S. A.; Brown, M. H. *J Mol Microbiol. Biotechnol.*

(200) Mahlapuu, M.; Håkansson, J.; Ringstad, L.; Björn, C. *Front. Cell Infect. Microbiol.* **2016**, *6*, 194.

(201) Hancock, R. E.; Sahl, H. G. *Nat. Biotechnol.* **2006**, *24*, 1551.

(202) Bahar, A. A.; Ren, D. *Pharm. J.* **2013**, *6*, 1543.

(203) Hancock, R. E.; Diamond, G. *Trends Microbiol.* **2000**, *8*, 402.

(204) Diamond, G. *Biologist* **2001**, *48*, 209.

(205) Wang, G.; Li, X.; Wang, Z. *Nucleic Acids Res.* **2016**, *44*, D1087.

(206) Wang, Z.; Wang, G. *Nucleic Acids Res.* **2004**, *32*, D590.

(207) Wang, G.; Li, X.; Wang, Z. *Nucleic Acids Res.* **2009**, *37*, D933.

(208) Li, J.; Koh, J. J.; Liu, S.; Lakshminarayanan, R.; Verma, C. S.; Beuerman, R. W. *Front.*

Neurosci. **2017**, *11*, 73.

(209) Matsuzaki, K.; Sugishita, K.; Harada, M.; Fujii, N.; Miyajima, K. *Biochim. Biophys. Acta* **1997**, *1327*, 119.

(210) Wilson, D. N.; Guichard, G.; Innis, C. A. *Oncotarget.* **2015**, *6*, 16826.

(211) Hale, J. D.; Hancock, R. E. *Expert Rev. Anti Infect.* **2007**, *5*, 951.

(212) Brogden, K. A. *Nat. Rev. Microbiol.* **2005**, *3*, 238.

(213) Sim, S.; Wang, P.; Beyer, B. N.; Cutrona, K. J.; Radhakrishnan, M. L.; Elmore, D. E. *FEBS Lett.* **2017**, *591*, 706.

(214) Vasilchenko, A. S.; Vasilchenko, A. V.; Pashkova, T. M.; Smirnova, M. P.; Kolodkin, N. I.; Manukhov, I. V.; Zavilgelsky, G. B.; Sizova, E. A.; Kartashova, O. L.; Simbirtsev, A. S.; Rogozhin, E. A.; Duskaev, G. K.; Sycheva, M. V. *J. Pept. Sci.* **2017**, *23*, 855.

(215) Knappe, D.; Piantavigna, S.; Hansen, A.; Mechler, A.; Binas, A.; Nolte, O.; Martin, L. L.; Hoffmann, R. *J. Med. Chem.* **2010**, *53*, 5240.

(216) Krizsan, A.; Volke, D.; Weinert, S.; Strater, N.; Knappe, D.; Hoffmann, R. *Angew. Chem. Int. Ed.* **2014**, *53*, 12236.

(217) Devocelle, M. *Front. Immunol.* **2012**, *3*, 309.

(218) Graf, M.; Mardirossian, M.; Nguyen, F.; Seefeldt, A. C.; Guichard, G.; Scocchi, M.; Innis, C. A.; Wilson, D. N. *Nat. Prod. Rep.* **2017**, *34*, 702.

(219) Mardirossian, M.; Grzela, R.; Giglione, C.; Meinnel, T.; Gennaro, R.; Mergaert, P.; Scocchi, M. *J. Biol. Chem.* **2014**, *21*, 1639.

(220) Ishida, Y.; Inouye, M. *AMB Express.* **2016**, *6*, 19.

(221) Gagnon, M. G.; Roy, R. N.; Lomakin, I. B.; Florin, T.; Mankin, A. S.; Steitz, T. A. *Nucleic Acids Res.* **2016**, *44*, 2439.

(222) Roy, R. N.; Lomakin, I. B.; Gagnon, M. G.; Steitz, T. A. *Nat. Struct. Mol. Biol.* **2015**, *22*, 466.

(223) Seefeldt, A. C.; Nguyen, F.; Antunes, S.; Perebaskine, N.; Graf, M.; Arenz, S.; Inampudi, K. K.; Douat, C.; Guichard, G.; Wilson, D. N.; Innis, C. A. *Nat. Struct. Mol. Biol.* **2015**, *22*, 470.

(224) Goldbach, T.; Knappe, D.; Reinsdorf, C.; Berg, T.; Hoffmann, R. *J. Pept. Sci.* **2016**, *22*, 592.

(225) Krizsan, A.; Prahl, C.; Goldbach, T.; Knappe, D.; Hoffmann, R. *Chembiochem.* **2015**, *16*, 2304.

(226) Otvos, L., Jr.; Wade, J. D.; Lin, F.; Condie, B. A.; Hanrieder, J.; Hoffmann, R. *J. Med. Chem.* **2005**, *48*, 5349.

(227) Holm, M.; Borg, A.; Ehrenberg, M.; Sanyal, S. *Proc. Natl. Acad. Sci.* **2016**, *113*, 978.

(228) Mandal, S. M.; Roy, A.; Ghosh, A. K.; Hazra, T. K.; Basak, A.; Franco, O. L. *Front. Pharmacol.* **2014**, *5*, 105.

(229) Wimley, W. C.; Hristova, K. *J. Membr. Biol.* **2011**, *239*, 27.

(230) Wu, C.-H.; Liu, I. J.; Lu, R.-M.; Wu, H.-C. *Int J Biomed Sci.* **2016**, *23*, 8.

(231) Colangelo, W., *In vivo* display : a selection and its derivatives for antimicrobial lead identification, PhD Dissertation, Wayne State University, **2017**.

(232) Guralp, S. A.; Murgha, Y. E.; Rouillard, J.-M.; Gulari, E. *PloS one* **2013**, *8*, e59305.

(233) Choi, K., Kim, HR., Park, YS. *Biotechnol. Lett.* **2002**, 24, 251. https://doi.org/10.1023/A:1014076426705.

(234) Walker, J. R.; Roth, J. R.; Altman, E. *J. Pept. Res.* **2001**, *58*, 380.

(235) Bray, B. L. *Nat. Rev. Drug Discov.* **2003**, *2*, 587.

(236) Seo, H., Ligand binding studies of a peptide targeting helix 69 of 23s rRNA in bacterial ribosomes, PhD Dissertation, Wayne State University, **2017**.

(237) Sakakibara, Y.; Abeysirigunawardena, S. C.; Duc, A. C.; Dremann, D. N.; Chow, C. S. *Angew. Chem. Int. Ed.* **2012**, *51*, 12095.

(238) Sakakibara., Y., Exploring conformational variability in the ribosome: from structure and function to potential antibiotic targeting, PhD Dissertation, Wayne State University, **2012**.

(239) Sakakibara, Y.; Chow, C. S. *Org. Biomol. Chem.* **2017**, *15*, 8535.

(240) Lobell, R. B.; Schleif, R. F. *Science* **1990**, *250*, 528.

(241) Reed, W. L.; Schleif, R. F. *J Mol Biol.* **1999**, *294*, 417.

(242) Kapust, R. B.; Waugh, D. S. *Protein Expr. Purif.* **2000**, *19*, 312.

(243) Kapust, R. B.; Routzahn, K. M.; Waugh, D. S. *Protein Expr. Purif.* **2002**, *24*, 61.

(244) Phan, J.; Zdanov, A.; Evdokimov, A. G.; Tropea, J. E.; Peters, H. K., 3rd; Kapust, R. B.; Li, M.; Wlodawer, A.; Waugh, D. S. *J. Biol. Chem.* **2002**, *277*, 50564.

(245) Fox, J. D.; Waugh, D. S. *Methods Mol Biol.* **2003**, *205*, 99.

(246) Sun, P.; Austin, B. P.; Tozser, J.; Waugh, D. S. *Protein Sci.* **2010**, *19*, 2240.

(247) Renicke, C.; Spadaccini, R.; Taxis, C. *PloS one* **2013**, *8*, e67915.

(248) Fechter, P.; Parmentier, D.; Wu, Z.; Fuchsbauer, O.; Romby, P.; Marzi, S. *Methods Mol Biol.* **2016**, *1490*, 83.

(249) Tijerina, P.; Mohr, S.; Russell, R. *Nat. Protoc.* **2007**, *2*, 2608.

(250) Peattie, D. A.; Gilbert, W. *Proc. Natl. Acad. Sci.* **1980**, *77*, 4679.

(251) Moazed, D.; Noller, H. F. *Cell* **1986**, *47*, 985.

(252) Behm-Ansmant, I.; Helm, M.; Motorin, Y. *J. Nucleic Acids.* **2011**, *2011*, 408053.

(253) Peattie, D. A. *Proc. Natl. Acad. Sci.* **1979**, *76*, 1760.

(254) Maxam, A. M.; Gilbert, W. *Proc. Natl. Acad. Sci.* **1977**, *74*, 560.

(255) Muth, G. W.; Ortoleva-Donnelly, L.; Strobel, S. A. *Science* **2000**, *289*,

(256) Bayfield, M. A.; Dahlberg, A. E.; Schulmeister, U.; Dorner, S.; Barta, A. *Proc. Natl. Acad. Sci.* **2001**, *98*, 10096.

(257) Russell, R.; Zhuang, X.; Babcock, H. P.; Millett, I. S.; Doniach, S.; Chu, S.; Herschlag, D. *Proc. Natl. Acad. Sci.* **2002**, *99*, 155.

(258) Muth, G. W.; Chen, L.; Kosek, A. B.; Strobel, S. A. *RNA* **2001**, *7*, 1403.

(259) Stern, S.; Wilson, R. C.; Noller, H. F. *J Mol Biol.* **1986**, *192*, 101.

(260) Egebjerg, J.; Leffers, H.; Christensen, A.; Andersen, H.; Garrett, R. A. *J Mol Biol.* **1987**, *196*, 125.

(261) Svensson, P.; Changchien, L. M.; Craven, G. R.; Noller, H. F. *J Mol Biol.* **1988**, *200*, 301.

(262) Sakakibara, Y.; Chow, C. S. *J. Am. Chem. Soc.* **2011**, *133*, 8396.

(263) Woodcock, J.; Moazed, D.; Cannon, M.; Davies, J.; Noller, H. F. *EMBO J.* **1991**, *10*, 3099.

(264) Spickler, C.; Brunelle, M. N.; Brakier-Gingras, L. *J Mol Biol.* **1997**, *273*, 586.

(265) Ehresmann, C.; Baudin, F.; Mougel, M.; Romby, P.; Ebel, J. P.; Ehresmann, B. *Nucleic Acids Res.* **1987**, *15*, 9109.

(266) Brunel, C.; Romby, P. *Methods Enzymol.* **2000**, *318*, 3.

(267) Wells, S. E.; Hughes, J. M.; Igel, A. H.; Ares, M., Jr. *Methods Enzymol.* **2000**, *318*, 479.

(268) Climie, S. C.; Friesen, J. D. *J Biol Chem.* **1988**, *263*, 15166.

(269) Moazed, D.; Robertson, J. M.; Noller, H. F. *Nature* **1988**, *334*, 362.

(270) Mayford, M.; Weisblum, B. *EMBO J.* **1989**, *8*, 4307.

(271) Ares, M., Jr.; Igel, A. H. *Genes Dev.* **1990**, *4*, 2132.

(272) Harris, K. A., Jr.; Crothers, D. M.; Ullu, E. *RNA* **1995**, *1*, 351.

(273) Zaug, A. J.; Cech, T. R. *RNA* **1995**, *1*, 363.

(274) Mereau, A.; Fournier, R.; Gregoire, A.; Mougin, A.; Fabrizio, P.; Luhrmann, R.; Branlant, C. *J Mol Biol.* **1997**, *273*, 552.

(275) Wiegand, I.; Hilpert, K.; Hancock, R. E. *Nat. Protoc.* **2008**, *3*, 163.

(276) Andrews, J. M. *J. Antimicrob. Chemother.* **2001**, *48*, 5.

(277) Clinical and Laboratory Standards Institute. Performance standards for antimicrobial susceptibility testing; sixteenth informational supplement. **2006** CLSI document M100-S16CLSI, Wayne, PA.

(278) European Committee for Antimicrobial Susceptibility Testing of the European Society of Clinical, M.; Infectious, D. *Clinical Microbiology and Infection* **2003**, *9*, 9.

(279) Kahlmeter, G.; Brown, D. F.; Goldstein, F. W.; MacGowan, A. P.; Mouton, J. W.; Osterlund, A.; Rodloff, A.; Steinbakk, M.; Urbaskova, P.; Vatopoulos, A. *J. Antimicrob. Chemother.* **2003**, *52*, 145.

(280) Li, J.; Xie, S.; Ahmed, S.; Wang, F.; Gu, Y.; Zhang, C.; Chai, X.; Wu, Y.; Cai, J.; Cheng, G. *Front. Pharmacol.* **2017**, *8*, 364.

(281) Wiegand, I.; Wiedemann, B. *Curr. Mol. Pharmacol.*; Offermanns, S., Rosenthal, W., Eds.; Springer Berlin Heidelberg: Berlin, Heidelberg, **2008**, 769.

(282) De Stasio, E. A.; Moazed, D.; Noller, H. F.; Dahlberg, A. E. *EMBO J.* **1989**, *8*, 1213.

(283) Jorgensen, J. H.; Ferraro, M. *J.Clin. Infect. Dis.* **2009**, *49*, 1749.

(284) Zhou, Y.; Hou, Z.; Fang, C.; Xue, X.; Da, F.; Wang, Y.; Bai, H.; Luo, X. *Folia Microbiol.* **2013**, *58*, 9.

(285) Anunthawan, T.; Yaraksa, N.; Phosri, S.; Theansungnoen, T.; Daduang, S.; Dhiravisit, A.; Thammasirirak, S. *Bioorganic Med. Chem. letters* **2013**, *23*, 4657.

(286) Nicolas, P. *The FEBS journal* **2009**, *276*, 6483.

(287) Casteels, P.; Ampe, C.; Jacobs, F.; Vaeck, M.; Tempst, P. *EMBO J.* **1989**, *8*, 2387.

(288) Gennaro, R.; Skerlavaj, B.; Romeo, D. *Infect. Immun.* **1989**, *57*, 3142.

(289) Knappe, D.; Kabankov, N.; Hoffmann, R. *Int. J. Antimicrob. Agents* **2011**, *37*, 166.

(290) Cociancich, S.; Dupont, A.; Hegy, G.; Lanot, R.; Holder, F.; Hetru, C.; Hoffmann, J. A.; Bulet, P. *The Biochem. J.* **1994**, *300 (Pt 2)*, 567.

(291) Chernysh, S.; Cociancich, S.; Briand, J.-P.; Hetru, C.; Bulet, P. *J. Insect Physiol.* **1996**, *42*, 81.

(292) Schneider, M.; Dorn, A. *J. Invertebr. Pathol.* **2001**, *78*, 135.

(293) Runti, G.; Lopez Ruiz Mdel, C.; Stoilova, T.; Hussain, R.; Jennions, M.; Choudhury, H. G.; Benincasa, M.; Gennaro, R.; Beis, K.; Scocchi, M. *Int J Bacteriol.* **2013**, *195*, 5343.

(294) Hansen, A.; Schafer, I.; Knappe, D.; Seibel, P.; Hoffmann, R. *Antimicrob. Agents Chemother.* **2012**, *56*, 5194.

(295) Schmidt, R.; Ostorhazi, E.; Wende, E.; Knappe, D.; Hoffmann, R. *J. Antimicrob. Chemother.* **2016**, *71*, 1003.

(296) Knappe, D.; Zahn, M.; Sauer, U.; Schiffer, G.; Strater, N.; Hoffmann, R. *Chembiochem.* **2011**, *12*, 874.

(297) Acharya, K. R.; Lloyd, M. D. *Trends Pharmacol. Sci.* **2005**, *26*, 10.

(298) Swaminathan, G. J.; Holloway, D. E.; Colvin, R. A.; Campanella, G. K.; Papageorgiou, A. C.; Luster, A. D.; Acharya, K. R. *Structure* **2003**, *11*, 521.

(299) Bulkley, D.; Innis, C. A.; Blaha, G.; Steitz, T. A. *Proc. Natl. Acad. Sci.* **2010**, *107*, 17158.

(300) Arenz, S.; Meydan, S.; Starosta, A. L.; Berninghausen, O.; Beckmann, R.; Vazquez-Laslop, N.; Wilson, D. N. *Mol. Cell.* **2014**, *56*, 446.

(301) Arenz, S.; Ramu, H.; Gupta, P.; Berninghausen, O.; Beckmann, R.; Vazquez-Laslop, N.; Mankin, A. S.; Wilson, D. N. *Nat. Commun.* **2014**, *5*, 3501.

(302) Vazquez-Laslop, N.; Klepacki, D.; Mulhearn, D. C.; Ramu, H.; Krasnykh, O.; Franzblau, S.; Mankin, A. S. *Proc. Natl. Acad. Sci.* **2011**, *108*, 10496.

(303) Vazquez-Laslop, N.; Thum, C.; Mankin, A. S. *Mol. Cell.* **2008**, *30*, 190.

(304) Berisio, R.; Schluenzen, F.; Harms, J.; Bashan, A.; Auerbach, T.; Baram, D.; Yonath, A. *Nat. Struct. Biol.* **2003**, *10*, 366.

(305) Dunkle, J. A.; Xiong, L.; Mankin, A. S.; Cate, J. H. *Proc. Natl. Acad. Sci.* **2010**, *107*, 17152.

(306) Yonath, A. *Annu. Rev. Biochem.* **2005**, *74*, 649.

(307) Sigmund, C. D.; Ettayebi, M.; Morgan, E. A. *Nucleic Acids Res.* **1984**, *12*, 4653.

(308) Polikanov, Y. S.; Steitz, T. A.; Innis, C. A. *Nat. Struct. Mol. Biol.* **2014**, *21*, 787.

(309) Jin, D. J.; Gross, C. A. *J Mol Biol.* **1988**, *202*, 45.

(310) Yonath, A. *Angew Chem. Int. Ed.* **2010**, *49*, 4340.

(311) Hancock, R. E. *J. Antimicrob. Chemother.* **1981**, *8*, 249.

(312) Hancock, R. E.; Farmer, S. W.; Li, Z. S.; Poole, K. *Antimicrob. Agents Chemother.* **1991**, *35*, 1309.

(313) Cabanas, M. J.; Vazquez, D.; Modolell, J. *Biochem. Biophys. Res. Commun.* **1978**, *83*, 991.

(314) Becker, B.; Cooper, M. A. *ACS Chem Biol.* **2013**, *8*, 105.

(315) Raychaudhuri, S.; Conrad, J.; Hall, B. G.; Ofengand, J. *RNA* **1998**, *4*, 1407.

(316) Ejby, M.; Sorensen, M. A.; Pedersen, S. *Proc. Natl. Acad. Sci.* **2007**, *104*, 19410.

(317) O'Connor, M.; Gregory, S. T. *Int J Bacteriol.* **2011**, *193*, 154.

(318) Uno, M.; Ito, K.; Nakamura, Y. *Biochimie.* **1996**, *78*, 935.

(319) Scheunemann, A. E.; Graham, W. D.; Vendeix, F. A.; Agris, P. F. *Nucleic Acids Res.* **2010**, *38*, 3094.

(320) Wade, H. E.; Robinson, H. K. *Biochem. J.* **1965**, *97*, 747.

(321) Kurylo, C. M.; Alexander, N.; Dass, R. A.; Parks, M. M.; Altman, R. A.; Vincent, C. T.; Mason, C. E.; Blanchard, S. C. *Genome Biol. Evol.* **2016**, *8*, 742.

(322) Wade, H. E.; Robinson, H. K. *Biochem. J.* **1965**, *96*, 753.

(323) Dinçbas-Renqvist, V.; Engström, Å.; Mora, L.; Heurgué-Hamard, V.; Buckingham, R.; Ehrenberg, M. *EMBO J.* **2000**, *19*, 6900.

(324) Touchon, M.; Hoede, C.; Tenaillon, O.; Barbe, V.; Baeriswyl, S.; Bidet, P.; Bingen, E.; Bonacorsi, S.; Bouchier, C.; Bouvet, O.; Calteau, A.; Chiapello, H.; Clermont, O.; Cruveiller, S.; Danchin, A.; Diard, M.; Dossat, C.; Karoui, M. E.; Frapy, E.; Garry, L.; Ghigo, J. M.; Gilles, A. M.; Johnson, J.; Le Bouguénec, C.; Lescat, M.; Mangenot, S.; Martinez-Jéhanne, V.; Matic, I.; Nassif, X.; Oztas, S.; Petit, M. A.; Pichon, C.; Rouy, Z.; Ruf, C. S.; Schneider, D.; Tourret, J.; Vacherie, B.; Vallenet, D.; Médigue, C.; Rocha, E. P. C.; Denamur, E. *PLoS Genet.* **2009**, *5*, e1000344.

(325) Benveniste, R.; Davies, J. *Antimicrob. Agents Chemother.* **1973**, *4*, 402.

(326) Llano-Sotelo, B.; Azucena, E. F., Jr.; Kotra, L. P.; Mobashery, S.; Chow, C. S. *J. Biol. Chem.* **2002**, *9*, 455.

(327) Lin M., Y. L., Liu Y., Shi G., Yang C., Zhou C., Xu W., TaoK., H Taiping., Afr J *Biotechnol*. **2010**, *9*, 8445.

(328) Abeysirigunawardena, S. C.; Chow, C. S. *RNA* **2008**, *14*, 782.

(329) Sakakibara, Y.; Chow, C. S. *ACS Chem Biol.* **2012**, *7*, 871.

(330) Korostelev, A.; Zhu, J.; Asahara, H.; Noller, H. F. *EMBO J.* **2010**, *29*, 2577.

(331) Korostelev, A. A. *RNA* **2011**, *17*, 1409.

(332) Ali, I. K.; Lancaster, L.; Feinberg, J.; Joseph, S.; Noller, H. F. *Mol. Cell.* **2006**, *23*, 865.

(333) Kipper, K.; Sild, S.; Hetenyi, C.; Remme, J.; Liiv, A. *Biochimie* **2011**, *93*, 834.

(334) Weixlbaumer, A.; Jin, H.; Neubauer, C.; Voorhees, R. M.; Petry, S.; Kelley, A. C.; Ramakrishnan, V. *Science* **2008**, *322*, 953.

(335) Korostelev, A.; Asahara, H.; Lancaster, L.; Laurberg, M.; Hirschi, A.; Zhu, J.; Trakhanov, S.; Scott, W. G.; Noller, H. F. *Proc. Natl. Acad. Sci.* **2008**, *105*, 19684.

(336) Salian, S.; Matt, T.; Akbergenov, R.; Harish, S.; Meyer, M.; Duscha, S.; Shcherbakov, D.; Bernet, B. B.; Vasella, A.; Westhof, E.; Bottger, E. C. *Antimicrob. Agents Chemother.* **2012**, *56*, 6104.

(337) Modolell, J.; Vazquez *Eur. J. Biochem.* **1977**, *81*, 491.

(338) Knappe, D.; Ruden, S.; Langanke, S.; Tikkoo, T.; Ritzer, J.; Mikut, R.; Martin, L. L.; Hoffmann, R.; Hilpert, K. *Amino acids* **2016**, *48*, 269.

(339) Schmidt, N. W.; Deshayes, S.; Hawker, S.; Blacker, A.; Kasko, A. M.; Wong, G. C. *ACS nano* **2014**, *8*, 8786.

(340) Bera, S.; Zhanel, G. G.; Schweizer, F. *Bioorganic Med. Chem. letters* **2010**, *20*, 3031.

(341) Jiang, L.; Watkins, D.; Jin, Y.; Gong, C.; King, A.; Washington, A. Z.; Green, K. D.; Garneau-Tsodikova, S.; Oyelere, A. K.; Arya, D. P. *ACS Chem Biol.* **2015**, *10*, 1278.

ABSTRACT

INVESTIGATION OF THE *IN VIVO* ACTIVITY OF RIBOSOME-TARGETING PEPTIDES AND AMINOGLYCOSIDES IN *ESCHERICHIA COLI*

by

NISANSALA SARANGI THILAKARATHNE MUTHUNAYAKE

August 2018

Advisor: Dr. Christine S Chow

Major: Chemistry (Biochemistry)

Degree: Doctor of Philosophy

The development of short peptides that specifically bind to higher-order structures of ribosomal RNA is one promising way to address the problem of antibiotic resistance. However, the poor correlation between *in vitro* and in *vivo* activities of these peptides is one of the major questions in antibiotic peptide research. Therefore, one of the main objectives of this dissertation work was to utilize a plasmid-based system to *in vivo* express ribosome-targeting peptides and study their direct inhibitory effects on bacteria. A specific plasmid system was optimized to *in vivo* express oncocin, a proline-rich antimicrobial peptide and its variants in bacteria. Our data showed that the *in vivo*-expressed peptide completely inhibited bacterial growth and displayed bactericidal activity. The *in vivo* dimethyl sulfate (DMS) footprinting data revealed interactions of oncocin with the PTC region of the bacterial ribosome. The optimized plasmid system was utilized to *in vivo* express short peptides that are known to target the helix 69 (H69) region of the ribosome. In the first approach, peptides were expressed as GFP-fusion proteins, and in the second approach they were expressed as free peptides. In both systems, we found that the NQAANHQ peptide had slightly better inhibition compared to other H69-targeting peptides.

Based on *in vivo* and *in vitro* data, we consider NQAANHQ as a potential drug lead, but it will need considerable modifications or alterations to improve its activity.

The bactericidal nature of 2-deoxystreptamine aminoglycoside antibiotics is still poorly understood despite decades of clinical use and biochemical studies. Previous work showed that Ψ modifications are important for efficient binding of aminoglycosides to H69. However, the effects of Ψ modifications on the bactericidal activity of aminoglycosides have not been examined. Antibacterial activities of 2-deoxystreptamine aminoglycosides were assessed by performing minimum inhibitory concentration (MIC) studies using wild-type and Ψ-deficient bacterial strains. Our data revealed that loss of Ψ modifications conferred resistance to 4,6-linked-2-DOS aminoglycosides, gentamicin and kanamycin, whereas the effect was not significant with 4,5-linked-2-DOS aminoglycosides, neomycin and paromomycin. However, bacterial strains carrying mutant release factor 2 (RF2, Ala246Thr) showed resistance to neomycin and paromomycin in the Ψ-deficient background. The observed results could be a combined effect of loss of Ψs and defective RF2 that perturb the ribosome-drug interactions. Collectively, the information gained from these studies provides deeper insight into the underlying mechanism of action of ribosome-targeting drugs, which is important for the development of unique antibiotics that target the bacterial ribosome at novel sites such as H69.

AUTOBIOGRAPHICAL STATEMENT

NISANSALA SARANGI THILAKARATHE MUTHUNAYAKE

ADVISOR: Dr. Christine S Chow

THESIS TITLE: INVESTIGATION OF THE *IN VIVO* ACTIVITY OF RIBOSOME-TARGETING-PEPTIDES AND AMINOGLYCOSIDES IN *ESCHERICHIA COLI*

EDUCATION

- **PhD.; Biological Chemistry, 2018 August, Wayne State University, Detroit, MI, USA**
- **B.S. (First Class Honors); Chemistry, 2009, University of Kelaniya, Sri Lanka**

PUBLICATIONS

1. **Muthunayake NS**, Colangelo W, Gamage S, Cunningham PR, Chow C, *In vivo* expression and ribosome mapping of peptide antibiotics in bacteria. Manuscript in preparation

2. Gamage S, **Muthunayake NS**, Sonousi A, Crich D, Chow C, Carbohydrate-linked cisplatin analogue: reactivity studies with RNA and DNA. Manuscript in preparation

3. Mathur A, Cano A, Kohl M, **Muthunayake NS**, Vaidyanathan P, Wood ME, (2018) Visualization of gender, race, citizenship and academic performance in association with career outcomes of 15-year biomedical doctoral alumni at a public research university. PLOS ONE 13(5): e0197473.

4. Mathur A, Chow C, Feig AL, Kenaga H, Moldenhauer J, **Muthunayake NS**, Ouellett M, Pence LE, Straub V, (2018) Exposure to Multiple Career Pathways by Biomedical Doctoral Students at a Public Research University, PLOS ONE 13(6): e0199720.

5. **Muthunayake NS**, Weerasooriya MKB, (2009) The use of rice bran lipase to enhance the washing performance of commercial detergents. Proceeding of Sri Lanka Association for the Advancement of Science, 2009, 65, 219